DOE/CH/46656--16-Rev.0

DE88 012368

SALT REPOSITORY PROJECT
SHAFT DESIGN GUIDE

Revision O

DECEMBER 1987

PREPARED FOR THE

U.S. DEPARTMENT OF ENERGY
OFFICE OF CIVILIAN RADIOACTIVE WASTE MANAGEMENT
SALT REPOSITORY PROJECT OFFICE

BY

FLUOR TECHNOLOGY, INC.
AND PARSONS BRINCKERHOFF/PB-KBB

IN CONJUNCTION WITH

MORRISON-KNUDSEN ENGINEERS, INC.

SCIENCE APPLICATIONS INTERNATIONAL CORPORATION

WOODWARD-CLYDE CONSULTANTS

ROCKWELL INTERNATIONAL, INC.

DISCLAIMER

BIBLIOGRAPHIC DATA

Fluor Technology, Inc., and Parsons Brinckerhoff/PB-KBB, 1987. *Salt Repository Project Shaft Design Guide,* Revision O, DOE/CH/46656-16 prepared for the U.S. Department of Energy, Salt Repository Project Office, Hereford, TX.

NOTICE

Printed in the United States of America
Available from
National Technical Information Service
U S Department of Commerce
5285 Port Royal Road
Springfield, VA 22161

NTIS price codes
Printed copy 12
Microfiche copy AO1

BMI/ONWI/C-57

DOE/CH/46656-16
Distribution Category UC-70

SALT REPOSITORY PROJECT
SHAFT DESIGN GUIDE

Revision O

DECEMBER 1987

PREPARED FOR THE

U.S. DEPARTMENT OF ENERGY
OFFICE OF CIVILIAN RADIOACTIVE WASTE MANAGEMENT
SALT REPOSITORY PROJECT OFFICE

BY

FLUOR TECHNOLOGY, INC.
AND PARSONS BRINCKERHOFF/PB-KBB

IN CONJUNCTION WITH

MORRISON-KNUDSEN ENGINEERS, INC.

SCIENCE APPLICATIONS INTERNATIONAL CORPORATION

WOODWARD-CLYDE CONSULTANTS

ROCKWELL INTERNATIONAL, INC.

This report was prepared for the U S Department of Energy by Fluor Technology, Inc., under Contract No. DE-ACO2-83WM46656 and Parsons Brinckerhoff/PB-KBB under Contract No. DE-ACO97-86WM46664.

ABSTRACT

The Salt Repository Project (SRP) Shaft Design Guide (SDG) and the accompanying SRP Input to Seismic Design define the basic approach for developing appropriate shaft designs for a high-level nuclear waste repository in salt at a proposed site in Deaf Smith County, Texas. The SDG is based on current mining industry standards and practices enhanced to meet the special needs of an underground nuclear waste repository. It provides a common approach for design of both the exploratory and repository shafts.

The SDG defines shaft lining and material concepts and presents methods for calculating the loads and displacements that will be imposed on lining structures. It also presents the methodology and formulae for sizing lining components. The SDG directs the shaft designer to sources of geoscience and seismic design data for the Deaf Smith County, Texas repository site.

In addition, the SDG describes methods for confirming shaft lining design by means of computer analysis, and it discusses performance monitoring needs that must be considered in the design.

FOREWORD

The National Waste Terminal Storage (NWTS) program was established in 1976 by the predecessor of the U.S. Department of Energy (DOE), the Energy Research and Development Administration. In September, 1983, this program became the Civilian Radioactive Waste Management (CRWM) program. Its purpose is to develop technology and provide facilities for safe, environmentally acceptable, permanent disposal of high-level nuclear waste (HLW). HLW includes wastes from both commercial and defense sources, such as spent (used) fuel from nuclear power reactors, accumulations of wastes from production of nuclear weapons, and solidified wastes from fuel reprocessing.

The information in this document pertains to the Exploratory Shaft Facility (ESF) and the repository studies of the Salt Repository Program (SRP) of the Office of Geologic Repositories in the CRWM Program. The SRP Shaft Design Guide and the SRP Input to Seismic Design were prepared to provide a common design approach for all repository shafts.

Fluor Technology, Inc., is the prime contractor to DOE for conceptual design of a high-level nuclear waste repository in salt, and Parsons Brinckerhoff/PB-KBB is the prime contractor to DOE for the design of the exploratory shaft facility at the Deaf Smith County, Texas site.

SUMMARY

The purpose of the SRP Shaft Design Guide (SDG) is to define the basic approach for designing shafts at a proposed site in Deaf Smith County, Texas. The SDG is based on traditional shaft design and construction concepts which have been enhanced to meet the special needs of an underground nuclear waste repository. The requirements for the Salt Repository Program (SRP) shafts go beyond those for conventional shafts. The design approach in the SDG recognizes that the salt repository must be licensed by the U.S. Nuclear Regulatory Commission (NRC) and the SRP shafts must be designed for a nominal 100-year operational life. Also, the construction methods must be selected to minimize disturbance to the host rock to the extent practicable and allow for the installation of decommissioning seals. The SDG is to be applied to the design of all the SRP shafts to provide a common basis for design of the repository and exploratory shafts.

The objective of the SDG is to provide the shaft designer with the necessary knowledge for designing the SRP shafts. The SDG covers reference design data bases, shaft linings and materials, loads acting on shaft structures, seismic considerations, shaft lining sizing procedures, computer design analysis, and performance monitoring.

The identification of specific licensing requirements for the SRP shafts is beyond the scope of the SDG. Licensing guidance will be provided by subsequent SRP documents. The shaft systems, structures, and components important to safety and the engineered barrier systems important to waste isolation will be identified by the shaft designer following approved Salt Repository Project Office (SRPO) procedures.

The functional requirements, performance criteria, and constraints will be identified in the SRP requirements document. As this information is developed and baselined, it will form part of the design criteria for the SRP shafts. Shaft and related design activities will be conducted in accordance with the SRP Quality Assurance (QA) requirements.

The following is a brief summary of the contents and purpose of the information provided in the SDG.

REFERENCE DESIGN DATA BASES

The geological, geotechnical, hydrological, and seismic information necessary for shaft design are contained in two separate data base documents. These include the Synthetic Geotechnical Design Reference Data for the Deaf Smith Site (SRP Data Base) (DOE, 1986) and the SRP Input to Seismic Design (ISD) (DOE, 1987). The SRP Data Base contains the geotechnical data for the Deaf Smith County, Texas site. The ISD contains the seismic stratigraphy and material properties for seismic design. These data can be used in a seismic analysis of the shafts. These and any other data bases used for the shaft design will be revised as new information becomes available from engineering design boreholes and other site characterization activities.

SHAFT LININGS AND MATERIALS

The lining and sealing systems described in the SDG are suitable for the ground and water conditions at the Deaf Smith County repository site. These systems are applicable for circular shafts and include single steel with concrete, double steel with concrete, ductile cast iron tubbing, and concrete. Operational seal systems for the watertight lining include chemical seal rings, asphaltic sealant material, and picotages. The selection of lining types and the location of operational seals will depend on ground and water conditions as identified in the reference data base. The linings will also be designed to accommodate decommissioning seal requirements.

LOADS ACTING ON SHAFT STRUCTURES

Uniform and nonuniform loads and displacements affecting the design of shaft lining components are discussed, and detailed methods and formulae are identified for calculation of loads, displacements, or strains which will act upon the lining. These loads will be used to develop the shaft design.

SHAFT LINING SIZING PROCEDURES

The dimensions of the lining components selected for the shafts will also be determined by means of closed-form solutions. The equations presented in this chapter incorporate allowable stresses, categorized according to load combinations, for all the load-bearing lining structures. This represents a traditional design approach used in conventional shaft design. In addition, seismic loads on the shafts will be considered in terms of transient wave forms which cause deformations in the ground around the shafts. The effects of seismic activity are not generally considered in the design of conventional mine shafts.

COMPUTER DESIGN ANALYSIS

Computer modeling techniques, including finite-element and finite-difference models, for shaft design analysis are described. These techniques can be used interactively with the closed-form methods for shaft structure design. The computer models can analyze the shaft lining structures and surrounding rock for the conditions envisioned during the construction phase and at various times during the shaft operational life. During the construction phase the model can depict freezing, excavation, lining installation, and thawing. For each period, the model can simulate the various loadings to which the linings will be subjected and the resulting stresses, strains, and displacements. Other factors such as salt creep, concrete shrinkage and creep, and local imperfections in the structures can also be considered during the modeling.

PERFORMANCE MONITORING

Monitoring of the exploratory shaft lining and seal systems will be undertaken during and after construction to provide the designer with input data, to confirm the design and construction concepts, and to monitor the stability of the shafts. It is anticipated that some form of monitoring will take place throughout the life of all repository shafts. This could include geotechnical instrumentation to determine rock and water conditions behind the lining and instrumentation in the shaft lining itself to determine stresses, strains, and displacements. The placement of these instruments must be taken into account at the commencement of the design of the shafts.

SHAFT DESIGN GUIDE
TABLE OF CONTENTS

TABLE OF CONTENTS
(Continued)

TABLE OF CONTENTS
(Continued)

TABLE OF CONTENTS
(Continued)

TABLE OF CONTENTS
(Continued)

TABLE OF CONTENTS
(Continued)

TABLE OF CONTENTS
(Continued)

TABLE OF CONTENTS
(Continued)

TABLE OF CONTENTS
(Continued)

SHAFT DESIGN GUIDE
LIST OF TABLES

LIST OF FIGURES

LIST OF FIGURES
(Continued)

1 INTRODUCTION

1.1 PURPOSE

The purpose of the SRP Shaft Design Guide (SDG) is to provide a common approach for the design of circular shafts such as those planned for the proposed SRP repository in Deaf Smith County, Texas. The SDG is specifically intended for use by both exploratory and repository shaft designers.

The Mission Plan for the Civilian Radioactive Waste Management (CRWM) Program (DOE, 1985a) specifies that:

> "The DOE intends to use the exploratory shafts, as required, to ensure that the construction of the repository can be completed in time to meet the January 1998 date mandated by the act and will continue to evaluate the most cost-effective use of the exploratory shafts in the operating repository."

As reflected in Appendix E to the Generic Requirements for a Mined Geologic Disposal System (GRMGDS) (DOE, 1985b), implementation of the cited Mission Plan requires providing exploratory shafts that can be incorporated into the repository and can be used to support repository construction. Another requirement from Appendix E of the GRMGDS mandates providing exploratory shaft design and construction methods that will, among other things, demonstrate constructibility for the candidate repository shafts. Successful implementation of these programmatic requirements requires that a common design approach be employed by both exploratory and repository shaft designers.

The geological regime at the Deaf Smith County, Texas repository site, to which this SDG specifically relates, is described fully in the Synthetic Geotechnical Design Reference Data for the Deaf Smith Site (SRP Data Base) (DOE, 1986). Briefly, the shafts will be constructed through horizontally-bedded sedimentary deposits consisting of unconsolidated and weakly cemented soils, variable strength rocks, and evaporite sequences. The soils include uncemented and unindurated cohesive or noncohesive material, such as the loess of the Blackwater Draw Formation, and the silty sand and gravel of the Ogallala Formation. Sediments, exhibiting varying degrees of cementation, induration, and water content, exist throughout the stratigraphic sequence, and range from very low- to high-strength rock. Two major aquifers, known as the Ogallala Formation and Dockum Group occur at the site. In addition, salt strata of various thicknesses exist in the

Upper Seven Rivers, Upper San Andres and Lower San Andres (five units) formations. Unit 4 of the Lower San Andres Formation has been selected as the repository horizon.

The design approach defined in the SDG is based on traditional shaft design and construction concepts enhanced to meet the special needs of an underground nuclear waste repository. This includes seismic analyses, which are not normally employed in the design of conventional shafts. The exploratory and repository shaft designs will be completed according to approved QA procedures.

The design approach of the SDG takes into account the following requirements which exceed those for conventional shaft design:

1. The shafts must have a nominal design life of 100 years.
2. Excavation methods must minimize overbreak and disturbance of the host rock.
3. Design and construction must allow for the installation of decommissioning seals.
4. Define monitoring requirements and concerns for confirmation of shaft performance.

The identification of specific licensing requirements for the SRP shafts is beyond the scope of the SDG. Licensing guidance will be provided by subsequent SRP documents. The shaft systems, structures, and components important to safety and the engineered barrier systems important to waste isolation will be identified by the shaft designer following approved Salt Repository Project Office (SRPO) procedures.

The SDG presents a conservative approach to shaft lining design for the Deaf Smith Site or for sites with similar geological conditions. However, it does not provide the only way to design shafts. The SDG shall form the basis for lining design, but the designer would have the option of using a different approach. In such cases the designer would be required to demonstrate the adequacy of his design approach against the SDG approach.

1.2 OBJECTIVE

The objective of the SDG is to ensure that all the repository shafts are designed to common bases. To meet this objective, the SDG requires the designer to:

1. Incorporate information from the reference design data bases.
2. Use the types of linings and seals identified in the SDG as the basis for selecting suitable shaft lining structures.
3. Use the methods and formulae identified in the SDG as the basis for calculating loads, stresses, and displacements of lining and seal components.
4. Calculate lining dimensions using the closed form solutions and/or computer analysis methods described in the SDG or comparable methods.
5. Identify monitoring requirements for performance confirmation of the shaft design.

It is recognized that to address U.S. Nuclear Regulatory Commission (NRC) licenseability of the SRP shafts, the designer must fulfill requirements in addition to those listed above. The identification of these requirements is beyond the scope of the SDG and will be addressed in subsequent SRP documents.

1.3 SCOPE

The SDG addresses the design of vertical circular shafts requiring both watertight and nonwatertight lining sections. These shafts will accommodate waste handling, mined salt handling, intake and exhaust ventilation, and service access. The SDG describes the following components and requirements that influence the shaft lining design: operational seals, shaft bottom plug, and station areas; surrounding rock and soil structures; attachments to the liners; instrumentation and monitoring requirements; and decommissioning bulkhead requirements.

The SDG does not address ground freezing design or the design of hoisting systems including headframes, hoists, guides, hoist ropes, and conveyances.

1.4 BACKGROUND

The prime design contractors are Parsons Brinckerhoff/PB-KBB, for the exploratory shafts, and Fluor Technology, Inc., for the repository shafts. According to the Mission Plan, the exploratory shafts may be incorporated into the repository, and so they must be designed to the same criteria as the repository shafts. To help achieve this commonality of design, the DOE directed the prime contractors to prepare this SDG as a means of documenting the design approach.

The SDG is supplemented by data bases including the SRP Data Base (DOE, 1986) and the Input to Seismic Design (ISD) (DOE, 1987). The data in these supporting documents are specific to the Deaf Smith County, Texas repository site. The SRP Data Base contains the stratigraphic, hydrogeological, geochemical, geomechanical, and thermal design data. The ISD contains information on the seismic stratigraphy and material properties, seismic assessments, seismic design parameters, and host media stability analyses. These data bases will be revised as new site information becomes available.

2 REFERENCE DESIGN DATA BASE

The purpose of this chapter is to identify the sources of the geotechnical and seismic information which the designer must use in designing the Salt Repository Program (SRP) shafts. The objective of the chapter is to give the designer a summary overview of the nature of these sources.

The data are contained in the Synthetic Geotechnical Design Reference Data for the Deaf Smith Site (SRP Data Base) (DOE, 1986) and the Input to Seismic Design (ISD) (DOE, 1987) which were developed for the Deaf Smith County, Texas repository site. The objective of these documents is to provide all entities involved in the design of the shafts with a common data base.

The SRP Data Base contains information and design values relating to the geology (stratigraphy), hydrogeology, and the geochemical, geomechanical, and thermal properties of the regime in which the SRP shafts will be constructed. The ISD is a companion document to the Shaft Design Guide (SDG) and contains design-related information on seismic stratigraphy and material properties which may be used to analyze the seismic response of the shaft lining. The ISD also contains results of the free-field site response required to perform seismic analysis of the shaft lining.

Other base data which will be developed, and which may be required for the design of the shafts, include:

1. Site and Regional Data.
2. Existing Infrastructure Data.
3. Construction Materials Data.
4. Chemical and Physical Properties Data.
5. Performance Data.

This information, which will be referenceable from external sources, will be incorporated with the existing SRP Data Base and the ISD to form a Design Data Base (DDB) for the proposed Deaf Smith County repository site. The reference data bases will be revised as updated or additional information becomes available. The shaft designer should use this information as the basis for the shaft designs.

3 SHAFT LININGS AND MATERIALS

The purpose of this chapter is to provide the shaft designer with descriptions of (1) the shaft lining components and their functions, (2) excavation methods, (3) ground control methods, (4) lining installation sequence, (5) current plans for decommissioning seals, and (6) material properties and limitations. The objective is to ensure that the shaft designer has sufficient understanding of the concepts to enable him to specify the appropriate elements, materials, and construction techniques to comply with the design criteria.

The shaft lining system consists of the shaft lining, seals, ground control systems, and the host rock. Four lining concepts are discussed: a lining composed of a single welded steel sheet with inside plain or reinforced concrete support; a welded double-steel lining with plain or reinforced concrete support between the steel sheets; ductile cast iron tubbing backed with concrete and grout; and a plain or reinforced concrete lining with or without a compressible material backing. The operational seal concepts discussed are chemical sealant, asphaltic sealant material (ASM), and wooden picotage. The discussion of shaft construction concepts focuses on ground control, the sequencing of lining and seal installation, the shaft equipping sequence, and the installation of performance monitoring instrumentation in the shafts. The section on decommissioning discusses the functions of the decommissioning seals in relation to the shaft design. Shaft lining materials discussed are cementitious materials, steel, ductile cast iron tubbing, compressible backfill material, rock bolt grouts, ASM, chemical seal rings, picotage wood, and lining accessories.

The designer has the option to incorporate lining elements not specified in this guide if it can be demonstrated that they are appropriate in satisfying the design criteria.

3.1 SHAFT LINING CONCEPTS

Figures 3.1 through 3.14 schematically depict the shaft lining concepts presented in this chapter. The shaft lining concepts consider that the host rock is part of the shaft system. The mechanical functions of typical shaft system components are defined in Table 3.1 and should be considered in the design. See Table 3.2 for the system component abbreviations used in the figures.

The shaft lining components generally have distinct watertight and rock control functions. The chapter describes several methods for water and rock control which can be used with different primary ground support and sealing methods.

Table 3.1 Mechanical Functions of Typical Shaft System Components

System Components	MECHANICAL FUNCTION		
	Load Bearing	Water Barrier	
		Horizontal	Vertical
Asphaltic Sealant Material	Yes[a,c]	Yes	Yes
Cementitious Grout	Yes	Yes[b]	Yes[b]
Cementitious Grout – Sanded	Yes	No	No
Concrete Primary (Plain or Reinforced) or Concrete Blocks	Yes	No	No
Concrete Final (Plain or Reinforced)	Yes	No	No
Chemical Seal Ring	Yes[c]	Yes	Yes
Grout Pipe	No	Yes	No
Grout Plug	No	Yes	No
Lead Base Plate	Yes	No	No
Liner Plate	No[d]	No	No
Picotage	Yes[c]	Yes	Yes
Rock	Yes	Yes[e]	Yes[e]
Rock Bolt	No[d]	No	No
Compressible Material	Yes[f]	No	No
Steel	Yes	Yes	No
Sanded Asphalt	Yes[a]	Yes	Yes
Steel Wedge Ring	Yes	Yes	No
Tubbing	Yes	Yes	No
Tubbing Wedge Ring	Yes	Yes	No
Wire Mesh	No[g]	No	No

(a) = Load bearing in terms of fluid column only
(b) = Horizontal and vertical water barrier only when injected into fractures, pore spaces, and component interfaces as in contact grouting
(c) = Load bearing in terms of resistance to hydraulic pressure
(d) = Load bearing only in support and control of disturbed rock
(e) = Aquicludes only
(f) = Load bearing only in the form of support pressure against creeping of rock face when supported by lining
(g) = Used for control of surface spalling during construction only

Table 3.2 Shaft Lining Systems Component Abbreviations

A_{SM}	- Asphaltic Sealant Material
C_G	- Cementitious Grout
C_{GS}	- Cementitious Grout - Sanded
C_M	- Compressible Material
C_P	- Concrete Primary (Plain or Reinforced)
C_F	- Concrete Final (Plain or Reinforced)
C_{SR}	- Chemical Seal Ring
G_P	- Grout Pipe
G_{PL}	- Grout Plug
L_{BP}	- Lead Base Plate
L_P	- Liner Plate
P_K	- Picotage
R	- Rock
R_B	- Rock Bolt
S	- Welded Steel Membrane
S_A	- Sanded Asphalt
S_{BP}	- Steel Base Plate
S_{WR}	- Steel Wedge Ring
T	- Tubbing
T_{WR}	- Tubbing Wedge Ring
W_M	- Wire Mesh

3.1.1 Single Steel Membrane with Concrete

The single steel membrane with concrete is a watertight lining system.

The basic components of this shaft lining system are a load-bearing, watertight, welded-steel membrane with load-bearing concrete installed towards the inside of the shaft. The steel plate is lowered

down the shaft in segments that are then welded together to form a continuous membrane. The steel plate segments are welded according to the American Welding Society (AWS), Structural Welding Code - Steel, D1.1-86. The membrane serves as an impermeable barrier to prevent fluid penetration through the load-bearing concrete. Any cementitious materials on the outside of the membrane are regarded as being nonwatertight. This lining system is used in shaft sections that must be fully watertight.

Although the principal function of the outer steel membrane is to serve as a water migration barrier rather than a load-bearing member, its contribution, in combination with the inner concrete shell, to the overall lining strength should be considered. The primary lining provides support to the excavation wall until the final lining is installed and may contribute to the overall strength of the total lining system.

3.1.1.1 Single Steel Membrane with Concrete and Asphaltic Sealant Material in Incompetent Rock (Figure 3.1, Detail 1)

A single welded-steel membrane and load-bearing plain or reinforced concrete with ASM, primary concrete, liner plate, and cementitious grout is applicable for the incompetent strata (i.e., lacking self-supporting characteristics) lying above the water table and requiring immediate ground control. The liner plate with cement grout backfill provides temporary support to the excavation wall. The concrete primary lining forms the rock support element of the lining. The ASM is a dense, viscous layer which mitigates the effects of radial pressure from the surrounding strata on the final lining and prevents vertical fluid migration at the interface of the primary lining and ASM. The ASM extends from above the groundwater table to below the depth of the frozen ground section to provide a hydrostatic head greater than the formation waters.

3.1.1.2 Single Steel Membrane with Concrete and Asphaltic Sealant Material in Competent Rock (Figure 3.1, Detail 2)

A single welded-steel membrane and load-bearing plain or reinforced concrete with ASM and primary concrete is applicable where soil or rock are stable enough that immediate ground control is not required. Rock bolts and wire mesh are used to provide temporary support to the excavation wall. The concrete primary lining acts as the rock support element. The effect of the ASM on ground and water control is described in 3.1.1.1, Single Steel Membrane with Concrete and Asphaltic Sealant Material in Incompetent Rock.

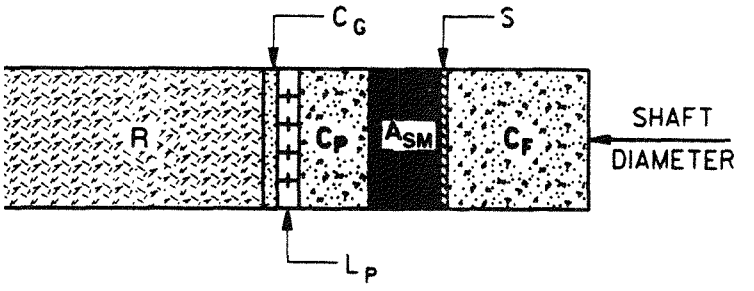

DETAIL 1

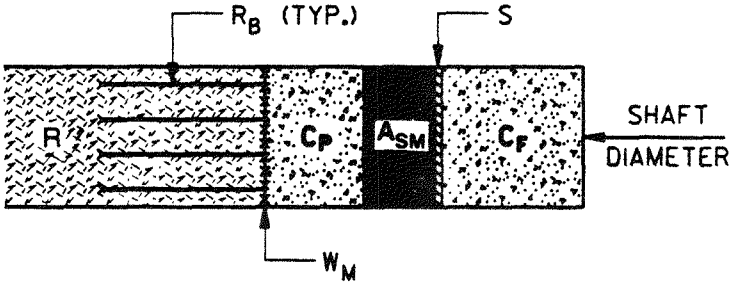

DETAIL 2

SHAFT LINING SYSTEMS
SINGLE STEEL WITH CONCRETE
DETAILS 1 and 2

FIGURE 3.1

3.1.1.3 Single Steel Membrane with Concrete and Cementitious Grout (Figure 3.2, Detail 3)

A single welded-steel membrane and load-bearing plain or reinforced concrete with cementitious grout and primary concrete is applicable in any shaft section where ASM is not used. The primary concrete has the same function as described in Section 3.1.1.2, Single Steel Membrane with Concrete and Asphaltic Sealant Material in Competent Rock. The thickness of the cementitious grout backfill behind the steel membrane is dictated by working room requirements for the assembly and welding of the steel membrane. However, the cementitious grout does not prevent water migration and operational seals are required to confine and/or prevent vertical fluid migration along the material interfaces with the grout. Typical examples of such seals are depicted by Figures 3.7 and 3.8, and described in Section 3.2.1, Chemical Seal with Single Steel Lining.

3.1.1.4 Single Steel Membrane with Concrete, Cementitious Grout, and Compressible Backfill Material (Figure 3.2, Detail 4)

A single load-bearing, impermeable, welded-steel membrane and load-bearing plain or reinforced concrete with cementitious grout, primary concrete, and compressible backfill material is applicable where the rock pressure from creeping strata, specifically salt, cannot bear on the lining. To prevent rock pressure bearing on the shaft lining the creeping rock is over-excavated to a radial dimension equal to the calculated radial creep convergence plus the required thickness of the compressible material when compressed. The compressible material is placed into the over-excavated space, and will provide increasing support pressure against the rock and retard creep as it is compressed.

The functions and limitations of the other lining components are identical to those described in Section 3.1.1.3, Single Steel Membrane with Concrete and Cementitious Grout.

3.1.2 Double Steel Membrane with Concrete

Double steel membrane with concrete is a watertight lining system. The basic components of this lining system are two load-bearing steel shells with load-bearing concrete installed between them. The outer steel shell is a watertight membrane. Confining the concrete between the two steel shells increases its compressive strength providing an added safety factor. The double steel membrane and primary concrete configuration is applicable in shaft sections where the large shaft diameter and great depth make single steel with concrete impractical. Both the outside and inside steel shells are lowered down the shaft in segments which are then

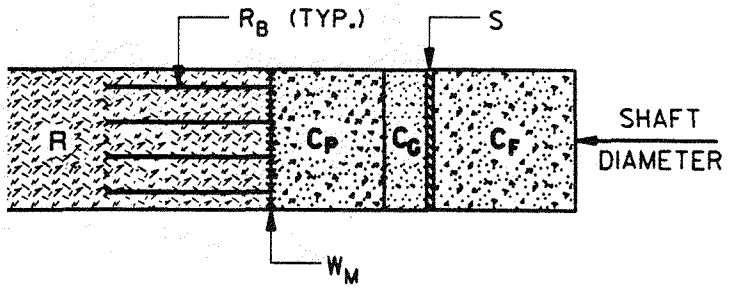

DETAIL 3

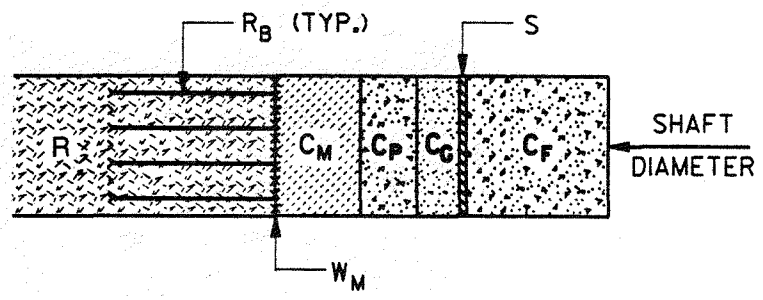

DETAIL 4

SHAFT LINING SYSTEMS
SINGLE STEEL WITH CONCRETE
DETAILS 3 and 4

FIGURE 3.2

welded together to form continuous membranes. The inside shell provides additional insurance of watertightness and therefore must be anchored to the final concrete. Alternatively, cast iron tubbing, instead of a steel membrane, can be used as the inside lining. Section 3.1.4, Tubbing, describes the tubbing system of lining.

3.1.2.1 Double Steel Membrane with Concrete and Asphaltic Sealant Material (Figure 3.3, Detail 1)

The functions of the double steel membrane with concrete are the same as those described in Section 3.1.1, Single Steel Membrane with Concrete, with the addition of an inner steel shell described in Section 3.1.2, Double Steel Membrane with Concrete. The functions of the ASM are the same as those described in Section 3.1.1.1, Single Steel Membrance with Concrete and Asphaltic Sealant Material in Incompetent Rock.

3.1.2.2 Double Steel Membrane with Concrete and Cementitious Grout (Figure 3.3, Detail 2)

Double welded-steel lining with cementitious grout and a concrete primary lining is similar to the single steel lining described in Section 3.1.1.3, Single Steel Membrane with Concrete and Cementitious Grout. The functions and limitations for the lining elements are also similar to those described in Section 3.1.1.3.

3.1.2.3 Double Steel Membrane with Concrete, Cementitious Grout, and Compressible Backfill Material (Figure 3.4, Detail 3)

Double welded-steel lining with a concrete primary lining, cementitious grout, and compressible backfill material is similar to the single steel lining described in Section 3.1.1.4, Single Steel Membrane with Concrete, Cementitious Grout, and Compressible Backfill Material. This concept is applicable for shaft sections where rock creep will occur. The functions and limitations of this system are the same as those of the single steel system described in Section 3.1.1.4.

3.1.3 Concrete

This lining consists of a plain or reinforced concrete shell that supports the shaft walls. Concrete lining should not be considered watertight. It can be installed in segments or monolithically in one continuous pour without cold joints. The concrete may be plain or reinforced depending on load-bearing and seismic requirements.

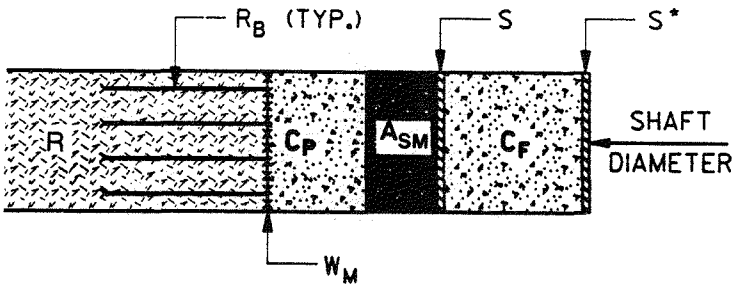

DETAIL 1

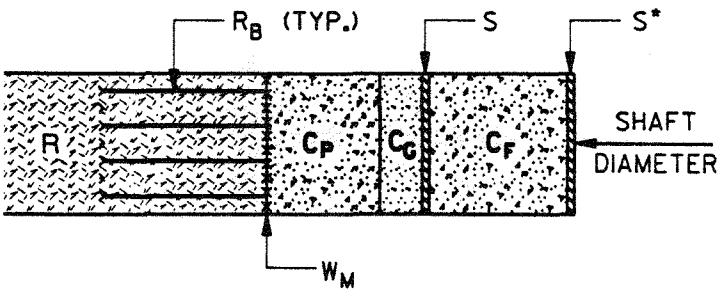

DETAIL 2

*** INNER SHELL MAY BE TUBBING INSTEAD OF WELDED STEEL**

SHAFT LINING SYSTEMS
DOUBLE STEEL WITH CONCRETE
DETAILS 1 and 2

FIGURE 3.3

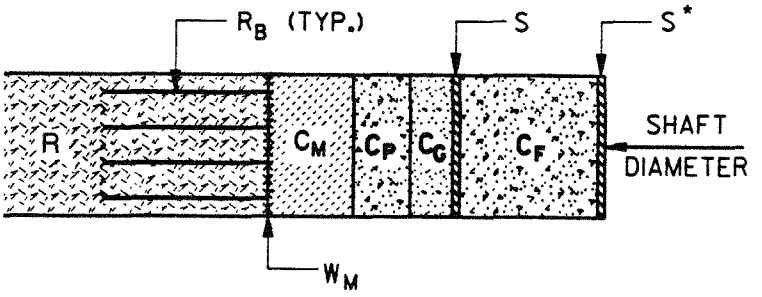

DETAIL 3

*** INNER SHELL MAY BE TUBBING INSTEAD OF WELDED STEEL**

SHAFT LINING SYSTEMS
DOUBLE STEEL WITH CONCRETE
DETAIL 3

FIGURE 3.4

3.1.3.1 Basic Concrete (Figure 3.5, Detail 1)

A basic plain or reinforced concrete shell with rock bolts and wire mesh is applicable in shaft sections with stable rock and dry conditions. The rock bolts temporarily support the rock, and the wire mesh controls rock spalling until the concrete shell is installed.

3.1.3.2 Concrete with Compressible Material (Figure 3.5, Detail 2)

Plain or reinforced concrete shell with compressible material is used in shaft sections where rock creep occurs, particularly in salt strata (see Section 4.5, Salt Creep). This lining concept requires over excavation of the rock to make room for the calculated radial creep convergence, plus the thickness of the compressible material when compressed. This retards the full lithostatic pressure due to creep acting on the concrete shell. The functions and limitations of the lining elements are the same as those for the corresponding elements described in Section 3.1.1.4, Single Steel Membrane with Concrete, Cementitious Grout, and Compressible Backfill Material.

3.1.4 Tubbing

The basic element of this shaft structure system is a column constructed of ductile cast iron tubbing segments. The tubbing acts as a watertight barrier and as a load-bearing structure. Individual segments of tubbing are bolted into a circular column. The horizontal and vertical joints are sealed with lead gaskets. The gap between the tubbing column and the rock or primary concrete lining is filled with cementitious grout. The grout is not considered to be a load-bearing member of the shaft lining system. The tubbing column may also be integrated with load-bearing concrete on the outside to form a load-bearing compound lining. Watertightness of the segmented tubbing column requires periodic caulking of the joints between the tubbing segments, especially in intake ventilation shafts. Pressure grouting behind the tubbing through grout holes may also be necessary to control leakage.

3.1.4.1 Tubbing with Cementitious Grout (Figure 3.6, Detail 1)

Tubbing with cementitious grout is applicable where a watertight lining and immediate support of weak strata is required. The tubbing column acts as the load-bearing component, and the cementitious grout integrates the tubbing column with the strata.

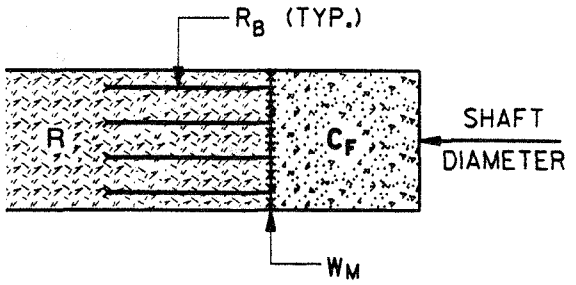

DETAIL 1

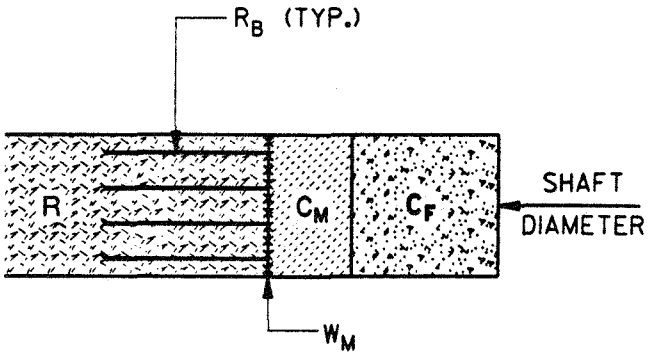

DETAIL 2

SHAFT LINING SYSTEMS
CONCRETE
DETAILS 1 and 2

FIGURE 3.5

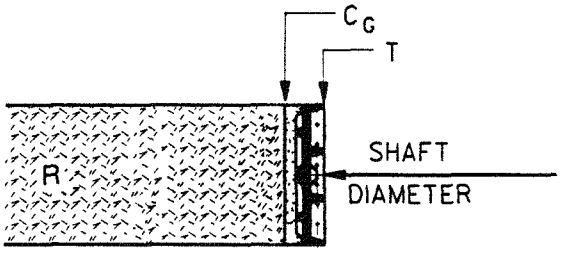

DETAIL 1

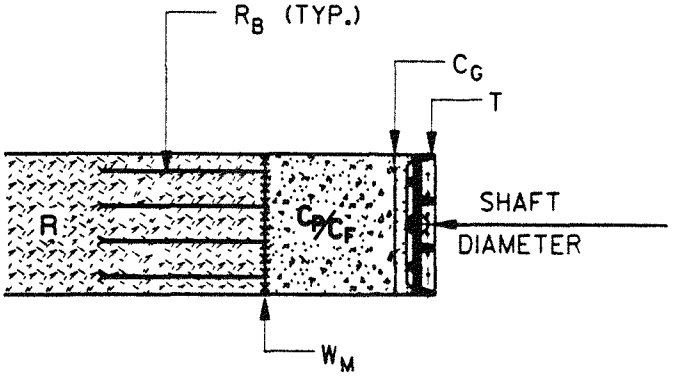

DETAIL 2 *

*** LOCAL CONDITIONS AND INSTALLATION SEQUENCE WILL DETERMINE USE OF CEMENT GROUT OR CONCRETE POURED AGAINST TUBBING.**

SHAFT LINING SYSTEMS
TUBBING
DETAILS 1 and 2

FIGURE 3.6

3.1.4.2 Tubbing with Concrete (Figure 3.6, Detail 2)

Tubbing may be combined with the primary concrete lining. This concept can be used where it is necessary to control the extent of the relaxed rock zone. The primary concrete lining in conjunction with the tubbing column acts as a load-bearing member.

The strength characteristics of the strata will determine the method and sequence of installing the tubbing and primary concrete lining. The primary concrete and cementitious grout may be replaced totally with load-bearing concrete. The cementitious grout, as shown, is backfilled in the space behind the tubbing. The functions and limitations for the rock bolts and wire mesh if used with this method, are the same as those described in Section 3.1.1.2, Single Steel Membrane with Concrete and Asphaltic Sealant Material in Competent Rock.

3.2 SHAFT SEAL CONCEPTS

Shaft seals are installed at terminations of watertight lining sections to prevent vertical fluid migration behind the watertight lining. The seals should be installed in strong impermeable and undamaged strata. Formation damage in the seal zones can be limited by employing controlled or smooth-wall blasting techniques inside the final excavation line, followed by chipping and hand-spading to the final excavation limits. Seal materials include picotage wood, ASM, chemical sealant, and cementitious grouts. Viscous and plastic sealants will penetrate into rock cracks and openings, enhancing the effectiveness of the seal. The selection of the type and number of seals depends on the lining type, the strata, and hydrogeological conditions. The nominal 100-year life of any of the selected seal materials is achieved through monitoring, maintenance, and repairs.

3.2.1 Chemical Seal with Single Steel Lining (Figures 3.7 and 3.8)

Chemical seal ring material is placed behind a watertight steel membrane. The chemical seal ring provides a fluid-tight seal between the shaft lining and the shaft excavation wall. The chemical sealant, which expands when in contact with water, is confined above and below by cementitious grout. Confinement is enhanced by pressure grouting the seal area through grout pipes provided in the lining. Penetration of the steel membrane, through the grout pipes, is achieved by drilling through the steel shell when required. The configuration shown in Figure 3.7 is applied to the bottom of a watertight lining section, and that in Figure 3.8 applies to the top of the section. Grout pipes not required for continued seal maintenance will be plugged to maintain watertightness of the lining.

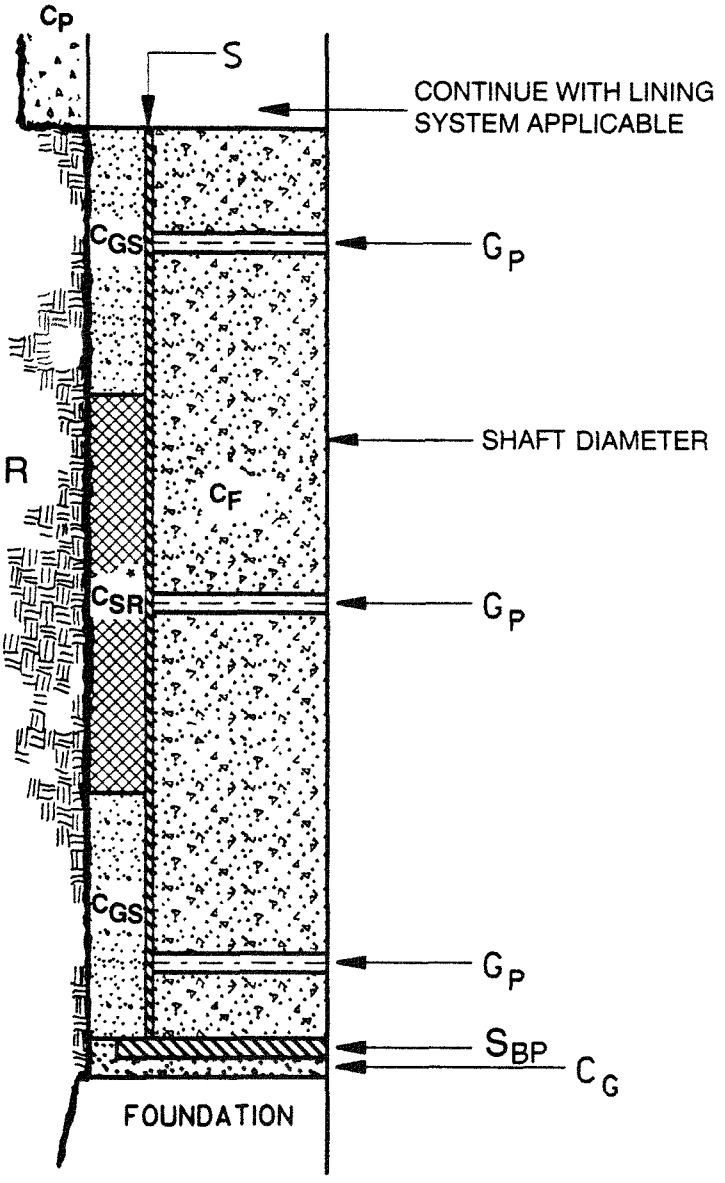

* SPACE PERMITTING, AN ADDITIONAL C_{SR} INTERVAL MAY BE PLACED ABOVE FOR SEAL REDUNDANCY

NOTE:
THIS SEAL APPLICABLE TO LINING SYSTEMS SHOWN ON FIGURES:
3.2–DETAILS 3 and 4, 3.3–DETAIL 2, 3.4–DETAIL 3.

SHAFT LINING SYSTEMS CHEMICAL SEAL RING (ALTERNATIVE 1)
FIGURE 3.7

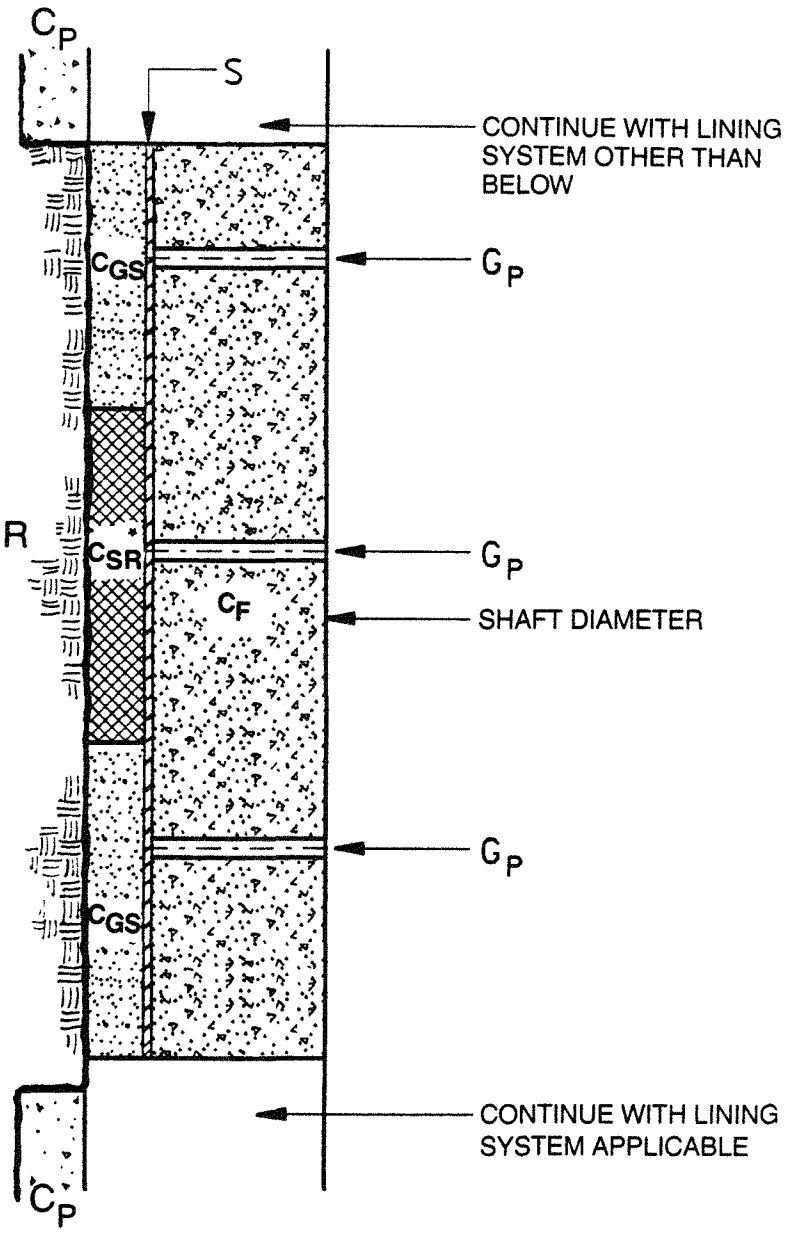

* **SPACE PERMITTING, AN ADDITIONAL C_{SR} INTERVAL MAY BE PLACED BELOW FOR SEAL REDUNDANCY**

NOTE:
THIS SEAL APPLICABLE TO LINING SYSTEMS SHOWN ON FIGURES: 3.2–DETAILS 3 and 4, 3.3–DETAIL 2, 3.4–DETAIL 3.

SHAFT LINING SYSTEMS CHEMICAL SEAL RING (ALTERNATIVE 2)

FIGURE 3.8

3.2.2 Asphaltic Sealant Material with Single Steel Lining (Figures 3.9 and 3.10)

Asphaltic sealant material is placed behind the watertight steel membrane. The basic sealing element is the ASM which is in contact with the surrounding rock. The height of the ASM column, which extends from the seal area to surface, and its high density and viscosity prevents migration of less dense formation fluids. The ASM also reduces fluid migration in the seal area strata immediately surrounding the shaft by invading fluid-filled or empty pore spaces and fractures in the rock. The use of the higher viscosity asphalt and sanded asphalt at the bottom of the ASM column prevents the less viscous ASM from leaking around the bearing key (foundation). A picotage may be placed at the base of the steel lining for seal redundancy as shown in Figure 3.10. The cementitious grout material below the sanded asphalt provides additional containment. A steel base plate and a lead base plate installed at the bottom of the lining section immediately above the foundation, as shown in Figure 3.9, accommodates any irregularities in the contact surfaces. A lead base plate may be placed above the steel wedge ring, as shown in Figure 3.10, for the same reason.

3.2.3 Seal for Tubbing (Figures 3.11 and 3.12)

Chemical sealant and a picotage may also be used in combination. The chemical seal ring in this system has the same functions and limitations as described in Section 3.2.1, Chemical Seal with Single Steel Lining. The picotage is a redundant (back up) seal for the chemical seal ring. The picotage is placed between strong and impermeable strata and a tubbing wedge ring, and it is compressed to a density that prevents fluid migration. Figure 3.11 illustrates the bottom of a tubbing section, and Figure 3.12, the top of a tubbing section. Supplemental pressure grouting is carried out through grout holes in the tubbing segments, which are drilled through when needed. Plugs are used to close the grout access openings after grouting has been completed.

3.2.4 Seal for Double or Single Steel Lining (Figures 3.13 and 3.14)

A chemical seal may also be combined with a picotage in a steel lining seal system. The concept is the same as that for tubbing described in Section 3.2.3, Seal for Tubbing. It applies to single steel and double steel lining systems with equal effectiveness. Seal redundancy may also be achieved by replacing the picotage with an additional chemical seal.

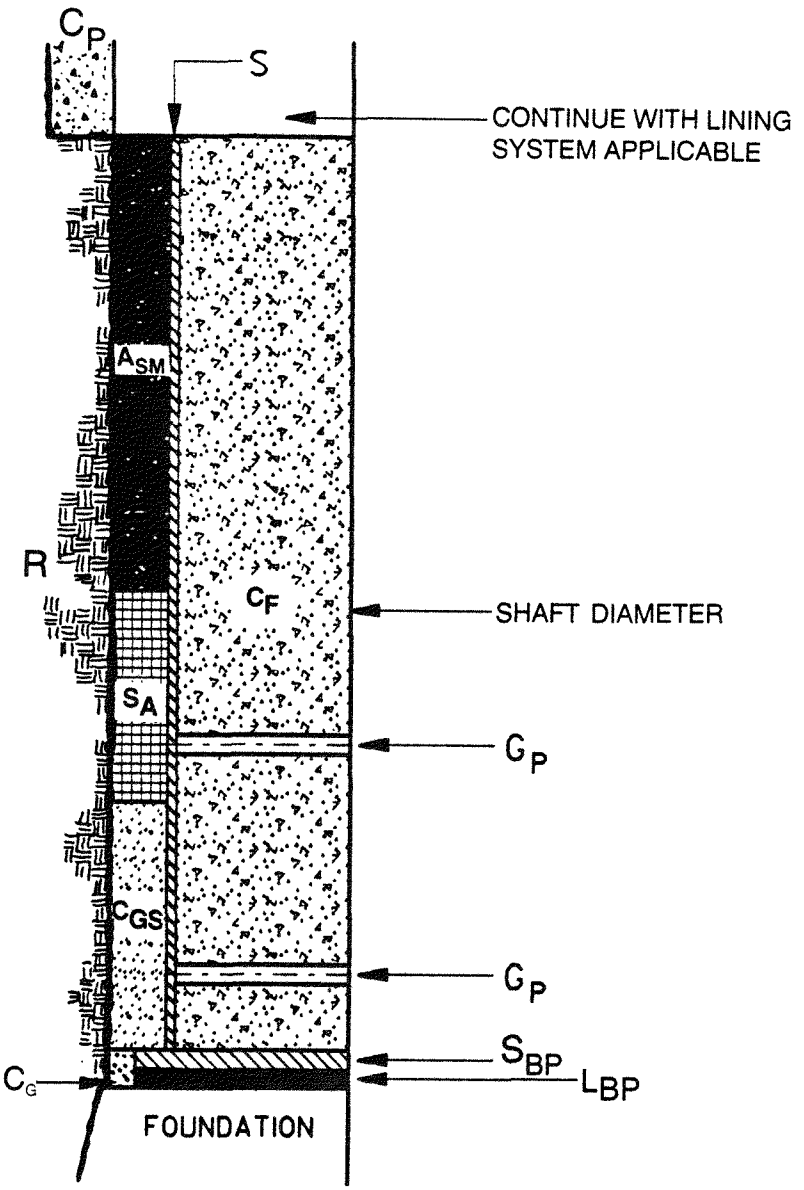

NOTE:
THIS SEAL APPLICABLE TO LINING SYSTEMS SHOWN ON FIGURES:
3.1–DETAILS 1 and 2, 3.3–DETAIL 1

SHAFT LINING SYSTEMS
ASPHALTIC SEALANT MATERIAL
AND SANDED ASPHALT SEAL

FIGURE 3.9

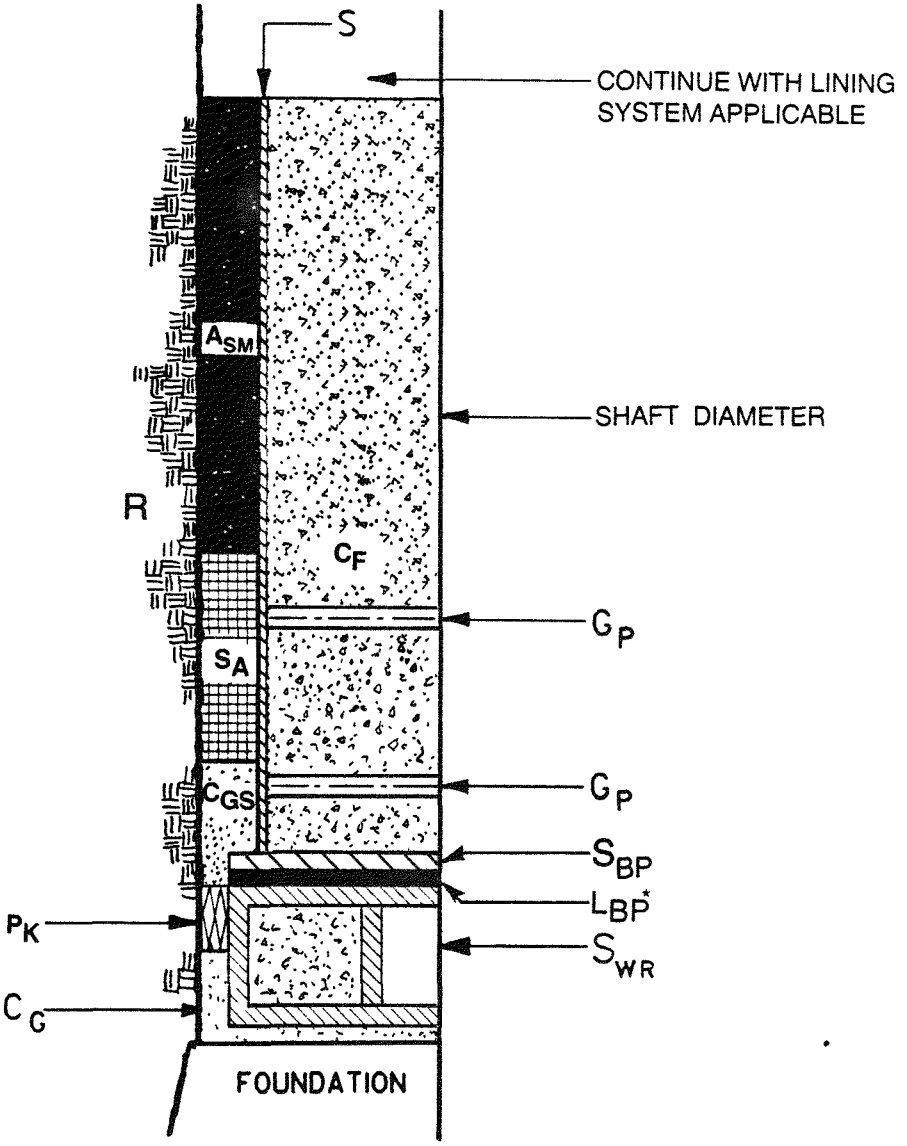

NOTE:
THIS SEAL APPLICABLE TO LINING SYSTEMS SHOWN ON FIGURES:
3.1–DETAILS 1 and 2, 3.3–DETAIL 1

*** MAY BE USED.**

SHAFT LINING SYSTEMS
ASPHALTIC SEALANT MATERIAL,
SANDED ASPHALT SEAL AND PICOTAGE

FIGURE 3.10

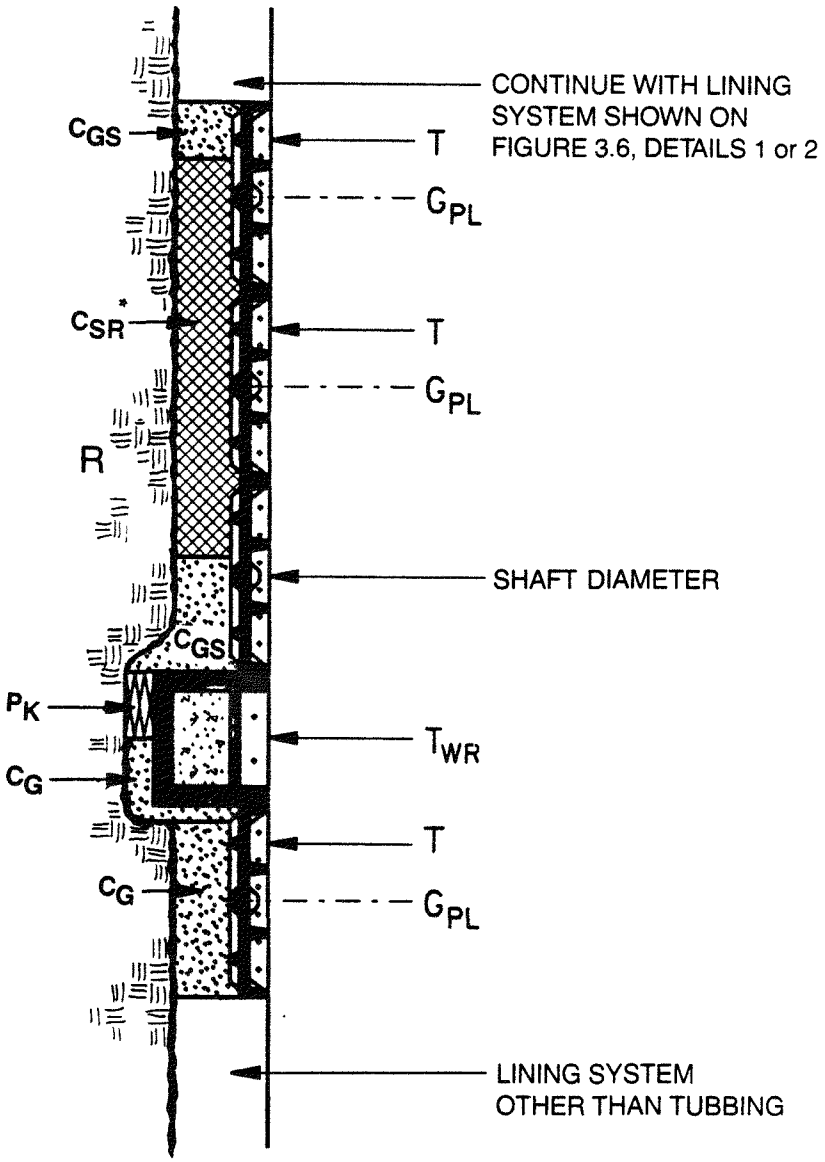

* SPACE PERMITTING AN ADDITIONAL C_{SR} INTERVAL MAY BE PLACED ABOVE FOR SEAL REDUNDANCY

SHAFT LINING SYSTEMS CHEMICAL SEAL RING AND PICOTAGE (ALTERNATIVE 1)

FIGURE 3.11

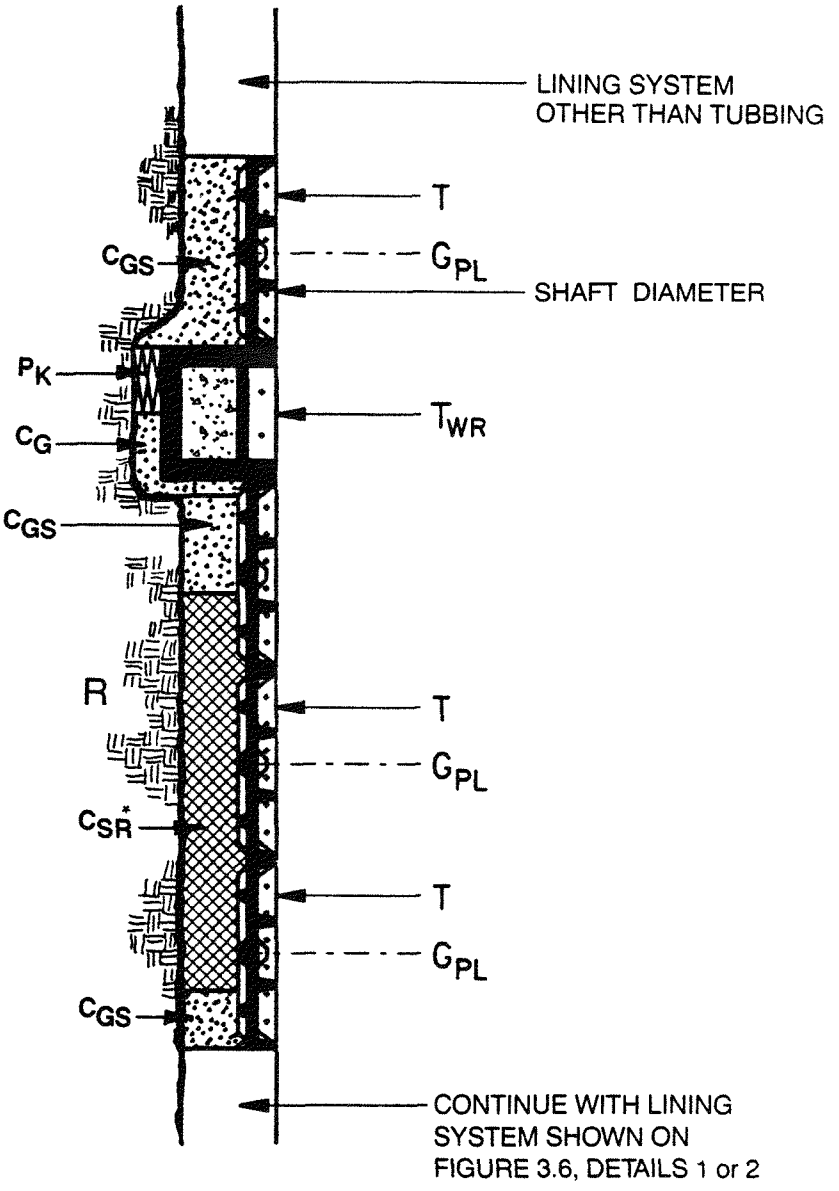

*** SPACE PERMITTING, AN ADDITIONAL C_{SR} INTERVAL MAY BE PLACED BELOW FOR SEAL REDUNDANCY**

SHAFT LINING SYSTEMS CHEMICAL SEAL RING AND PICOTAGE (ALTERNATIVE 2)
FIGURE 3.12

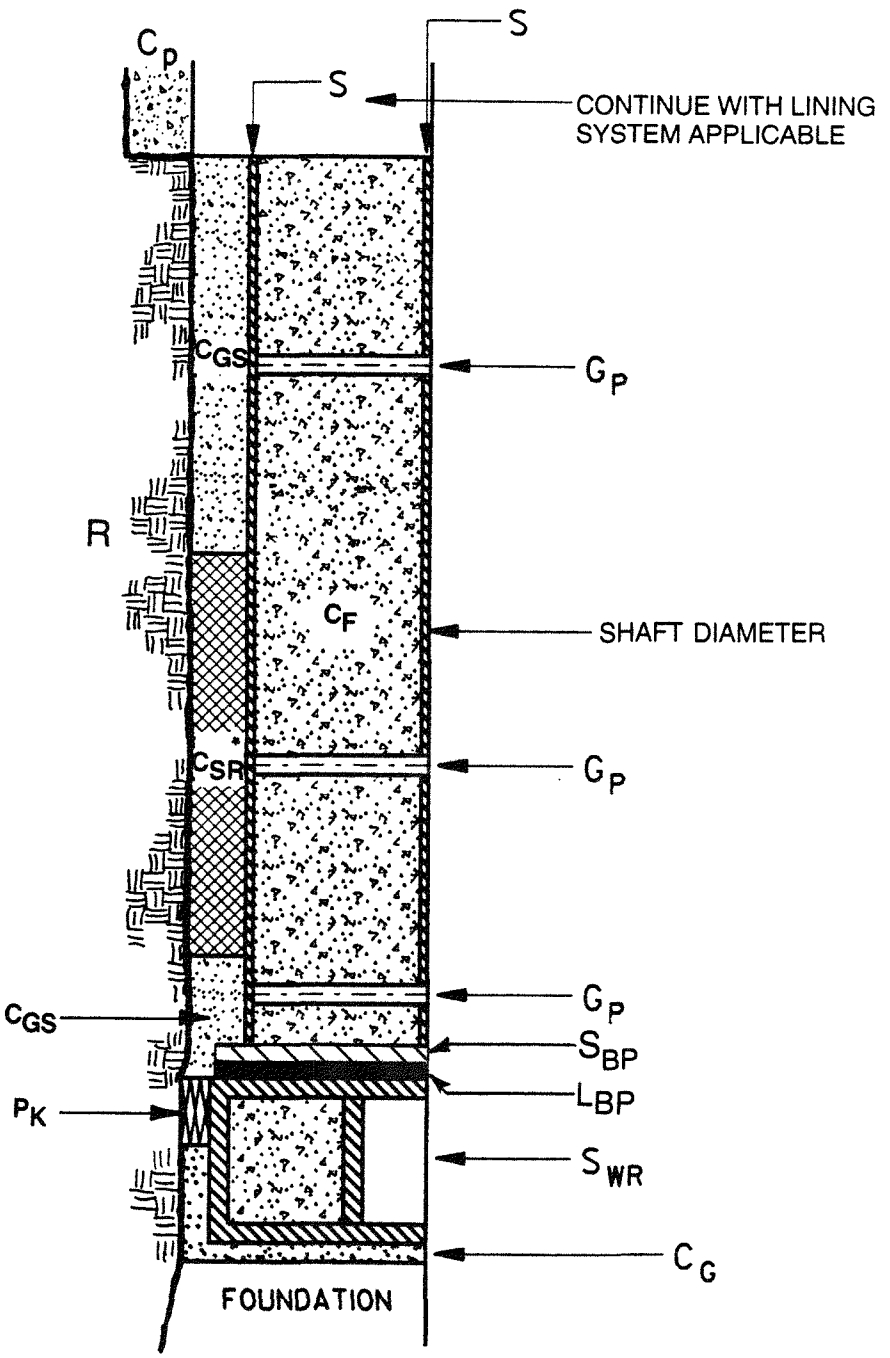

*** SPACE PERMITTING, AN ADDITIONAL C_{SR} INTERVAL MAY BE PLACED ABOVE FOR SEAL REDUNDANCY**

NOTE:
THIS SEAL APPLICABLE TO LINING SYSTEMS SHOWN ON FIGURES:
3.2–DETAIL 3 and 4
3.3–DETAIL 2, 3.4–DETAIL 3

SHAFT LINING SYSTEMS CHEMICAL SEAL RING AND PICOTAGE (ALTERNATIVE 3)

FIGURE 3.13

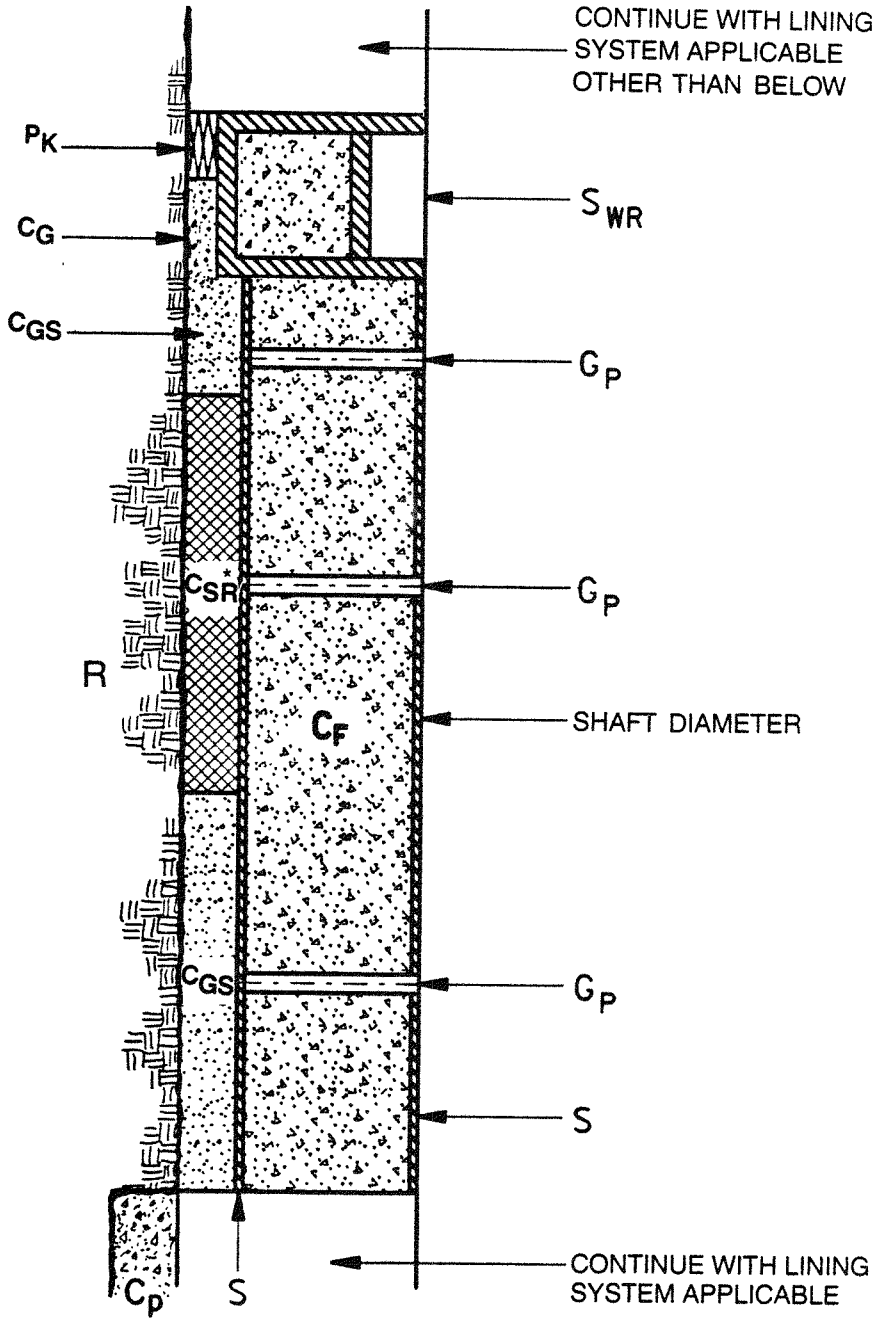

* SPACE PERMITTING, AN ADDITIONAL C_{SR} INTERVAL MAY BE PLACED BELOW FOR SEAL REDUNDANCY

NOTE:
THIS SEAL APPLICABLE TO LINING SYSTEMS SHOWN ON FIGURES:
3.2–DETAILS 3 and 4
3.3–DETAIL 2, 3.4–DETAIL 3

SHAFT LINING SYSTEMS CHEMICAL SEAL RING AND PICOTAGE (ALTERNATIVE 4)

FIGURE 3.14

3.3 SHAFT CONSTRUCTION CONCEPTS

The shaft will be constructed using conventional methods. Construction encompasses excavation methods, ground control methods, and lining installation and sequencing methods. Construction methods selected must have minimal effect on the surrounding strata and provide for safe working conditions.

3.3.1 Ground Control

Ground control is an integral part of the shaft design and must provide safe working conditions in the shaft and, at the same time, control the surrounding strata.

3.3.1.1 Ground Control for Working Conditions

To achieve safe working conditions in the shaft and to stabilize the rock strata, ground control methods must be designed according to the characteristics of the surrounding strata. Incompetent water-bearing strata can be stabilized by dewatering, grout injection, freezing, or other appropriate methods. Competent strata, as a rule, are self-supporting and do not require extensive artificial support. Other weak strata will be supported as necessary.

3.3.1.2 Control of Surrounding Strata

Minimum disturbance of the surrounding strata will be achieved by applying appropriate excavation methods in conjunction with timely installation of suitable ground support systems.

3.3.1.2.1 Excavation Methods. The design will specify an excavation method or combination of methods chosen in response to the characteristics of the strata. Excavation methods analyzed will include the following:

1. Controlled blasting at the shaft perimeter.
2. Controlled blasting by limiting the amount of explosives per firing sequence.
3. Controlled blasting by considering hole size, burden, spacing, depth, and orientation.
4. Spading and or chipping with pneumatic hammers.
5. Mechanical cutting of perimeter slots.
6. Mechanical face cutting with roadheader-type cutting heads.

3.3.1.2.2 Rock Reinforcement. Rock reinforcement is a ground support technique which can be either temporary or permanent and which serves to enhance the structural properties of relaxed or jointed rock. Rock reinforcement systems are designed for specified conditions and rock loads. Metal components can be protected against corrosion from groundwaters with protective coatings. The basic parts of a rock reinforcement system are:

1. Rock bolt assemblies.
2. Wire mesh.
3. Grout (resin or cement).
4. Shotcrete.

The lengths and sizes of rock bolts are determined by estimating the radii of the elastic rock zones surrounding the shaft (see Section 4.1.1.2, Rock Pressures). Rock bolt patterns will be determined by using conventional practices. The designer is referred to Hoek and Brown (1982) and U.S. Corps of Engineers (1980). Timing in placing rock support depends on the deformational characteristics of the strata and the support pressure available from the support system. Rock bolts are placed as early as practicable. Where welded wire mesh is installed at the excavation wall in the freeze zone, it is pinned to the wall with short bolts to avoid damage to the freeze pipes and the freeze wall.

3.3.2 Lining Installation and Sequencing

Lining installation methods and the sequence of shaft construction are governed by the type of shaft structure and ground and water conditions. Appropriate excavation and ground support methods must be considered. The sequence of construction for the shaft lining concepts shown in Figures 3.1 through 3.6 are described in the following paragraphs.

3.3.2.1 Single Steel with Concrete (Figure 3.1, Detail 1)

Steel liner plates are usually placed at, or near, the shaft bottom to ensure immediate ground control as the shaft is deepened. Primary concrete is placed as soon as practical after installation of the steel liner plate. The steel membrane is installed from the bottom upwards by assembling and welding the steel plate segments. The final concrete lining is poured as installation of the steel sections is completed. The ASM is placed behind sections of completed steel and concrete lining at specified intervals.

3.3.2.2 Single Steel with Concrete (Figure 3.1, Detail 2 and Figure 3.2, Detail 3)

Rock bolts and wire mesh are installed near the advancing shaft bottom. The primary concrete is placed as shaft sinking progresses with sufficient clearance being left for the shaft bottom equipment. It is placed within a time frame dictated by the support requirements of the shaft wall. The steel lining and concrete are installed from the bottom up and the cementitious grout or ASM are placed at predetermined intervals.

3.3.2.3 Single Steel with Concrete (Figure 3.2, Detail 4)

The compressible material forms a part of the primary support. When compressible material is used, it may be necesssary to excavate the shaft using rock bolts and wire mesh as temporary support, and then install the compressible material (e.g., resin foam, vermiculite) and primary concrete upwards. In this approach, the steel membrane, final concrete, and cementitious grout are also placed from the bottom upwards.

3.3.2.4 Double Steel with Concrete (Figure 3.3, Details 1 and 2)

Rock bolts and wire mesh are placed from the top of the shaft excavation downwards. The primary concrete lining is placed as shaft sinking progresses with sufficient clearance being left for the shaft bottom equipment. The steel, concrete, and ASM or cementitious grout are installed from the bottom upwards. The lining installation sequence is the same as that described for the single steel lining in Section 3.3.2.2, Single Steel with Concrete.

3.3.2.5 Double Steel with Concrete (Figure 3.4, Detail 3)

The concept illustrated in Figure 3.4, Detail 3 requires that rock bolts and wire mesh be installed as the shaft is deepened. The compressible material, steel, and concrete elements are constructed from the bottom upwards. Placement of cementitious grout follows the installation of steel and concrete at specific intervals.

3.3.2.6 Concrete (Figure 3.5, Details 1 and 2)

With concrete as the main lining element, the rock bolts and wire mesh are installed as the shaft is deepened near the shaft bottom. The concrete is placed near the shaft bottom in much the same manner as the primary concrete in other systems.

The installation illustrated in Figure 3.5, Detail 2 requires the same design decisions as described in Section 3.3.2.3, Single Steel with Concrete.

3.3.2.7 Tubbing (Figure 3.6, Details 1 and 2)

Cast iron tubbing rings may be installed by suspending segments from the rings above and keeping them close to the shaft bottom to provide ground control in weak rock as illustrated in Figure 3.6, Detail 1. The tubbing is bonded to the surrounding strata by backfilling with cementitious grout. Alternately, the tubbing rings may be installed from the bottom upwards as illustrated in Figure 3.6, Detail 2, in intervals determined by ground conditions and the overall lining design. Rock bolts, wire mesh, and primary concrete are installed as the shaft is deepened. Backfilling with cementitious grout bonds the tubbing to the concrete. In strong rock, shaft sinking may proceed using rock bolts and wire mesh for primary support. The tubbing column can then be installed from the bottom upwards and backfilled with concrete as each ring is installed.

3.3.3 Seal Installation

The installation of the seal systems illustrated in Figures 3.7 through 3.14 logically follows the lining installation sequence described in the preceding paragraphs. The designer must select methods which will preserve the integrity of the strata at each seal location. This may be accomplished by temporary support, such as shotcreting, which is removed prior to seal placement, or by sequencing rock removal so that the shaft opening is excavated to the design dimension until just prior to seal placement. All operational seal systems should be installed from the bottom up.

3.3.4 Shaft Equipping

Shaft equipping consists of two steps. The first step covers installation of utilities and services required for shaft construction. These are installed as the shaft is deepened, but are removed as the final linings are installed from the bottom up.

The second step covers installation of utilities and services required for normal operations. These are installed upon completion of shaft sinking or at specific intervals.

All items required for shaft equipping are either attached to the concrete lining with concrete anchors, welded to the steel lining, or bolted to the tubbing.

3.3.5 Shaft Instrumentation Installation

Site characterization, monitoring of shaft performance, and design verification will require installation of instruments in the shaft. The designer must be satisfied that these instruments can be integrated with the shaft structure without violating the integrity of the lining structures or the requirements of the shaft design criteria.

3.4 SHAFT LINING MATERIALS

3.4.1 Cementitious Materials

Much research on cementitious material has been conducted for the SRP, and many reports are available, especially concerning the longevity of cements, grouts, and concretes. The designer is referred to BMI/ONWI-536 (Roy, et. al., 1985) and BMI/ONWI-568 (Grutzeck and Roy, 1985) when specifying cement, concrete, or grout.

Cementitious materials selected for shaft lining components must be compatible with the geochemistry of the rock zones in which they are to be placed. For example, brine-based concretes and grouts can be used in salt zones, and sulfate-resistant concretes where hydrogen sulfide is present in the groundwater. Site-specific geochemical data must be thoroughly examined to ensure chemical compatibility.

3.4.1.1 Cast-In-Place Concrete

Concrete is used in shaft construction principally for ground control and as a load-bearing material. The designer should therefore define its function and the required strength and properties. In general, all concrete structures should be designed and constructed according to the requirements of the American Concrete Institute, ACI 318-83, Building Code Requirements for Reinforced Concrete, and ACI 318.1-83/318.1R-83, Building Code Requirements for Structural Plain Concrete and Commentary.

3.4.1.2 Concrete Block Masonry

Concrete block masonry has limited usefulness as a primary shaft lining. However, concrete blocks can be used to construct the primary lining in frozen shaft sections where excessive creep may occur. Concrete blocks also provide a more flexible lining in the event of ground movement that may be caused by freezing and thawing. The concrete blocks are separated by wooden spacers.

3.4.1.3 Cementitious Grouts

Cementitious grouts have many applications in shaft construction. Examples include:

1. In-place modification of soils and rocks to increase their strength and integrity.
2. Sealing of cracks and fissures in rocks, and voids in granular materials, to reduce permeability.
3. Backfilling between the shaft lining and rock wall.
4. Backfilling the annulus between the primary and final linings.
5. Fixing rock bolts in place.

The properties and components of grout mixtures may be varied for different applications. Injection grouts used for sealing groundwater flow in rock formations may include microfine cements to enhance penetrability. For backfilling applications, fillers such as sand, fly ash, or bentonite may be added to the mixture to provide bulk. Like concrete, grout materials must be compatible with the rock formations and the fluids with which they will come into contact.

3.4.1.4 Concrete Admixtures

Admixtures may be added to concrete to improve or change its properties during curing. Admixtures should only be used as needed. The designer should obtain specifications and instructions from potential suppliers before specifying the use of any admixture.

3.4.1.4.1 Superplasticizers. Superplasticizers enhance the workability of high-strength concrete mixes where lower than normal water-to-cement ratios are required. Superplasticizers must meet or exceed the requirements of ASTM C494-86, Specification for Chemical Admixtures for Concrete, Type F Admixtures.

3.4.1.4.2 **Accelerators.** Accelerators develop a higher strength concrete at an early stage. An accelerator may be added to ensure stability or for other reasons.

If calcium chloride is used as an accelerator, it must conform with the requirements of ASTM D98-80, Specification for Calcium Chloride, and it must be tested in accordance with ASTM D345-80, Methods of Sampling and Testing Calcium Chloride for Roads and Structural Applications. Because of the potential corrosion effects of calcium chloride on steel reinforcement and embedded anchors, its use should be carefully evaluated.

3.4.2 Steel

3.4.2.1 Structural Steel

Welded structural steel plates are used for fabrication of the watertight steel lining membrane. High-strength, low-alloy, fine grained steels are conventionally used for this application. The steel lining should be designed to act in combination with concrete as one element of a composite load-bearing structure. Methods to mitigate corrosion must be provided where necessary to meet the design life of the lining component.

3.4.2.2 Rock Bolts

Rock bolts with a wide range of lengths, diameters, steel grades, and anchoring systems are available from different manufacturers. Anti-corrosion treatment can be requested, and stainless steel bolts can be used in special applications.

3.4.2.3 Reinforcing Steel

Embedment type reinforcing steel in the shaft lining must conform to ASTM A615-85, Specification for Deformed and Plain Billet-Steel Bars for Concrete Reinforcement, including Supplementary Requirement S1. Alternatively, the reinforcing may be coated for corrosion protection.

Designers should exercise caution in specifying reinforcement for lining sections where the concrete is in direct contact with a rock formation and subject to attack by saline or other potentially corrosive groundwater. Contact with groundwater can cause corrosion of the reinforcing steel, leading to spalling of the concrete.

3.4.3 Ductile Cast Iron Tubbing

Ductile cast iron is generally used today for shaft tubbing. In the absence of U.S. standards, German Industry Standards (DIN standards) must be used as a basis for design. The manufacture of cast iron tubbing and accessories is specified by DIN 21501, Shaft Linings of Cast Iron Tubbing (1963). DIN 1693, Cast Iron with Nodular Graphite (Part 1, 1983 and Part 2, 1977) and ASTM A536-84, Standard Specification for Ductile Iron Castings, specify the standards for ductile cast iron. Gaskets and washers are conventionally made of 99.9% virgin lead. However, antimonial lead is sometimes required for deep shafts where higher pressures are encountered. The antimonial lead has a higher yield point which prevents the gasket from being squeezed out between the tubbing flanges. The parts of the cast iron tubbing lining that are most vulnerable to corrosion are the connecting bolts.

3.4.4 Chemical Seal Ring

Chemical seal ring material is an elastic polymeric substance which swells as it absorbs water. It is mixed and placed as a slurry and, after setting, it remains flexible. It will not be damaged by predicted movements of the shaft lining or the rock and salt formations. Chemical seal rings resist biodegradation and are at least as permanent as cement grout (Dowell, Technical Report, Undated).

3.4.5 Compressible Backfill Material

Compressible backfill material includes resin foam, expanded polystyrene blocks, polystyrene prills in concrete, and vermiculite blocks. Bentonite clays and viscous fluids such as ASM, which are contained behind the primary concrete lining and allowed to escape through pressure relief holes, have also been suggested as a means of creating positive pressure against the salt. This would retard creep.

3.4.6 Rock Bolt Grouts

All rock bolts, except those in the freeze wall, should be fully grouted to retard water movement toward the shaft lining. Rock bolt grouts such as cementitious grouts or epoxy resins must be carefully selected to satisfy the design requirements.

3.4.7 Asphaltic Sealant Material

Asphalt is a solid or semi-solid hydrocarbon which may occur naturally or as a by-product of oil refining processes. Because the specific gravity of asphalt is less than 1.0, it must be weighted to increase its density so as not to be displaced by formation fluids. Pulverized limestone may be used for this purpose. The viscosity of the mix must ensure certain penetration into fractures and pores which may become pathways for groundwater migration. The mixing of asphalt and the pulverized limestone is referred to as asphaltic sealant material.

3.4.8 Picotage Wood

Picotage seals are made from Honduran Pitch Pine, Longleaf Southern Pine, or other woods with high pitch contents. Wood in the form of blocks, wedges, and needles is compacted in the seal annulus. Swelling of the wood induced by moisture or fluids enhances its sealing effectiveness. The pitch contained in the pore spaces of the wood prevents the migration of fluids via these spaces. If the picotage dries out or the shaft lining is displaced, pressure grouting may be required to repair the picotage.

3.4.9 Lining Accessories

Lining accessories are permanently embedded in, or connected to, the shaft lining. Examples include, but are not limited to:

1. Inserts embedded in concrete lining to provide bolted connections for shaft furnishings.
2. Water collection rings embedded in concrete lining for temporary water control.
3. Grout and drain pipes.
4. Brackets and other connectors welded to the steel lining for support of shaft furnishings.

Materials for these components should be selected for the required life and integrity of the shaft lining structure.

3.5 DECOMMISSIONING CONSIDERATIONS

3.5.1 Decommissioning Purpose and Shaft Seal Functions

A decommissioning plan is one of the requirements for repository licensing. The purpose of the plan is to facilitate permanent closure of the repository and long-term waste isolation. The design philosophy for isolation includes short- and long-term seals, with both kinds installed at the time of decommissioning. Short-term seals must become functional soon after installation and remain so until the long-term seals become effective.

The current decommissioning plan requires a seal system comprised of concrete bulkheads and various backfills. The primary function of all sealing components in the shafts is to restrict groundwater flow into the repository. A secondary function is to provide structural support to the host rock, limiting long-term deformation of the rock mass. Shaft lining design must include provisions to accommodate the shaft sealing system when the shafts are abandoned and the repository is decommissioned.

Concrete bulkheads will be the major postclosure components in the shafts, and their primary function will be to prevent intrusion of groundwater into the repository from overlying aquifers. They must be designed for low permeability through the bulkhead concrete and excavation-disturbed rock zone, for maintaining a tight seal between the bulkhead-rock interface, for chemical and structural compatibility with the host rock, and to provide adequate redundancy against leakage. The backfill material placed between the concrete bulkheads will form the long term sealing component. The shaft linings must be removed prior to placing backfill material.

3.5.2 Alternative Decommissioning Seal System Design

The early schematic seal system designs for the Permian Basin suggested lining removal and excavation of keyways for installation of concrete shaft bulkheads. These conceptual designs emphasized the need to minimize the disturbed rock zone for adequate seal performance.

An alternative to removing the shaft lining prior to installing bulkheads is to incorporate the periphery of the bulkhead as a shell in the shaft. At decommissioning, a concrete plug would be installed in the central

portion of the shell, thereby completing the bulkhead. The shells would be independent of the shaft lining and would be constructed of materials that meet decommissioning specifications. Mechanical excavation methods can be utilized to limit rock disturbance in the bulkhead locations during shaft sinking.

Performance monitoring of the shaft lining and any pre-installed bulkhead shells during the operational period will be critical for final seal system design. Design issues that should be addressed include: (1) the need for re-excavation, (2) shell-rock interface and lining-rock interface leakage, and (3) stress in the lining at the end of the operational life.

4 LOADS ACTING ON SHAFT STRUCTURES

The purpose of this chapter is to describe the methods to be used for determining loads that may act on the shaft linings. Its objective is to ensure that the shaft designer fully understands these methods. Methods for calculating static ground pressure, frozen ground pressure, fluid pressure, seismic loading, salt creep, and foundation loading are described. In addition, other loading conditions are discussed.

The lining design load can be determined on the basis of uniform horizontal soil and rock pressures with an allowance added for nonuniform loads. Calculations of uniform rock loads acting on the lining should be based on the strength and the state of equilibrium of the host strata. Discontinuities in the rock, any disturbance caused by excavation and construction, and how these discontinuities and disturbances may affect the development of uniform pressures should be considered. Nonuniform loads due to formation and lining anisotropy, and lining out-of-roundness are accounted for in an allowance. Other nonuniform loads, including those due to discontinuities, grouting, and ground freezing and thawing, must be considered in more detail as described in Section 4.6.3, Other Loads. Calculations of loads exerted by soil and rock below the groundwater table should include fluid pressures as described in Section 4.1.1.3, Fluid Pressures.

The general tectonic setting of Deaf Smith County, Texas, and recent measurements of in situ stresses both indicate that significant nonuniform, anisotropic, in situ horizontal stresses are unlikely at the repository site. Accordingly, the designer may assume that in situ stresses are isotropic. Any unbalanced stresses that do occur may be assumed to result from fabrication and construction and should be addressed on that basis.

The guidelines described for calculating ground pressures are appropriate if the horizontal stress field is reasonably uniform or isotropic, and if there are no significant differences between site-specific geotechnical and hydrological conditions and those portrayed in the SRP Data Base for the Deaf Smith County, Texas repository site. Site-specific data will be used to verify the application of the equations presented in this chapter, and provide a basis for modifying these guidelines, if appropriate.

4.1 STATIC GROUND PRESSURE

While several methods of calculating soil and rock pressures for shaft designs are available, the methods presented in the following subsections are appropriate for expected conditions at the Deaf Smith County, Texas repository site. Rock mass properties should be used in the equations presented in this section.

If these are not available from in situ test data, the rock properties should be scaled from available laboratory test data, or be otherwise estimated by the designer.

4.1.1 Uniform Components of Design Loads at Depth

The loads calculated from the equations in this section are assumed to act in a uniform, radial direction. If site-specific data indicate the presence of discontinuities that in combination with one another could form blocks or wedges, then pressures resulting from these discrete bodies will be individually analyzed. In addition, if anisotropic conditions are encountered in site-specific investigations, or during shaft construction, the application of these methods must be re-evaluated.

The equations defined in this section for calculating soil pressures should be used for materials described in soils terms, such as "clay, silt, sands, or any combination thereof." Rock pressure equations should be used for materials described in conventional rock terms and for specifically defined cemented materials. The SRP Data Base describes topsoil, loess of the Blackwater Draw Formation, and portions of the Ogallala Formation in soils terms and, therefore, the soil pressure methods are appropriate. The rock pressure methods are appropriate for the cemented strata in the Ogallala and for the underlying formations.

4.1.1.1 Soil Pressures

Soil pressures for shallow depths may be conservatively calculated using active earth pressure equations such as:

$$P_S = K_a \, \bar{\sigma}_V \tag{4-1}$$

where:
P_S = soil pressure (psf, kPa)
K_a = coefficient of active earth pressure
$\bar{\sigma}_V$ = effective vertical stress (psf,kPa)

and:
$$K_a = \frac{1 - \sin \phi}{1 + \sin \phi} \tag{4-2}$$

where: ϕ = angle of internal friction (degrees)

and: $\bar{\sigma}_v = \Sigma z_i \gamma_i + \Sigma z_k (\gamma_k - \gamma_w)$ (4-3)

Assuming flow pressures are negligible,

where: z_i = thickness of the $_i$th soil layer above the water table (ft,m)

z_k = thickness of the $_k$th soil layer below the water table (ft,m)

γ_i = unit weight of moist (partially saturated) soil in the $_i$th soil layer (pcf,kg/m^3)

γ_k = unit weight of saturated soil in the $_k$ soil layer (pcf)

γ_w = unit weight of formation water (pcf, kg/m^3) (See Section 4.1.1.3, Fluid Pressures)

Σ = summation of different layers

The pressures calculated using Equations 4-1 through 4-3 may be limited for deep soil conditions at the shaft according to procedures given in NAVFAC (1971), if considered appropriate by the designer.

4.1.1.2 Rock Pressures

When in situ horizontal stresses are uniform in all directions, and do not exceed one-half the unconfined strength of the rock mass, the shaft wall may resist yielding or spalling without a lining support (Springer, et. al., 1984). This limiting condition for in situ horizontal stress can be expressed as:

$$\sigma_h \leq \frac{q_u}{2} \quad (4\text{-}4)$$

where: σ_h = in situ horizontal stress (psi, kPa), which shall be assumed equal to the vertical stress unless actual field measurement (e.g., hydraulic fracture test) data are available and indicate otherwise

q_u = unconfined compressive strength of rock mass (psi, kPa) measured either by in situ testing or scaled from laboratory test data (Heuze, 1980).

If unconfined rock mass strength data are not available, and if cohesion and the angle of internal friction are known, Equation 4-4 can be restated using Mohr's envelope (Obert and Duvall, 1967):

$$\sigma_h \leq \frac{c \cdot \cos \phi}{1 - \sin \phi} \tag{4-5}$$

where: c = cohesion (psi, kPa)

If σ_h is greater than $\frac{1}{2} q_u$, an inelastic zone (hereafter referred to as the plastic or relaxed zone) with a radius of R (ft, m) will develop around the excavation and require support. The radius R to the boundary between the plastic and the elastic zone may be calculated using the following equation. (The derivations of Equations 4-6 and 4-7 are described in Appendix A.)

$$\left(\frac{a}{R}\right)^2 = \sin \phi + \frac{c \cdot \cos \phi}{\sigma_h} \tag{4-6}$$

where: a = radius of excavation (ft,m)

The uniform rock pressure P_r (psi, kPa) acting on the shaft support can be calculated using the following equations:

$$P_r = (\sigma_h + c \cdot \cot \phi)(1 - \sin \phi) \cdot \left(\frac{a}{R}\right)^{t^2 - 1} - c \cdot \cot \phi \tag{4-7}$$

where: P_r = rock pressure (positive direction is acting inward toward center of shaft)

σ_h = horizonal in situ stress (positive direction is acting inward toward center of shaft)

and:
$$t^2 - 1 = \frac{2 \sin \phi}{1 - \sin \phi} \tag{4-8}$$

The limit of $\frac{R}{a}$ expressed in equation 4-9 applies to the value calculated from equation 4-6 if a minimum support pressure, $P_{R(min)}$, is applied. This limit is based on practical ranges for rock mass properties, past experience, and a desired practical limit of the plastic zone thickness.

$$\frac{R}{a} \leq \sqrt{e} \leq 1.65 \tag{4-9}$$

where: e = natural logarithm = 2.7183

and: $$P_{R(min)} = \frac{\sigma_V - 2\,c \bullet t}{t^2} \text{ if } \sigma_V > q_u \qquad (4\text{-}10)$$

or: $$P_{R(min)} = 0 \text{ if } \sigma_V \leq q_u$$

where: σ_V = vertical in situ stress at depth

The design procedure is summarized as follows:

1. Determine applicable values for σ_h, ϕ, and c.
2. Check if elastic or inelastic condition will prevail by calculating $\frac{a}{R}$ ratio using Equation 4.6.
3. If $\frac{a}{R} < 1.0$, then inelastic conditions prevail.
4. If $\frac{a}{R} \geq 1.0$, then elastic conditions prevail.
5. Check against maximum values given by Equation 4-9.
6. From $\frac{a}{R}$ ratio, find P_r using Equation 4-7, compare with $P_{R(min)}$ using Equation 4-10, use greater of P_r values.

The above procedures are appropriate for the subsurface conditions and the range of rock strengths and resulting stresses expected at the Deaf Smith County, Texas repository site. Supplemental procedures for analyzing ground/support interaction that may be useful where adequate experimental or in situ rock mass properties are known, or where displacement (convergence) data may be available, are found in Brown, et. al., (1983) and Hoek and Brown (1982).

For a nearly frictionless plastic material such as a soft clay shale, the appropriate ground pressure calculation is:

$$P_s = (\sigma_h - c) - 2c \bullet \ln\left(\frac{R}{a}\right) \qquad (4\text{-}11)$$

with a limit of $P_s = (\sigma_h - 2c)$, when $\frac{R}{a} \leq \sqrt{e}$

These closed-form solutions are valid for isotropic horizontal conditions only. They do not take into account anistropy of the in situ materials or stresses, time-dependent behavior, the presence of discontinuities in the rock mass, nor the effects of excavation and construction. The designer should consider these conditions and more complex situations and critical structural elements, such as intersections, shaft support rings, and seal locations, on a case by case basis. Applicable methods and analytical solutions can be found in Hoek and Brown (1982), Ostrowski (1972), and Szechy, (1973). Computer modeling techniques described in Section 6, Computer Design Analysis, are also applicable for analysis of the more complex rock conditions and critical lining structural elements.

The procedures described for calculating rock pressures on a lining are based on past experience using conventional analyses that assume: 1) an elastic-plastic material model for the rock, wherein rock in the plastic zone deforms at constant volume; and 2) a linear Mohr-Coloumb strength criterion for the rock mass. In contrast, it is recognized that experimental data generally indicate that rock in the plastic zone undergoes dilation and that strength criteria for in situ rock masses are usually nonlinear. Newer models have been proposed to fit such experimental data and closed-form solutions have been developed for use with such models (Brown, et. al., 1983), including procedures for determining ground/support interaction as a function of convergence (Hoek and Brown, 1982). However, the results obtained with any of the models can only be as good as the designer's characterization of the in situ rock mass properties. Such a characterization is a formidable task. Therefore, it is appropriate to use a conservative estimate of these properties with the relatively simple model proposed. Experienced designers may wish to test the range of results possible using other models, and perhaps refine estimates of the rock mass properties to be used in the simple model, but detailed recommendations for doing so are beyond the scope of the SDG.

4.1.1.3 Fluid Pressures

The calculation of fluid pressures P_W should be based on the specific gravity of the rock formation fluids. If specific data are not available, hydrostatic pressures can be calculated for fresh water using a gradient of 0.43 psi/ft (9.72 kPa/m) of depth below the groundwater table. For brine, a gradient of 0.52 psi/ft (11.91 kPa/m) of depth below the fresh water/brine interface should be used. The fresh water gradient of 0.43 psi/ft (9.72 kPa/m) is for formation fluids with a total dissolved solids (TDS) content of 10,000 ppm or less. The brine gradient of 0.52 psi/ft (11.91 kPa/m) is for fluids with a TDS content greater than 10,000 ppm. An exact determination of the fluid pressure gradient can be made using the following equation.

$$\text{Fluid pressure gradient (psi/ft)*} = \frac{\text{SG (62.43 pcf)**}}{\text{144 si/sf}} \qquad (4\text{-}12)$$

where: SG = specific gravity of fluid

*Multiply by 22.6 to obtain kPa/m

**Water at 4°C, maximum density and SG = 1.0.

Where asphaltic sealant material (ASM) is placed between the primary and final lining, the final lining must be designed to bear the ASM pressure. This is equal to the weight per unit area of the column of ASM from the point of application to its free surface. The minimum ASM pressure must be 110% of the formation fluid pressure, and the ASM pressure should be uniform around the lining. The specific gravity of ASM should not exceed 1.3.

Fluid pressures at any given point z should be calculated as follows (see Figure 4.1):

For fresh water: $P_w' = 0.43\ (H - h)$ (psi), $9.72\ (H - h)$(kPa) (4-13)

For brine: $P_w'' = 0.52\ h$ (psi), $11.91\ h$(kPa) (4-14)

Total Fluid Pressure P_W (psi, kPa):

For ASM Surrounded Linings: $P_W = P_f \geq 1.1\ (P_w' + P_w'')$ (4-15)

where: P_f = ASM pressure (psi, kPa)

For all other linings: $P_W = P_w' + P_w''$ (4-16)

where: H = total depth (ft,m) below water table

h = thickness of brine saturated formation (ft,m)

4.1.2 Nonuniform Component of Design Loads at Depth

Calculations of the lining design load should include a component P_ϕ to allow for nonuniform loads due to formation and lining anistropy and lining out-of-roundness. The maximum value of this component is P_1 at the point of loading on the perimeter of the lining. Its minimum value is zero at a point 90° from the point of maximum value. The distribution of this load may be calculated according to the method by Link, et. al., (1985), as follows (see Figure 4.2):

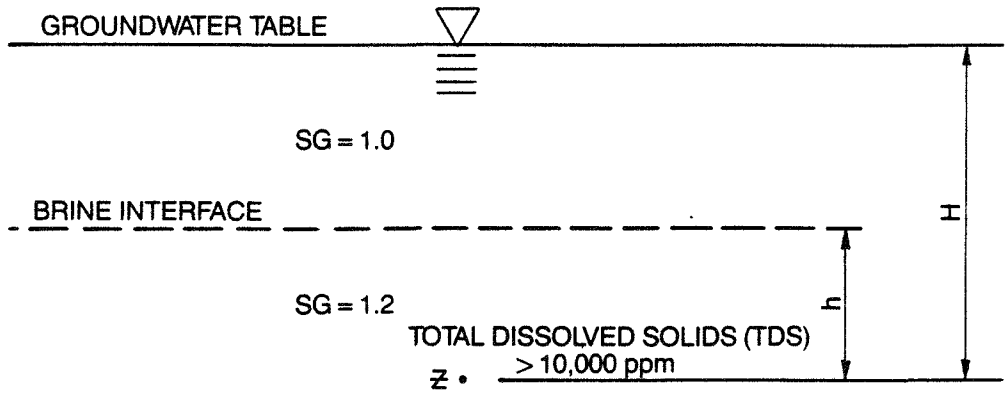

BASIS FOR CALCULATING FLUID PRESSURE

FIGURE 4.1

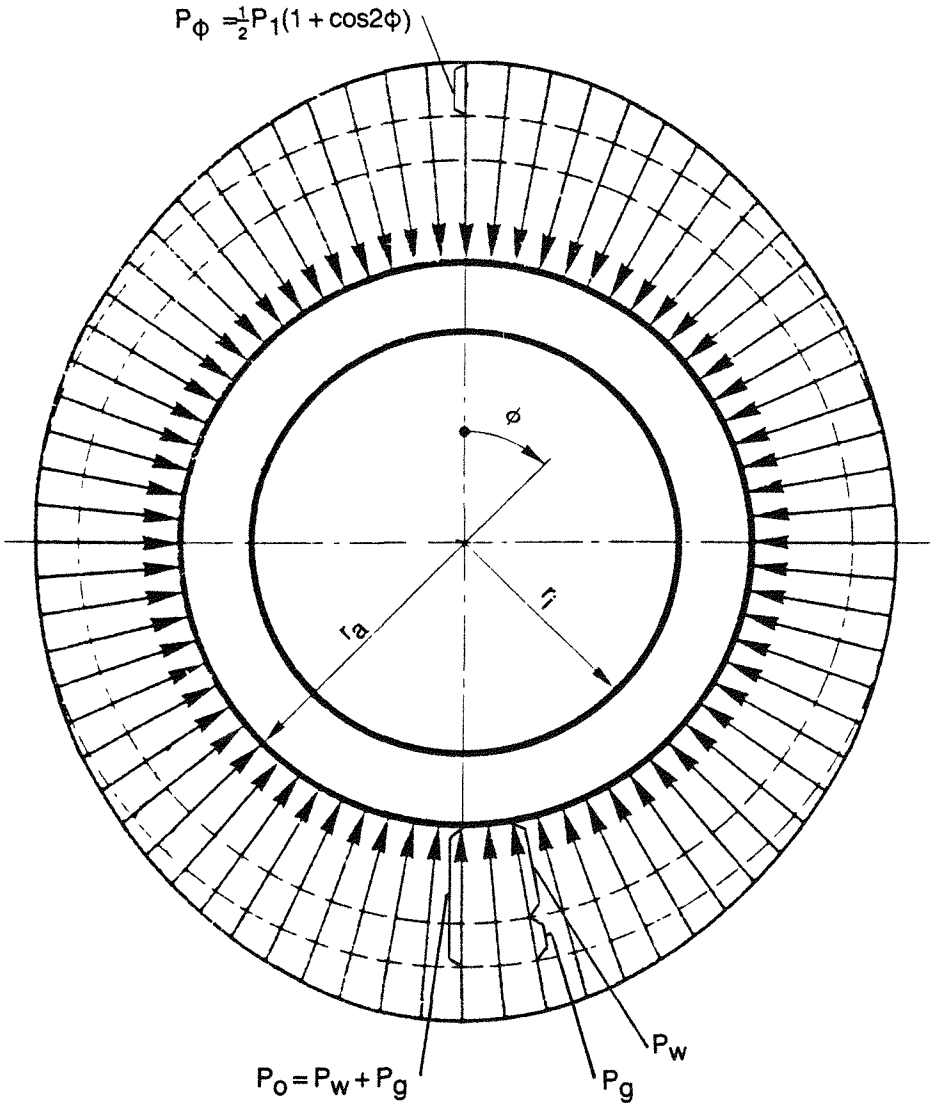

NON UNIFORM LINING LOADS

FIGURE 4.2

$$P_\phi = \frac{1}{2} P_1 (1 + \cos 2\phi) \qquad (4\text{-}17)$$

where: ϕ = circular vector angle ($0° \leq \phi \leq 90°$)

$P_1 = 0.10\ P_O$ (psi,kPa)

and: P_O = total pressure (psi,kPa) (see Section 4.6.1, Uniform Horizontal Pressure)

The component P_1 is only valid when the inside shaft radius r_i does not vary by more than 0.833% and the lining thickness is not less than specified by the designer. Where it is expected or verified that r_i varies by more than 0.833%, and the lining thickness is less than specified, P_1 must be increased by a value determined as follows:

$$\Delta P_1 = 6 \cdot \frac{(\Delta r_i - 0.00833 r_a)}{r_a} \cdot P_O \qquad (4\text{-}18)$$

where: r_a = outside radius of the lining (ft,m)

However, the actual radius or actual lining thickness should not exceed the maximum tolerances specified.

4.1.3 Grouting

Bending and other nonuniform loads that may act on the shaft lining as a result of grouting should be analyzed using such methods as Bodrov-Gorelik, the polygonal method, or the Bougayeva method, as described by Szechy (1973). The loads should be estimated and included in the design of the shaft lining.

Contact grouting may be used to completely fill all voids between the completed shaft lining and the excavated shaft wall. Contact grout is injected under pressure through holes drilled as deep as five feet into the rockwall. Access to the holes is provided through pipe nipples set in the shaft lining forms prior to concrete placement or through threaded port openings installed in the steel lining of the shaft. Grout may also be injected through holes drilled after the shaft lining is constructed. In general, contact grouting should begin at the lowest point in an ungrouted section of shaft, and move upward, forcing air and water ahead of the rising grout column.

It is important to limit injection pressures so as not to overstress the lining and the surrounding rock. In some cases reported (Grant, 1983), injection pressures have been limited to 1.25 times the design uniform pressure for nonwatertight linings and 1.25 times the hydrostatic pressure for watertight linings.

The above paragraphs describe the effects of contact grouting. Other types of grouting, such as formation grouting ahead of the shaft bottom, typically do not affect the shaft lining and should be examined on an individual basis.

4.2 FROZEN GROUND PRESSURE

4.2.1 General Remarks and Load Assumptions

When ground freezing is used to control groundwater inflow or to stabilize loose or low-strength water bearing materials, load components arising from freezing and thawing should be included in the lining design.

4.2.2 Loads on Primary Lining

When the primary lining rests directly against the freeze wall, the support pressure $P_{g'}$ required is either 200 psi or the total of the soil, rock, and hydrostatic pressures, whichever is greater. A minimum support pressure of 200 psi is used for dimensioning the shaft lining to provide an allowance for material handling, quality control, and performance considerations. Soil and rock pressures can be calculated using the equations in Section 4.1, Static Ground Pressure, and strength parameters c and ϕ for frozen and thawed materials. Where test data are not available for thawed materials, ground pressures may be evaluated using empirical values of 0.2 c and 0.9 ϕ of the unfrozen ground. To support the design analysis the designer is referred to Sage and D'Andrea (1982), and Andersland, et. al., (1978) for the mechanical properties of frozen and thawed materials. In addition, the designer is referred to Jessberger (1980), Vyalov, et. al., (1962), and Klein (1985) for methods of calculating ground pressures resulting from frozen and thawed materials, and for methods of designing primary linings in frozen ground.

4.3 OTHER LOADING CONSIDERATIONS

It may be necessary to include in the design loads the loads arising from miscellaneous factors P_m such as shaft furnishings, operational effects, or construction activities. These loads may be of importance in

critical areas such as seals and foundation. These loads can be evaluated by closed-form solution or computer modeling methods. Other loading considerations are briefly summarized below.

4.3.1 Loads from Time-Delayed Rock Displacements

Excavation can cause subsidence, and temperature changes can cause heave or settlement of the strata surrounding the shaft. Over time, these movements may cause bending of the shaft axis and displacement at the collar. The lining design must consider this displacement.

For a shaft lining bonded to the strata, the stresses in the lining caused by bending should be calculated relative to the shaft center line with a longitudinal bending radius R:

$$R = 197{,}000 \text{ in } (5{,}003{,}800\text{mm}) \qquad \text{(Link, et. al., 1985) (4-19)}$$

For a shaft lining separated from the strata by ASM, the stresses should be calculated relative to the shaft center line with a longitudinal bending radius R:

$$R = \frac{L^2}{2f} \qquad \text{(Appendix F) (4-20)}$$

where: L = 4000 in (101,600mm) if shaft length $L \geq 4000$ in (101,600mm)

or: L = actual shaft length if $L < 4000$ in (101,600 mm)

and: f = horizontal displacement of shaft axis (in,mm). The f dimension may be the thickness of the ASM or the tolerance provided in the lining restraining device at the shaft collar.

Stresses caused by bending of the shaft axis with a bending radius R are calculated using Equations 5-28 and 5-30.

For an ASM surrounded lining, shear stresses at the interface of the lining with the ASM are calculated as follows:

$$\tau_{max} = \pm \mu \cdot \frac{V_{max}}{b} \qquad \text{(Link, et. al., 1985) (4-21)}$$

where: τ_{max} = axial shear stress (psi,kPa)

μ = dynamic viscosity of ASM (day • psi, day • kPa)

b = radial ASM thickness (in,mm)

V_{max} = maximum vertical displacement velocity

use: V_{max} = 0.5 inch/day (12.7mm/day)

In an ASM surrounded lining, the tilt resulting from delayed rock displacement affects only the lining foundation. This results in axial bending of the shaft lining which is included in the bending loads calculated as described in Section 5.3.4.1, Rock Coupled Lining, and Section 5.3.4.2, Lining Surrounded by Asphaltic Sealant Material.

The effects of delayed rock displacements can be reduced through appropriate provisions in the lining system, for example, by using ASM or individual concrete rings.

4.3.2 Loads from Internal Residual Stresses

Concrete shrinkage and residual stresses from welding (e.g., steel lining plate) can create additional stresses on the lining system. The designer should attempt to minimize any adverse effect of residual and shrinkage stresses on the strength of the lining by specifying standard fabricating procedures and avoiding stress raisers. This is a conventional procedure. The designer is referred to ACI 318-83.

4.3.3 Thermal Loads

The in situ rock temperature T_i is determined from the geothermal gradient. At any depth below the surface, this temperature is given by:

$$T_i = \frac{dT_o}{dH} \cdot H + T_o \ (°F, °C) \qquad (4\text{-}22)$$

where: T_o = mean annual ground surface temperature (°F, °C)

$\frac{dT_o}{dH}$ = average geothermal gradient (°F/ft, °C/m)

and: H = depth below ground surface (ft,m)

The values for T_O and $\frac{dT_O}{dH}$ are given in the SRP Data Base.

Thermal changes in the lining and in the host rock will induce thermal stresses in the lining system. These stresses can be calculated using conventional thermal equations.

The designer must consider two conditions which result in ventilation-related thermal stresses. These are (1) the gradual change in rock temperature in the period between commissioning and the time when the rock mass reaches thermal equilibrium and (2) daily changes in the ventilation air temperature.

The temperature of ventilation air varies with depth due to heat transfer at the lining surface and due to autocompression. These changes can be calculated using heat conduction and heat convection equations. Radiant heat transfer need not be considered. Simplified analyses of steady-state thermal responses can be performed using one-dimensional solutions. Transient responses may require more detailed analyses using two-dimensional solutions. These two-dimensional solutions can be evaluated using numerical models listed in NUREG-CR3450 (Curtis, et. al., 1983).

Simplified thermomechanical analyses of the thermoelastic response of a hollow cylinder can be performed with a closed form, steady-state solution. More sophisticated analyses should include the effects of ventilation heat. These analyses are much more complicated and are best performed by numerical models. These numerical models can either access the results of the thermal analyses identified above (e.g., output from DOT) or calculate the temperatures simultaneously. Applicable codes are identified in NUREG-CR3450 (Curtis, et. al., 1983).

In the long run, thermal uplift resulting from the heat of the emplaced waste will create differential loads on the shaft lining. Although these loads might eventually be more significant than vertical or horizontal loads created by groundwater and rock pressures, they are unlikely to have any effect during the operational period. Nevertheless, the thermal changes in the rock mass around the shaft opening should be monitored to verify this assumption.

4.3.4 Effects of Proposed Construction Methods

The designer should specify excavation and rock support methods that minimize disturbance to the surrounding strata. In particular, the influence of ground stabilization procedures (e.g., dewatering, pressure grouting, freezing) on the shaft structure and surrounding rock should be analyzed. Also, installation procedures for shaft lining components should be appropriate for the design stability of each component.

4.3.5 Shaft Equipping Loads

In addition to the actual weight of the shaft lining, the lining design should also consider loads arising from shaft furnishings; hoisting and equipment reactions and forces at shaft support brackets; instrumentation penetrations; and instruments installed and operated in the shafts.

4.3.6 Shaft Station Area

Loads, if any, arising from the transition from the shaft lining to the horizontal repository entries should be incorporated in the design.

4.3.7 Shaft Bottom Plug

The shaft lining will terminate at the shaft bottom with a shaft plug. This plug should be designed to protect the shaft bottom against uplift pressures caused by creeping strata and groundwater in the basal nonsalt units, and to provide a barrier to water migration. Loads arising from the shaft plug interacting with the lining should be considered in the lining design.

4.3.8 Decommissioning Seals

The designer should consider loads arising from decommissioning seal components that are installed as part of the shaft lining.

4.3.9 Shaft Abandonment

The effects of shaft abandonment seals and backfill should be taken into account.

4.3.10 Rock Discontinuities and Tectonic Disturbances

Loading conditions resulting from rock discontinuities and tectonic disturbances in the rock formations should also be considered in the lining design. Examples can be found in Hoek and Brown (1982).

4.4 SEISMIC LOADING

4.4.1 Response Spectra and Control Motions

Methods to obtain estimates of temporal and spatial variations in seismic motion throughout the site profile require that a control point and a control motion be specified. Control motions are represented by artificial acceleration time histories which are constrained to have response spectra that envelop the design response spectra. Further constraints on the control motion involves duration characteristics (Dobry, et al, 1978) in addition to peak values of ground acceleration, velocity, and displacement (PGA, PGV, and PGD, respectively) which are consistent with the magnitude and distance of the Design Basis Earthquake (DBE). Response spectra and control motions are specified using median plus-one-standard-deviation estimates of the PGA, PGV, and PGD for the DBE. Horizontal response spectral values are determined by employing median spectrum amplification factors following the procedure recommended by Newmark and Hall (1978). By employing peak acceleration, velocity, and displacement values to scale response spectral ordinates, this procedure converts earthquake magnitude dependence into spectral shapes. The use of median amplification factors applied to median plus-one-sigma peak ground motion values provides for conservative estimates of spectral ordinates. The control point is specified at an assumed outcrop of competent material within the site profile since the control motions are representative of recordings at a competent rock site.

Response spectral ordinates for the vertical motion are taken as a fraction of the horizontal design response spectrum. (See Section 4.3 of the SRP Input to Seismic Design [ISD].) The scale factor is specified so that reasonable and conservative values are produced for vertical surface motion caused by vertically propagating compressional waves. Both horizontal and vertical motions computed at the surface are compared to appropriate recorded time histories to demonstrate that they are reasonable. The response spectra and time histories prepared for the Deaf Smith County site are contained in the ISD.

4.4.2 Site Response Analysis

Site response analyses are performed to determine the depth-dependent free field strains and accelerations associated with the specified seismic environment. These strains and accelerations are used to determine shaft lining stresses (Section 5.4, Stresses Due to Earthquakes) and shaft furnishing reactions (Section 5.10, Shaft Equipping Effects on Shaft Lining). Many of the elements which are used to calculate the site response either cannot be precisely defined or they have expected variations from their measured values. Accordingly, the several parameters influencing the analysis should be varied in order to arrive at realistic and reasonably conservative estimates of site response.

For curvature and shear deformation, the seismic environment consists of vertically propagating shear waves, inclined horizontally polarized shear waves (SH), and inclined compressional (P) and vertically polarized shear waves (SV).

For axial deformation, the seismic environment consists of vertically propagating compressional waves and inclined compressional and SV waves.

For uniform hoop deformation, the seismic environment consists of vertically propagating compressional waves. For nonuniform hoop deformation, the seismic environment consists of inclined SH waves and inclined P-SV waves.

The control motions consist of 100% of the specified horizontal motion for both the vertically propagating shear waves and the inclined SH waves. For the vertically propagating compressional waves and for the inclined P-SV waves, the control motion consists of a percentage of the specified vertical control motion (see Section 4.3 of the ISD).

The control point is specified at an imaginary outcrop of competent material.

Surface waves need not be included in the site response analysis since their effects are small and similar to those caused by the assumed inclined and vertically propagating waves in the frequency range of interest (Chen, et al, 1981).

To analyze vertical wave propagation, an appropriate computer program should be used to determine the maximum strain field for P waves and shear strain field for S waves for parametric variations in dynamic site properties. For P waves the normal strains on horizontal planes are specified. For S waves the shear strains on horizontal planes are specified.

To analyze inclined wave propagation, appropriate computer programs may be used to determine the maximum tangential normal strain field (P-SV waves) and maximum tangential shear strain field (SH waves) for parametric variations in dynamic site properties and incidence angles.

The free field strains and accelerations described above have been calculated for the Deaf Smith County, Texas site, and are contained in the ISD.

4.4.3 Host Media Stability

The following seismic hazards are considered to have little likelihood of occurring at the Deaf Smith County, Texas site:

1. Liquefaction of the loess soils at or near the ground surface.
2. Fatigue of clay layers in proximity to the ground surface.
3. Settlement due to seismic shaking.
4. Seismically-induced slope instability.
5. Movement of discrete blocks against the shaft lining.

These seismic hazards and their expected conditions at the Deaf Smith County, Texas site are discussed in the ISD.

4.5 SALT CREEP

In strata that are subject to long-term creep deformations, shaft linings should be designed to withstand full lithostatic pressure unless the pressure can be isolated from the lining during its design life or the lining is omitted. Calculations of lithostatic pressure should be based either on the measured vertical stress or on the gradient of the vertical stress that is appropriate for the level of the lining section. A nonuniform component

(P_ϕ) of the full lithostatic pressure will not be required unless it can be demonstrated that anisotropic horizontal creep rates exist and that the shaft lining dimensional requirements set forth in Section 4.1.2, Nonuniform Component of Design Loads at Depth, are exceeded. Where full lithostatic pressure can be retarded by overexcavation and backfilling with compressible material, the rate of creep closure and the development of creep pressures can be calculated using the constitutive properties of the strata and steady state creep laws. Although the initial creep rate will be larger than later rates, it will not last long and will contribute a small portion of the total strain over the required service life of the shafts.

The steady state creep laws are in the form of an exponential time law. The following equation is the constitutive law for salt creep commonly used in the Salt Repository Program (Pfeifle, et. al., 1983):

$$\dot{\epsilon} = A \cdot \sigma^n \cdot e^{\left(-\frac{Q}{RT}\right)} \tag{4-23}$$

where:
- $\dot{\epsilon}$ = steady state creep rate (s^{-1})
- A = material-dependent coefficient ($MPa^{-n} \cdot s^{-1}$)
- σ = effective stress (MPa)
- n = material-dependent stress exponent
- Q = activation energy (cal/mole)
- R = Universal Gas Constant (1.987 cal $mole^{-1}$ $°K^{-1}$)
- T = absolute temperature (°K)
- s = seconds

The parameters A, n, and $\frac{Q}{R}$ are taken from the SRP Data Base. Preliminary estimates of creep closure may be calculated using a closed-form solution for the radial velocity of a point on the excavation wall (see Appendix B) as follows:

$$V = \left(\bar{A} \cdot \frac{(\sqrt{3})^{n+1}}{2} \cdot a \cdot \left(\frac{\sigma_o}{n} \right)^n \right) \cdot C \tag{4-24}$$

where:
- V = radial closure velocity (m/s)
- $\bar{A}$ = material-dependent coefficient at a given temperature in the steady state creep law, e.g., $\bar{A} = A \cdot e^{\left(-\frac{Q}{RT}\right)}$ ($MPa^{-n} \cdot s^{-1}$)
- n = material-dependent stress exponent of steady state creep law

a = excavation radius (m)

σ_O = $\sigma_H - P_i$ (MPa)

P_i = support pressure (MPa)

C = a scalar factor accounting for initially higher transient effects during early shaft life. This factor is conservatively estimated to be 10 for Permian Basin salt properties and stress conditions (see Appendix B, Figure B.1)

4.6 SUMMARY OF LINING LOADS

The loads acting on the shaft lining are summarized below. Abbreviations and symbols used in the equations are described in Sections 4.1.1, 4.1.2, and 4.2.2.

4.6.1 Uniform Horizontal Pressure (P_O)

Where salt bears directly against the shaft lining:

$$P_O = P_O'$$

where: P_O' = full lithostatic pressure (psi, kPa)

For all other linings:

$$P_O = P_g + P_w$$

where: P_g = ground pressure (psi, kPa)

and: $P_g = P_s$ for soil

$P_g = P_r$ for rock

$P_g = P_g'$ for frozen ground

$P_g = P_i$ for salt with compressible backfill material

P_g = O for ASM surrounded lining

P_w = fluid pressure (see Section 4.1.1.3, Fluid Pressures)

4.6.2 Nonuniform Loads (P_ϕ)

$$P_\phi = \frac{1}{2} P_1 (1 + \cos 2\phi)$$

where: $P_1 = 0.10\ P_O$ with limits described in Section 4.1.2.

4.6.3 Other Loads (P_m)

1. Loads from time-delayed rock displacements.
2. Loads from internal residual stresses.
3. Thermal loads.
4. Seismic loads.
5. Effects of construction loads.
6. Shaft equipping loads (including those created by shaft furnishings, hoisting, and instrumentation).
7. Shaft station area.
8. Shaft bottom plug.
9. Decommissioning seals.
10. Shaft abandonment.
11. Grouting pressures.
12. Rock discontinuities.
13. Tectonic forces (if present).

4.6.4 Total Combined Loads (P_T)

The total combined loads acting on the final shaft lining are the sum of uniform horizontal pressures, nonuniform loads, and other loads, except as noted below.

In cases where the salt bears directly against the shaft lining:

$$P_T = P_O + P_m$$

For all other final linings:

$$P_T = P_O + P_\phi + P_m$$

4.7 FOUNDATION LOADING

Figure 4-3 shows a typical arrangement of the foundation at the bottom of a watertight lining section through a freeze zone. A similar configuration may be used for support of intermediate sections of watertight lining.

Foundations for nonwatertight lining systems are conceptually the same as those for watertight lining sections. Loading considerations are also similar. These foundations consist of massive reinforced concrete trapezoidal section rings that are keyed into the surrounding rock formations and designed to transfer all loads to them. It is essential that foundations be located in rock formations that contain no fluids.

4.7.1 Loads Acting on Foundations

In addition to its own weight, each foundation must be designed to bear the following loads:

1. The total weight of the final shaft lining, consisting of concrete and one or two steel shells.
2. The total weight of the ASM or grout filler in the annulus between the primary and final linings.
3. A fraction of the combined weight of the primary lining and the unconsolidated thawed formations.

The value of the fraction χ of the combined weight of the primary lining and unconsolidated thawed formations is left to the judgment of the designer, but typically it lies within the range of 0.3 to 0.4. The foundation should be sized so that the bearing pressure on the rock formation will not exceed one third of the unconfined compressive strength of the formation (Figure 4.4). A greased lead plate approximately 2 in (51mm) thick may be placed between the base plate of the lining and the top of the foundation (Figure 4.3) to permit independent radial deflection of the lining resulting from horizontal ground pressure. This plate will serve to eliminate the horizontal component of the lining load and ensure that the load on the foundation remains vertical and uniform.

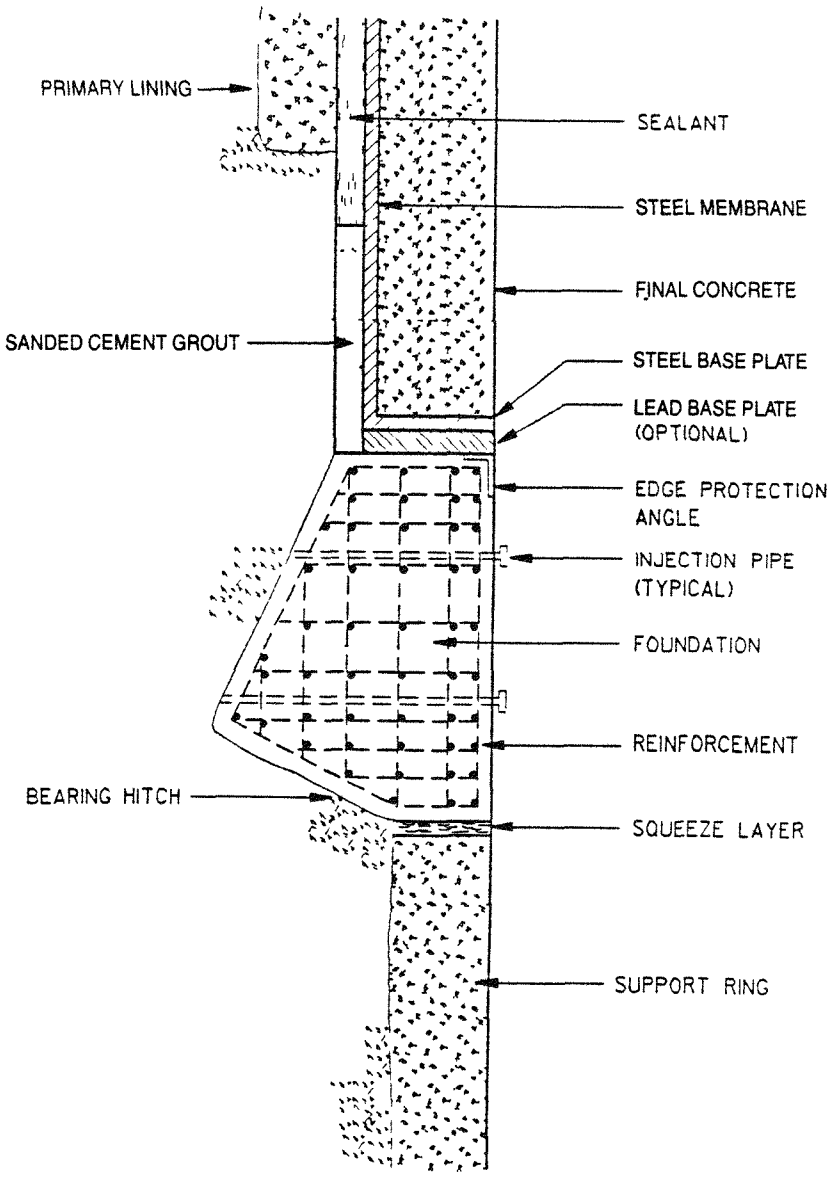

FOUNDATION (TYPICAL)

FIGURE 4.3

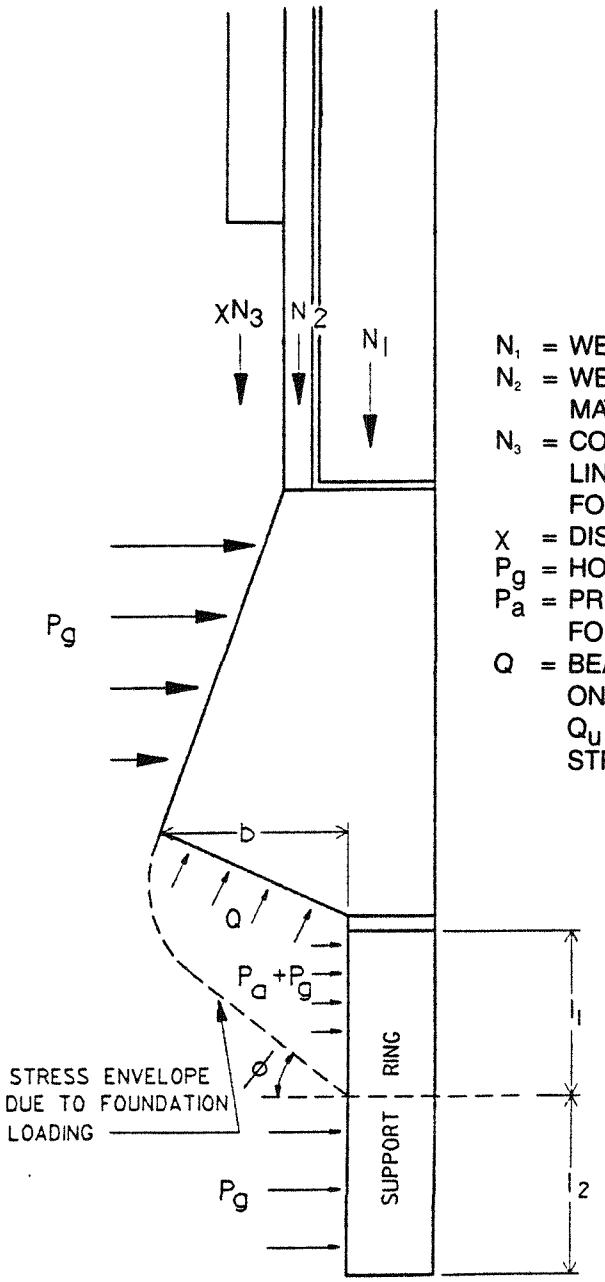

N_1 = WEIGHT OF FINAL LINING COLUMN.
N_2 = WEIGHT OF ASPHALTIC SEALANT MATERIAL OR GROUT COLUMN.
N_3 = COMBINED WEIGHT OF PRIMARY LINING AND UNCONSOLIDATED FORMATION.
X = DISCRETIONARY LOAD FACTOR.
P_g = HORIZONTAL GROUND PRESSURE.
P_a = PRESSURE SURCHARGE DUE TO FOUNDATION LOADING.
Q = BEARING PRESSURE OF FOUNDATION ON FORMATION. $Q \leq 0.33\ Q_u$ (WHERE Q_u = UNCONFINED COMPRESSIVE STRENGTH OF FORMATION).

FOUNDATION SUPPORT RING
$(l_1 + l_2) \geq 10'$
$l_2 \geq 5'$
$l_1 \geq b \tan \phi \geq 5'$
b = DEPTH OF KEY
ϕ = INTERNAL FRICTION ANGLE OF HOST FORMATION.

TYPICAL FOUNDATION LOADING

FIGURE 4.4

5 SHAFT LINING SIZING PROCEDURES

The purpose of this chapter is to guide the designer in the procedures for sizing load-bearing linings for vertical circular shafts constructed through competent and incompetent strata which may be dry or waterbearing. The procedures do not apply to primary linings which provide temporary support for the shaft excavation. The procedures allow the shaft designer to determine the stresses induced in the individual lining components by various loading combinations to ensure that the overall shaft lining design is safe.

5.1 SHAFT LINING MATERIALS

5.1.1 Reinforced Concrete

Reinforced concrete for shaft linings should be designed according to the requirements of the American Concrete Institute (ACI) 318-83, Building Code Requirements for Reinforced Concrete (Appendix B, Alternate Design Method) except that the allowable material stresses should be as calculated using the factors and values shown in Tables 5.1, 5.2, 5.3, 5.4, and 5.5.

To be considered reinforced concrete, the minimum ratio of the horizontal or vertical reinforcement area to the gross concrete area must be 0.002 for deformed bars not larger than No. 5, with a specified yield strength not less than 60 ksi (413 mPa). Where steel lining shells are employed, they must be securely bonded to the concrete for the structure to be considered reinforced.

5.1.1.1 Concrete Reinforcement

Reinforcing bars must be sized and provided with sufficient concrete cover to be in accordance with ACI 318-83.

5.1.2 Plain Structural Concrete (Unreinforced)

Plain structural concrete for shaft lining should be designed according to ACI 318-83/318.1R-83, Building Code Requirements for Structural Plain Concrete and Commentary, using the "Alternate Design Method" except that the allowable material stresses should be as calculated using the factors shown in Tables 5.1, 5.2, 5.3, and 5.5.

5.1.3 Concrete Block Masonry

Concrete block masonry should be designed according to the National Concrete Masonry Association (NCMA), Specification for the Design and Construction of Load-Bearing Concrete Masonry, and the allowable material stresses should be as calculated using the factors shown in Tables 5.1 and 5.5.

5.1.4 Steel

Steel combined with concrete in the shaft lining should be designed in accordance with the requirements of the American Institute of Steel Construction (AISC), Specification for the Design, Fabrication and Erection of Structural Steel for Buildings, except that the allowable material stresses should be as calculated using the factors shown in Tables 5.1, 5.2, 5.3, and 5.5.

5.1.5 Ductile Cast Iron Tubbing

The allowable stresses for ductile cast iron are based on the German Industry Standard, DIN 1693, Modular Graphite Cast Iron, and American Society for Testing and Materials (ASTM) A536-84, Standard Specification For Ductile Iron Castings, and should be calculated using the factors shown in Tables 5.1 and 5.5.

5.1.6 Connectors (Bolts and Weldments)

Bolted connections in tubbing construction should comply with the requirements of DIN 21501, Shaft Lining of Cast Iron Tubbing. Other bolted connections should comply with the allowable stresses specified for the selected bolts.

Welded connections for the steel lining plate should be designed using the allowable material stress values determined from the factors shown in Tables 5.1 and 5.5, provided that the strength and ductility of the weld is equal to or greater than that of the material being welded. Other allowable material stresses for lining connections may be permitted if verified by acceptable tests or codes.

5.1.7 Material Imperfections

Shaft lining materials may contain minor imperfections. As these are accounted for by the allowable stress factors and values shown in Tables 5.1, 5.2, 5.3, 5.4, and 5.5, they need not be analyzed separately. Since the SRP shafts will be subjected to a stringent Quality Control and Quality Assurance Program, the stress factors, which have been developed based on standard industrial practice, are considered conservative.

5.2 MATERIAL PROPERTIES

5.2.1 Moduli of Elasticity

The following moduli of elasticity should be used for ductile cast iron and steel:

1. Ductile Cast Iron; E_i = 25,000,000 psi (172,250,000 kPa)
2. Steel; E_S = 29,000,000 psi (199,810,000 kPa)

The modulus of elasticity E_C (psi, kPa) for concrete should be calculated according to ACI 318-83, using the equation:

$$E_C^* = W_C^{1.5}\, 33\sqrt{f'_C} \qquad (5\text{-}1)$$

for values W_C between 90 pcf (1,442 kg/mm^2) and 155 pcf (2,483 kg/mm^2).

where: W_C = weight of concrete (pcf)

f'_C = compressive strength of concrete (psi)

For normal weight concrete (145 pcf, 2,322 kg/mm^2), E_C should be calculated using the equation:

$$E_C^* = 57{,}000\sqrt{f'_C} \qquad (5\text{-}2)$$

* Multiply by 6.89 to obtain (kPa)

5.2.2 Value of n

The ratio of moduli of elasticity is given by n.

where: $n = \frac{E_S}{E_C}$ for a composite steel and concrete shaft lining.

Table 5.1 Allowable Compressive Stress Factors

Loads	Steel f_s/f'_s	Ductile Cast Iron f_i/f'_i	Concrete [a]		Concrete Block f_m/f'_m
			Reinforced f_c/f'_c	Plain f_c/f'_c	
Uniform (P_O)	0.60 [d]	0.60 [d]	0.55 [b]	0.45 [c]	0.33 [e]
Uniform plus Nonuniform ($P_O + P_\phi$)	0.85 [d]	0.75 [d]	0.66 [d]	0.55 [d]	0.45 [f]
Total (P_T)	0.95 [d]	0.90 [d]	0.75 [d]	0.61 [d]	0.55 [f]

Note: The application of the stress factors for reinforced concrete that are shown in this table requires a minimum reinforcing using #4 deformed bars (Grade 40) tangentially at the outer and inner concrete surfaces on 8-inch (203 mm) centers.

where:
- P_O = Uniform component of total load
- P_ϕ = Nonuniform component of total load
- P_T = Total combined loads (see Section 4.6.4, Total Combined Loads)
- f_s = allowable stress for steel (psi, kPa)
- f'_s = yield stress of steel (psi, kPa)
- f_i = allowable stress for ductile cast iron (psi, kPa)

f'_i = yield stress of ductile cast iron (psi, kPa)

f_c = allowable compressive strength of concrete (psi, kPa)

f'_c = specified compressive strength of concrete (psi, kPa)

f_m = allowable compressive strength of concrete block lining system (psi, kPa)

f'_m = compressive strength of individual block (psi, kPa)

a. All stress factors are valid for concrete with a 28-day compressive strength, f'_c, of 6,500 psi (44,785 kPa) or less, based on tests in accordance with ACI.

b. Source of stress factor: ACI 307-79, Sections 4.9.3 and 4.9.4

c. Source of stress factor: ACI 318-83, Appendix B, Section 8.3.1

d. Source of stress factor: Link, et al., 1985

e. Source of stress factor: ACI 531-79, Table 10-1

f. Source of stress factor: ACI 531-79, Table 10-1, scaled in accordance with Link, et al., 1985

Table 5.2 Allowable Tensile Stress Factors for Concrete

Loads	Concrete Lining	
	Reinforced [a, b] $f_t/\sqrt{f'_c}$	Plain [b] $f_t/\sqrt{f'_c}$
Uniform (P_o)	7.9	1.25
Uniform and Nonuniform ($P_o + P_\phi$)	7.9	1.25
Total (P_T)	7.9	1.25

where: f_t = allowable tensile strength of concrete (psi, kPa)

f'_c = specified compressive strength of concrete (psi, kPa)

a. Total tension is carried by tensile reinforcing.

b. Source of Stress Factor: Link, et. al., 1985

Table 5.3 Allowable Shear Stress Factors for Concrete: Values for s

Material	Applicability	s
Reinforced Concrete	In concrete without shear reinforcing	2.6
	If τ_o is carried by total cross section (concrete and reinforcing)	5.3
	At the interface of concrete/steel or concrete/ cast iron	0
Plain Concrete	In concrete	2.3

Note: Source of stress factors: Link, et. al., 1985

The allowable shear stress τ_a (psi, kPa) for concrete is given by:

$$\tau_a = \tau_o + \mu\sigma_r \qquad \text{(Link, et. al., 1985) (5-3)}$$

where: $\tau_o = s\sqrt{f'_c}$

s = shear stress coefficient from Table 5.3

and: τ_o = allowable shear stress for $\sigma_r = 0$

σ_r = smallest normal radial compressive stress at the plane of shear (psi, kPa)

$\sigma_r = 0$ if in tension

and: μ = coefficient of friction

$\mu = 1.0$ if inside the concrete mass

or: $\mu = 0.5$ at the interface of concrete/steel or concrete/cast iron

Table 5.4 Allowable Tensile Stresses in Reinforcement Steel

Loads	Reinforcement Steel	
	Grade 60	Grade 40
Uniform (P_O)	24,000 psi (165,360 kPa)	20,000 psi (137,800 kPa)
Uniform plus Nonuniform ($P_O + P_\phi$)	24,000 psi (165,300 kPa)	20,000 psi (137,800 kPa)
Total (P_T)	32,000 psi (220,480 kPa)	27,000 psi (186,030 kPa)

Note: Stresses meet requirements of ACI 318-83, Appendix B, Section B.3.2

Table 5.5 Allowable Buckling Stress Factors

Material	σ_{cr}/f'	
Steel	0.95[a]	$f' = f'_s$
Reinforced Concrete	0.75[a]	$f' = f'_c$
Plain Concrete	0.61[a]	
Concrete Block	0.55[b]	$f' = f_m$

a. Source of Stress Factors: Link, et. al., 1985.

b. Source of Stress Factors: ACI 531-79, Table 10-1, scaled in accordance with Link, et. al., 1985.

where: σ_{cr} = critical buckling stress (psi, kPa)

5.2.3 Allowable Material Stress Summary

Lining stresses determined for uniform, uniform plus nonuniform, and total loads should not exceed the allowable material stresses determined by using the factors and values specified in Tables 5.1, 5.2, 5.3, 5.4, and 5.5.

5.2.4 Lining Stresses for Total Load

The following yield criteria will limit the stresses. These criteria apply to two-dimensional states of stress. The stresses in the third dimension are omitted because the values are too small to govern.

Stresses in steel and ductile cast iron

For steel and ductile cast iron, the following expression for the stress intensity factor σ_v provides a value which is limited by the yield stress.

$$\sigma_v = \sqrt{\sigma^2_t + \sigma^2_z - \sigma_t\sigma_z + 3\tau^2_{tz}} \qquad \text{(Link, et. al., 1985) (5-4)}$$

Stresses in concrete

For concrete, the principal stress values, calculated as follows, should not exceed the appropriate allowable tensile or compressive stresses.

$$\sigma_v = \frac{\sigma_t + \sigma_z}{2} \pm \sqrt{\left(\frac{\sigma_t - \sigma_z}{2}\right)^2 + \tau^2_{tz}} \qquad \text{(Link, et. al., 1985) (5-5)}$$

where:
- σ_v = allowable stress obtained by using the factors shown in Tables 5.1, 5.2, 5.3, and 5.5 (psi, kPa)
- σ_t = all tangential stresses acting in horizontal plane (psi, kPa)
- σ_z = all stresses acting in a vertical direction (psi, kPa)
- τ = shear stress (psi, kPa)

For total load combinations which include seismic loads, the steel lining shell(s) must be stress checked using Equation 5-4 (with hoop, axial, and in-plane shear stresses as written) to ensure σ_v does not exceed the yield stress for the material.

Equation 5-5 for concrete is written to examine the stress conditions in a vertical plane through the axis of the lining. It is not used for seismic load evaluation. For seismic evaluation, the stress behavior of the concrete lining shell should be checked for hoop compression only, using the following Mohr's circle expression:

$$\sigma_v = \frac{\sigma_t + \sigma_r}{2} \pm \sqrt{\left(\frac{\sigma_t - \sigma_r}{2}\right)^2 + \tau^2_{rt}} \qquad (5\text{-}6)$$

The maximum shear stress τ_{max} (psi, kPa) should also be calculated and compared with the allowable shear stress for non seismic load conditions:

$$\tau_{max} = \pm \sqrt{\left(\frac{\sigma_t - \sigma_z}{2}\right)^2 + \tau^2_{tz}} \qquad (5\text{-}7)$$

See Section 5.4, Stresses Due to Earthquakes, for a discussion of nonhoop behavior and reinforcement to control cracks during seismic deformation.

5.3 DETERMINATION OF LINING STABILITY

Lining stability is a function of the loads acting on the lining, its material properties, and lining geometry. Lining stability against buckling is based on the resistance to buckling in individual lining rings of unit height. An individual lining ring is a theoretical lining section of unit height. Buckling safety is determined by calculating the loads that cause instability to occur in one of the buckling modes. Material failure is determined by calculating the stresses in the lining, after which Equations 5-4 and 5-5 are used to establish whether or not the lining can withstand these stresses.

All shaft lining systems consisting of several shells of different materials must be considered basically as compound linings and design calculations must be performed taking this into account. Shaft lining systems with a complete or partial bond between shells require a calculation showing that the bond will cause the shells to act as a unit rather than individually. Shaft lining systems without bond require that the buckling safety and stresses of each shell be analyzed individually.

The equations included in this guide are only valid for shaft linings having a constant cross sectional area. Variations in the cross sectional area, e.g., because of joints in a tubbing column, require a special determination of lining stability. Where the shaft lining is cast in direct contact with an excavation wall of irregular surface, all analyses should be performed using the minimum lining thickness.

5.3.1 Lining Stress Analysis

Equations should be used to determine the stresses in the lining as a result of uniform, nonuniform, and total loads acting on the outside of the lining.

5.3.1.1 Stresses Due to Uniform Horizontal Pressure P_o

Tangential stress should be calculated for all lining types by assuming that the pressure P_o acts on the exterior surface of the lining.

Tangential stresses are calculated using the equation:

$$\sigma_t = - \frac{P_o \cdot r_a}{A} \cdot \left(1 + \frac{y}{r_s}\right) \qquad \text{(Link, et. al., 1985) (5-8)}$$

where:
- P_o = uniform horizontal pressure (psi, kPa) (Section 4.6.1, Uniform Horizontal Pressure)
- r_a = outer liner radius (in, mm)
- r_s = radius of neutral axis (in, mm)
- A = cross-sectional area of lining per unit height (in^2/in, mm^2/mm)
- y = distance from neutral axis (see Figure 5.1)

The value y is considered positive towards the shaft opening. Compressive stresses derived from Equation 5-8 are negative.

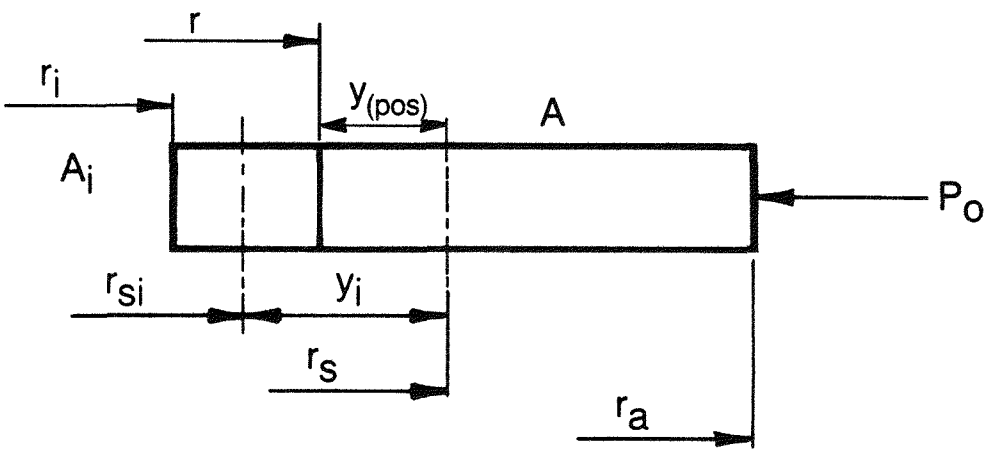

RADIAL STRESS IN A SURFACE SHELL

FIGURE 5.1

Equation 5-8 can be used for shaft linings with a thickness $< 0.3\ r_i$. With increasing lining thickness, the linear component in Equation 5-8 deviates for the tangential stress at the outer surface of the lining as determined by the more accurate quadratic Lamẽ statement. For thick linings ($\geq 0.3\ r_i$), the multiplication constants shown in Table 5.6 may be used to modify the values obtained from Equation 5-8.

Table 5.6* Multiplication Constants for Thick Linings

$\frac{t}{r_i}$	Multiplication Constant (Tangential stress outer lining surface)
0.3	1.035
0.35	1.045
0.40	1.057
0.45	1.070
0.50	1.083
0.55	1.098
0.60	1.113
0.65	1.128
0.70	1.161
0.75	1.178

where: r_i = inner lining radius
t = lining thickness

*See Appendix E.

The radial stress in a shell at radius r is given by the following equation:

$$\sigma_r = - \frac{P_o \bullet r_a \bullet A_i}{r \bullet A} \bullet \left(1 + \frac{y_i}{r_s} \right) \qquad \text{(Link, et. al., 1985) (5-9)}$$

where: A_i = area of unit height cross section bounded by r and r_i (in^2/in, mm^2/mm)

$y_i = r_s - r_{si}$

r_{si} = radius of the neutral axis of A_i (in, mm)

r = variable radius where stresses are calculated (in, mm) $r_i \leq r \leq r_a$

(See Figure 5.1)

In this load assumption, the shear stress τ is zero throughout.

5.3.1.2 Stresses Due to Nonuniform Horizontal Pressure Surcharge

The pressure P_ϕ (Section 4.1.2, Nonuniform Component of Design Loads at Depth) acts on the outermost surface of the lining. Stresses must be calculated for all linings assuming an existing bond between the shells.

The tangential stresses are given by:

$$\sigma_t = - 0.5 \bullet \omega \bullet \frac{P_o \bullet r_a}{A} \left[\left(1 + \frac{y}{r_s} \right) - \frac{1}{3} \left(1 + \frac{r_s \bullet y}{i^2} \right) \frac{\zeta}{\zeta - 1} \bullet \cos 2\phi \right] \qquad (5\text{-}10)$$

(Link, et. al., 1985)

where: $\zeta = \frac{3 E \bullet I}{P_o \bullet r_a \bullet r^2_s}$ (Link, et al., 1985)

$\omega = \frac{P_1}{P_o}$

ω = coefficient of nonuniform pressure

P_l = maximum value of nonuniform horizontal pressure P_O (Section 4.1.2, Nonuniform Component of Design Loads at Depth) (psi, kPa)

A = area per unit height of the entire transformed cross section (in^2/in, mm^2/mm)

ϕ = circular vector angle (Section 4.1.2, Nonuniform Component of Design Loads at Depth)

i = radius of gyration (in, mm)

$i = \sqrt{\frac{I}{A}}$

I = Moment of inertia per unit height (in^4/in, mm^4/mm)

This analysis must be carried out for the cross sections where $\phi = 0°$ and $\phi = 90°$ because tangential stresses at these points result in extreme values.

When $\phi = 0°$

$$\sigma_t = -0.5\ \omega \cdot \frac{P_O \cdot r_a}{A} \left[\left(1 + \frac{y}{r_s} \right) - \frac{1}{3} \left(1 + \frac{r_s \cdot y}{i^2} \right) \frac{\zeta}{\zeta - 1} \right] \quad (5\text{-}11)$$

(Link, et. al., 1985)

When $\phi = 90°$

$$\sigma_t = -0.5\ \omega \cdot \frac{P_O \cdot r_a}{A} \left[\left(1 + \frac{y}{r_s} \right) + \frac{1}{3} \left(1 + \frac{r_s \cdot y}{i^2} \right) \frac{\zeta}{\zeta - 1} \right] \quad (5\text{-}12)$$

(Link, et. al., 1985)

In addition, the shear stresses and radial stresses must be analyzed. The shear stresses are determined using the equation:

$$\tau = \frac{1}{3} \cdot \omega \cdot P_O \cdot \frac{r_a \cdot r_{si}}{r^2} \cdot \frac{A_i}{A} \left[\left(1 + \frac{r_s \cdot y_i}{i^2} \right) - \frac{r_s \cdot i_i^2}{r_{si} \cdot i^2} \right] \frac{\zeta}{\zeta - 1} \cdot \sin 2\phi \quad (5\text{-}13)$$

(Link, et. al., 1985)

where: i_i = radius of gyration of the cross sectional area bounded by r_i and r (in, mm)

and: $i_i = \sqrt{\frac{I_i}{A_i}}$

I_i = moment of inertia of unit height cross section bounded by r_i and r (in^4/in, mm^4/mm)

Shear stresses are greatest near the center of gravity of the cross section at $\phi = 45°$.

The nonuniform radial stress components are given by the equation:

$$\sigma_r = -0.5 \cdot \omega \cdot P_o \cdot \frac{r_a}{r} \cdot \frac{A_i}{A} \left\{ \left(1 + \frac{y_i}{r_s} \right) + \left[\left(1 + \frac{r_s \cdot y_i}{i^2} \right) \left(1 - \frac{4r_{si}}{3r} \right) + \right.\right.$$

$$\left.\left. \frac{4r_s}{3r} \cdot \frac{i_i^2}{i^2} - \left(1 + \frac{y_i}{r_s} \right) \frac{1}{\zeta} \right] \frac{\zeta}{\zeta - 1} \cdot \cos 2\phi \right\} \qquad (5\text{-}14)$$

(Link, et. al., 1985)

(see Figure 5.2)

The shear stresses τ and radial stresses σ_r in the concrete must be calculated at the interfaces of the different materials.

If the shear stresses τ or the combined uniform or nonuniform radial stresses exceed the permissible values determined as described in Section 5.2, Material Properties, then a mechanical bond must be provided or the method described in Section 5.3.3, Stress Determination in Linings with No Bond or Partial Bond, will govern. This is also true if the combined radial stresses are positive, which indicates that the interface is in tension. For design of mechanical bonds between shells see Sections 5.3.6, Anchoring to Prevent Shell Separation.

5.3.1.3 Stresses Due to Combined Uniform and Nonuniform Horizontal Pressures

Tangential Stress

$$\sigma_t = - \frac{P_o \cdot r_a}{A} \left[\left(1 + \frac{\omega}{2} \right) \left(1 + \frac{y}{r_s} \right) - \frac{\omega}{6} \left(1 + \frac{r_s \cdot y}{i^2} \right) \frac{\zeta}{\zeta - 1} \cdot \cos 2\phi \right] \qquad (5\text{-}15)$$

(Link, et. al., 1985)

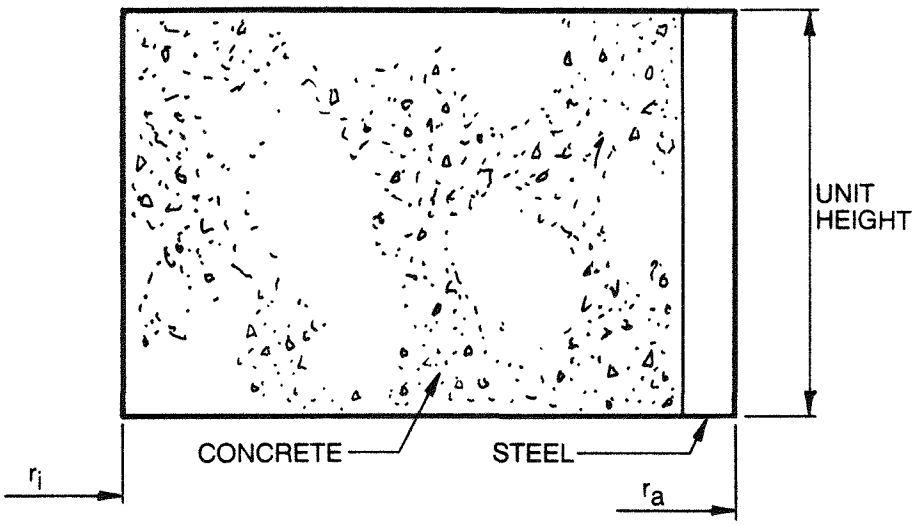

DETAIL 1
ACTUAL LINING CROSS SECTION

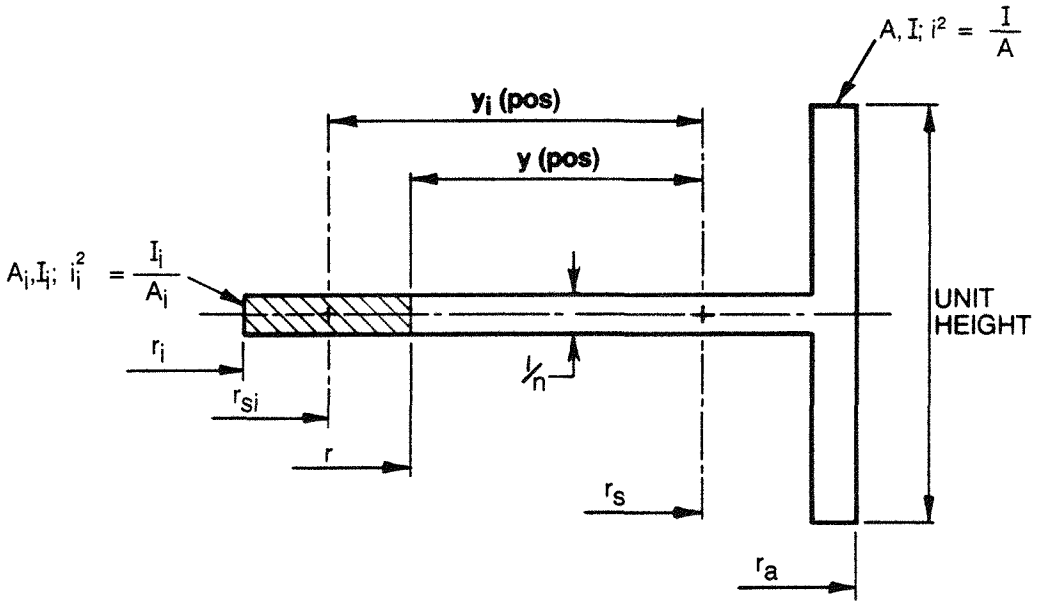

DETAIL 2
EQUIVALENT CROSS SECTION OF DETAIL 1 APPLYING N-FACTOR (SECTION 5.2.2)

NOTE: A concrete/single steel composite lining was chosen because it is the most common watertight lining type presently planned for the ESF and Repository Shafts

LINING CROSS SECTION DETAILS 1 and 2

FIGURE 5.2

Radial Stress:

$$\sigma_r = -\frac{P_o \cdot r_a}{r} \cdot \frac{A_i}{A}\left\{\left(1+\frac{\omega}{2}\right)\left(1+\frac{y_i}{r_s}\right)+\frac{\omega}{2}\left[\left(1+\frac{r_s \cdot y_i}{i^2}\right)\left(1-\frac{4r_{si}}{3r}\right)+\right.\right.$$

$$\left.\left.\frac{4r_s}{3r}\cdot\frac{i^2_i}{i^2}-\left(1+\frac{y_i}{r_s}\right)\frac{1}{\zeta}\right]\frac{\zeta}{\zeta-1}\cdot\cos 2\phi\right\} \qquad (5\text{-}16)$$

(Link, et. al., 1985)

where: $\phi = 45°$

$\sigma_r > 0$ for tensile stresses

$\sigma_r < 0$ for compressive stresses

Shear Stress

$$\tau = \frac{1}{3}\, P_o \cdot \omega \cdot \frac{r_a \cdot r_{si}}{r^2} \cdot \frac{A_i}{A}\left[\left(1+\frac{r_s \cdot y_i}{i^2}\right)-\frac{r_s \cdot i^2_i}{r_{si} \cdot i^2}\right]\frac{\zeta}{\zeta-1}\cdot \sin 2\phi \qquad (5\text{-}17)$$

(Link, et. al., 1985)

(See Figure 5.2)

The shear resistance τ_{ALL} at the interface of concrete/steel or concrete/cast iron is given by:

$$\tau_{ALL} = (\sigma_{r_{UL}} + \sigma_{r_{NL45}})\mu \qquad (5\text{-}18)$$

where: $\sigma_{r_{UL}}$ = radial stress due to uniform loading

$\sigma_{r_{NL45}}$ = radial stress due to nonuniform loading at 45°

μ = coefficient of friction = 0.5 between concrete and steel

(See Figure 5.2)

The tangential stresses determined by using Equation 5-15 depend upon the equivalent section whose area per unit height is A. The equivalent Section A in turn depends on the material selected for the equivalent section. In Figure 5.2, Detail 2, the selected material is steel. The tangential stresses in the concrete are determined by multiplying the calculated stress for steel by $\frac{1}{n}$.

If concrete is selected for the analysis, then the calculated stress for concrete is transformed into the stresses for steel by multiplying the concrete stress by n. The radial stresses determined by using Equation 5-16 and the shear stresses given by Equation 5-17 are independent of the material selected for analysis. They are, therefore, the true stresses for the material selected for analysis.

Equations 5-15, 5-16, and 5-17 are valid also for uniform horizontal pressures acting on the shaft lining only. When using these equations to determine stresses for uniform horizontal pressure, use $\omega = 0$.

5.3.1.4 Stresses Due to Uniform, Nonuniform, and Other Lining Loads

Total loads on a lining system are a combination of uniform and nonuniform loads, plus other loads as described in Sections 4.1.3, Grouting; Section 4.6, Summary of Lining Loads; and Section 5.4, Stresses Due to Earthquakes. All other lining loads are added as a supplement to P_O. Equations 5-15 through 5-17, therefore, are valid for calculating lining stresses using the adjusted value of P_O.

5.3.2 Stress Determination for Nonstandard Lining Configurations

For purposes of the guide, composite lining configurations are considered nonstandard if the watertight membrane is not the outermost shell.

For a lining with a permeable outer shell, the tangential stresses and radial stresses should also be calculated where the hydrostatic pressure P_W (Section 4.1.1.3, Fluid Pressures) acts on the surface of the outermost watertight shell and the ground pressure P_g (Section 4.6.1, Uniform Horizontal Pressure) acts on the outermost lining shell. By assuming that a bond between the lining shells exists, tangential stresses are determined using the equation:

$$\sigma_t = - \frac{(P_W \cdot r_W + P_g \cdot r_a)}{A} \left(1 + \frac{y}{r_s} \right) \qquad \text{(Link, et. al., 1985) (5-19)}$$

where: $y = r_s - r$ (> 0 for $r_s > r$, < 0 for $r_s < r$)

Radial stresses are calculated using:

$$\sigma_r = -\frac{(P_w \cdot r_w + P_g \cdot r_a)}{r} \cdot \frac{A_i}{A}\left(1 + \frac{y_i}{r_s}\right) \qquad \text{(Link, et. al., 1985) (5-20)}$$

where: $r_i \leq r \leq r_w$

and: $$\sigma_r = \frac{P_w \cdot r_w}{r} - \frac{(P_w \cdot r_w + P_g \cdot r_a)}{r} \cdot \frac{A_i}{A}\left(1 + \frac{y_i}{r_s}\right) \qquad \text{(Link, et. al., 1985) (5-21)}$$

where: $r_w \leq r \leq r_a$

(see Figure 5.3)

For the radius r_w of the watertight shell surface, the uniform component of the radial stress is determined using:

$$\sigma_{r_w} = P_w - \left(P_w + P_g \cdot \frac{r_a}{r_w}\right) \cdot \frac{A_i}{A}\left(1 + \frac{y_i}{r_s}\right) \qquad \text{(Link, et. al., 1985) (5-22)}$$

For the radius r_w of the outermost watertight shell surface, the nonuniform component of the radial stresses are determined by the equation:

$$\sigma_{r_w} = -0.5 \cdot \omega \cdot P_o \cdot \frac{r_a \cdot A_i}{r_w \cdot A}\left\{\left(1 + \frac{y_i}{r_s}\right) + \left[\left(1 + \frac{r_s \cdot y_i}{i^2}\right)\left(1 - \frac{4r_{si}}{3r_w}\right) + \frac{4r_s}{3r_w} \cdot \frac{i^2_i}{i^2} - \left(1 + \frac{y_i}{r_s}\right)\frac{1}{\zeta}\left[\frac{\zeta}{\zeta - 1} \cdot \cos 2\phi\right]\right\} \qquad \text{(Link, et. al., 1985) (5-23)}$$

For the radius r_w of the outermost watertight shell surface, the shear stresses are calculated using:

$$\tau_w = \frac{1}{3} \cdot \omega \cdot P_o \cdot \frac{r_a \cdot r_{si}}{r_w^2} \cdot \frac{A_i}{A}\left[\left(1 + \frac{r_s \cdot y_i}{i^2}\right) - \frac{r_s \cdot i^2_i}{r_{si} \cdot i^2}\right]\frac{\zeta}{\zeta - 1} \cdot \sin 2\phi \qquad \text{(5-24)}$$

(Link, et. al., 1985)

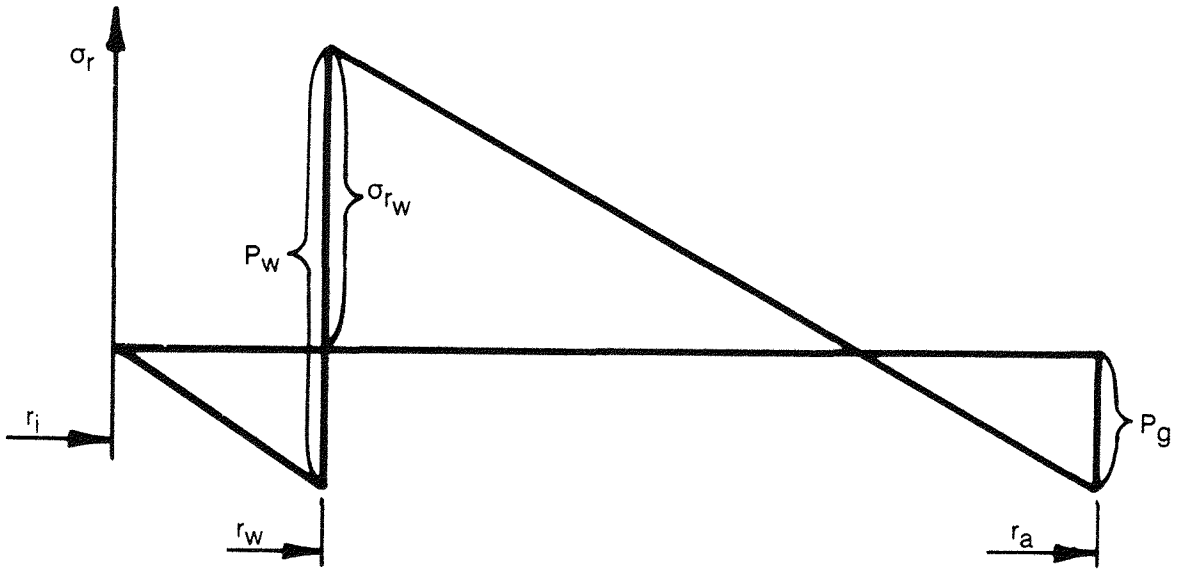

RADIAL STRESS

RADIAL STRESS
FIGURE 5.3

If the sums of uniform plus nonuniform components of radial stress are positive values, then the stresses are tensile and the bond between shells must be secured by mechanical means for the lining to be considered bonded. For design of mechanical bonds between shells see Section 5.3.6, Anchoring to Prevent Shell Separation. If this is not done, then proceed as described in Section 5.3.3, Stress Determination in Linings with No Bond or Partial Bond. This is also true if the shear stress exceeds the allowable shear τ_a as determined by Equation 5-3 or if negative values of the sums of uniform plus nonuniform components of radial stress exceed the allowable compressive stress as shown in Table 5.1.

5.3.3 Stress Determination in Linings with No Bond or Partial Bond

When, in a lining consisting of several shells, stresses between the shells exceed the allowable stress values determined as described in Section 5.2, Material Properties, and the bond is not mechanically secured, the stress determination must be repeated. It is then assumed that the shells are separated at the lining interfaces and are loaded by uniform and nonuniform pressures. Stresses from this analysis should not exceed the allowable stress values calculated as described in Section 5.2, Material Properties. If they do, the lining must be redesigned.

Buckling analysis for this type of lining should be conducted in accordance with Section 5.3.5.3, Buckling Safety for Linings with No Bond or Partial Bond.

5.3.4 Shaft Lining Stresses Due to Time Delayed Rock Displacements

5.3.4.1 Rock Coupled Lining

Axial (compression or tension) stress with ϵ_{max}

$$\sigma_{max} = \pm E \bullet \epsilon_{max} \qquad (5\text{-}25)$$

where: E = modulus of elasticity of lining materials

and ϵ_{max} = maximum axial strain of shaft lining column

For values of ϵ_{max}, see Kratzsch (1983).

Although it is unlikely that the exploratory and repository shafts will be exposed to shear deformation caused by repository subsidence, the shear stress may be calculated as follows:

$$\tau_{max} = G \bullet \beta \qquad \text{(Link, et. al., 1985)} \quad (5\text{-}26)$$

where: β = angle of displacement of strata due to subsidience (radians) (See Figure 5.4)
G = shear modulus (psi, kPa)

and:
$$G = \frac{E}{2(1+\nu)} \qquad (5\text{-}27)$$

where: ν = Poisson's Ratio

with: $\nu = \frac{1}{3}$ for steel and ductile cast iron
$\nu = \frac{1}{6}$ for concrete

Longitudinal bending stress, with R as in Section 4.3.1, Loads from Time-Delayed Rock Displacements, are calculated by:

$$\sigma_{max} = \pm E \bullet \left(\frac{1}{R}\right) \bullet r_a \qquad (5\text{-}28)$$

where: E = modulus of elasticity of the lining material (psi, kPa)
r_a = radius of the outer lining surface being analyzed (in, mm)
R = Longitudinal Bending Radius (Section 4.3.1, Loads from Time-Delayed Rock Displacements)

The axial, shear, and longitudinal bending stresses must be superimposed on the uniform and nonuniform stresses in their proper plane of analysis. The resultant total stress must not exceed the allowable material stresses. Where stresses exceed the allowable material stresses, provisions must be made in the lining configuration to negate the effect of the stress combinations.

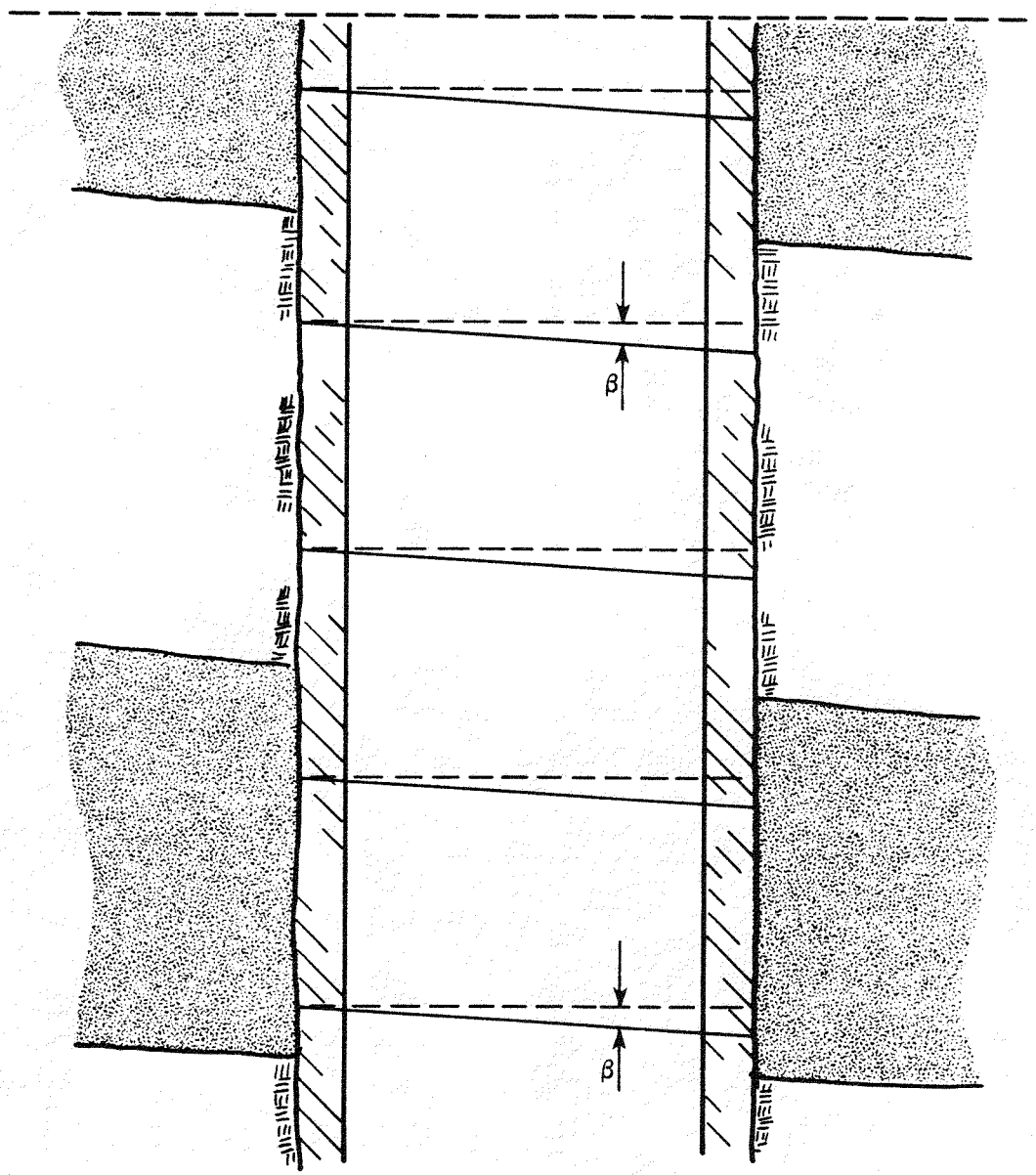

ANGULAR DISPLACEMENT OF SHAFT AND SURROUNDING STRATA DUE TO SUBSIDENCE

FIGURE 5.4

5.3.4.2 Lining Surrounded by Asphaltic Sealant Material

Axial stress within the lining column surrounded by ASM with τ_{max} as shown in Section 4.3, Other Loading Considerations, is calculated by:

$$\sigma_{max} = \pm 2r_a \cdot \pi \cdot \tau_{max} \cdot \frac{L}{F} \qquad (5\text{-}29)$$

where: L = lining length (in, mm)

F = horizontal lining cross-sectional area (in^2, mm^2)

$F = (r^2_a - r^2_i)\pi$

τ_{max} = axial shear (psi, kPa)

Longitudinal bending stress:

$$\sigma_{max} = \pm E \cdot \left(\frac{1}{R}\right) \cdot r_a \qquad (5\text{-}30)$$

The axial stresses and the longitudinal bending stresses must be superimposed on the uniform and nonuniform stresses in their proper plane of analysis. The resultant total stress must not exceed the allowable material stresses calculated by using the factors shown in Tables 5.1, 5.2, 5.3, and 5.5, and the procedures presented in Section 5.2.4, Lining Stresses for Total Load.

5.3.5 Buckling Safety of Lining Rings

The buckling safety of lining rings in all lining types must be determined by assuming that the uniform pressure P_O acts on the outer surface of the lining. As the approach taken is conservative, the nonuniform component of load P_ϕ is not considered in the buckling analysis (Link, et. al., 1985).

The slenderness ratio λ of the lining dictates the approach taken to determine buckling safety:

$$\lambda = \frac{\pi \cdot r_s}{\sqrt{3} \cdot i} \qquad \text{(Link, et. al., 1985)} \quad (5\text{-}31)$$

where: $\lambda \geq 66$ is considered a thin shell

$\lambda < 66$ is considered a thick shell

where: $\lambda \leq 20$ is considered an extremely thick shell and no further buckling analysis is required

To calculate λ when P_o acts on the outer lining surface, consider the real cross section of all shell materials and determine the radius r_s to the neutral axis of the total cross section and its radius of gyration $i = \sqrt{\frac{I}{A}}$. If the lining consists of several unbonded concentric shells, and P_o acts on the outer shell and a portion of the pressure P_o acts on the surface of the next interior shell, radial tensile stresses are created and should be calculated for σ_{r_w} using Equations 5-22 and 5-23. In this case, the slenderness ratio of each individual cross section must be calculated separately and the buckling safety proven (see section 5.3.5.3, Buckling Safety for Linings with No Bond or Partial Bond).

5.3.5.1 Buckling Safety of Lining Rings with a Slenderness Ratio $\lambda \geq 66$ (Thin Shell)

The buckling safety of all linings should be determined using:

$$\sigma_{cr_i} = \frac{3\, E_{\phi i} \bullet i_i^2}{r_{s_i}^2} \qquad \text{(Link, et. al., 1985) (5-32)}$$

where:
- σ_{cr_i} = critical buckling stress of shell
- $E_{\phi i}$ = modulus of elasticity of shell material (psi, kPa)
- i_i = radius of gyration of shell (in, mm)
- r_{s_i} = radius of neutral axis of shell (in, mm)

If σ_{cr_i} is less than σ_{cr} determined from Table 5.5, use σ_{cr} obtained from Table 5.5.

The factor of safety FS required to preclude material failure is determined by:

$$FS = \frac{\Sigma(A_i \bullet \sigma_{cr_i})}{P_o \bullet r_a} \geq 1.5 + \frac{\lambda}{120} \qquad \text{(Link, et. al., 1985) (5-33)}$$

- A_i = unit cross sectional area of each shell (in^2, mm^2)
- P_o = uniform component of total load (psi, kPa)
- r_a = outer radius of the lining (in, mm)

5.3.5.2 Buckling Safety of Lining Rings with a Slenderness Ratio of $20 < \lambda < 66$ (Thick Shell)

The factor of safety (FS) required to preclude material failure is determined by:

$$FS = \frac{\Sigma(A_i \bullet \sigma_{cr_i})}{P_o \bullet r_a} \bullet \frac{r_s}{r_a} \geq 1.5 + \frac{\lambda}{120} \qquad \text{(Link, et. al., 1985) (5-34)}$$

where: σ_{cr_i} = critical buckling stress from Table 5.5 of each shell (psi, kPa)

r_s = radius to neutral axis of lining (in, mm) (Figure 5.2)

For composite linings properly anchored, use the real cross sectional area A of the individual shell materials and for σ_{cr} use the corresponding values from Table 5.5.

5.3.5.3 Buckling Safety for Linings with No Bond or Partial Bond

The buckling stresses for the individual shells should be calculated separately by assuming that (1) the hydrostatic pressure P_w acts on the exterior surface of the watertight inner shell, (2) the ground pressure P_g acts on the exterior surface of the concrete lining, and (3) that the watertight shell is separated from the concrete. In this case, an analysis based on Amstutz (1970) should be performed on the forces acting between the inner steel shell and the outer concrete lining. Because these are confining forces, they restrain buckling. Buckling safety of the inner lining should be calculated using:

$$\zeta_{cr} = \frac{P_{cr}}{P_o} \geq 2.0 \qquad (5\text{-}35)$$

and: $$P_{cr} = \frac{3EI}{r^3} \qquad \text{(Euler's Formula)}$$

For thin steel shells the Amstutz (1970) and Hertrich (1965) results must be examined. For a cast iron tubbing with a concrete envelope with no bond or partial bond see Section 5.5.2, Cast Iron Tubbing and Concrete Envelope Stress Analysis.

5.3.6 Anchoring to Prevent Shell Separation

5.3.6.1 Types of Anchoring

Bonding between inner steel lining shells and concrete can be achieved by straight, flat bar anchors welded to the steel shells. Tensile radial stresses can be compensated by anchors only. Between the outer steel and the concrete, shear transfer by friction is possible if the radial stress at the interface is $\sigma_r \geq \frac{\tau}{\mu}$ (see Section 5.2, Table 5.3), otherwise, bonding should be established by installing anchors. Where ductile cast iron tubbing is used as a lining, shear transfer by the tubbing ribs only is allowable.

The design of welds used to connect the anchors to the steel shells should be executed in compliance with applicable paragraphs of the AISC Specification for the Design, Fabrication and Erection of Structural Steel for Buildings, Section 5.1 (1978), and with applicable sections of the Prestressed Concrete Institute, PCI Design Handbook, (1985).

5.3.6.2 Dimensioning of Anchors

The stresses σ_r and τ at the interface between concrete and steel should not exceed the values calculated by using the factors shown in Tables 5.2 and 5.3.

If the separating stresses are carried by anchors which are positioned at an angle α to the inside steel lining, the anchor cross section (f_a) should be calculated using:

$$f_a = \frac{F_A}{2\sigma_A}\left(\frac{\tau}{\cos\alpha} + \frac{\sigma_r}{\sin\alpha}\right) \qquad \text{(Link, et. al., 1985) (5-36)}$$

where:
- f_a = cross sectional area of one anchor (in^2, mm^2)
- F_A = lining area influenced by a pair of anchors (in^2, mm^2)
- α = angle between anchor and the inside steel lining (degrees)
- σ_r = radial compressive stress (psi, kPa)
- τ = shear stress (psi, kPa)
- σ_A = maximum allowable stress in anchor (psi, kPa) in both anchor directions. The tensile stress used in dimensioning the anchor shall not exceed the allowable stress of the material used.

The force separating the shells produces tension in both anchor directions. The tensile stress used in dimensioning the anchor should not exceed the allowable material stress.

If $\sigma_r > 0$, and $a < \delta$

$$f_a = \frac{F_A}{\sigma_A} \cdot \frac{\tau + \mu \sigma_r}{\cos a + \mu \sin a} \qquad \text{(Link, et. al., 1985) (5-37)}$$

where: δ = angle between resultant of the radial and shear stresses and the inside steel lining (degrees)

The force separating the shells produces tension in an anchor in one direction and compression between the concrete and inner shell in the other direction which deviates from the vertical orientation relative to the shaft wall by an angle of ρ where ($\tan \rho = \mu$).

If $\sigma_r > 0$ and $a > \delta$, or when $\sigma_r < 0$, the angle δ is determined by:

$$\delta = \tan^{-1}\left(\frac{\sigma_r}{\tau}\right) = \text{angle in degrees whose arc tangent is the ratio of the radial compressive stress to the shear stress}$$

To compensate for the shear stresses, the anchors may be arranged either at a right angle or askew to the wall. If askew anchors are used ($\alpha \neq 90°$) they must be arranged in two directions corresponding to the possible orientation of the shear stresses. Also, they must be arranged in groups dimensioned by f_a as determined by Equations 5-36 or 5-37.

Furthermore, the following stresses must be analyzed:

1. Stresses in the concrete caused by the anchor.
2. Stresses where the anchor is joined to the steel shell.
3. Bending stresses in the steel shell caused by the anchor.

If shear stresses are to be resisted by anchors, then the required anchor capacity D is derived from the shear stress using:

$$D = \tau \cdot F_A \qquad \text{(Link, et. al., 1985) (5-38)}$$

The average concrete stress at the anchor should not exceed the values for total load calculated by using the factors shown in Table 5.2. The stresses where the anchor is joined to the steel shell and the bending stresses in the steel shell caused by the anchor must also be determined.

The bending moment of the anchor M_D acting on the steel shell is determined using:

$$M_D = D \cdot \frac{h + d}{2} \qquad \text{(Link, et. al., 1985) (5-39)}$$

where: h = anchor length (in, mm)
d = steel shell thickness (in, mm)

5.3.6.3 Anchor Connections

All bolted connections and welds should be designed according to the AISC Manual of Steel Construction (1980) with the exception that allowable stresses should be increased for specified load combinations as detailed in Section 5.1, Shaft Lining Materials.

Note: Equation numbers 5-40 to 5-43 intentionally not used.

5.4 STRESSES DUE TO EARTHQUAKES

When evaluating seismic effects on the shaft the designer must keep in mind that an earthquake imposes oscillating displacements and strains on the shaft. Accordingly, the shaft will not continue to freely deflect under these conditions; the displacements will be quite small and limited. The calculated stresses will vary between plus and minus values. It is not a static loading problem, where applied forces could drive a structure to failure. Cracking of the concrete shell of the lining due to possible induced tension is not a design concern because the cracks will be small and the transitory nature of the strain field means the cracks will close after

the passage of the seismic disturbance and restore the normal load-carrying capability of the concrete. To ensure this behavior, where calculated seismic stresses exceed the concrete tensile strength, welded wire mesh or bar reinforcement to meet nominal temperature reinforcement requirements shall be used to maintain crack distribution and containment of the concrete shell. Further, the concrete shell will be reinforced in the circumferential direction where necessary (and stress checked by Equation 5-6) to ensure that hoop compression does not induce a concrete crushing failure.

The overall seismic design philosophy is to evalute the shaft structure for the transient strains to ensure that watertightness, which is especially important in areas of potential water inflow, is maintained and collapse is prevented. In general, these criteria are met by the presence of a steel lining whose total stress is kept below yield and by providing proper reinforcing of the concrete portion of the lining to preclude hoop failure. Reinforcement of the concrete lining to resist longitudinal seismic stresses is considered unnecessary because circumferential cracking (if any) would be similar to the condition of a segmented lining. The segments, or cracks, accommodate the longitudinal strain, reduce the longitudinal stress to zero and do not contribute to a collapse mechanism. Likewise, reinforcement of the concrete lining to resist circumferential tension is considered unnecessary because the development and temporary opening of radial cracks does not contribute to a collapse mechanism.

In the discussion that follows, induced seismic strains are converted to stresses for simplicity's sake. Also, the benefits of interaction of soil and structure are ignored, except as related to induced shear strains in a vertical plane through the shaft and nonuniform hoop deformations. For these two load conditions the simplified approach is simply too conservative so interaction is not neglected.

The effects of earthquake ground motion are amplified near the ground surface because of interactions between incoming and reflected waves. For the Deaf Smith County, Texas site that amplification is enhanced because the near surface materials have a relatively low modulus. The seismic effects are greatest near the surface and diminish significantly with depth to values that are most likely negligible for design. At depths greater than a few hundred feet it is expected that the calculated seismic stresses will be so small that when they are combined, and then added to the stresses caused by nonseismic loads, they can still be accommodated within the parameters allowed for the materials. If this is not the case, the seismic effects are to be considered as induced strains in a nonlinear analysis or should be treated by a soil-structure interaction analysis as described later.

The passage of earthquake waves through the soil causes four distinct deformation patterns of the shaft opening. These are: (1) longitudinal or axial strains which are uniform over the section, (2) shear strains acting on horizontal sections of the shaft, (3) flexural strains resulting from bending of the shaft which in this case is considered to be a vertical beam and, (4) hoop strains arising either from the influence of axial strains as described by Poisson's ratio or from ovaling deformations (see Figure 5.5).

The design significance of seismic loads as an induced strain problem is that, if computed stresses are too high, a corresponding increase in lining thickness (and/or stiffness) will, in effect, attract greater loads into the lining and therefore do little to reduce the overstress. The proper design response for an overstress condition is to use a strain acceptance criterium and to employ ductile detailing. The seismic design objective is to focus on the stresses in a horizontal plane through the lining. For the steel lining shell the axial, hoop, and shear stresses are limited by the Hencky-von Mises yield criteria (Equation 5-4) to ensure structural integrity. For the concrete lining shell, hoop compression stresses are limited to design allowables in order to prevent crushing. Concrete tension can be ignored, however, because nominal temperature reinforcement and the steel lining ensure crack distribution and containment.

The notation used for the seismic analyses of the site quite properly corresponds to Cartesian coordinates (see Figure 5.6), so the free-field ground strains are also expressed in this system, e.g., ϵ_{xx}, ϵ_{zz} and γ_{xz}. Consequently, the free-field stresses (where these are used) are also expressed in this system, e.g., σ_x, σ_y, σ_z and τ_{xz}. However, once the vertical shaft is introduced into the system, it is easier to use a cylindrical coordinate system to express strains, e.g., ϵ_t, ϵ_r and γ_{tz} and stresses, e.g., σ_t, σ_r, σ_z and τ_{tz} in the lining (see Figure 5.6). The relationship between these systems and those subsequently used in Section 5.2.4, Lining Stresses for Total Load, for allowable stresses is described at the end of this section by two detailed examples and explanatory sketches.

The nomenclature traditionally used in earthquake engineering has been adopted for use in this section on stresses caused by earthquakes. Because some of the terms differ from those used elsewhere in this guide, a separate list of the abbreviations and symbols used in this section is provided in Section 10.3, Abbreviations and Symbols (used in Section 5.4).

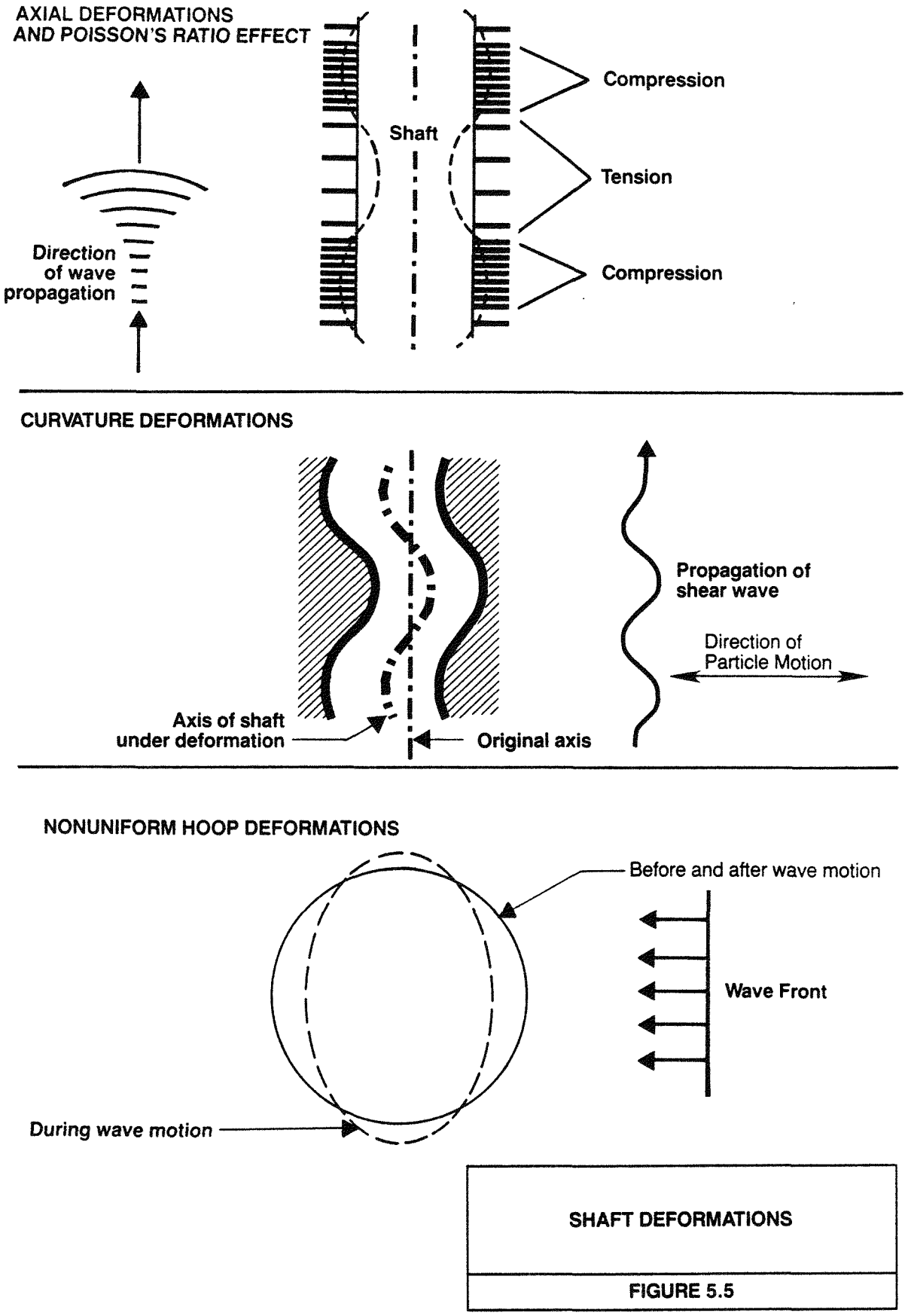

SHAFT DEFORMATIONS

FIGURE 5.5

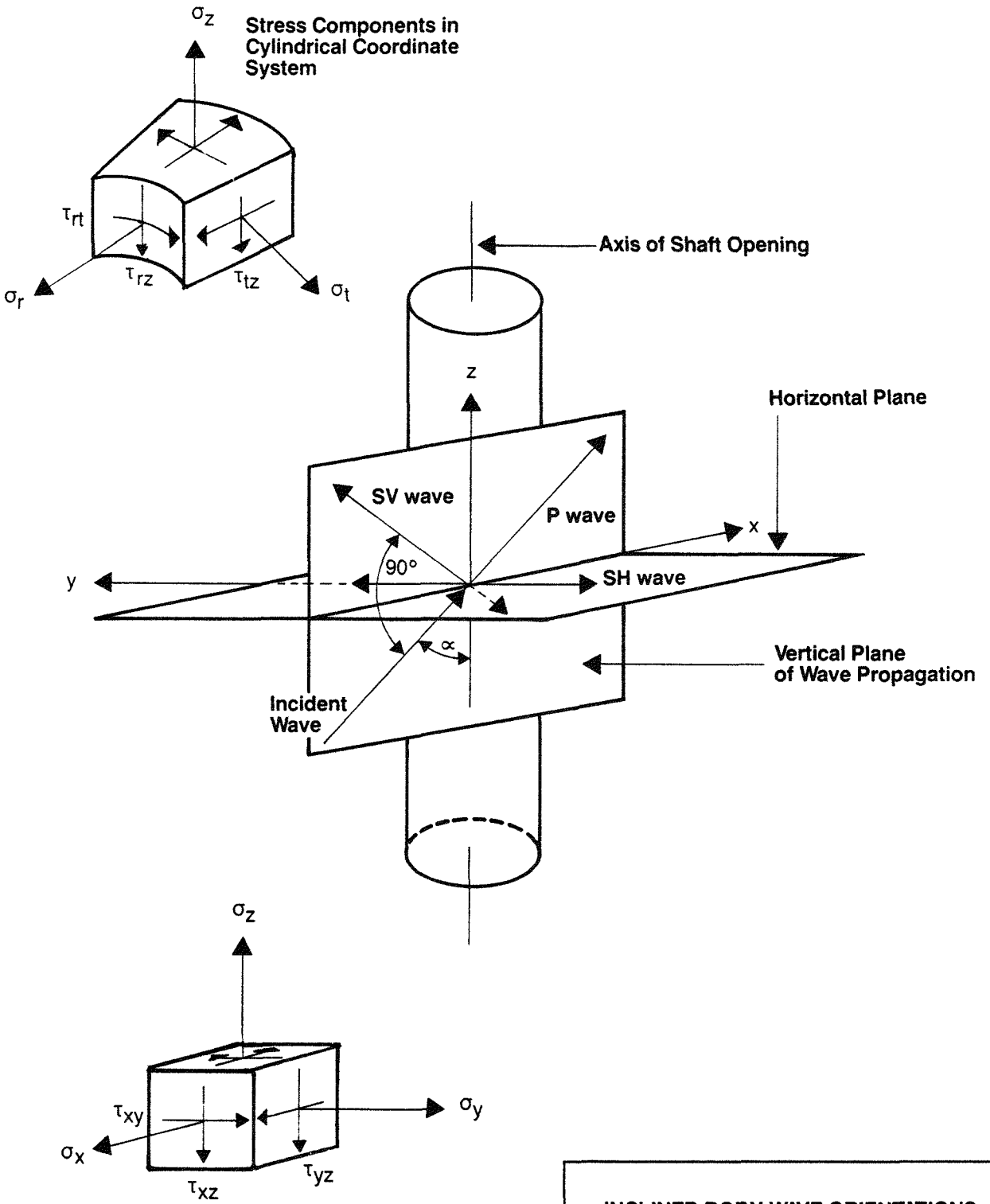

INCLINED BODY WAVE ORIENTATIONS AND STRESS COMPONENTS

FIGURE 5.6

5.4.1 Seismic Loads on Shaft

The response of a vertical shaft to seismic motions should be considered in terms of transient wave forms which cause deformations in the ground around the shaft. A conservative assumption that the shaft lining will deform in accordance with the surrounding ground should be made. In general, ground accelerations, velocities, displacements, and strains which are calculated to occur in the free field in the absence of the shaft are imposed on the lining as design requirements. The exceptions to this general approach have been discussed in the introduction above.

In the discussion that follows, the ground deformations are treated as static load effects. It is appropriate to ignore dynamic amplification when the length of waves impinging on an underground opening is on the order of eight times or more greater than the opening width (Hendron and Fernandez, 1983). When the shaft opening is 20 ft. (6.1 m) in diameter and apparent horizontal wave velocities are on the order of 5000 ft/sec (1525 m/sec), incident ground motions with frequencies less than 30 Hz will not cause significant dynamic amplification. Therefore, the seismic loading can be considered as a pseudo-static load.

Compression and shear waves are assumed to propagate in a direction parallel to the axis of the shaft. This is consistent with the methodology used to obtain the site response with depth (Section 4.4.2, Site Response Analysis). Compression waves produce axial strains, both tension and compression, parallel to the shaft axis (see Figure 5.5) and uniform hoop deformations due to Poisson's ratio effect. Shear waves result in shear strains and curvature of the shaft opening (see Figure 5.5).

In addition, nonuniform hoop deformations can develop in the lining because the horizontal component of body waves (both compression and shear) propagate upward at an angle of incidence (other than parallel) to the shaft axis (see Figure 5.6).

Less conservative assumptions can be made which account for interaction between the lining and shaft opening and result in stresses lower than those given by the expressions in the following sections. An alternative analysis approach which includes full interaction is the dynamic-stiffness matrix method (Wolf, 1985). If an alternative analysis is used, it must be qualified by supporting documentation.

5.4.2 Longitudinal Stresses

The maximum longitudinal (axial) stress (psi, kPa) in the shaft lining is given by Yeh (1974):

$$\sigma_a = E'_d \epsilon_{zz} \tag{5-44}$$

where: E'_d = dynamic Young's modulus of the lining material (psi, kPa)

ϵ_{zz} = maximum vertical ground strain (in/in, mm/mm) in free field (Section 4.4.2 Site Response Analysis, and SRP Input to Seismic Design (ISD), Chapter 4, Development of Seismic Design Parameters) at the depth under consideration

The stress σ_a is one of the contributors to the vertical lining stress, σ_z.

5.4.3 Shear Stresses

When calculating the effect of shear strains on the lining, two alternative types of behavior should be evaluated and the larger of the two computed values of shear strain used for design.

When the wavelengths of concern are relatively short and the lining stiff in comparison to the soil, the primary mode of shaft behavior is bending. In this circumstance the bending is calculated by assuming that the shaft centerline moves with the soil. The amplitude of that motion is calculated from the free field shear strain and the wavelength as given in the subsequent discussion.

For larger wavelengths and closer correspondence between the lining and the soil stiffnesses, there is a more direct transfer of shear strain into the lining. In this case the maximum shear strain in the lining is calculated from a pure shear interaction solution given in the following discussion.

For primary bending behavior, the maximum induced shear strain acting on a horizontal section (or plane) of the lining is given by (see Appendix D):

$$\gamma^*_{zy} = \frac{8\pi^2 E'_d I}{G'_d A L^2} \gamma_{zy} \tag{5-45}$$

where: I = moment of inertia of the shaft cross section (in^4, mm^4)

A = cross-sectional area of the shaft lining (in^2, mm^2)

L = wavelength corresponding to the predominant frequency of the maximum free-field shear strain (in, mm) as given in ISD, Section 4.4.6, Strain Compatible Moduli and Poisson's Ratio

γ_{zy} = maximum horizontal shear strain (in/in, mm/mm) in free field (Section 4.5.2, Site Response Analysis and ISD, Chapter 4, Development of Seismic Design Parameters) at the depth under consideration

G'_d = dynamic shear modulus of the lining material (psi, kPa)

The shear strains on horizontal sections given above by Equation 5-45 are based upon simple beam theory. Their distribution over a horizontal section of the shaft varies from the maximum value (as computed), which occurs on the neutral axis of the shaft considered as a vertical beam, to zero at the outer most point. Induced shearing strains computed in accordance with beam theory are substantially less than those that would be calculated by assuming the shaft lining to undergo pure shear deformations equal to the free field values at typical frequencies (1 Hz) at the Deaf Smith County site. Soil-structure interaction (SSI) studies, using the soil properties at the site from the SRP Data Base, indicate that at the predominant wavelengths of interest in soft soils, the shaft structure deflects elastically in bending, not shear. The related shear strains are simply and conservatively calculated by imposing on the shaft lining a sinusoidal flexural deflection pattern whose maximum slope is equal to the free field shear strain. Such SSI studies have shown the maximum shear strain in the lining to be reduced from free field values by a factor of 10 or more.

With longer wavelengths and soil stiffness approaching that of the lining, the free field shear strains are more readily coupled into the shaft such that the resulting lining shear strains approach those in the free field. This behavior, however, tends to occur at depth where the free field shear strains are much smaller. For this case of pure shear interaction, the maximum induced shear strain acting on a horizontal section (or plane) of the lining is given by (see Appendix D):

$$\gamma^*_{zy} = \frac{2\left(1 - \frac{a^2}{R^2}\right)\gamma_{zy}}{\left(1 + \frac{a^2}{R^2}\right) + \frac{G'_d}{G_d}\left(1 - \frac{a^2}{R^2}\right)} \qquad (5\text{-}46)$$

where: R = outer radius of lining (in, mm)

a = inner radius of lining (in, mm)

G_d = dynamic shear modulus of the soil (psi, kPa)

The shear strain given above by Equation 5-46 varies from the maximum value (as computed), which occurs on the outer radius of the lining on the y axis, to zero at the inner radius of the lining on the y axis. Induced shear strains computed in accordance with Equation 5-46 are typically much less than the free field shear strains.

The maximum shear stress (psi, kPa) acting on a horizontal section (or plane) of the lining is now given by:

$$\tau_{zy} = \tau_{yz} = G'_d \gamma^*_{zy} \tag{5-47}$$

where: γ^*_{zy} = induced shear strain (in/in, mm/mm) from Equations 5-45 or 5-46, whichever is greater

Except for very stiff soil layers, the horizontal shear stresses are likely to be negligible and can be ignored in design as has been the traditional practice for buried pipelines (American Society of Civil Engineers, 1983).

5.4.4 Flexural Stresses

Curvature along the shaft axis results in maximum longitudinal flexural stresses (psi, kPa) in the shaft lining given by Yeh (1974):

$$\sigma_b = \pm E'_d r \kappa \tag{5-48}$$

where: E'_d = dynamic Young's modulus of the lining material (psi, kPa)

r = distance from the shaft centerline to the fiber under consideration (in, mm), (see Figure 5.8)

κ = free-field ground curvature (1/in, 1/mm) (Section 4.4.2, Site Response Analysis, and ISD Chapter 4, Development of Seismic Design Parameters) at the depth under

consideration, or curvature resulting from shear deformation discussed in Section 5.4.3, Shear Stresses, whichever is greater. In the latter case, the curvature is given by (see Appendix D):

$$\kappa = \frac{2\pi\gamma_{zy}}{L} \tag{5-49}$$

Note in Equation 5-49 that the expression is for curvature in the zy plane, corresponding to the free-field shear strain γ_{zy}. Accordingly, when computing curvature for motions in the zx plane, the free field shear strain γ_{zx} should be used.

At locations away from strata layer interfaces, the free-field ground curvature is equal to the ratio of the free field acceleration to the square of the shear wave propagation velocity at the depth under consideration.

The stress σ_b is one of the contributors to the vertical lining stress σ_z. The calculated results using Equations 5-44, 5-47 and 5-48 are valid only for continuous shaft linings.

5.4.5 Hoop Stresses

Circumferential stresses in the lining caused by both uniform and nonuniform hoop deformation of the shaft opening are treated by first calculating the free-field strains for each wave type. These strains are then converted to free-field principal stresses. Finally, shaft lining stresses are evaluated for the two cases – with and without ground interaction.

Nonuniform hoop deformations arise from two kinds of free-field strain fields: one due to inclined P-SV waves (both incident P and incident SV) and the other due to inclined SH waves (see Figure 5.6). Inclined P-SV waves result in the following nonzero, three-dimensional strain components:

γ_{xz}, ϵ_{xx} and ϵ_{zz}

These are available from an inclined wave analysis (see Section 4.4.2, Site Response Analysis, and the ISD, Chapter 4, Development of Seismic Design Parameters). All such strains can be either plus or minus.

In the following discussion they consistently do not have a sign. However, because the most critical stress conditions are caused when the strains are considered as either all positive or all negative, they should be so treated. Hence, all subsequent calculated stresses and strains can be of either sign.

Using conventional stress-strain relationships (Timoshenko and Goodier, 1970), the corresponding stress field (psi, kPa) is given by the following (see also Figure 5.7):

$$\sigma_x = 2G_d\epsilon_{xx} + \lambda_d(\epsilon_{xx} + \epsilon_{zz}) \quad (5\text{-}50)$$

$$\sigma_y = \lambda_d(\epsilon_{xx} + \epsilon_{zz}) \quad (5\text{-}51)$$

$$\sigma_z = 2G_d\epsilon_{zz} + \lambda_d(\epsilon_{xx} + \epsilon_{zz}) \quad (5\text{-}52)$$

$$\tau_{xz} = \tau_{zx} = G_d\gamma^*_{zx} \quad (5\text{-}53)$$

where: G_d = dynamic shear modulus of the soil (psi, kPa)

$\lambda_d = \frac{\nu_d E_d}{(1 + \nu_d)(1 - 2\nu_d)}$; dynamic Lamé's constant of the soil

E_d = dynamic Young's modulus of the soil (psi, kPa)

ν_d = dynamic Poisson's ratio of the soil

γ^*_{zx} = the maximum induced shear strain (in/in, mm/mm) calculated from either Equation 5-45 (with γ_{zy} replaced by γ_{zx}) or Equation 5-46 (with γ_{zy} replaced by γ_{zx}), whichever is greater

Hoop deformations are obtained by examining the stresses on a horizontal slice through the shaft (see Figure 5.7). Because the horizontal shear stresses are zero on the vertical faces of such sections, the normal stresses σ_x and σ_y, calculated using Equations 5-50 and 5-51, are also the principal stresses σ_1 and σ_3, respectively. The out-of-plane shear stress τ_{xz} does not induce any in-plane direct stress because the medium is assumed to be isotropic.

Uniform hoop deformations arise from vertically propagating P waves. These stress effects are greatest near the surface and should be considered acting in conjunction with other lining stresses caused by

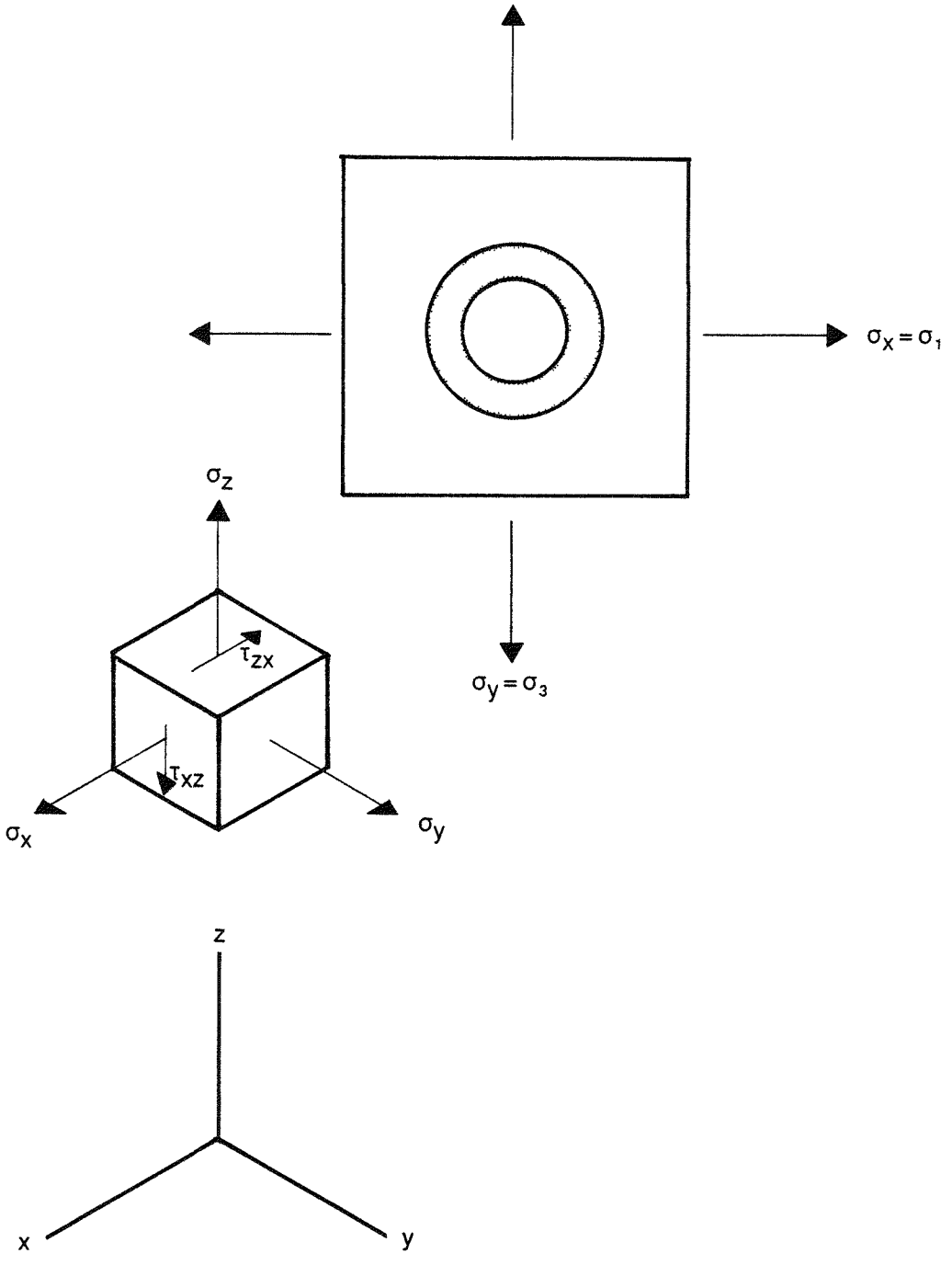

FREE FIELD PRINCIPAL STRESS STATE FOR SHAFT HOOP DEFORMATION UNDER INCLINED P AND SV WAVES

FIGURE 5.7

vertically propagating P waves. Vertically propagating P waves result in a single nonzero, three-dimensional strain component, ϵ_{zz}, obtained from the site response analysis for vertically propagating body waves (Section 4.4.2, Site Response Analysis). The corresponding free-field normal stresses are given by Equations 5-50 and 5-51 as $\sigma_x = \sigma_y = \lambda_d \epsilon_{zz}$. Lining stresses (uniform hoop deformations) are obtained in the same manner as that used for nonuniform hoop deformations (see Figure 5.7), except in this case the principal stresses are equal, viz., $\sigma_1 = \sigma_3 = \sigma_x$.

Inclined SH waves result in the following nonzero, three-dimensional strain components:

$$\gamma_{xy} \text{ and } \gamma_{yz}$$

These are available from the inclined wave analysis (see Section 4.4.2, Site Response Analysis, and the ISD Chapter 4, Development of Seismic Design Parameters). Using conventional stress-strain relationships, the corresponding stress field (psi, kPa) is given by the following (see also Figure 5.8):

$$\tau_{xy} = \tau_{yx} = G_d \gamma_{xy} \tag{5-54}$$

$$\tau_{yz} = \tau_{zy} = G_d \gamma^*_{zy} \tag{5-55}$$

where: γ^*_{zy} = the maximum induced shear strain (in/in, mm/mm) calculated from either Equation 5-45 or Equation 5-46, whichever is greater. These shear stresses are shown in Figure 5.8

The horizontal shear stresses (see Figure 5.8) are seen to be the principal shear stresses. Accordingly, the principal normal stresses, σ_1 and σ_3, can be derived directly from τ_{xy}, given in Equation 5-54, i.e., $\sigma_1 = \tau_{xy}$, and $\sigma_3 = -\sigma_1$.

With the free-field principal horizontal stresses and axial strain known, the stresses in the lining can now be calculated using one of two approaches given in the following discussion. A simplified conservative method is given first followed by the interaction solution.

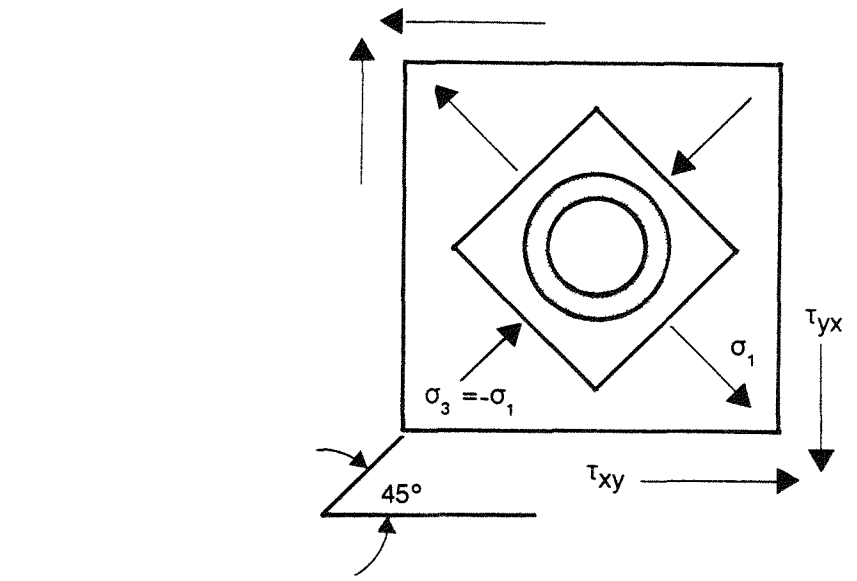

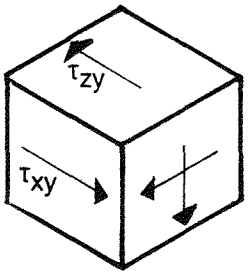

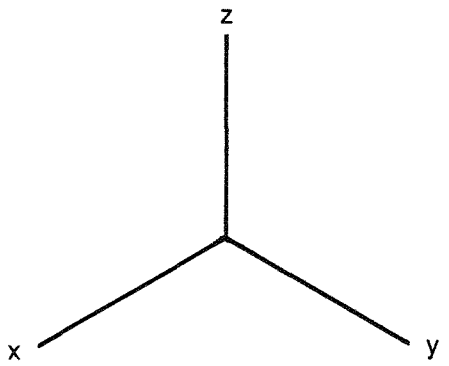

FREE FIELD PRINCIPAL STRESS STATE FOR SHAFT HOOP DEFORMATION UNDER INCLINED SH WAVES

FIGURE 5.8

For simplicity in computing lining stress effects, it is conservative to impose on the outer surface of the shaft lining the hoop strains that would exist at the edge of the circular shaft opening in the absence of the lining. This approach assumes the lining to have no stiffness. It should be noted, however, that this approach is excessively conservative when the ratio of elastic moduli of the shaft lining to the soil is high. The circumferential (hoop) stress σ_t in the ground at the edge of the opening is given by the following (Timoshenko and Goodier, 1970):

$$\sigma_t = (\sigma_1 + \sigma_3) - 2(\sigma_1 - \sigma_3) \cos 2\theta \tag{5-56}$$

where: σ_1 and σ_3 = the free-field principal stresses (psi, kPa)
θ = the angle measured from σ_1

The corresponding hoop strain, ϵ_t, at this intersection is given by:

$$\epsilon_t = \frac{1}{E_d}(\sigma_t - \nu_d \sigma_z) \tag{5-57}$$

In the following discussion a plane strain field is assumed in the out-of-plane direction. That is, ϵ_{zz} is taken as a constant equal to the free field value.

For the case of inclined P and SV waves the hoop strain is obtained by substitution of Equations 5-50, 5-51 and 5-56 into Equation 5-57; and noting that $\sigma_z = E_d \epsilon_{zz} + \nu_d \sigma_t$ because of the assumption of a uniform strain, ϵ_{zz}:

$$\epsilon_t = \epsilon_{tA} - \epsilon_{tB} \cos 2\theta \tag{5-58}$$

where:
$$\epsilon_{tA} = \frac{(1 - \nu_d)}{(1 - 2\nu_d)} \cdot \epsilon_{xx} + \frac{\nu_d}{(1 - 2\nu_d)} \cdot \epsilon_{zz} \tag{5-59}$$

$$\epsilon_{tB} = 2(1 - \nu_d)\, \epsilon_{xx} \tag{5-60}$$

Likewise, for the case of inclined SH waves, Equations 5-54 and 5-56 are combined with Equation 5-57 to yield the maximum hoop strain given by:

$$\epsilon_t = -2(1 - \nu_d)\, \gamma_{xy} \cos 2\theta \tag{5-61}$$

Using conventional stress-strain relationships, the resulting hoop-axial stress field in the lining is given by the following (see Appendix D):

$$\sigma_t = \frac{E'_d}{1-\nu'^2_d}(\epsilon_t + \nu'_d \epsilon_{zz}) \tag{5-62}$$

$$\sigma_z = \frac{E'_d}{1-\nu'^2_d}(\epsilon_{zz} + \nu'_d \epsilon_t) \tag{5-63}$$

where: ϵ_t = hoop strain computed by Equations 5-58 or 5-61, as appropriate
ν'_d = dynamic Poisson's ratio of the lining material

Note in the foregoing that the soil and rock material properties are used in Equations 5-58 and 5-61 to compute imposed strains, whereas the shaft lining material properties are used in Equations 5-62 and 5-63 to compute resulting stresses. Further, if axial stress is treated by Equation 5-44 for ϵ_{zz}, then the ϵ_{zz} term in Equation 5-63 for σ_z above should be disregarded.

The stresses from Equations 5-62 and 5-63 are now considered in conjunction with the other seismic stresses as described in Section 5.4.6, Combined Seismic Stresses.

If the foregoing levels of imposed nonuniform hoop stress in combination with other seismic stresses can be accommodated by the lining structure, the more refined analysis given in the following is not necessary for this loading case. If not, the following closed-form analytical solution for an elastic, thick-walled cylinder embedded in an elastic medium (St. John, Van Dillen, and Detournay, 1985) should be used for this and all other hoop deformation stress conditions. This approach considers the interaction between the lining and ground, and it is the complete solution, provided stresses do not exceed the elastic limit. For the typical case where the elastic modulus of the soil is much less than that of the shaft lining, the interaction solution provides a great reduction in lining stresses compared to the simplified Equations 5-56 through 5-63.

Let σ_1 and σ_3 be the free field principal stresses, as sketched in Figure 5.9.

Define: $M = \frac{r}{a}$ = radius ratio, and $T = \frac{R}{a}$

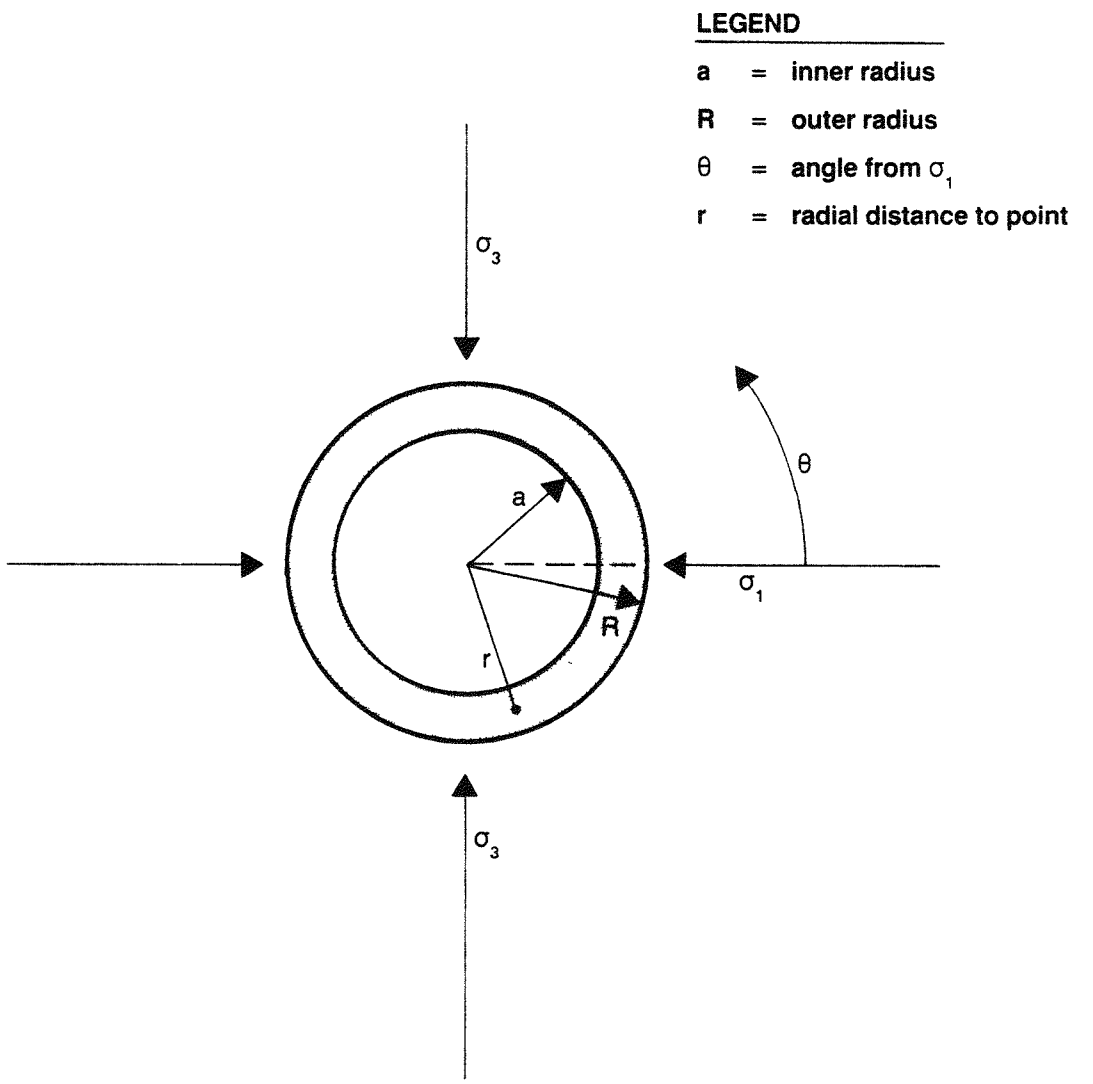

SHAFT CROSS SECTION WITH NORMAL PRINCIPAL STRESSES

FIGURE 5.9

$$P = \frac{\sigma_1 + \sigma_3}{2} = \text{mean stress (hydrostatic component) (psi, kPa)}$$

$$S = \frac{\sigma_1 - \sigma_3}{2} = \text{deviator stress (shear component) (psi, kPa)}$$

E_d and ν_d = material properties for medium
E'_d and ν'_d = material properties for lining

(E_d and E'_d are dynamic Young's moduli, and ν_d and ν'_d are dynamic Poisson's ratios)

In the following equations, use actual E_d, E'_d, ν and ν'_d when considering plane stress, i.e., at the surface. For any prescribed axial strain ϵ_{zz}, including plane strain ($\epsilon_{zz} = 0$), make the following substitutions:

$$E^*_d = \frac{E_d}{1 - \nu^2_d}$$

$$E'^*_d = \frac{E'_d}{1 - \nu'^2_d}$$

$$\nu^*_d = \frac{\nu_d}{1 - \nu_d}$$

$$\nu'^*_d = \frac{\nu'_d}{1 - \nu'_d}$$

The hoop, σ_t, radial, σ_r, and shear, τ_{rt}, stresses (psi, kPa) in the lining are given by the following:

$$\sigma_t = -\frac{A}{r^2}(1 + M^2) + \left[\frac{C}{r^4}(1 - M^4 + 4M^6) + \frac{2D}{r^2}(3M^4 - M^2)\right]\cos 2\theta \qquad (5\text{-}64)$$

$$\sigma_r = \frac{A}{r^2}(1 - M^2) + \left[\frac{C}{r^4}(M^4 - 1) + \frac{2D}{r^2}(M^2 - 1)\right]\cos 2\theta \qquad (5\text{-}65)$$

$$\tau_{rt} = \left[\frac{C}{r^4}(2M^6 - M^4 - 1) + \frac{D}{r^2}(3M^4 - 2M^2 - 1) \right] \sin 2\theta \qquad (5\text{-}66)$$

where: $$A = \frac{(-2P - B\epsilon_{zz})R^2}{\frac{E_d}{E'_d} \cdot [(1 + \nu'_d) + T^2(1 - \nu'_d)] - (1 + \nu_d)(1 - T^2)}$$

$$B = 0 = \text{plane stress}$$

$$B = E_d \left[\frac{\nu'}{1 + \nu'} - \frac{\nu}{1 + \nu} \right] = \text{generalized plane strain}$$

The values of C and D depend on the condition at the lining/rock interface.

For No-Slip:

$$C = \frac{12S \cdot R^4}{\Delta} [(1 + \nu_d)T^4 - (2F_3 + F_4 + 1 + \nu_d)] \qquad (5\text{-}67)$$

$$D = \frac{4S \cdot R^2}{\Delta} [-2(1 + \nu_d)T^6 + (F_1 + F_2 + 2(1 + \nu_d))] \qquad (5\text{-}68)$$

For Full-Slip, i.e., no shear strength:

$$C = \frac{12S \cdot R^4}{\Delta^*}(3T^4 - 2T^2 - 1) \qquad (5\text{-}69)$$

$$D = -\frac{12S \cdot R^2}{\Delta^*}(2T^6 - T^4 - 1) \qquad (5\text{-}70)$$

For No-Slip:

$$\Delta = [(\nu_d+1)(\nu_d-3)]T^8 + 4[(5-\nu_d)F_3 + (2-\nu_d)F_4 - (\nu_d+1)(\nu_d-3)]T^6 + [(\nu_d-5)F_1 + 2(\nu_d-2)F_2 + 6(\nu_d-3)F_3 + 3(\nu_d-3)F_4 + 6(\nu_d+1)(\nu_d-3)]T^4 - 2[(\nu_d-3)(F_1+F_2) + 2(\nu_d+1)(\nu_d-3)]T^2 + [F_1(F_4-1+\nu_d) - 2F_3(F_2+1+\nu_d) + F_4(1+\nu_d) - 2F_2 + (\nu_d+1)(\nu_d-3)] \quad (5\text{-}71)$$

For Full-Slip:

$$\Delta^* = [(\nu_d - 5)]T^8 + 4[(5 - \nu_d) + 3F_3]T^6 + 3[2(\nu_d - 5) - F_1 - 2F_3]T^4 + 2[2(5 - \nu_d) + F_1]T^2 + [(\nu_d - 5) + F_1 - 6F_3] \quad (5\text{-}72)$$

For Both Cases:

$$F_1 = \frac{E_d}{E'_d}[4\nu'_d T^6 - (1 + \nu'_d)(1 + 3T^4)] \quad (5\text{-}73)$$

$$F_2 = \frac{E_d}{E'_d}[-2(3 + \nu'_d)T^6 + (1 + \nu'_d)(3T^4 - 1)] \quad (5\text{-}74)$$

$$F_3 = \frac{E_d}{E'_d}[\nu'_d T^4 - (1 + \nu'_d)T^2 - 1] \quad (5\text{-}75)$$

$$F_4 = \frac{E_d}{E'_d}[-(\nu'_d + 3)T^4 + 2(1 + \nu'_d)T^2 + (1 - \nu'_d)] \quad (5\text{-}76)$$

5.4.6 Combined Seismic Stresses

When considering lining stress effects caused by different wave types and directions, it might be assumed that the various effects are decoupled and can be treated separately (ASCE, 1983). This is largely because it is recognized that the maximum stresses produced by compression and shear waves are likely to occur at different times, owing to their different propagation velocities. Further, peak shear and curvature-related stresses are caused by maximum particle velocity and acceleration, respectively, which do not occur simultaneously.

Despite this possibility, it is recommended that the more conservative approach be used of simultaneous occurrence of the maximum response of one effect with a lesser contribution from the other

effects using the 100-40-40 combination rule published by Newmark and Hall (1978). Fundamentally, this approach combines 100% of the peak of all stress contributions that must occur simultaneously (because they are associated with the same wave type and direction of the same particle motion) with 40% of the peak value of those stress effects caused by different wave type or particle motion.

Both the incident inclined P waves and incident inclined SV waves will generate a P-SV wave-field within the layered site profile. This P-SV wave-field will result in strain components ϵ_{zz}, γ_{xz}, ϵ_{xx} and curvature in the xz plane. Since the design earthquake is at a distance exceeding 30 miles (48 km), the arrival times of the P wave group and S wave group will be separated by at least five seconds. As a consequence of this time separation, application of the 100-40-40 load combination rule to stresses resulting from incident P waves and incident SV waves is considered inappropriate and would result in excessive conservatism. As a result these two wave types are not combined.

The net response to earthquake ground motion at any depth is computed separately for vertically propagating P and S waves, and for inclined P, SH and SV waves. The combinations are shown in Tables 5.7 and 5.8. The combination (either vertical or inclined waves) that produces the worst case stress effects is the net seismic response at the depth under consideration. Stress combinations for vertically propagating P and S waves (Table 5.7) include contributions from both wave types because motions from the two waves, when added, produce 100% of the surface ground motion. On the other hand, with inclined waves, 100% of the surface ground motion is associated with: (1) the P wave (x-z plane) combined with the SH wave (y-z plane) as well as (2) with the SV wave (x-z plane) combined with the SH wave (y-z plane). This pattern is reflected in Table 5.8.

Table 5.7 Seismic Stress Combinations for Vertical P and S Waves

Seismic Stress Combination	Stress Component (%)			
	Vertical P Wave		Vertical S Wave	
	Axial	Uniform Hoop	Shear	Flexural
1	100	100	40	40
2	40	40	100	40
3	40	40	40	100

Table 5.8 Seismic Stress Combinations for Inclined P-SV and SH Waves

STRESS COMPONENT (%)

Seismic Stress Combination	Incident P				Incident SV				Inclined SH		
	Axial	Shear	Flexural	Hoop	Axial	Shear	Flexural	Hoop	Shear	Flexural	Hoop
1	100	40	40	100					40	40	40
2	40	100	40	40					40	40	40
3	40	40	100	40					40	40	40
4					100	40	40	100	40	40	40
5					40	100	40	40	40	40	40
6					40	40	100	40	40	40	40
7					40	40	40	40	100	40	40
8					40	40	40	40	40	100	40
9	40	40	40	40					100	40	100
10	40	40	40	40					40	100	40

When combining stress effects for inclined waves the analyst must recognize and account for the circumferential variation of nonuniform hoop and flexural stresses as well as the 90 degree difference in orientation of shear stresses due to SH and P-SV waves. For example, with inclined SH waves (assumed to cause horizontal particle motion parallel to the y-axis as shown in Figure 5.6) the maximum flexural stress occurs along the y axis whereas the maximum nonuniform hoop stress given by Equation 5-62 occurs along the axes 45 degrees to x and y, and is zero on the y-axis. For inclined P-SV waves the horizontal particle motion is now parallel to the x-axis (as shown in Figure 5.6) such that the maximum flexural stress occurs on the x-axis, whereas, the nonuniform hoop stresses reach a maximum on the y-axis where the flexural stress is zero.

The designer can take advantage of the above noted variations and orientations of stress when combining stress effects, for example, as required by Equation 5-4. This distinction is in addition to the stress combination values given in Tables 5.7 and 5.8. Because of the number of stress components which vary

over the shaft cross section, it is not possible to preselect the worst case stress location. Therefore, it will be necessary to examine the stress state at a number of positions around the shaft in order to determine the worst case stress condition.

As an alternative, the designer can conservatively neglect the above stress variations by using the maximum of each stress contribution to be combined in accordance with Table 5.7 or Table 5.8, as appropriate. This latter approach will provide an upper bound by assuming that all deformation patterns produce their maximum effects at the same point and in the same direction.

Example 1

Consider a 144 in (3658 mm) I.D., 195 in (4953 mm) O.D. concrete lined shaft with a 0.5 in (13 mm) steel outer lining at a depth of 35 ft (10.7m). In this and the following example, scientific notation is written in typical computer format, e.g., 4×10^{-3} is written as 4E-03. The free-field strains are given in Table 5.9:

Table 5.9 Maximum Strains at 35 ft (10.7 m) Depth

Wave Type	ϵ_{zz}	ϵ_{xx}	γ_{xz}	γ_{yz}	γ_{xy}	κ^* (l/ft)
Vertical P and S	2E-04			1E-03		4E-05
Inclined SH				2.1E-03	7E-05	5E-05
Inclined P-SV Incident P	3E-04	1E-05	4E-04			9E-06
Inclined P-SV Incident SV	2E-04	4E-05	2E-03			4E-05

* Multiply by 3.28 to obtain (l/m)

For soil (see ISD, Section 4.5.6, Strain Compatible Moduli and Poisson's Ratio):

E_d = 5480 psi (37,780 kPa)

ν_d = 0.33

G_d = $5480/(2\bullet(1+0.33))$ = 2060 psi (14,200 kPa)

λ_d = $0.33\ (5480)/((1+0.33)\bullet(1-0.66))$ = 4000 psi (27,580 kPa)

L = 236 ft (72 m)

For f'_c = 6000 psi (41,370 kPa) concrete:

E'_d = 3,000,000 psi (20,690,000 kPa)

ν'_d = 0.167

G'_d = 1,285,000 psi (8,860,000 kPa)

λ'_d = 645,000 psi (4,447,000 kPa)

For A-633 Grade C steel:

E'_d = 29,000,000 psi (200,000,000 kPa)

ν'_d = 0.33

G'_d = 10,900,000 psi (75,160,000 kPa)

λ'_d = 21,200,000 psi (146,200,000 kPa)

For purposes of illustration, stresses for the incident SV and incident SH waves (subsequently to be used in Seismic Stress Combination 5 of Table 5.8) are calculated for the concrete lining as follows (note, as mentioned in Section 5.4.5, Hoop Stresses, all stresses can be considered as either tension or compression):

Incident SV Wave

1. Axial stress, Equation 5-44:

   $\sigma_a = \sigma_z$ = 3E06(2E-04) = 600 psi (4140 kPa)

2. Flexural stress:

   Imposed flexural deformation curvature, Equation 5-49:

   $\kappa = 2\pi$(2E-03)/236 = 5.3E-05 1/ft (1.7 E-04 1/m) (governs)

   Free-field curvature, Table 5.9:

   κ = 4E-05 1/ft (1.3E-04 1/m)

   Flexural stress, Equation 5-48:

   $\sigma_b = \sigma_z = \pm$ 3E06(195)(0.5)(5.3E-05)/12 = 1292 psi (8908 kPa)

   (These stresses vary from zero on the y axis to the value calculated on the x axis.)

3. Shear stress:

   Imposed shear strain from Equations 5-45 and 5-46:

$$\gamma^*_{zx} = \frac{8\pi^2(3E06)[(97.5)^2 + (72)^2](2E-03)}{1.285E06(4)(236)^2(12)^2}$$

$$= 1.7E\text{-}04 \text{ (governs)}$$

and: $$\gamma^*_{zx} = \frac{2(1 - C^2) \cdot (2E\text{-}03)}{(1 + C^2) + \frac{1.285E06}{2060}(1 - C^2)}$$

$$= 6.4E\text{-}06$$

where: $$C = \left(\frac{72}{97.5}\right)$$

Shear stress, Equation 5-47:

$$\tau_{zx} = 1.7E\text{-}04\ (1.285E06) = 217 \text{ psi } (1496 \text{ kPa})$$

These stresses are not applied to the concrete portion of the liner because they do not represent a failure mechanism. See the introduction of Section 5.4, Stresses Due to Earthquakes.

4. Hoop stresses:

Using the simplified approach of Equations 5-56 to 5-63, the imposed hoop strains are given by Equation 5-58 as:

$$\epsilon_{t_A} = \frac{(1 - 0.33)}{(1 - 2(0.33))}\ (4E\text{-}05) + \frac{0.33}{(1 - 2(0.33))}\ (2E\text{-}04)$$

$$= 2.7E\text{-}04$$

$$\epsilon_{t_B} = 2(1 - 0.33)(4E\text{-}05) = 5.4E\text{-}05$$

$$\epsilon_t = \epsilon_{t_A} - \epsilon_{t_B} \cos 2\theta$$

where: θ is measured from the x axis

$\epsilon_t(\theta = 0) = 2.7E\text{-}04 - 5.4E\text{-}05 = 2.2E\text{-}04$

$\epsilon_t(\theta = 45°) = 2.7E\text{-}04$

$\epsilon_t(\theta = 90°) = 2.7E\text{-}04 + 5.4E\text{-}05 = 3.2E\text{-}04$

Resulting lining stresses, Equations 5-62 and 5-63 (for illustration purposes, only one circumferential position is examined in what follows):

$$\sigma_t(\theta = 0) = \frac{3E06}{(1-(0.167)^2)}(2.2E\text{-}04 + (0.167)(2E\text{-}04)) = 782 \text{ psi } (5392 \text{ kPa})$$

$$\sigma_Z = \frac{3E06}{(1-(0.167)^2)} \cdot (0.167)2.2E\text{-}04 = 113 \text{ psi } (779 \text{ kPa})$$

A more realistic evaluation of the hoop stress effects is obtained using the interaction approach of Equations 5-64 to 5-66. For free-field stresses of:

$$\sigma_1 = \sigma_X \text{ (Eq 5-50)} = 2(2060)(4E\text{-}05) + 4000\,(4E\text{-}05 + 2E\text{-}04) = 1.12 \text{ psi } (7.7 \text{ kPa})$$

and:

$$\sigma_3 = \sigma_y \text{ (Eq 5-51)} = 4000\,(4E\text{-}05 + 2E\text{-}04) = 0.96 \text{ psi } (6.6 \text{ kPa})$$

Equations 5-64 to 5-66 yield (full slip) at $\theta = 0$, $\sigma_t = 9$ psi (62 kPa), $\sigma_r = 1.6$ psi (11 kPa), and $\tau_{rt} = 0$ at the lining outer radius compared to $\sigma_t = 782$ psi (5392 kPa) calculated by the simplified method. The corresponding $\sigma_Z = 0.167(9) = 1.5$ psi (10.3 kPa) which can be ignored. In this case, with a small soil to shaft stiffness ratio, i.e., the soil is much less stiff than the lining, the simplified method overstates the hoop stress by a factor of about 85.

The above calculated SV wave stress effects and their variation and orientation over the lining are shown in Figure 5.10. A cylindrical coordinate system is used, except for the shear on the horizontal plane, τ_{ZX}. This is done to emphasize that the stress has the same direction regardless of angular position. As a result, for the location shown in the upper right hand portion of Figure 5.10, where $\theta = 0$, the stress τ_{ZX} is also τ_{Zr}. At the upper left, where $\theta = 90°$, τ_{ZX} becomes τ_{Zt}.

Incident SH Wave

1. Axial stress: $\sigma_a = \sigma_Z = 0$

2. Flexural stress:
   Imposed flexural deformation curvature, Equation 5-49:
   $\kappa = 2\pi(2.1E\text{-}03)/236 = 5.6E\text{-}05$ 1/ft (1.8 E-04 1/m) (governs)

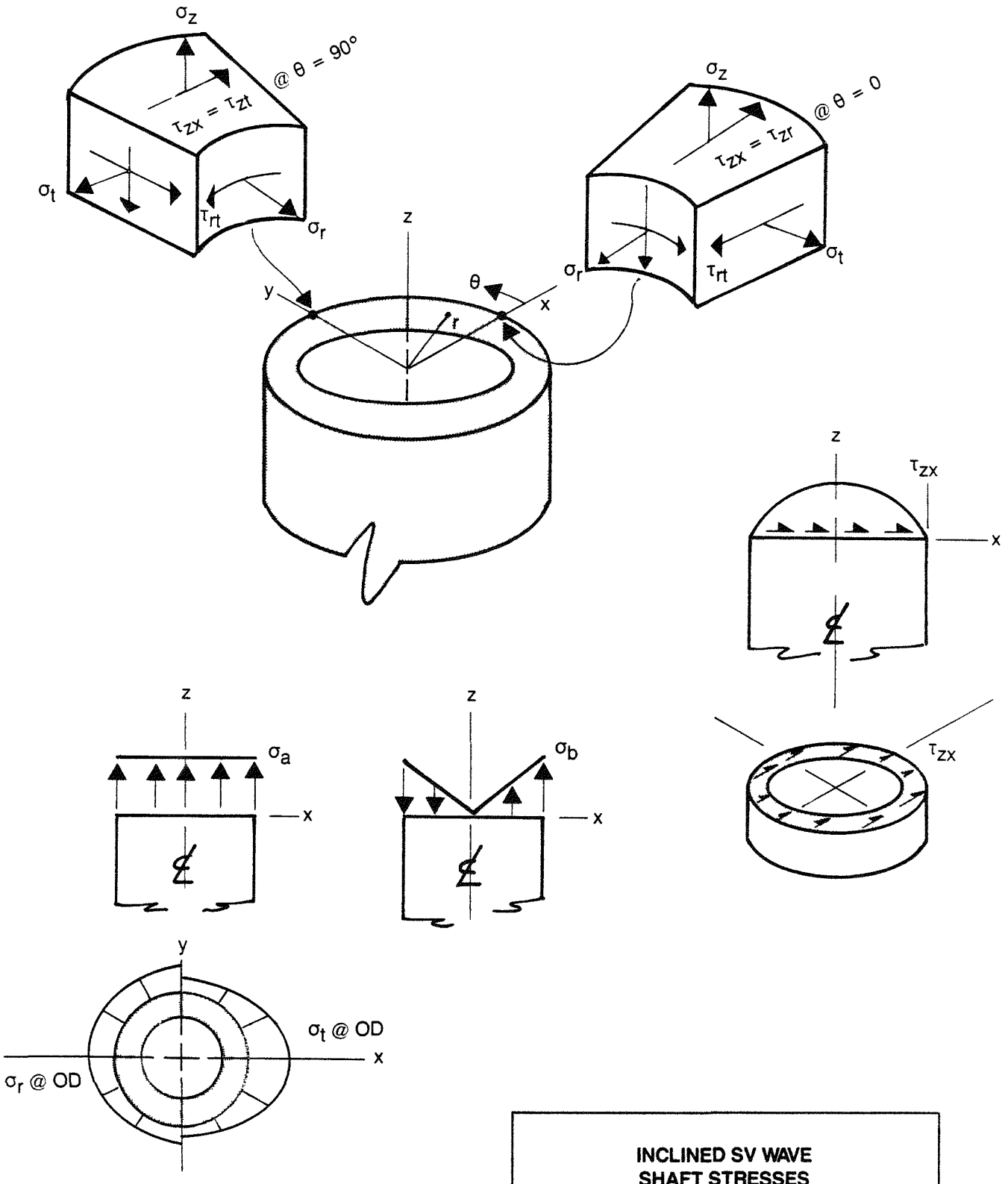

INCLINED SV WAVE SHAFT STRESSES

FIGURE 5.10

Free-field curvature, Table 5.9:

κ = 5E-05 1/ft (1.6E-04 1/m)

Flexural stress, Equation 5-48:

$\sigma_b = \sigma_z = \pm 3E06(195)(0.5)(5.6E-05)/12 = 1365$ psi (9412 kPa)

(These stresses vary from zero on the x axis to the value calculated on the y axis)

3. Shear stress:

Imposed shear strain from Equations 5-45 and 5-46:

$$\gamma^*_{zy} = \frac{8\pi^2(3E06)[(97.5)^2 + (72)^2](2.1E-03)}{1.285E06(4)(236)^2(12)^2}$$

$$= 1.8E-04 \text{ (governs)}$$

and:
$$\gamma^*_{zx} = \frac{2(1 - C^2) \bullet (2.1E-03)}{(1 + C^2) + \frac{1.285E06}{2060}(1 - C^2)}$$

$$= 6.7E-06$$

where:
$$C = \left(\frac{72}{97.5}\right)$$

Shear stress, Equation 5-58:

$\tau_{zy} = 1.285E06(1.8E-04) = 227$ psi (1565 kPa)

4. Hoop stresses:

Clearly, the simplified approach is too conservative for the low soil modulus at this depth. The interaction method requires the free-field stresses:

$$\sigma_1 = \tau_{xy} \text{ (Eq 5-54)} = 2060(7E-05) = 0.14 \text{ psi (0.97 kPa)}$$

and:
$$\sigma_3 = -0.14 \text{psi } (-0.97 \text{ kPa})$$

Equations 5-64 to 5-66 yield at the outside radius:

	Stress (psi)*			
$(\theta°)$	σ_t	σ_r	τ_{rt}	$\sigma_z = \nu'_d\sigma_t$
0	7	0.3	0	1(ignore)
45	0	0	0	0
90	−7	−0.3	0	−1(ignore)
135	0	0	0	0

* Multiply by 6.89 to obtain (kPa)

where θ = 45° corresponds to the x axis, and θ = 135° corresponds to the y axis.

The inclined SH wave stress effects calculated above and their variation over the lining are shown in Figure 5.11. The conversion from Cartesian to cylindrical coordinate notation for the τ_{zy} shear is illustrated in the figure and must be made as described for the SV wave.

The seismic stresses are now combined in accordance with Tables 5.7 and 5.8 for each of the various radial and circumferential lining locations under investigation. For example, Combination 5 from Table 5.8 results in the following stresses for a point on the x axis at the outer radius of the concrete:

a. Longitudinal stress:

40% axial incident SV = 0.4(600) = 240 psi (1655 kPa)
40% flexural incident SV = 0.4(1292) = 517 psi (3565 kPa)
40% flexural incident SH = 0.4(0) = 0 psi
Total σ_z = 757 psi (5220 kPa)

b. Shear stress:

100% shear SV(τ_{zx}) = 1.0(217)
τ_{zx} = 217 psi (1496 kPa) = τ_{zr}
40% shear SH(τ_{zy}) = 0.4(227)
τ_{zy} = 91 psi (627 kPa) = τ_{zt}

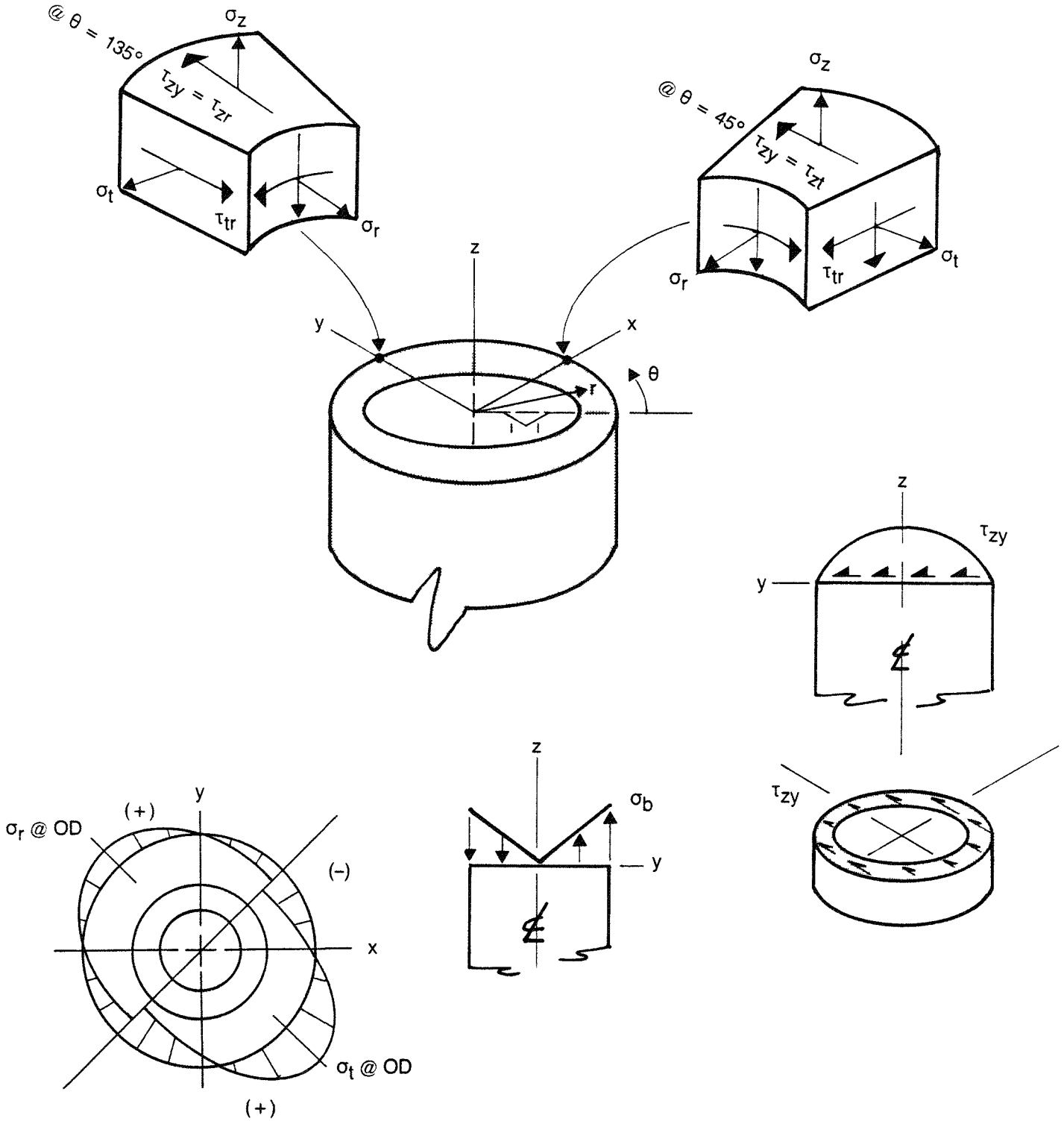

INCLINED SH WAVE SHAFT STRESSES

FIGURE 5.11

c. Hoop stress:

σ_t: 40% SV = 0.4(9) = 3.6 psi (25 kPa)
40% SH = 0.4(0) = 0
σ_t = 3.6 psi (25 kPa)

σ_r: 40% SV = 0.4(1.6) = 0.6 psi (4 kPa)
40% SH = 0.4(0) = 0
σ_r = 0.6 psi (4 kPa)

τ_{rt}: 40% SV = 0.4(0) = 0
40% SH = 0.4(0) = 0
τ_{rt} = 0

The above calculated stresses are shown in Figure 5.12.

Similar calculations are performed for other radial and circumferential positions both in the concrete and steel shells. This is required because the various stress components do not reach their maximum at the same point in the lining. These calculations are then repeated for all the other seismic stress combinations. Each calculated seismic stress state is then combined with horizontal pressures and other loads in accordance with Section 4.6.4, Total Combined Loads. The resulting total load combination stress state is then checked against the acceptance criteria given in Sections 5.1 and 5.2, Shaft Lining Materials, and Material Properties, respectively.

For purposes of this example, it is clear that the hoop direction seismic stresses, viz., σ_t, σ_r and τ_{rt}, are trivial. When substituted into Equation 5-6 for checking concrete, σ_v is calculated to be 4 psi (28 kPa). The allowable stress (from Table 5.1) is 0.75 f'_c = 4500 psi (31,030 kPa). For reasons stated previously, stresses on other planes in the concrete are not checked.

Example 2

In order to demonstrate the reduced effects of seismic strains with depth and how this can simplify the calculations, the lined shaft of Example 1 is now considered for induced seismic strains corresponding to a depth of 300 ft (91.5 m). The maximum value for each stress condition is used without regard for actual

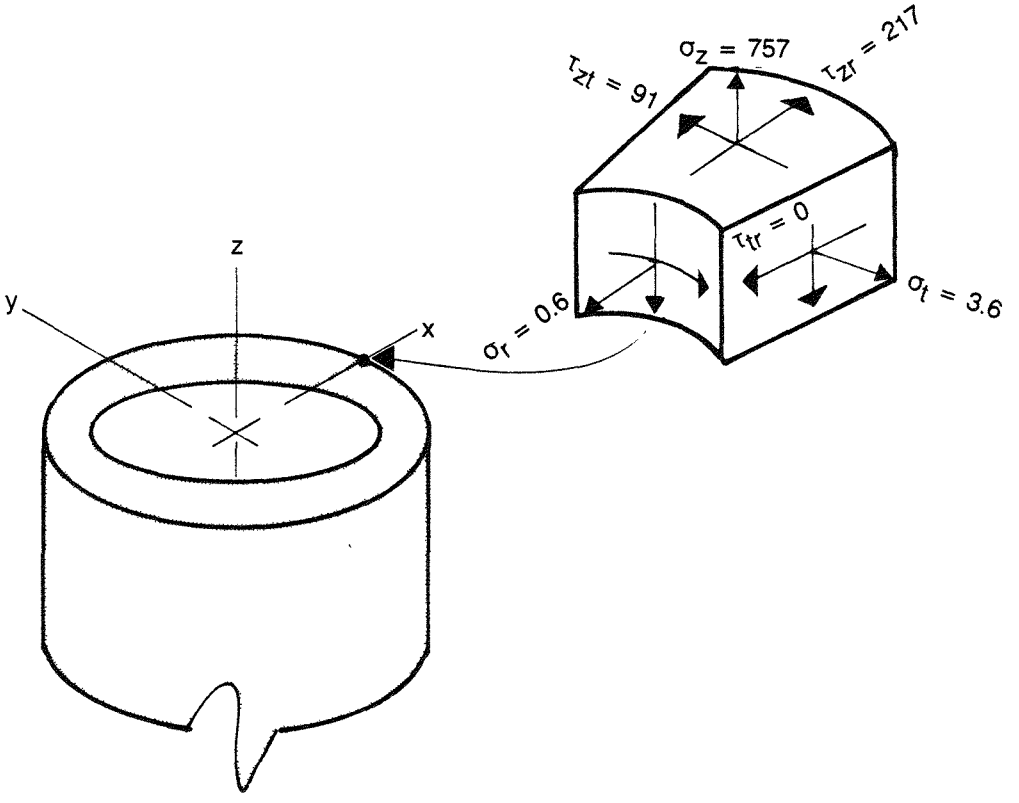

LINING STRESSES (psi) ON X AXIS AT O.D. FOR SEISMIC STRESS COMBINATION 5

FIGURE 5.12

variation or orientation, in order to demonstrate the simplification this approach can introduce. The free-field strains are given in Table 5.10:

Table 5.10 Maximum Strains at 300 ft (91.5 m) Depth

Wave Type	ϵ_{zz}	ϵ_{xx}	γ_{xz}	γ_{yz}	γ_{xy}	κ^* (1/ft)
Vertical P and S	3E-05			2E-04		2E-06
Inclined SH				1E-04	4E-05	1E-06
Inclined P-SV, Incident P	4E-05	8E-06	8E-05			4E-07
Inclined P-SV, Incident SV	1E-05	2E-05	7E-05			6E-07

* Multiply by 3.28 to obtain (1/m)

Soil properties at this depth are assumed to be as follows:

E_d = 150,000 psi (1,034,000 kPa)
ν_d = 0.33
G_d = 56,400 psi (388,900 kPa)
λ_d = 109,000 psi (752,000 kPa)
L = 2240 ft (683 m)

Stresses in the steel shell are calculated for incident SV and incident SH waves in the following:

Incident SV Wave

1. Axial stress: $\sigma_a = \sigma_z$ = 29E06(1E-05) = 290 psi (2000 kPa)

2. Flexural stress: $\kappa = 2\pi$ (7E-05)/2240 = 2E-07 1/ft (6.6E-07 1/m)

   κ (Table 5.10) = 6E-07 1/ft (2 E-06 1/m)(governs)

   Flexural stress: $\sigma_b = \sigma_z = \pm$ 29E06 (196)(0.5)(6E-07)/12 = 142 psi (979 kPa)

3. Shear stress:

$$\gamma^*_{zx} = \frac{8\pi^2(29E06)[(98)^2 + (72)^2](7E\text{-}05)}{10.9E06(4)(2240)^2(12)^2}$$

$$= 7.5E\text{-}08$$

and:
$$\gamma^*_{zx} = \frac{2(1 - C^2) \bullet (7E\text{-}05)}{(1 + C^2) + \frac{10.9E06}{5.64E04}(1 - C^2)}$$

$$= 7E\text{-}07 \text{ governs}$$

where:
$$C = \left(\frac{72}{98}\right)$$

$$\tau_{zx} = 10.9E06(7E\text{-}07) = 8 \text{ psi (55 kPa)}$$

4. Hoop stress: (Using the simplified method)

Imposed strain is given by Equation 5-58 as

$$\epsilon_{tA} = \frac{(1 - 0.33)}{(1 - 2(0.33))} \bullet (2E\text{-}05) + \frac{0.33}{(1 - 2(0.33))} \bullet (1E\text{-}05)$$

$$= 4.9E\text{-}05$$

$$\epsilon_{tB} = 2(1\text{-}0.33)(2E\text{-}05) = 2.7E\text{-}05$$

$$\epsilon_{t_{max}} = 4.9E\text{-}05 + 2.7E\text{-}05 = 7.6E\text{-}05$$

The corresponding steel lining stresses are derived from Equations 5-62 and 5-63:

$$\sigma_t = \frac{29E\text{-}06}{1 - (0.33)^2}(7.6E\text{-}05) + 0.33(1E\text{-}05)) = 2581 \text{ psi (17,800 kPa)}$$

$$\sigma_z = \frac{29E06}{(1-(0.33)^2)} \cdot [0.33(7.6E\text{-}05)] = 816 \text{ psi } (5626 \text{ kPa})$$

The interaction solution gives a maximum hoop stress of 43 psi (296 kPa). Although this reduced value is theoretically correct, the simplified, conservative value will be used.

Incident SH Wave

1. Axial stress: $\sigma_a = \sigma_z = 0$

2. Flexural stress:
   $\kappa = 2\pi(1E\text{-}04)/2240 = 3E\text{-}07$ 1/ft (9.8 E-07 1/m)
   κ (Table 5.10) = 1E-06 1/ft (3.3 E-06 1/m)(governs)
   $\sigma_b = \sigma_z = \pm 29E06(196)(0.5)(1E\text{-}06)/12 = 237$ psi (1634 kPa)

3. Shear stresses:

$$\gamma^*_{zy} = \frac{1E\text{-}04}{7E\text{-}05} \; 7E\text{-}08 = 1E\text{-}07$$

and:
$$\gamma^*_{zy} = \frac{1E\text{-}04}{7E\text{-}05} \; (7E\text{-}07) = 1E\text{-}06 \text{ (governs)}$$

$$\tau_{zy} = 10.9E06(1E\text{-}06) = 11 \text{ psi } (76 \text{ kPa})$$

4. Hoop stresses (using simplified method):
   Imposed strain is given by Equation 5-61.

$$\epsilon_t = -2(1-0.33)(4E\text{-}05)\cos 2\theta$$

$$\epsilon_t = -5.4E\text{-}05 \cos 2\theta$$

where $\theta = 45°$ corresponds to the x axis.

The corresponding stress in the steel lining is given by Equation 5-62 as:

$$\sigma_t = \frac{29E06}{(1-(0.33)^2)}(-5.4E\text{-}05-(0.33)(0))\cos 2\theta$$

$\sigma_{t\max}$ = 1744 psi (12,025 kPa)

σ_z = 0.33(1744) = 576 psi (3970 kPa)

The stress field for Seismic Stress Combination 5 is as follows:

a. Longitudinal stress:

40% axial incident SV	= 0.4(290)	= 116 psi (800 kPa)
40% flexural incident SV	= 0.4(142)	= 57 psi (393 kPa)
40% flexural incident SH	= 0.4(237)	= 95 psi (655 kPa)
40% hoop axial SV	= 0.4(816)	= 326 psi (2248 kPa)
40% hoop axial SH	= 0.4(576)	= 230 psi (1586 kPa)
	σ_z	= 824 psi (5682 kPa)

b. Shear stress:

100% shear SV(τ_{xz}) = 1.0(8)

τ_{xz} = 8 psi (55 kPa)

40% shear SH(τ_{yz}) = 0.4(11)

τ_{yz} = 4 psi (28 kPa)

c. Hoop stress:

σ_t: 40% SV = 0.4(2581) = 1032 psi (7116 kPa)

40% SH = 0.4(1744) = 698 psi (4813 kPa)

σ_t = 1730 psi (11,929 kPa)

For further simplicity, and conservatism, combine the shear stresses and assume they both act on the t-z planes. Thus, $\tau_{tz} = \tau_{zt} = 8+4 = 12$ psi (83 kPa). These stresses (σ_z, σ_t, and τ_{zt}) would now be combined

with other load stress effects in accordance with Section 4.6.4, Total Combined Loads. The resulting total would then be checked against the acceptance criteria given in Sections 5.1 and 5.2, Shaft Lining Materials and Material Properties, respectively.

One can assess the significance of the seismic stresses on the total stress state in the steel lining by substituting the above seismic stresses directly into Equation 5-4. The resulting stress when compared to the allowable (see Table 5.1) gives a measure of the fraction of available strength required to carry the seismic deformation. Accordingly, Equation 5-4 gives $\sigma_v = [(1730)^2 + (824)^2 - (1730)(824) + 3(12)^2]^{\frac{1}{2}} =$ 1500 psi (10,340 kPa) which is compared to the allowable stress of 47,500 psi (327,500 kPa). Hence, seismic effects use only about 3% of the steel lining design limit at this depth.

Although the above example does not consider other seismic stress combinations, it is believed the results are typical of those to be found at this and greater depths at the Deaf Smith County site.

If seismic stresses (computed in accordance with the foregoing linear procedures) combined with other load conditions exceed allowable total load material strength to the extent seismic effects become an important factor in design, they can alternatively be treated by nonlinear analysis as an induced strain, or using a SSI analysis described in Section 6.4.2, Overall Approach for Soil Structure Interaction (SSI) Analysis. In the former approach the free-field displacements are applied to a two dimensional static, nonlinear finite-element model of the shaft and surrounding ground. This method will provide a more refined estimation of the nonlinear response of the system. The resulting induced seismic strains in the shaft lining can then be superimposed on the existing lining stresses (due to other loads) to assess lining response as a constrained system.

5.5 CAST IRON TUBBING LINING

The design of cast iron tubbing should be based on DIN 21501. For ductile cast iron specifications, DIN 1693-1 and DIN 1693-2 should be used. The high quality ductile cast iron now available allows tubbing configurations which offer increased stability and strength with a smaller section size and weight than the grey cast iron previously available.

Material testing specifications for ductile cast iron should be based on the following ASTM standards:

ASTM E8-85b	Methods of Tension Testing of Metallic Materials
ASTM E114-85	Recommended Practice for Ultrasonic Pulse-Echo Straight-Beam Testing by the Contact Method
ASTM E142-86	Method for Controlling Quality of Radiographic Testing
ASTM E689-79 (Reapproved 1984)	Reference Radiographs for Ductile Iron Castings

The proposed dimensions of ductile cast iron tubbing segments for different wall thicknesses are shown in Table 5.11. These dimensions are based on those contained in DIN 21501.

Table 5.11
CAST IRON TUBBING DIMENSIONS

Wall Thickness*		1 3/4"	1 7/8"	2"	2 1/8"	2 1/4"	2 3/8"	2 1/2"	2 5/8"	2 3/4"	2 7/8"	3"	3 1/8"	3 1/4"	3 3/8"	3 1/2"	3 5/8"	3 3/4"	3 7/8"	4"	4 1/8"	4 1/4"
Item	Unit**																					
a	in.	1 3/4	1 7/8	2	2 1/8	2 1/4	2 3/8	2 1/2	2 5/8	2 3/4	2 7/8	3	3 1/8	3 1/4	3 3/8	3 1/2	3 5/8	3 3/4	3 7/8	4	4 1/8	4 1/4
b	in.	6	6	6	6	6	6	6	6	6	6	6	6	6	6	6	6	6	6	6	6	6
c	in.	1 3/8	1 3/8	1 3/8	1 3/8	1 3/8	1 3/8	1 3/8	1 7/16	1 9/16	1 11/16	1 13/16	1 15/16	2 1/16	2 3/16	2 5/16	2 7/16	2 9/16	2 11/16	2 13/16	2 13/16	2 13/16
d	in.	7 3/4	7 7/8	8	8 1/8	8 1/4	8 3/8	8 1/2	8 5/8	8 3/4	8 7/8	9	9 1/8	9 1/4	9 3/8	9 1/2	9 5/8	9 3/4	9 7/8	10	10 1/8	10 1/4
A	in.	2 7/8	2 7/8	2 7/8	2 7/8	2 7/8	2 7/8	2 7/8	2 14/16	3	3 1/8	3 1/4	3 6/16	3 1/2	3 5/8	3 3/4	3 14/16	4	4 1/8	4 1/4	4 14/16	4 1/2
B	in.	3 3/16	3 3/16	3 3/16	3 3/16	3 3/16	3 3/16	3 3/16	3 3/16	3 5/16	3 7/16	3 9/16	3 11/16	3 13/16	3 15/16	4 1/16	4 3/16	4 5/16	4 7/16	4 9/16	4 11/16	4 13/16
C	in.	2 1/2	2 1/2	2 1/2	2 1/2	2 1/2	2 1/2	2 1/2	2 1/2	2 5/8	2 3/4	2 7/8	3	3 1/8	3 1/4	3 3/8	3 1/2	3 5/8	3 3/4	3 7/8	4	4 1/8
D	in.	2 7/8	2 7/8	2 7/8	2 7/8	2 7/8	2 7/8	2 7/8	2 7/8	3	3 1/8	3 1/4	3 3/8	3 1/2	3 5/8	3 3/4	3 7/8	4	4 1/8	4 1/4	4 3/8	4 1/2
E	in.	1 7/8	1 7/8	1 7/8	1 7/8	1 7/8	1 7/8	1 7/8	2	2 1/8	2 1/4	2 3/8	2 1/2	2 5/8	2 3/4	2 7/8	3	3 1/8	3 1/4	3 3/8	3 1/2	3 5/8
F	in.	2 7/8	2 7/8	2 7/8	2 7/8	2 7/8	2 7/8	2 7/8	3	3 1/8	3 1/4	3 3/8	3 1/2	3 5/8	3 7/8	4 1/8	4 3/8	4 5/8	4 7/8	5 1/8	5 3/8	5 5/8
G	in.	1 7/8	1 7/8	1 7/8	1 7/8	1 7/8	1 7/8	1 7/8	1 7/8	1 7/8	1 7/8	1 7/8	1 7/8	1 7/8	1 7/8	1 7/8	1 7/8	1 7/8	1 7/8	1 7/8	1 7/8	1 7/8
H	in.	60	60	60	60	60	60	60	60	60	60	60	60	60	60	60	60	60	60	60	60	60
N	in.	3	3	3	3	3	3	3	3	3	3	3	3	3	3	3	3	3	3	3	3	3
A_T	in^2	172.05	179.55	187.05	194.55	202.05	209.55	217.05	225.9	237.6	249.3	261.0	272.7	284.4	297.2	309.9	322.7	335.4	348.2	360.9	372.6	384.3
I_{yy}	in^4	855	888	921	962.5	1004	1048	1092	1175	1291	1408	1526	1643	1760	1944	2128	2312	2497	2681	2865	3040	3216
e_i	in.	5.700	5.792	5.883	5.973	6.062	6.148	6.233	6.333	6.401	6.470	6.539	6.607	6.676	6.757	6.838	6.919	7.000	7.082	7.163	7.222	7.281
i^2	in^2	4.968	4.945	4.923	4.946	4.969	5.000	5.031	5.201	5.434	5.649	5.847	6.025	6.188	6.541	6.867	7.165	7.445	7.700	7.838	8.159	8.368

* Different tubbing types are denoted by different wall thicknesses, as shown here.

** Multiply in by 25.4 to obtain mm.

The items shown in Table 5.11 are described in Figure 5.13. The weight of tubbing segments varies with the type, or grade, of ductile cast iron tubbing used and its dimensions.

The recommended number of tubbing segments per ring with reference to finished shaft diameter are:

Shaft Diameter (Ft.)*	14	15	16	18	20	21	22	23
Segments/Ring (Z)	9	9	10	10	11	12	12	13

* Multiply by 0.305 to obtain m.

The design of a cast iron tubbing lining can be approached in two ways by considering the following cases:

1. Only the cast iron tubbing column.
2. A lining composed of cast iron tubbing and a concrete envelope.

5.5.1 Cast Iron Tubbing Column Stress Analysis

In the design of the cast iron tubbing column only, (Case 1), the following stress analyses should be performed:

a) Determine circumferential stresses in tubbing ring section resulting from:

   1. Uniform horizontal pressure (Equations 5-8, 5-9)
   2. Nonuniform horizontal pressure (Equations 5-10, 5-13, 5-14)

b) Determine buckling safety of tubbing rings at limited possibilities of deformation according to Amstutz (1970) and Hertrich (1965).

To determine the buckling safety of a tubbing ring for limited possibilities of deformation, the following should be considered:

1. Allowable out of roundness $\delta \leq 1\%$ (0.01)
2. The ratio $\frac{e_i}{e_{\phi a}} > 1.5$ and $\frac{e_i}{e_{\phi a}} \leq 1.5$

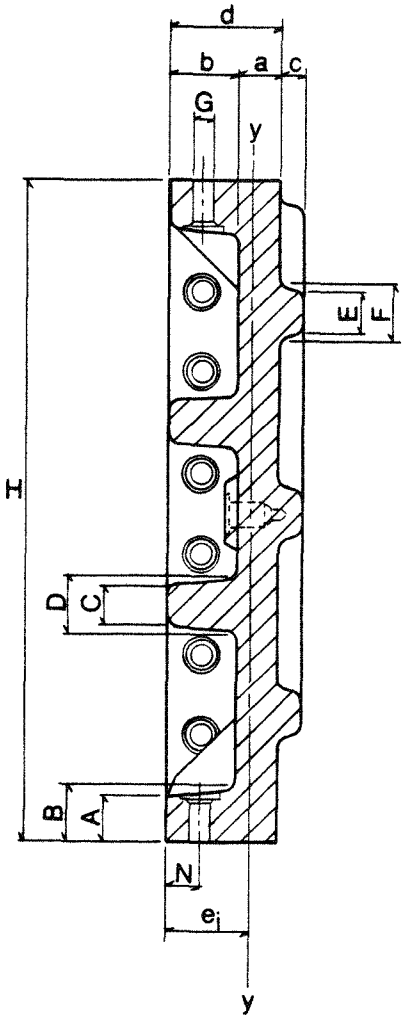

A_r = CROSS SECTIONAL AREA OF TUBBING SEGMENT
I_{yy} = RADIUS OF GYRATION OF TUBBING SEGMENT
i = RADIUS OF GYRATION OF TUBBING SEGMENT

SECTION THROUGH CAST IRON TUBBING SEGMENT

FIGURE 5.13

where: e_i = distance from neutral axis to the inside edge of the tubbing flange (in, mm)

$e_{\phi a}$ = distance from neutral axis to the outside edge of the tubbing flange (in, mm)

$e_{\phi a} = d - e$;

For: $\frac{e_i}{e_{\phi a}} \leq 1.5$

$$\frac{\sigma_N}{E_i}\left[1+\left(\frac{r_S+\xi}{i}\right)^2 \cdot \frac{\sigma_N}{E_i \cdot k_f}\right]^{\frac{3}{2}} = 1.68 \cdot \frac{r_S}{e_{\phi a}} \cdot \xi^2 \cdot \frac{\sigma_F-\sigma_N}{E_i \cdot k_f}\left[1-\frac{r_S}{4 \cdot e_{\phi a}} \cdot \xi \cdot \frac{\sigma_F-\sigma_N}{E_i \cdot k_f}\right] \quad (5\text{-}77)$$

Solve Equation 5-77 iteratively for the tangential stress σ_N.

From which the critical buckling stress σ_{cr} for ductile cast iron tubbing can be determined:

$$\sigma_{cr} = \frac{\sigma_N}{\xi}\left[1-\frac{r_S \cdot \xi}{e_{\phi a}} \cdot \frac{\sigma_F-\sigma_N}{\left(\frac{3\pi}{2}+1\right)E_i \cdot k_f}\right] \quad (5\text{-}78)$$

where: $\xi = \frac{1+2\delta}{1-\delta}$ = out of roundness factor

r_S = radius of neutral axis of the tubbing segment (in, mm)

$r_S = r_i + e_i$

i = radius of gyration of tubbing segment (in, mm)

E_i = modulus of elasticity of ductile cast iron (psi, kPa)

σ_F = yield point in bending for ductile cast iron (psi, kPa)

k_f = bending coefficient of the flange connection with lead gasket (Equation 5-81)

For: $\frac{e_i}{e_{\phi a}} > 1.5$

$$\frac{\sigma_N}{E_i}\left[1+\left(\frac{r_S \cdot \xi}{i}\right)^2 \frac{\sigma_N}{E_i \cdot k_f}\right]^{\frac{3}{2}} = 2.59\frac{r_S}{e_i}\,\xi^2 \cdot \frac{\sigma_F-\sigma_N}{E_i \cdot k_f}\left[1-0.389\,\frac{r_S}{e_i} \cdot \xi \cdot \frac{\sigma_F-\sigma_N}{E_i \cdot k_f}\right] \quad (5\text{-}79)$$

Solve Equation 5-79 iteratively for the tangential stress σ_n.

From which the critical buckling stress can be determined by:

$$\sigma_{cr} = \frac{\sigma_N}{\xi}\left[1 - \frac{r_s \cdot \xi}{e_i} \cdot \frac{\sigma_F - \sigma_N}{\left(\frac{3\pi}{2} - 1\right)E_i \cdot k_f}\right] \tag{5-80}$$

The bending coefficient k_f of the flange connection with a lead gasket is given by:

$$k_f = \frac{2r_s\pi\psi}{2r_s\pi\psi + Z \cdot E_i} \cdot I \tag{5-81}$$

where: I = moment of inertia of tubbing of unit height (in^4/in, mm^4/mm)

$I = I_{yy}/H$

ψ = stiffness of the flange connections with lead gasket (lb)

Z = number of segments in a tubbing ring

The stiffness of the flange connection with lead gasket is given by:

$$\psi = \frac{E_L}{12S}\left(d^2 - 2\sqrt{3} \cdot S \cdot A \cdot \frac{\sigma_o}{\sigma_{YL}}\right)^{\frac{3}{2}} \tag{5-82}$$

where: E_L = modulus of elasticity of lead = 284,000 psi (for $5{,}700 \le \sigma \le 11{,}400$ psi)*

d = width of the tubbing flange (in, mm)

A = unit cross-sectional area of tubbing segment (in^2/in, mm^2/mm)

σ_o = average tangential stress in the tubbing ring (psi, kPa)

σ_{YL} = yield stress of the lead gasket (psi, kPa)

S = thickness of lead gasket (in, mm)

* Multiply by 6.895 to obtain kPa

Required safety factor:

$$SF = \frac{P_{cr}}{P_o} \geq 2.0 \qquad (5\text{-}83)$$

where: P_{cr} = critical buckling horizontal pressure (psi, kPa)

$$P_{cr} = \frac{\sigma_{cr} A}{r_a}$$

$r_a = r_i + d$

P_o = uniform outside horizontal pressure (psi, kPa)

To determine the buckling safety of a tubbing ring for unlimited possibilities, refer to Section 5.3.5.1, Buckling Safety of Lining Rings with a Slenderness Ratio $\lambda \geq 66$ (Thin Shell).

5.5.2 Cast Iron Tubbing and Concrete Envelope Stress Analysis

In the design of a lining composed of cast iron tubbing and a concrete envelope (Case 2), the following stress analyses should be performed:

a) To determine circumferential stresses in the tubbing and concrete section resulting from uniform and nonuniform horizontal pressure, solve using the methods shown in Section 5.3.2, Stress Determination for Nonstandard lining Configurations.

b) If the analysis performed in the above paragraph indicates that the tubbing and concrete are bonded, then determine the buckling safety using the methods shown in Section 5.3.5.2, Buckling Safety of Lining Rings with a Slenderness Ratio of $20 < \lambda < 66$ (Thick Shell). If the analysis indicates that the tubbing and concrete are not bonded, then determine the buckling safety using the methods shown in Section 5.5.1, Cast Iron Tubbing Column Stress Analysis.

5.5.3 Corrosion

It has been found from field measurements that the thickness of the walls, flanges, and ribs of ductile cast iron tubbing segments decreases through corrosion by an average of 0.004 in (0.1 mm) per year. The dimensions of the tubbing segments should compensate accordingly for any expected loss.

5.5.4 Lead Gasket

Watertightness of the cast iron lining column is achieved by installing 0.12-inch-thick (3.05 mm) lead gaskets between the vertical and horizontal flanges of the tubbing segments. The gaskets are made of virgin lead (99.9% Pb) (ASTM B29-79) or antimonial lead (99.2% Pb and 0.8% Sb). The yield point of the virgin lead is approximately 1.1 ksi (7,579 kPa). The yield point of antimonial lead is higher.

A thin lead gasket confined by two flanges resists high compressive stress before it starts to exhibit plastic flow.

Compressive stress σ_{PL} in the middle of the flange at which plastic flow of the lead gasket will commence is given by:

$$\sigma_{PL} = \frac{d\sigma_{YL}}{\sqrt{3}\,S} \tag{5-84}$$

where: σ_{YL} = yield stress of lead gasket (psi, kPa)
d = width of tubbing flange (in, mm)
S = thickness of lead gasket (in, mm)

5.6 REINFORCED CONCRETE LINING

Figure 5.14 shows the factors used in Equations 5-86 through 5-95. The definitions of these factors are as follows:

r_i = inside radius of concrete (in)
r_s = radius to center of reinforced concrete section (in)
r_o = outside radius of concrete (in)
B = thickness of reinforced concrete section (in)
f = cross-sectional area of single reinforcing steel bar (in^2)
z = number of horizontal reinforcing steel bars per unit length of concrete lining section (ft^{-1})

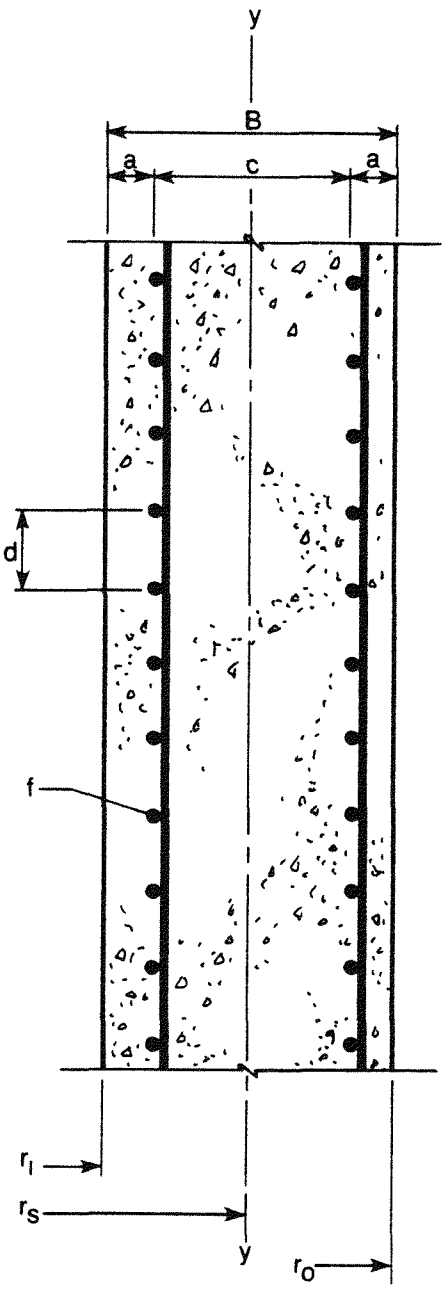

SECTION THROUGH REINFORCED CONCRETE LINING

FIGURE 5.14

c = distance between centers of horizontal reinforcing steel bars (in)

d = vertical spacing between centers of horizontal reinforcing steel bars (in)

a = distance between concrete surface and centers of horizontal reinforcing steel bars (in)

n = E_S/E_C

5.6.1 Properties of Reinforced Concrete Section

Area:

$$A_{total} = 12B + nfz \ (in^2/ft) \tag{5-85}$$

Where:

12 is (in/ft)

Moment of Inertia:

$$I_{yy} = B^3 + nfz \left(\frac{c}{2}\right)^2 (in^4/ft) \tag{5-86}$$

Radius of Gyration:

$$i = \sqrt{\frac{I_{yy}}{A_t}} \ (in) \tag{5-87}$$

Slenderness Ratio:

$$\lambda = 1.8135 \bullet \frac{r_s}{i} \tag{5-88}$$

5.6.2 Circumferential Stresses in Reinforced Concrete

1) Uniform Horizontal Outside Pressure:
   Coefficient for decrease of compressive stress in concrete due to placement of horizontal reinforcing steel is given by:

$$\delta = \frac{1}{1 + (n-1)\frac{fz}{12B}} \tag{5-89}$$

where: 12 is (in/ft)

Stresses in Reinforced Concrete:

$$\sigma_i = -\delta \cdot P_o \cdot \frac{2r^2_o}{r^2_o - r^2_i} \tag{5-90}$$

$$\sigma_o = -\delta \cdot P_o \cdot \frac{r^2_o + r^2_i}{r^2_o - r^2_i} \tag{5-91}$$

$$\sigma_{AV} = \frac{\sigma_i + \sigma_o}{2} \tag{5-92}$$

where: σ_i = tangential stress at inside face of reinforced concrete

σ_o = tangential stress at outside face of reinforced concrete

σ_{AV} = average tangential stress in reinforced concrete

Stresses in Reinforcing Steel Bars:

$$\sigma_{si} = n\left[\sigma_o + (\sigma_i - \sigma_o)\frac{a}{B}\right] \tag{5-93}$$

$$\sigma_{so} = n\left[\sigma_o + (\sigma_i - \sigma_o)\frac{B-a}{B}\right] \tag{5-94}$$

where: $n = \frac{E_s}{E_c}$

σ_{si} = tangential stress in the inner horizontal reinforcing steel

σ_{so} = tangential stress in the outer horizontal reinforcing steel

2) Nonuniform Outside Horizontal Pressure:

Reinforced Concrete: Use Equations 5-10 and 5-11 but substitute σ_{AV} for $\frac{P_o \cdot r_a}{A}$

Reinforcing Steel Bars: Use Equations 5-10 and 5-11 with following modifications:

1. Substitute σ_{AV} for $\frac{P_o \cdot r_a}{A}$.
2. Multiply the right side of Equations 5-10 and 5-11 by n.

3) Buckling Safety of Reinforced Concrete Lining Ring:

Buckling of a reinforced concrete ring in a shaft lining is calculated by using the equations shown in Section 5.3.5, Buckling Safety of Lining Rings.

The total cross sectional area of horizontal reinforcing bars should not exceed 3% of the total concrete section depending on the concrete thickness. Vertical reinforcement should amount to approximately one quarter of the horizontal steel bar section, provided that the longitudinal bending of the shaft lining column is not critical.

As it is shear stress which leads to failure of the concrete, the displacement of the concrete may proceed only towards the center of the shaft. Stirrups placed in horizontal planes will greatly increase the structural resistance of the concrete shaft wall. Methods of designing reinforced concrete are well known in the field of structural design, and can be easily adapted for shaft lining structures.

5.7 OPERATIONAL SEALS

5.7.1 Picotage Seals

Picotage seals may be used in conjunction with wedge rings for tubbing and steel lined shaft sections. The picotage height should be at least 12 inches (305 mm) and width not less than four inches (102 mm).

5.7.2 Chemical Seals

Chemical seals may be used in conjunction with ductile cast iron tubbing and steel lined shaft sections. The seal properties and its thickness-to-height ratio relative to the design pressure must conform to the technical data prepared by the manufacturers.

5.7.3 Asphaltic Sealant Material Seals

ASM seals can be used in conjunction with steel lined shaft sections. The ASM's specific weight and viscosity and the height of the ASM column section should be based on the calculated depth of ASM penetration into the open and fluid-filled pore spaces and fractures in the rock.

The ASM seal sections should be sufficiently ductile to make the seal self-healing at the selected height under hydrostatic pressure and at the design temperature.

5.8 SHAFT STATION AREA

The designer must recognize that the transition from the shaft to the horizontal subsurface entries imposes loads on the shaft lining which are different from those exerted on the shaft. In particular, the interaction of the shaft station with the shaft lining system requires adjustment of the horizontal design stress. The designer must consider adjusted coefficients of active stress and perform modeling of the shaft/shaft station interactive system.

5.9 DECOMMISSIONING SEALS

Repository shaft decommissioning seals will consist of concrete bulkheads and backfill materials designed to restrict groundwater flow and the migration of radionuclides. The shaft lining design is affected primarily by the dimensions and location of the bulkhead components. Therefore, backfilling is not discussed extensively in this guide.

5.9.1 Bulkhead Seals

5.9.1.1 Dimension Criteria

Bulkhead seals should be dimensioned to satisfy the low-leakage criteria. The design approach requires that the permeability of the host rock and the necessary thickness and strength of the stratum be determined. An evaluation of the disturbed zone, if any, and the long-term effects of thermal loading is also required.

5.9.1.1.1 Bulkhead Sizing. In order to dimension and locate bulkheads, the following criteria must be considered. A detailed explanation of each criterion is presented in Appendix C.

1. Rock mass, disturbed zone, and concrete bulkhead permeabilities.
2. Flow and pressure gradient across the length of the bulkhead.
3. Thickness of rock interval.
4. Strength of host rock.
5. In situ conditions at time of decommissioning.
6. Geochemistry.
7. Hydrochemistry.

5.9.1.1.2 Disturbed Zone. All excavation methods will induce some degree of disturbance in the adjacent host rock. The objective is to minimize this disturbance in locations where bulkheads are to be installed. Appendix C describes the disturbance caused by various excavation techniques. Additional disturbance may be caused by rock stress redistribution (see Section 4.1.1.2, Rock Pressures).

5.9.1.1.3 Thermal Loading. Thermal stresses in the host rock will not peak during the operational life of the lining, but rather some time after decommissioning. The strength of the concrete comprising the bulkhead should therefore be designed to accommodate these stresses.

5.9.1.2 Location

Bulkhead seal locations should be selected by reviewing the seal system philosophy and the availability of low-permeability, competent rock strata.

5.9.1.2.1 **Philosophy.** The number of bulkheads required is dependent on the expected flow and pressure gradients of water into, or out of, the repository horizon. Low-permeability rock strata below the major aquifers will retard groundwater flow. The rock should have few open discontinuities and not be highly influenced by the excavation process.

Sealing redundancy can be achieved by constructing successive pairs of bulkheads and by utilizing different rock strata for each pair, where possible.

5.9.1.2.2 **Configuration.** Bulkheads should be located below ASM/watertight lining sections and their associated bearing keys. If possible, the bearing keys may be considered for use as bulkhead shells, provided steel reinforcement can be removed upon decommissioning.

The salt strata above the repository horizon may be an ideal location for pairs of bulkheads since few critical lining components must be located in this section. However, because salt creep will induce full lithostatic loads, it may be necessary to install removable lining sections of compressible backfilling material behind the lining.

5.9.2 Backfill Seals

Backfilling is the second basic component of the shaft sealing system. Different materials will be used to fill the openings between bulkheads. Current schematic designs include engineered earthen materials which will retard the flow of groundwater and the migration of radionuclides. Crushed salt will be used for backfilling in the shaft areas adjacent to salt strata. Cementitious material will be used in areas where load-bearing capability is required.

Nonwatertight lining sections may have to be removed so that the backfilling material can be placed directly against the host rock. It is feasible to remove watertight tubbing provided it is properly destressed. However, watertight steel-lined sections are not easily removed unless they are specifically designed with removal in mind. Lining sections which most likely will not require removal prior to placing backfill will be installed in the upper aquifer horizons since removal would necessitate re-freezing. Removal of lining sections at decommissioning will also provide greater flexibility in locating bulkheads.

5.10 SHAFT EQUIPPING EFFECTS ON SHAFT LINING

The various brackets, support systems, embedments, and penetrations needed to accommodate shaft equipment and outfitting will result in secondary loading and local stress disturbances in the shaft lining. These local effects should be evaluated by means of closed form solutions, or by means of dedicated local finite-element models.

Equipment supporting areas should be checked for fatigue and impact loading if local vibration or dynamic loading is a possibility. The danger of crack initiation should be addressed on the basis of a minimum allowable flaw dimension. The general fracture mechanics approach to crack propagation should be limited to the evaluation of crack tip stress intensity factors in order to quantify crack growth, if any.

5.10.1 Fittings

Seismic reactions on brackets supporting conveyance attachments, utilities, and other furnishings should be considered in the shaft lining analysis. In-structure accelerations at the appropriate depth should be used for the seismic analysis of appurtenances and for safety checks of the corresponding reaction of equipment supports to seismic activity. Support brackets attached to the lining, and their anchoring, should be stress checked for seismic reactions acting in combination with other bracket loads. The localized stress effects of bracket reactions on the lining should also be included in the lining design verification, using allowable material strengths for extreme load conditions.

In-structure accelerations are obtained from the site response analysis described in Section 4.4.2, Site Response Analysis. In-structure response spectra at the surface and at selected depths are provided in the SRP Input to Seismic Design. Three directions of earthquake motion must be considered. In-structure response spectra must be assumed to vary linearly between depths where spectra are provided. To account for response phasing, the three orthogonal components of seismic response must be calculated using the 100-40-40 rule described in Newmark and Hall (1978).

5.11 INSTRUMENTATION AND MONITORING CONNECTION EFFECTS ON SHAFT LINING

Penetrations of the shaft lining for instrumentation and monitoring should be designed in such a manner that the connectors will not compromise the mechanical integrity or watertightness of the lining section. The

attachments, embedments, and penetrations provided for instrumentation and monitoring equipment constitute local stress raisers. Their effects on shaft integrity should be addressed in local studies. While penetrations cause local disturbances in the shaft structure, their extent depends on the penetration size and reinforcement. By rule of thumb, peripheral reinforcement should be provided for any penetration that is wider than the wall is thick. Penetrations should be circular whenever possible. No angular cuts or sharp corners are permitted.

The simplest reinforcement guideline is the so-called ''area replacement'' approach whereby the structural material eliminated through the opening is redistributed around the penetration by means of reinforcing steel, nozzle arrangements, and possibly local wall thickening.

Recommended reinforcement for penetrations of different sizes are:

1. For penetration diameters smaller than a quarter of the wall thickness, no special reinforcement needed.

2. For penetration diameters between a quarter of the wall thickness and the wall thickness, provide:

   a. Circumferential reinforcement concentrated within a two-diameter area.
   b. Orthogonal reinforcement within a five-diameter area.

3. For penetration diameters larger than the wall thickness, the orthogonal reinforcing arrangement should be complemented by a nozzle-type steel reinforcement.

Local stress analyses should be based on the application of plane stress concentration factors of $+3.0$ and -1.0 for circular openings in flat membranes subjected to uniaxial stresses. For local bending and transverse loading effects, appropriate elastic solutions should be supplied through the standard theory of shells.

Special purpose finite-element models can be used to address local problems for any load configuration in the elasto-plastic stress range.

6 COMPUTER DESIGN ANALYSIS

The purpose of this chapter is to describe computer modeling techniques that can be used for design of the Salt Repository Program (SRP) shafts. Computer modeling has two primary objectives. First, to verify shaft designs carried out by conventional closed-form calculations and, second, to examine the relationship of the lining structures to the surrounding rock and the changing stress conditions that are not easily characterized by conventional methods. Finite-element modeling extends the scope of the closed-form solution methods and provides greater detail in analysis of the interaction between the lining structures and the surrounding geological and hydrological environment. The goal of the chapter is to ensure that the designer understands how suitable modeling programs can be developed and applied to the design of the SRP shafts.

The chapter begins with a discussion of the computer methods and procedures that may be used in the design of the shaft components. Geometric model calibration, rheological material calibration, and load simulation of the different stress conditions expected during the life of the shafts are discussed. The second section of the chapter is a discussion of stress analysis. It begins with descriptions of three axisymmetric models and one nonsymmetric special purpose model.

Section 6.3, Lining System Stability, discusses the analysis of lining system stability. It first lists factors affecting lining buckling stability and then the three most distinct types of buckling problems. Section 6.4, Seismic Analysis Methodology Audit, is a discussion of the assessment of the seismic analysis methodology. It discusses an assessment made by computing the seismic response on the basis of a complete analysis of soil structure interaction (SSI) and comparing the results with those of the calculations described in Sections 4.4, Seismic Loading and 5.4, Stresses Due to Earthquakes. The final section deals with the analysis of local stresses.

6.1 COMPUTER MODELING

The designer can simulate and evaluate the interactive behavior of the lining and the rock strata surrounding it by using nonlinear, finite-element computer programs. These programs can be used to model the interaction between the lining structure and rock. They simulate rock freezing, creep, plastic yield, cracking, slippage, time and temperature dependence of material properties, and varying loading and boundary conditions. They also calculate the cumulative effect of large displacements on the lining. Input

data for modeling will be derived from the Synthetic Geotechnical Design Reference Data for the Deaf Smith Site (SRP Data Base) (DOE, 1986) which will be revised as new information becomes available during site characterization.

Computer codes used for design of the SRP shafts must comply with Quality Assurance Specifications set forth by the U.S. Nuclear Regulatory Commission in 10 CFR 50 Appendix B (NRC, 1986b), and in 10 CFR 21 (NRC, 1986a). A number of computer programs, which have been endorsed by the NRC upon validation and testing, are listed in NUREG/CR-3450 (Curtis, et. al., 1983). The parameters and variables appearing in repository design models are discussed in NUREG/CR-0856 (Silling, 1983). It is recommended that the shaft designer be acquainted with all information contained in these documents.

6.1.1 Model Calibration

Model calibration with respect to geometry and the constitutive laws of ground and support is necessary before modeling begins. Elastic solutions can be used, even though the behavior of the rocks may not be purely elastic, since these solutions allow the results to be compared with well known examples. Nonlinear solutions, if available, will provide a more accurate analysis.

6.1.1.1 Geometric Model Calibration

The development of a representative finite-element mesh model either for a typical section of rock and lining or for a particular component, such as the shaft bearing key, requires a preliminary calibration test in order to check for:

1. The adequacy of the model's extent, both radially and vertically.
2. The accuracy of the boundary conditions, as compared with the actual site and construction constraints.
3. Grid fineness (for proper representation of stress gradients and local discontinuities).
4. The choice of element types describing such items as rock mass, thin clay seams, concrete mass, steel lining, asphaltic sealant material (ASM), and void elements.

The procedure consists of applying unit loads and boundary deformations having elastic material characteristics to the final geometric model. The results may then be compared with known solutions, and the main geometric parameters and the boundary and initial conditions can be properly adjusted to limit parasitic disturbances. Special attention should be given to the lateral extent of the model and lateral boundary conditions for the case of creep simulation which is most sensitive to these factors.

6.1.1.2 Rheological Material Calibration

Major sources of error and inaccuracy are the constitutive equations describing the complete elastic, time, temperature, strain, and strain-rate dependent behavior of the various rock layers and shaft components. Errors can be minimized in these areas by comparing the computer simulations with the results of laboratory tests performed on sample specimens. Because soil and rock properties and concrete creep and shrinkage can vary widely, a range of values should be defined for the governing parameters. This approach will allow the user to single out the most sensitive parameters for further examination, if necessary. For example, the creep exponent in the strain-rate power law is by far the most important factor affecting stress redistribution under creep conditions. Changes in Young's moduli for dissimilar materials are essential for elastic solutions. Other parameters, such as the thermal expansion coefficient for soils that are to be frozen, are of importance where different types of materials interact.

6.1.2 TIME DEPENDENT LOADING AND SEQUENCING

In order to understand the behavior of the shaft system and to evaluate its performance capability from installation to the end of its service life, the designer can perform a complete time-history simulation of the interactive rock/lining system. This computer model study will trace the actual sequence of events as they are likely to occur. The example used in this section is a shaft lining that is similar to the lining design suitable for the repository shafts at the Deaf Smith County, Texas repository site. However, the example is somewhat simplified for convenience.

In this example, it is assumed that the upper portion of the shaft will be constructed in unconsolidated water-bearing strata that will require ground freezing to achieve safe working conditions during excavation. The lower shaft section will penetrate dry, consolidated strata that include multiple layers of salt. The lining

structure in the upper shaft section will consist of a primary concrete lining and a watertight steel and concrete final lining. ASM will be placed in the annulus between the primary lining and the final lining. The lower shaft section will be lined with concrete with a compressible material between the concrete and the shaft wall in salt strata.

The sequence of model development and analysis covering shaft construction, operation, and abandonment for this example can be summarized by the following steps:

1. Undisturbed lithostatic state of stress of the free field.
2. Freezing of soil and rock.
3. Excavation.
4. Installation of lining.
5. ASM loading.
6. Concrete shrinkage.
7. Thawing and steady state thermal regime.
8. Exterior loading and overburden.
9. Long-term creep, shrinkage, and relaxation regime.
10. Incidental loading (including subsidence, local settlement, slippage, thermal effects, and shaft equipping loads).
11. Shaft decommissioning.

These steps are illustrated in Figure 6.1 and briefly described in Sections 6.1.2.1 to 6.1.2.11. The duration of each step is dependent upon the construction, operation, and decommissioning schedule.

Explanation of Figure 6.1

(a) The model comprises only undisturbed rock elements identified as (1).

(b) Some of the rock elements are frozen and their properties might change. These frozen elements are identified as (2).

(c) Certain rock elements (undisturbed elements (1) and possibly frozen elements (2)) are excavated and become voids identified as (3).

(d) Shaft lining elements are added to the model. These are identified as (4).

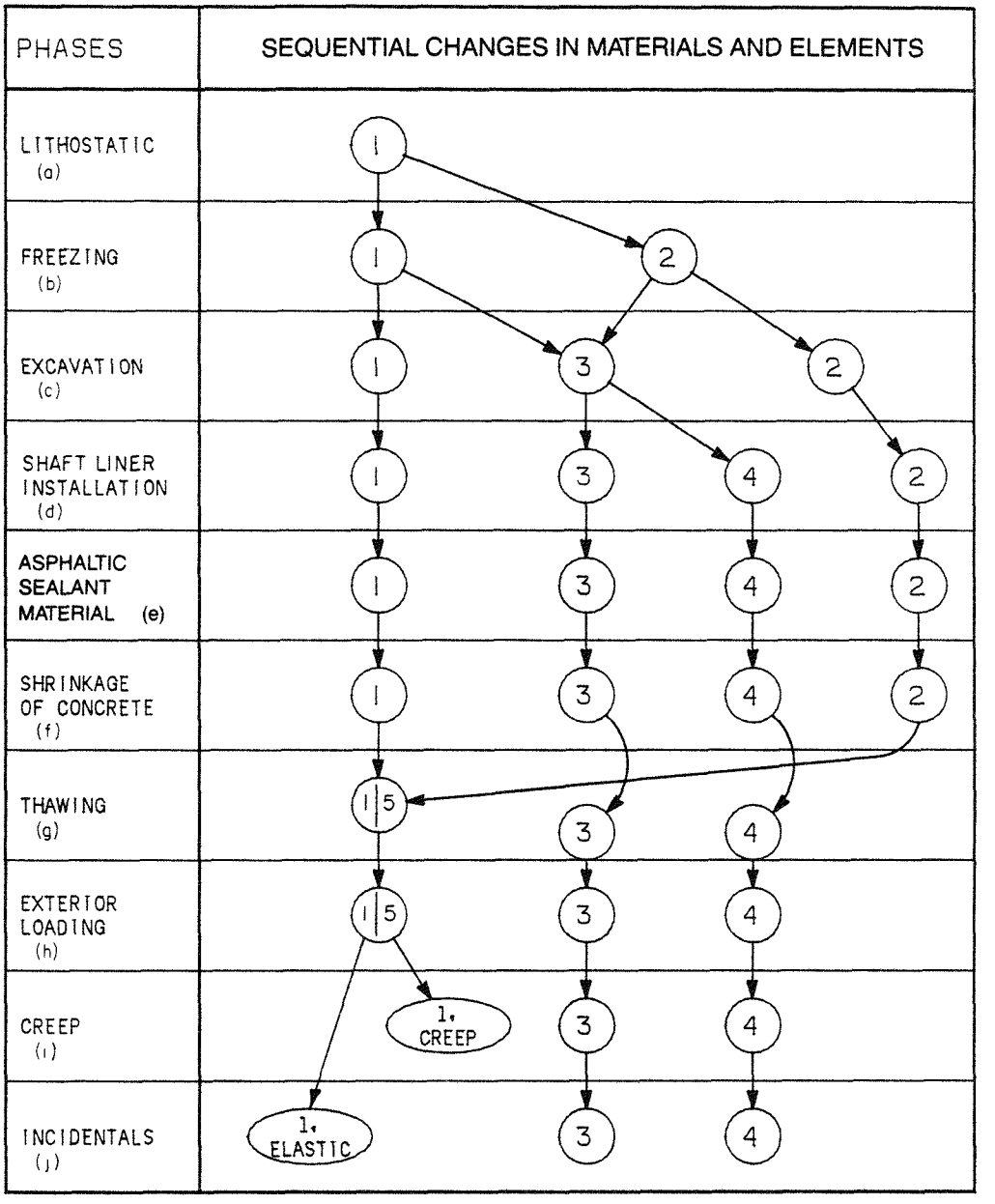

AXISYMMETRIC FINITE ELEMENT MODEL: SEQUENTIAL MATERIAL PROPERTY CHANGES

FIGURE 6.1

(e) Modeling of ASM loading is simulated by a radial pressure acting on both faces of the gap element. The gap element simulates the annulus between the primary lining and the steel membrane of the main lining.

(f) Concrete shrinkage strain is simulated by a specified volumetric strain in all concrete elements.

(g) All frozen rock elements revert to their initial temperature with material characteristics that may have been modified identified as (5).

(h) Simulation of loads caused by external factors such as settlement, earthquakes, and tectonic movements.

(i) Simulation of long-term, time-dependent deformation resulting from the interaction between salt creep and the lining.

(j) Simulation of long-term incidental loadings such as thermal stresses.

6.1.2.1 Undisturbed Lithostatic State of Stress of the Free Field

In this first phase of the analysis, where lining elements are to be examined, original "undisturbed" ground conditions are modeled as they are before construction begins. Gravity loading, lateral boundary confining pressure, and simple support conditions along the bottom boundary simulate these conditions. The rock layers are modeled with their original characteristics, that is, as undisturbed elastic material. Each layer and each seam is modeled using a separate set of finite elements (see Figure 6.2 and Table 6.1). The rock/shaft system can be described by plane-strain, axisymmetric, three-dimensional models. The extent of the model is limited at the top by a top boundary surface, at the bottom by the bottom boundary surface, and laterally by the lateral boundary.

6.1.2.2 Freezing of Soil and Rock

Once the first lithostatic loading configuration has been analyzed, the soil and rock to be frozen can be simulated using special purpose time- and temperature-dependent material properties. To do this, the original properties of the appropriate elements are gradually changed from the unfrozen to the frozen state. The corresponding temperature distributions are also adjusted until a steady state condition has been reached. This simulates the progression of radial and vertical freezing.

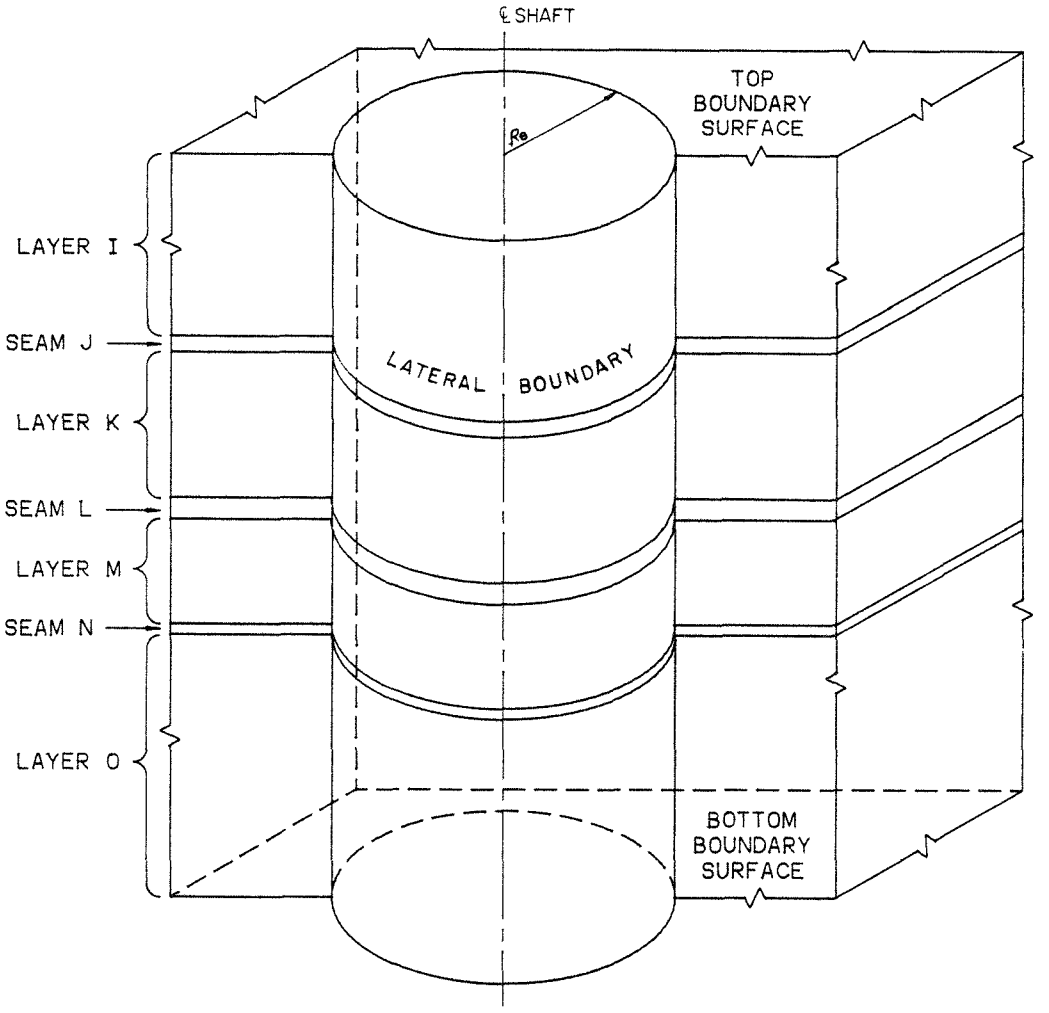

STRATIGRAPHIC CUT-AWAY VIEW OF THE SHAFT ZONE
FOR SIMPLIFIED MODEL SIMULATION

NOTE: See Table 6.1 for explanation of symbols.

MODEL OBJECT
FOR INITIAL PHASE
FREE FIELD
LITHOSTATIC STATE

FIGURE 6.2

Table 6.1 Symbols Used in Figures 6.2 through 6.14

1 = Elements representing rock in its natural state.

2 = Elements representing frozen material which might exhibit different material properties.

3 = Void elements (excavation).

4 = Lining elements simulating the complete lining system.

4a = Concrete.

4b = Inner steel lining.

4b′ = Outer steel lining.

4c = Primary lining.

4d = Gap element.

5 = Elements representing rock that has been frozen and thawed.

R_i = Inside radius of final lining.

t_i = Thickness of final lining.

R_e = Outside boundary radius of model.

R = Radial coordinate.

z = Axial coordinate (vertical).

O.D. = Outside shaft diameter.

I.D. = Inside shaft diameter.

Simulation of the freezing process through the various layers of rock material must take into account the water content of the rock in order to establish the resultant steady state swelling or shrinkage. High water content may cause swelling, but dry rock material tends to shrink when frozen. This difference of behavior becomes critical at the interface of wet and dry materials. During freezing, radial and circumferential cracks are likely to occur in dry, brittle rock layers. The bottom of the freezing zone in particular requires special attention because high stress gradients can lead to potential hemispherical cracking (Figures 6.3, 6.4, and 6.5). Special three-dimensional models simulating radial cracking as well as inclined failure surfaces can be developed in a second phase study.

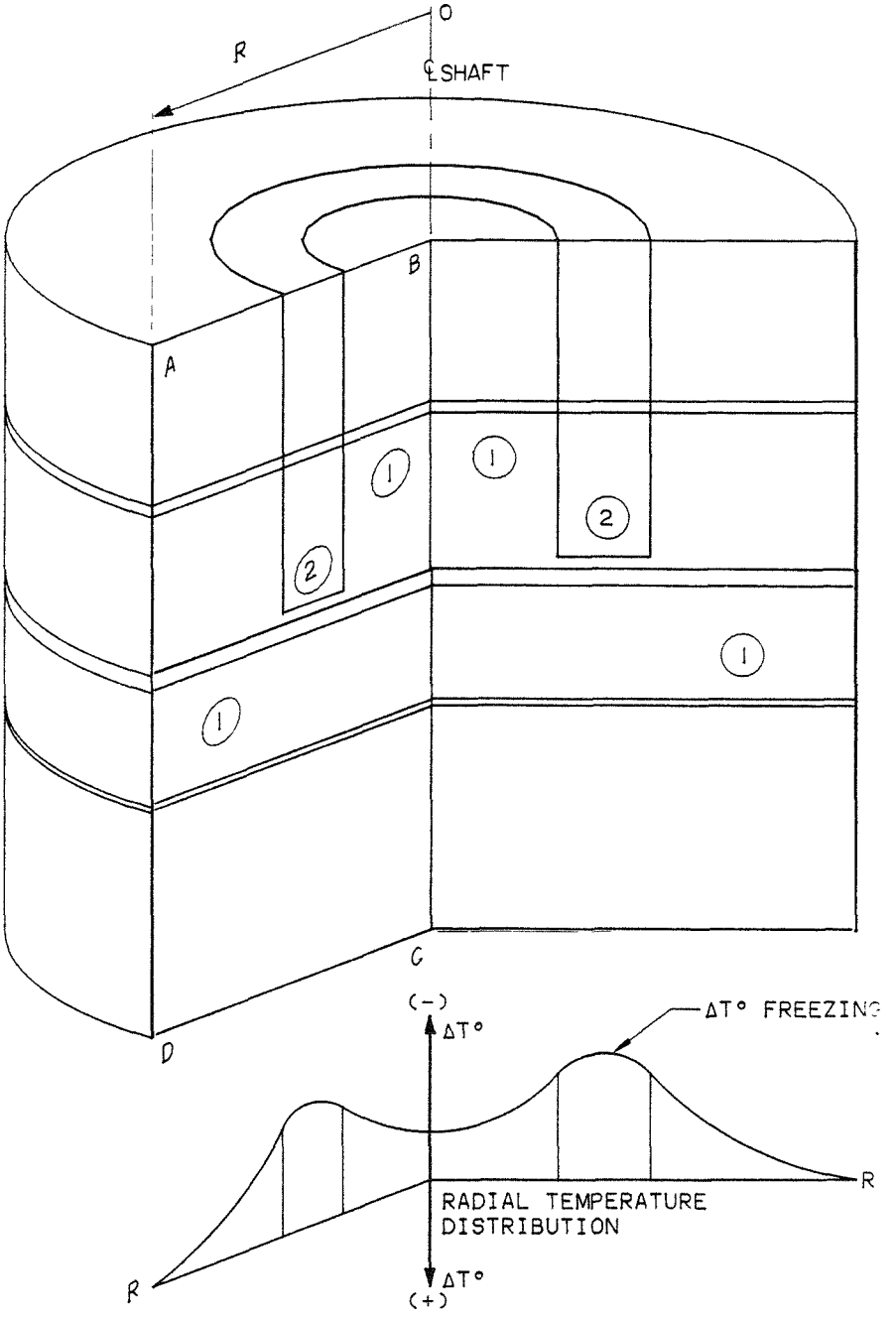

NOTE: See Table 6.1 for explanation of symbols.

MODEL OBJECT FREEZING OF A RING-SHAPED VOLUME

FIGURE 6.3

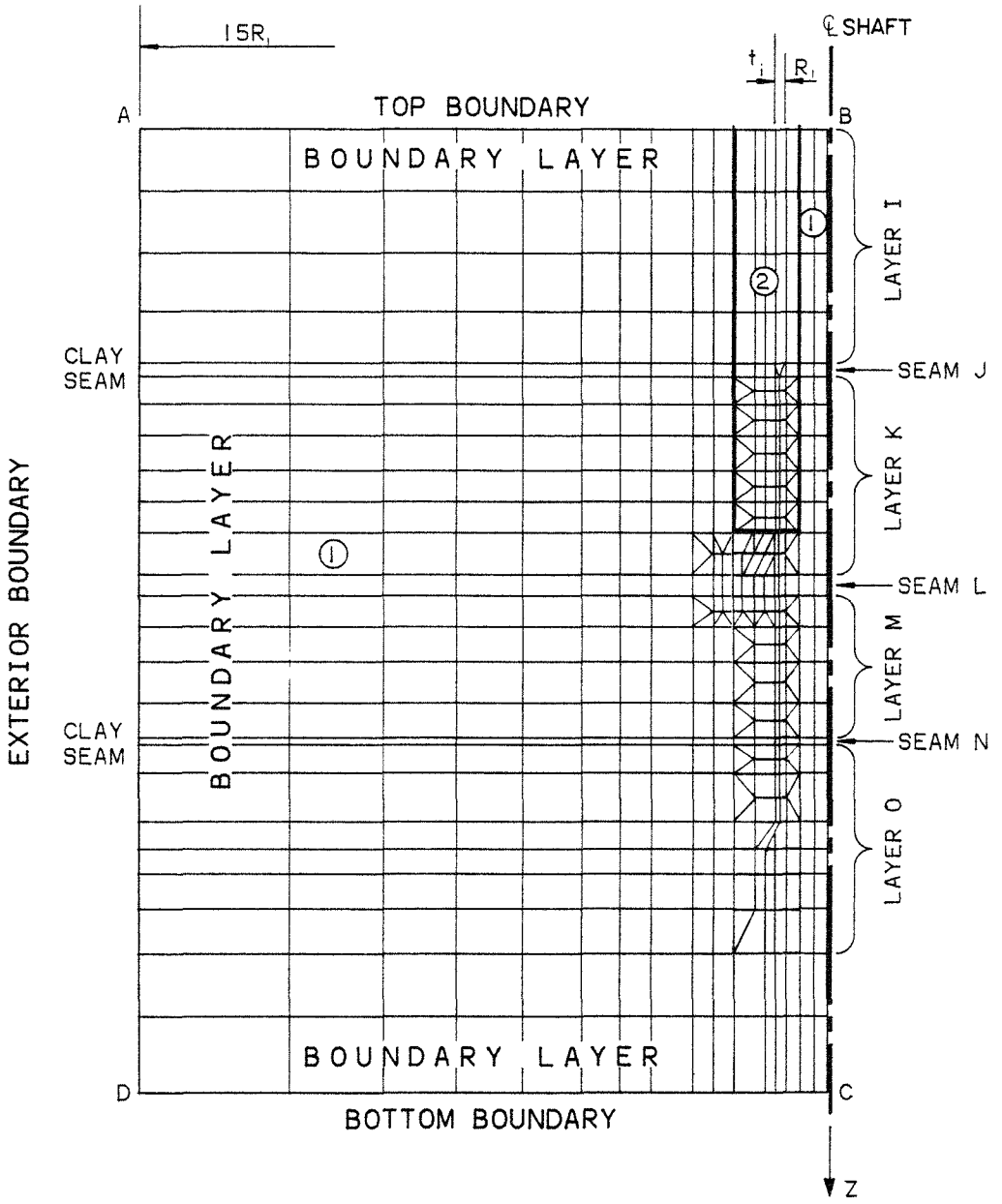

NOTE See Table 6.1 for explanation of symbols.

AXISYMMETRIC FINITE ELEMENT MODEL SIMULATING THE ROCK FREEZING PHASE

FIGURE 6.4

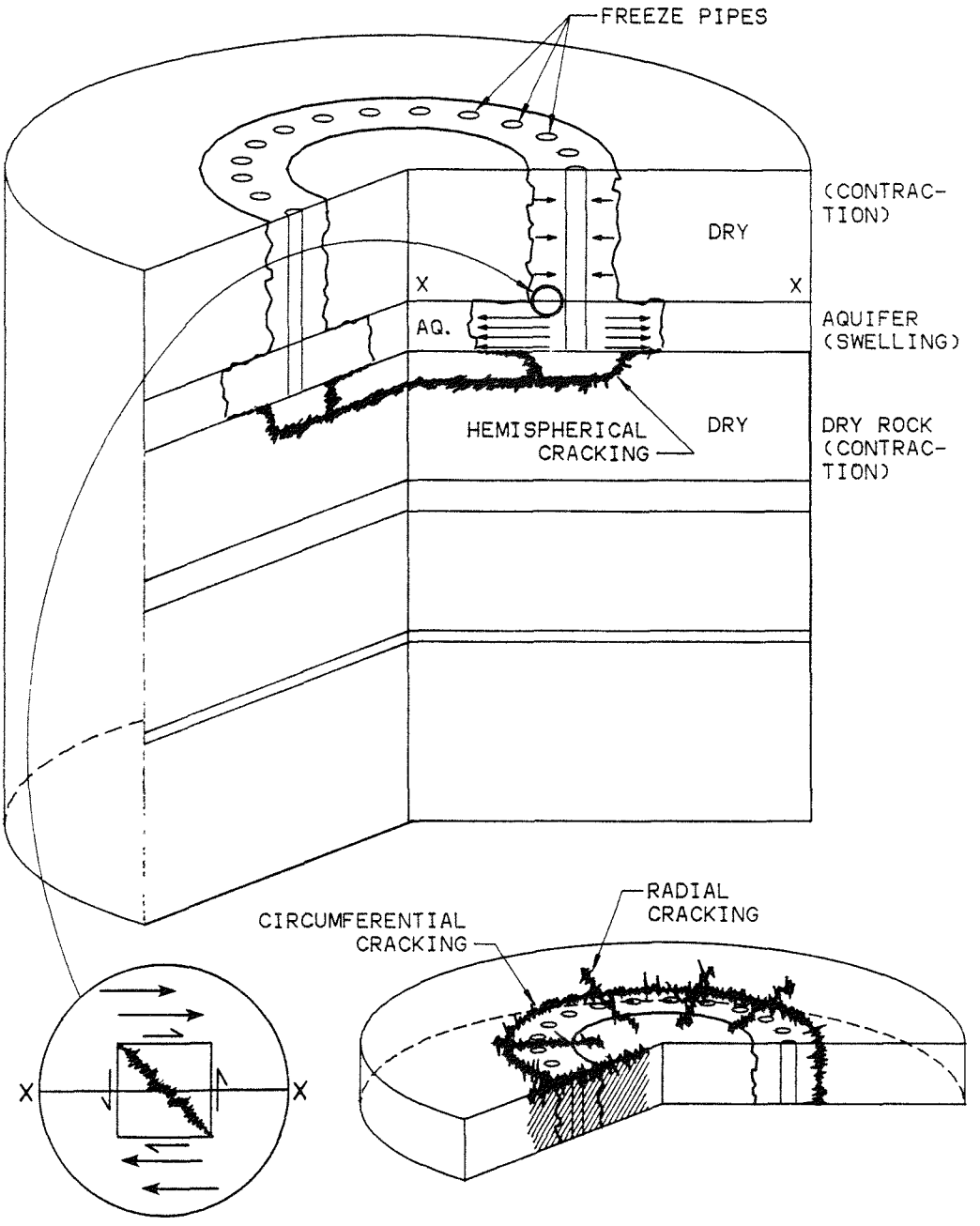

NOTE: 1. Radial and circumferential cracking has been observed in dry rock layers. Bottom hemispherical cracks occur as well below tip of freeze zone.

2. See Table 6.1 for explanation of symbols.

FREEZING CRACK GENERATION

FIGURE 6.5

6.1.2.3 Shaft Excavation

Excavation is simulated by progressive elimination of the elements located in the excavation zone of the shaft. The volume of rock to be excavated is represented by an axisymmetric center plug (see Figure 6.6). An optional procedure would be to change the material properties for all excavation elements.

6.1.2.4 Installation of Lining

Lining installation follows excavation and is simulated by activating a set of elements corresponding to the shaft lining system, including special provision for ASM. These elements model the steel lining plate, the concrete lining, and the interface between the lining and the rock. In this phase, these material properties are the short-term values for steel and concrete.

The gap to be filled with ASM is modeled using gap/contact elements. This allows resolution of contact problems caused by closure. Similar contact elements can be provided at the interface of the primary lining and the rock. Figure 6.7 illustrates the steel lining plate, the concrete lining, and the gap for ASM. Figure 6.8 represents the model elements which simulate the shaft structure.

6.1.2.5 Asphaltic Sealant Material Loading

A radial pressure load is applied to the ASM gap boundaries during simulation of sealant placement in the gap between the primary concrete lining and the outer steel lining.

6.1.2.6 Concrete Shrinkage

Concrete shrinkage occurs in both the primary and final lining. This changes the gap for ASM and also creates gaps between the primary lining and the rock if the concrete/rock bond is broken. To allow for these gaps, the model provides gap/contact elements in both locations. These elements allow for free shrinkage of the concrete lining without generating radial tensile stresses at the gap faces. Shrinkage strains are imposed on the concrete linings (see Figures 6.9 and 6.10.).

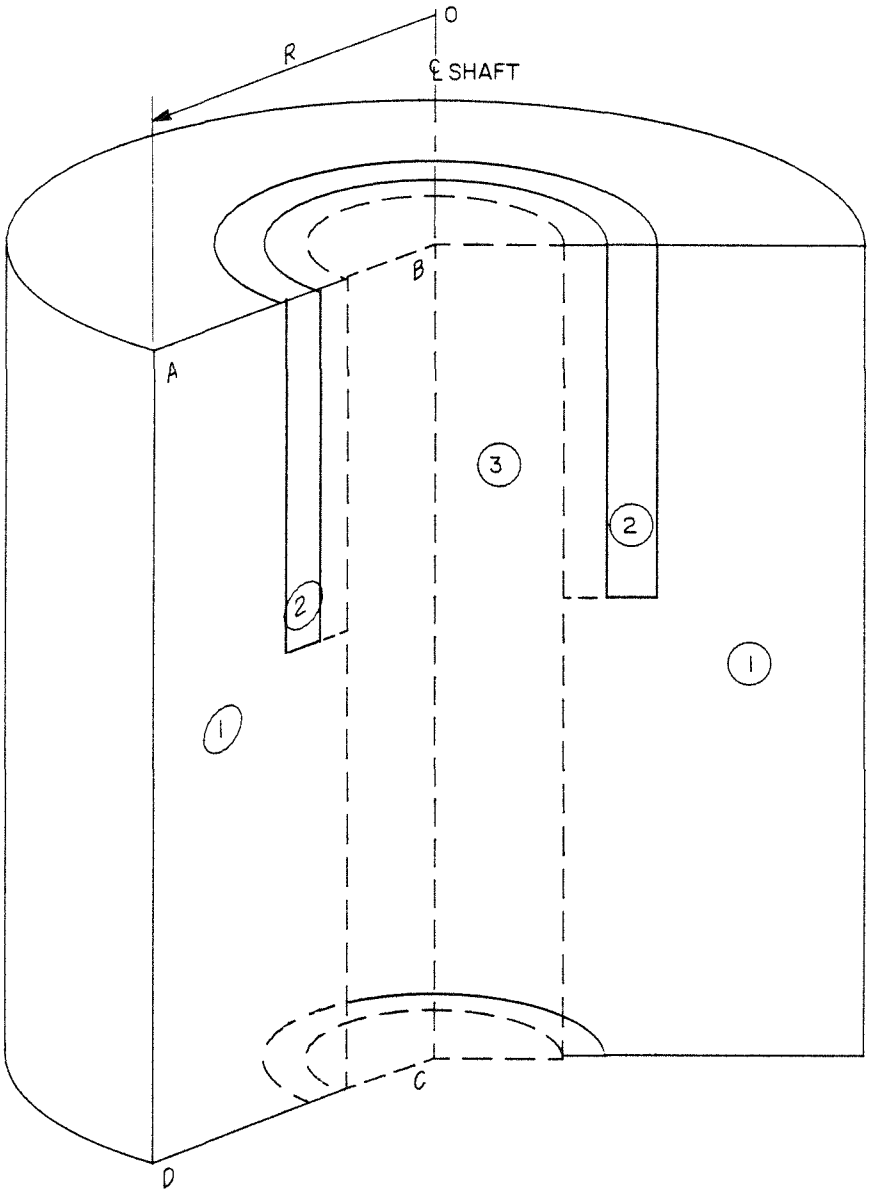

EXCAVATED ELEMENTS SIMULATED IN
FINITE ELEMENT MODEL THROUGH "VOID"
ELEMENT ③ MATERIAL PROPERTIES

NOTE: See Table 6.1 for explanation of symbols.

MODEL OBJECT:
EXCAVATION OF CENTER CYLINDRICAL PLUG

FIGURE 6.6

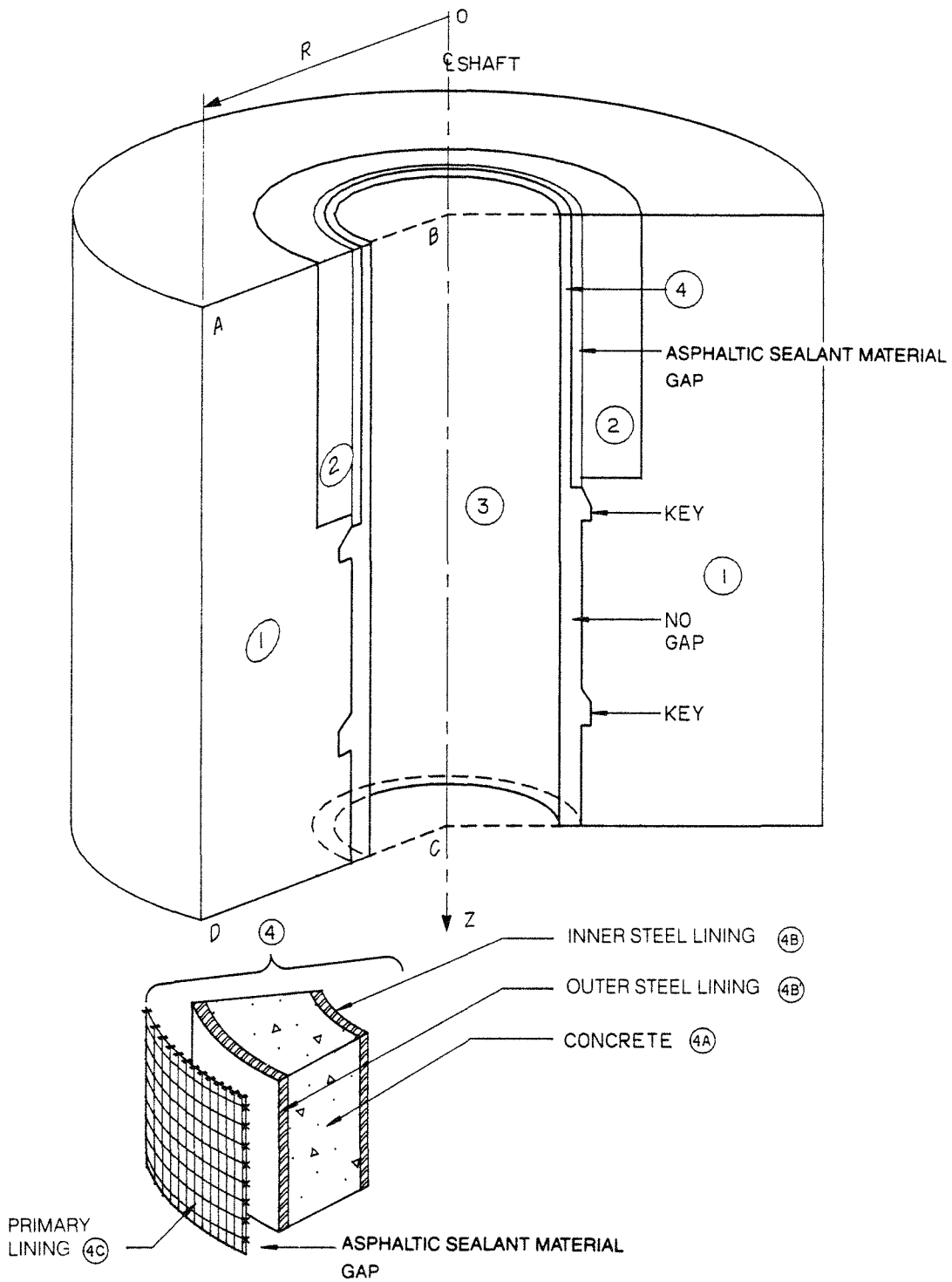

NOTE: 1. Asphaltic sealant material is poured into the gap between the primary lining and the outer steel lining.
2. See Table 6.1 for explanation of symbols.

MODEL OBJECT:
INSTALLATION OF
SHAFT LINING STRUCTURE

FIGURE 6.7

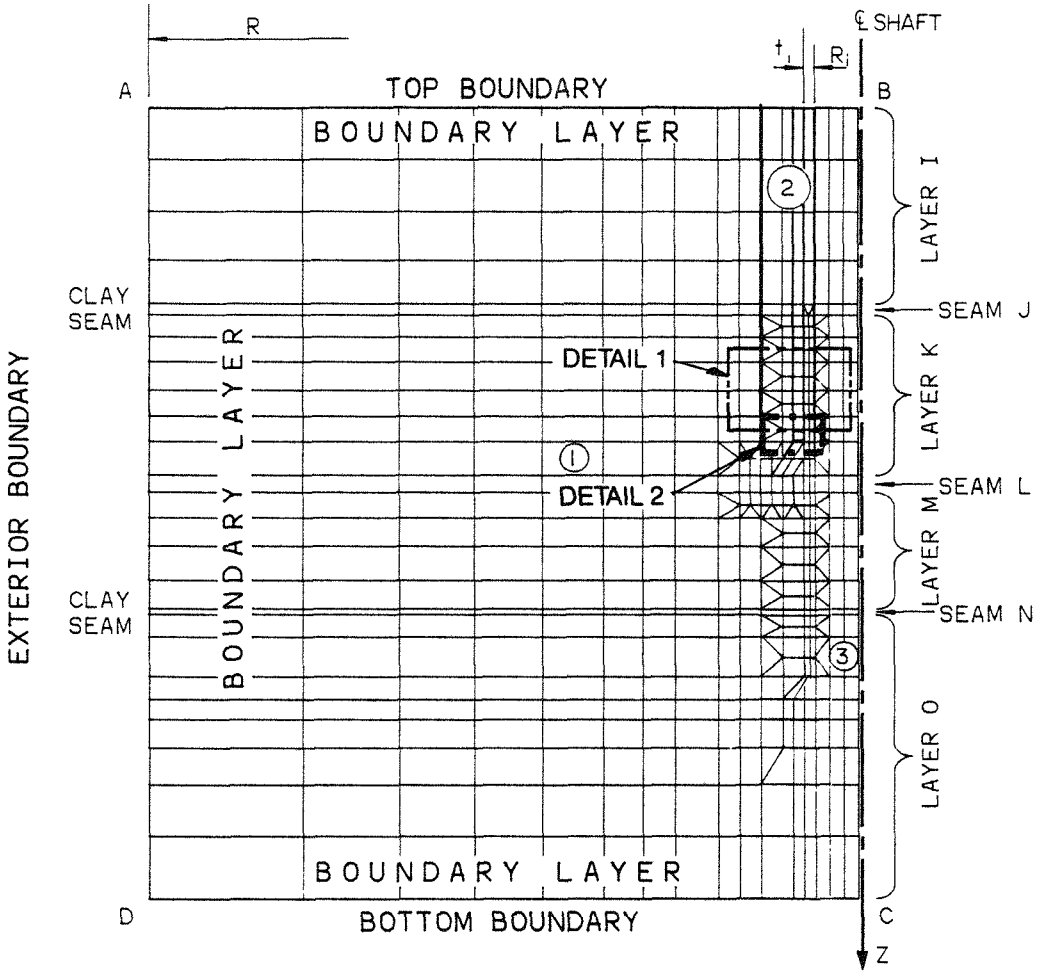

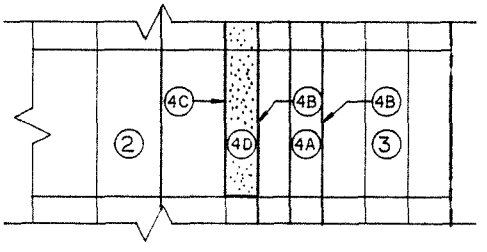

DETAIL 1

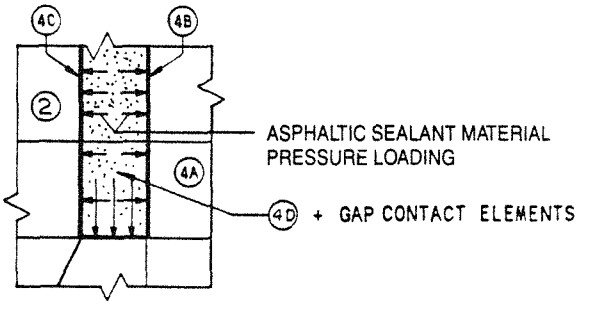

DETAIL 2

NOTE: 1. Asphaltic Sealant Material is modeled by gap contact elements. The gap contact elements are part of all subsequent model phases.

2. See Table 6.1 for explanation of symbols.

NOTE: Asphaltic Sealant Material loading is simulated through radial pressure applied to all faces of the gap.

AXISYMMETRIC FINITE ELEMENT MODEL SIMULATING THE SHAFT LINING INSTALLATION AND ASPHALTIC SEALANT MATERIAL PLACING PHASES

FIGURE 6.8

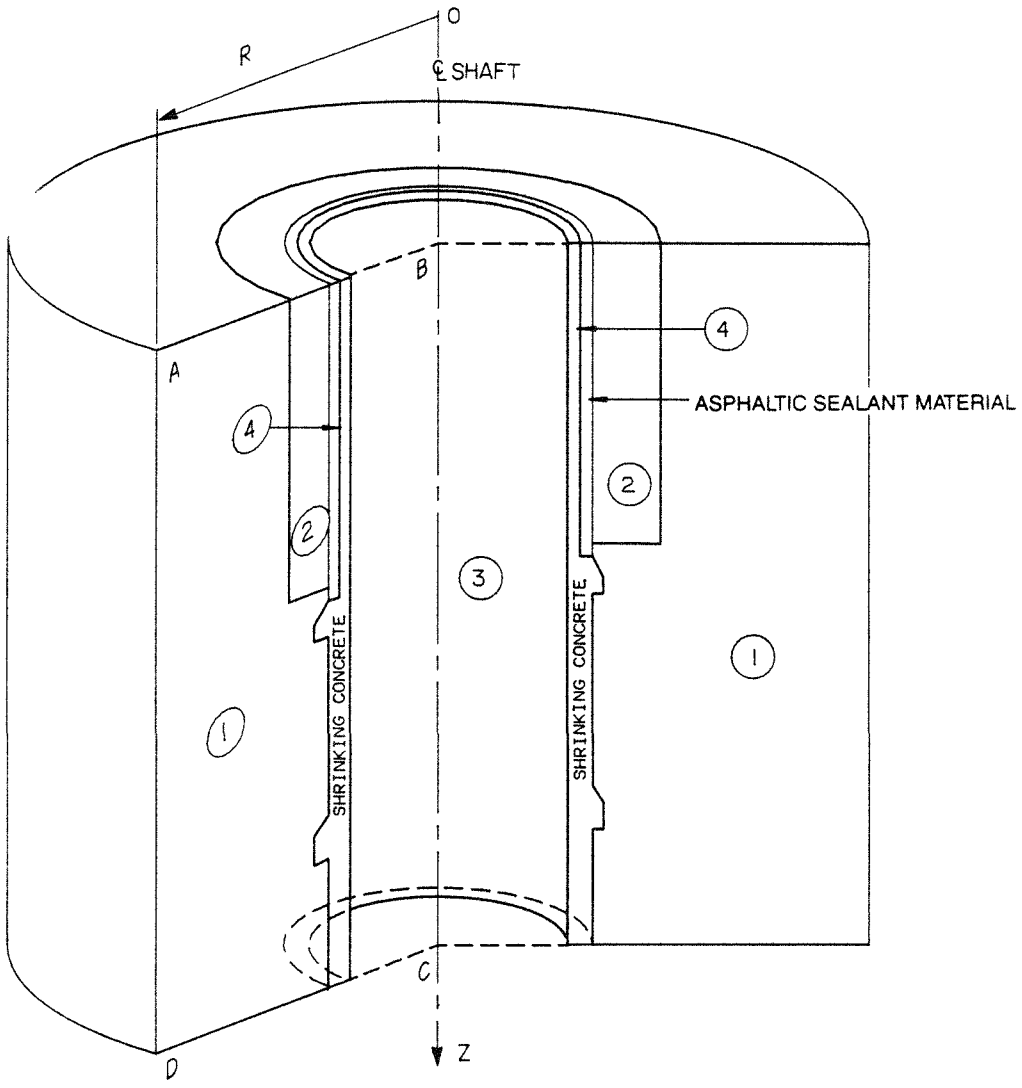

NOTE: 1. Shaft concrete shrinkage strains are imposed on all shaft concrete elements as a consequence, steel lining shells are subjected to membrane compression and the asphaltic sealant material gap increases slightly.

2. As frozen rock is thawed, the material properties revert to rock type ① or type ⑤ properties.

3. See Table 6.1 for explanation of symbols.

MODEL OBJECT: CONCRETE SHRINKAGE AND THAWING OF FROZEN ROCK

FIGURE 6.9

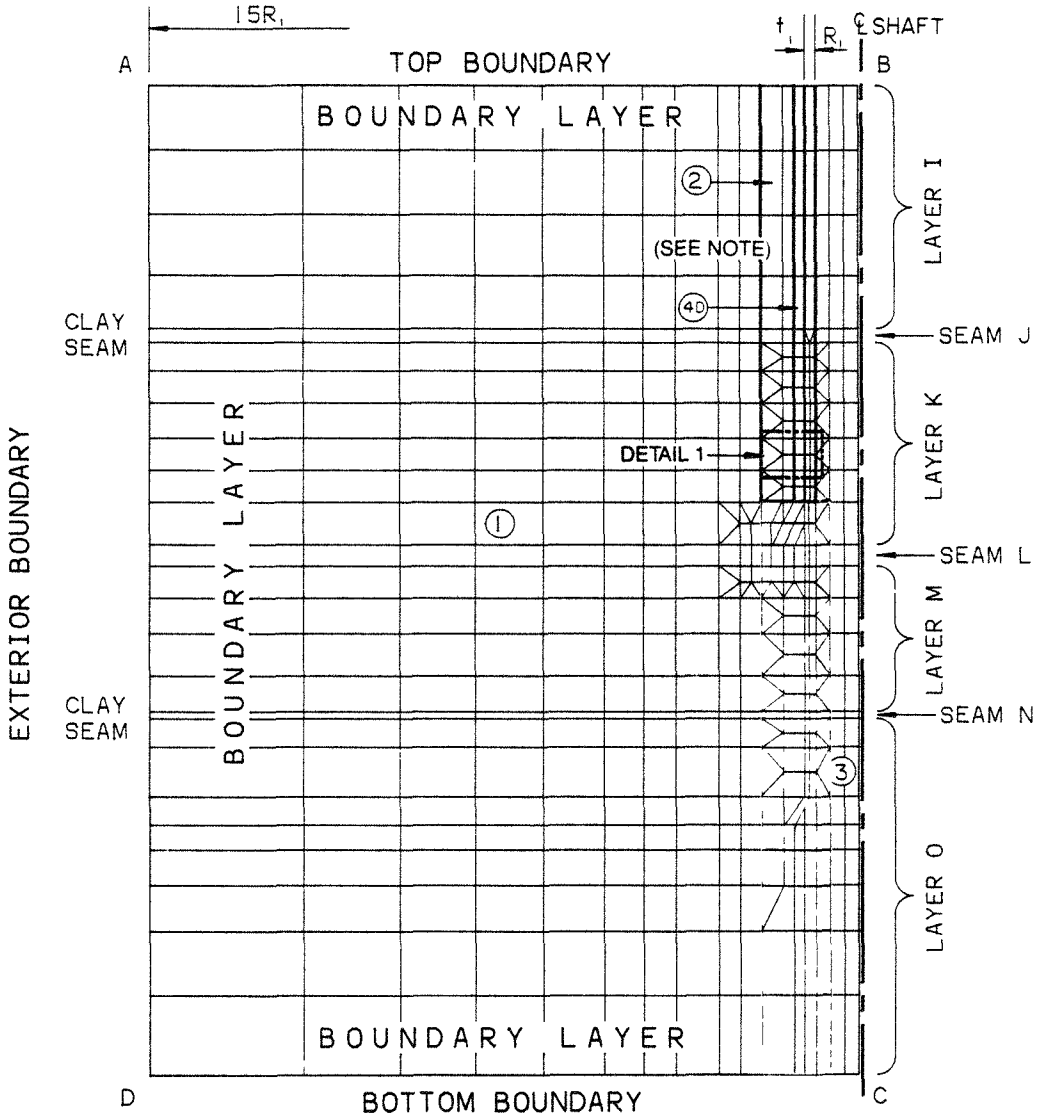

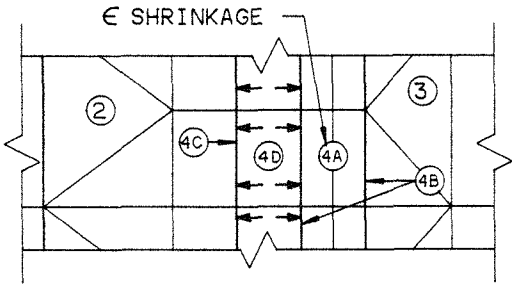

DETAIL 1

NOTE: ALL CONCRETE ELEMENTS (4A) ARE GIVEN A SHRINKAGE STRAIN.

NOTE: 1. All frozen material is changed back to type ① or type ⑤ and the "freezing" temperature field is brought back to the permanent steady state field configuration

2. See Table 6.1 for explanation of symbols.

AXISYMMETRIC FINITE ELEMENT MODEL SIMULATING SHAFT CONCRETE SHRINKAGE AND THAWING OF ALL FROZEN ROCK MATERIAL

FIGURE 6.10

The gap between the rock and the lining, if it exists, increases gradually as the concrete shrinks. As a consequence, the inner and outer steel lining shells are subjected to membrane compression. This continues until the limit of shrinkage is reached, or until closure catches up with the radial shrinkage deformations.

6.1.2.7 Thawing and Steady-State Thermal Regime

When the model elements representing the frozen rock are deactivated, the corresponding material properties revert to the original or modified rock properties (see Figures 6.9 and 6.10). Temperature differentials are simulated as thawing progresses by changing the temperature within each element until permanent steady-state temperatures are reached.

6.1.2.8 Exterior Loading and Overburden

Additional loads caused by hydrostatic pressure, tectonic movements, settlements, earthquakes, or overburden are applied to the model as separate load configurations. If permanent, these loads remain active throughout the rest of the simulation.

6.1.2.9 Long-Term Creep, Shrinkage, and Relaxation Regime

The SRP shafts will be designed for a nominal 100 year operational life. This requires that creep, relaxation, residual shrinkage, and concrete hardening be taken into consideration. Salt and concrete creep (see Figure 6.11) are expected to be the most important factors affecting long-term stress redistribution and closure. However, secondary effects such as water intrusion and percolation through the concrete mass, which can result in pressure build-up behind steel lining plate, are also of concern. All concrete must be considered permeable, hence treated as porous media.

The simulation of salt and concrete creep by using steady-state, secondary-creep power laws is a standard procedure. Primary creep can also be simulated through an equivalent time offset in the steady-state creep phase.

Although creep and relaxation can be reasonably well accounted for by a single steady-state power law, the designer might take creep-buckling safety into account in the finite-element analysis procedure.

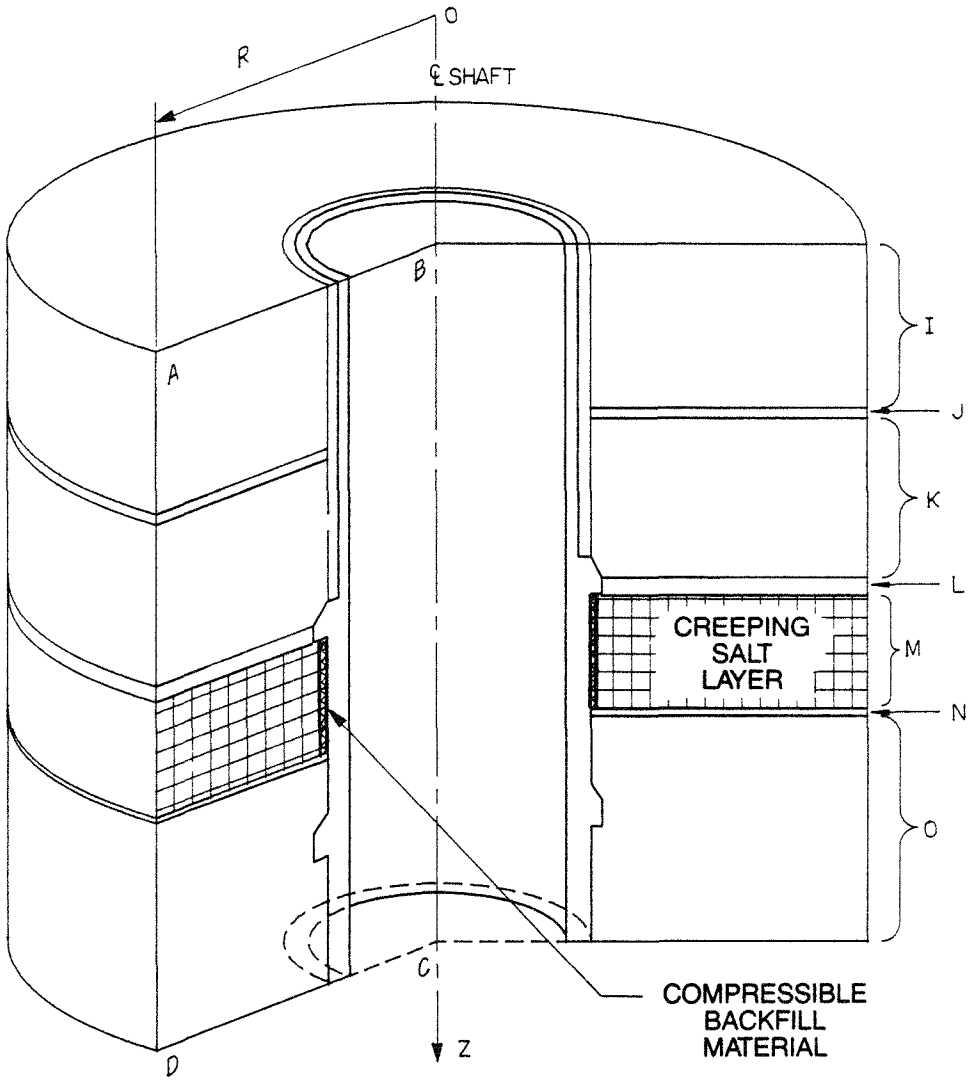

MODEL OBJECT:
CREEP OF SALT LAYERS

FIGURE 6.11

6.1.2.10 Incidental Loading Including Subsidence, Local Settlement, Slippage, and Thermal Effects

Incidental or local load conditions such as subsidence, are simulated by loads or displacements imposed on the model at any given time during the long-term creep phase. These loads are applied elastically and yield instant states of stress which are redistributed with time as a consequence of subsequent creep and relaxation.

The effect of local slippage in clay seams and rock joints, the disturbance caused by local settlements, and changes in thermal conditions are readily simulated.

6.1.2.11 Shaft Decommissioning

The model could be required to simulate the shaft decommissioning activities. These would include removal of sections of the concrete lining, excavation for, and installation of, the decommissioning seals, and backfilling. The model should simulate long-term conditions for approximately 100 years after decommissioning and beyond.

6.2 SPECIAL PURPOSE MODELS

The shaft lining structure and horizontally layered rock media are most conveniently modeled by axisymmetric elements. The load configurations described in Section 6.1.2, Time Dependent Loading and Sequencing, are typically axisymmetric. However, it is also possible to use special purpose models for local nonsymmetric configurations. Nonsymmetric loads include: (1) local grout pressure, (2) local elastic loads, (3) local overburden, (4) local uneven temperature changes, (5) differential settlements, (6) tectonic movements, and (7) uneven freezing configurations.

6.2.1 Axisymmetric Shaft Bearing Key Model

The shaft bearing-key sections, which are crucial to the stability of the lining, should be modeled to analyze the effects of local discontinuities. A schematic mesh plot similar to that illustrated in Figure 6.4 can be adapted to the characteristics of the rock formations at the site and to the actual shaft configuration. To minimize boundary effects, the model radius should be at least 15 times the excavation radius. For the same

reason, the vertical range from the top boundary to the bottom boundary should extend at least 40 ft (12m) and, if necessary, 100 ft (31m) or more as determined by the geometric calibration and stratigraphy.

Grid fineness is a function of rock layer thickness and the arrangement of the bearing-key structure. Important stress gradients require finer mesh configurations. Fineness can range from 6-inch-wide (152mm) inner ring elements to 60-inch-wide (1,524mm) outer ring elements. The height of the element should not exceed four times, nor be less than a quarter of, the ring width.

6.2.2 Axisymmetric Shaft Model for Layered Stratigraphy

Stratigraphic discontinuities combined with clay seams require a special axisymmetric model that focuses on rock layering and its discontinuous interaction with the shaft structure. The abrupt changes in rock stiffness or creep characteristics resulting from these discontinuities create high local strain gradients. To describe these gradients accurately, local mesh refinements are required. These refinements are attained by keeping the height of individual rock ring elements at a fraction of the layer thickness (See Figure 6.12).

6.2.3 Axisymmetric Plane Strain Model

Typical sections of the shaft that are located within thick or fairly uniform layers can be modeled by thin, plane-strain disks. These simple models are very cost-effective and efficient in the analysis of general radial and circumferential response behavior under uniform load configurations where vertical discontinuities are not considered. Axisymmetric radial discontinuities are also readily simulated in this type of model. The thickness of the model can be limited to 2 ft (0.61m) and the radial dimension to 15 times the excavation radius.

6.2.4 Nonsymmetric Special Purpose Model

Special loading configurations which are not axisymmetric can be modeled by either horizontal (Figure 6.13) or vertical (Figure 6.14) two-dimensional, plane-strain models. Standard quadrilateral plane-strain elements, combined with interface elements that simulate gap and contact friction, allow for assessment of the local behavior. Three-dimensional models can be utilized for special geometrical situations

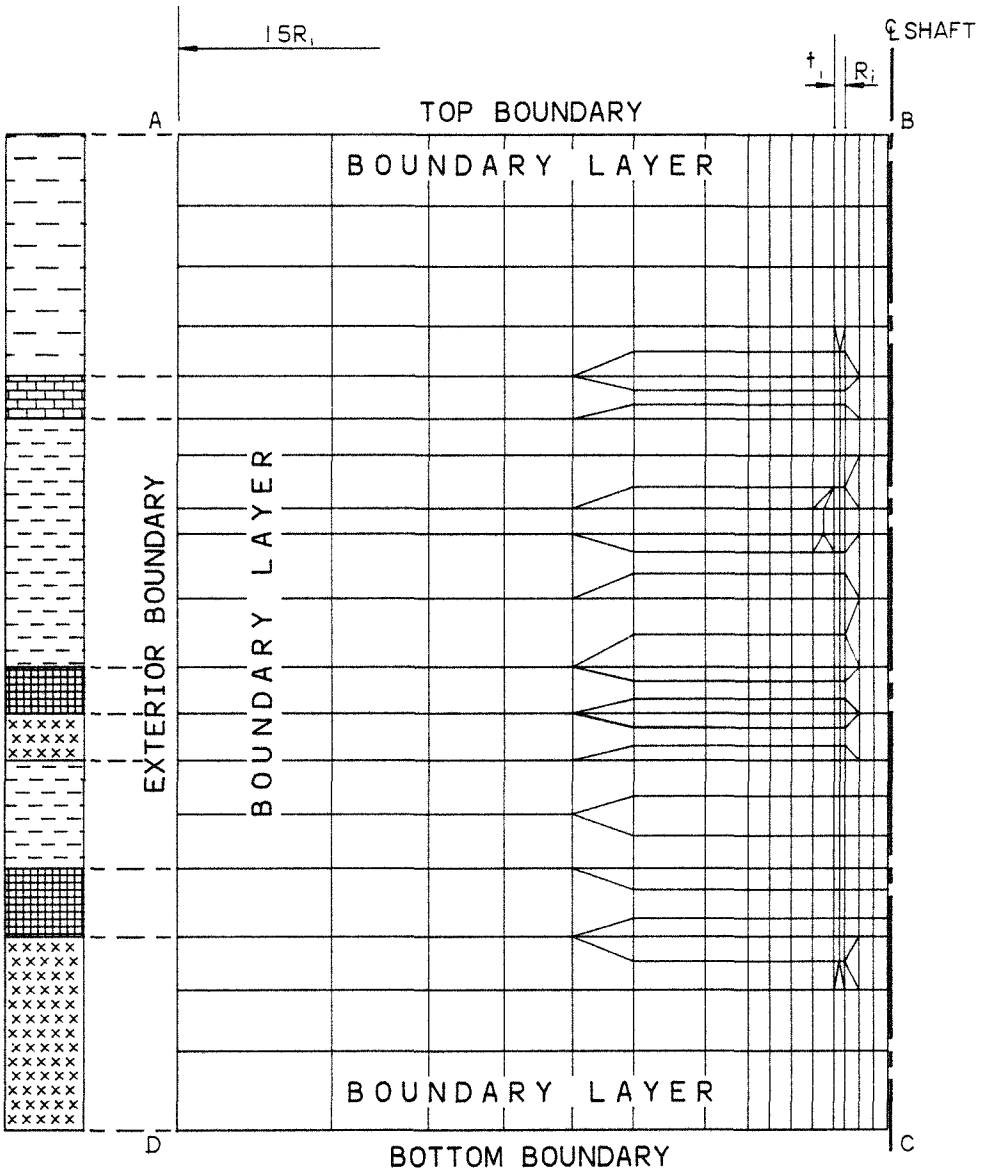

AXISYMMETRICAL SHAFT-LAYER MODEL

FIGURE 6.12

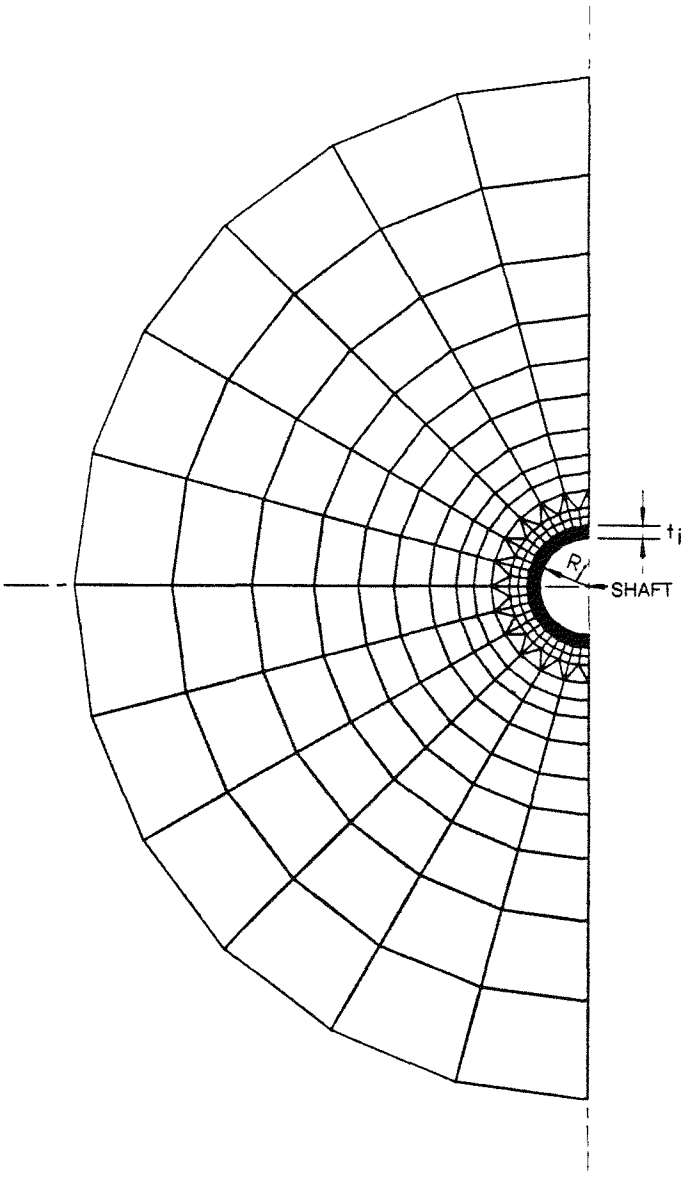

PLANE STRAIN HORIZONTAL FINITE ELEMENT MODEL (NO AXISYMMETRICAL EFFECTS)

FIGURE 6.13

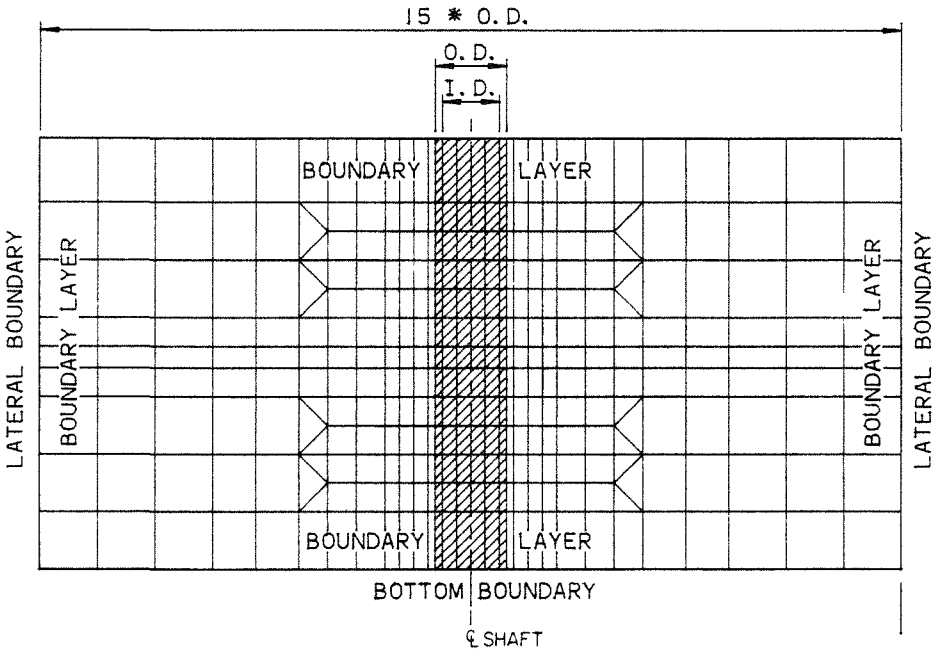

PLANE STRAIN MERIDIONAL FINITE ELEMENT MODEL (NONSYMMETRICAL EFFECTS)

FIGURE 6.14

or for particular loading arrangements. The extent of the model in this case is dictated by the configuration of the specific items and rock types and conditions to be modelled. For example, joint slip, if it occurs, is generally not axisymmetric. Its occurrence and subsequent effects can be simulated by means of appropriately oriented gap/friction elements with cohesion.

6.3 LINING SYSTEM STABILITY

Buckling stability of the composite shaft lining system is comprised of the overall buckling stability of the concrete and steel lining arrangement and the local buckling stability of the inner steel shell between anchors. Buckling stability is greatly affected by the following:

1. Geometric imperfections.

    a. Out-of-roundness.
    b. Local radial imperfections and dimples.
    c. Axial offsets and misalignments between successive lining sections.

2. Local restraints or boundary conditions.

    a. Encasements and embedments.
    b. Anchors, stiffeners, and bulkheads.

3. Residual stresses.

    a. Residual welding stresses in the steel lining.
    b. Locked-in, construction-induced stresses and strains.
    c. Shrinkage stresses and strains.

4. Loading.

    a. Uniform axial and radial pressures.
    b. Concentrated local loading.

c. Short-term loads.
d. Long-term creep-affected loading.

Three distinct types of buckling are likely to occur. These are:

1. Buckling of the steel and concrete shaft lining column when it is subject to the most critical load configuration. This is essentially creep-phase loading which includes both long-term creep of the concrete lining and incidental loads.
2. Local elasto-plastic buckling of the inner steel lining between anchor points caused by long-term hydrostatic pressure at the steel and concrete interface as a consequence of accidental leakage through the outer steel shell (non time-dependent).
3. Local buckling of the steel lining between anchor points (time-dependent).

6.4 SEISMIC ANALYSIS METHODOLOGY AUDIT

6.4.1 Design Approach

A one-time, independent verification of the seismic design approach (Section 4.4, Seismic Loading and Section 5.4, Stresses Due to Earthquakes) adopted for this guide should be performed on one shaft design for the Deaf Smith County site. To make this assessment, the designer should use a complete soil structure interaction (SSI) analysis to compute the seismic response of the uppermost section of the shaft and the medium surrounding it. This response should then be compared with the one computed by the simplified methods described in Sections 4.4 and 5.4. The most likely finding will be that the simplified methods have overestimated the seismic stresses and, hence, the simplified methods are acceptable as a conservative approach. In the unlikely event that the complete SSI analysis shows the simplified methods to have been unconservative for a particular stress effect, the shaft design should be reviewed using the SSI results for that stress effect.

The SSI analysis need only be performed on the uppermost section of the structure which includes the shaft collar and the lining to the depth of competent soil materials. Reasons for so limiting the SSI analysis are:

1. Seismically induced loads on the structure will be largest in this surface section of the shaft since ground motions at the shaft site and their associated strains will decrease rapidly with depth (Chang, et al., 1986).
2. Interaction effects between the structure and the surrounding medium will be largest in this surface section since the flexibility ratio for the shaft/medium system is low along this section (Hendron and Fernandez, 1983).
3. The configuration of the shaft is relatively complex in this surface section and, therefore, considerable approximation is involved when using the simplified procedures adopted in the seismic design approach.

Computer codes are available for complete three-dimensional analysis of seismic SSI problems. The details of procedures and methods for this analysis are dependent on the computer codes available (Johnson, 1981). Details of available SSI methods are not provided in this SRP Shaft Design Guide (SDG) and are left to the analyst. However, an overall approach for analysis, and general requirements for performing a seismic SSI analysis of the shaft are given below. Information required to perform an SSI analysis is contained in the SRP Input to Seismic Design (ISD).

6.4.2 Overall Approach for Soil-Structure Interaction (SSI) Analysis

A dynamic SSI analysis of the shaft involves the determination of the response of the shaft and the surrounding medium during a Design Basis Earthquake (DBE). Measures of seismic response to be determined should include relative displacements, velocities, accelerations, and strains and stresses induced throughout the soil-structure system.

The SSI analysis of the shaft and confirmation of the seismic design approach should involve the following steps:

1. Development of a numerical model of the soil structure system. The model should be compatible with the SSI computer code selected. Such a model will use finite elements to model the shaft and a portion of the surrounding medium, as appropriate. A horizontally layered finite-element model of the surrounding medium is used to solve the site response problem for free-field ground motions (Lysmer, et al., 1981).

2. Development of seismic input for analysis. Such input should be consistent with that provided in Section 5.4, Stresses Due to Earthquakes, used for design of the structure. It should consist of a control motion, a control point, and a seismic environment.
3. Computer analysis of the SSI problem.
4. Comparison of the seismic response computed through the SSI analysis with that used for design. Such comparison should be performed in terms of relative displacements, strains, and stresses induced in the shaft and the soil medium.
5. Determination of the implications of the above comparison for the design approach adopted in the SDG. This is a verification of the simplified seismic design approach. As noted in Section 6.4.1, Design Approach, the SSI analysis most likely will verify the simplified approach by virtue of the latter's relative conservatism. If not, the SSI analysis results should be adopted for design review.

6.4.3 General Requirements for SSI Analysis

In order to obtain meaningful results from the SSI analysis, it is essential it meet certain general requirements (Seed and Lysmer, 1978). These requirements are:

1. The analysis must account for the three-dimensional nature of the structure. Advantage may be taken of structural and medium symmetry as appropriate.
2. Free-field motions in the SSI analysis must correspond to the seismic environment used for design and should include inclined body waves.
3. The analysis must account for the semi-infinite nature of the problem (Lysmer, 1978). That is, it must properly model the medium extending to infinity horizontally and downward.
4. The analysis must account for all significant modes of deformation of the structure. For the shaft, these modes must include axial, shear, curvature, and hoop deformation (Owen and Scholl, 1981; and St. John and Zahrah, 1985).
5. The soil-structure model must be sufficiently refined to obtain an adequate representation of the spatial variation of stresses and displacements in the structure and the medium. Such a representation must permit an adequate comparison with stresses and displacements used in design and an adequate evaluation of structural performance.
6. The analysis must model the horizontal stratification of the site using linear viscoelastic and/or viscoplastic properties for the medium strata.

7. The analysis must account for the variation of material properties with strain level if this variation is significant. Such variation may be important in soils since the dynamic properties of these materials are highly dependent on the magnitude of the strains induced by seismic ground motion (Seed and Idriss, 1970).
8. To the extent practical, the analysis must account for the effects of shaft construction on material properties of the soil medium, if any. Construction effects may result from changes in the state of stress and disturbance of the soil medium in close vicinity to the shaft.

6.5 LOCAL STRESSES

Local effects, which are not simulated in the general shaft studies, are considered here in dedicated, small, finite-element models. The main concern is to control critical stress raisers in order to limit damage caused by local crushing or cracking. To ensure the steel lining shell remains watertight, disturbances resulting from local discontinuities, such as anchoring, grouting, attachments, and penetrations must be examined.

The actual stresses and strains derived in the main time-history analysis must be included in the local models. The local stresses computed in the dedicated finite-element models are additional to stresses existing in the system at the time of occurrence of local loads.

Local gap closure caused by clay seam slippage and elastic rock movement should be analyzed by the local studies. Corresponding stress and strain increments should be derived from initially prestressed models, as mentioned above.

Special problems resulting from differential local settlements, from high localized geotectonic load configurations, and from irregular thermal fields should also be analyzed by means of local models. The effect of freezing on highly dissimilar rock materials with differing water content and porosity in itself justifies such specially dedicated models.

7 PERFORMANCE MONITORING

The purpose of this chapter is to provide a conceptual description of the performance monitoring program for the exploratory and repository shafts. One objective of the chapter is to provide the designer with an understanding of the performance monitoring program, its purpose, and how it impacts the shaft design. Another objective is to provide the designer with sufficient information to assist in the development of a performance monitoring program for the shaft linings and seals. This program is to be developed in conjunction with the overall performance monitoring program.

The actual preparation of performance monitoring plans is beyond the scope of this document. However, it is important to identify the distinction between requirements for the monitoring programs of the exploratory shafts (ESs) and the repository shafts. The ES monitoring program will provide data to determine if the site is suitable for a repository. It will also gather data for repository shaft design and construction and for verifying the adequacy of the ES design and construction. The repository shaft monitoring program will not be as comprehensive as the ES monitoring program, and it will emphasize long-term data needs such as those for design and construction verification and postclosure.

7.1 MONITORING OBJECTIVES

The principal objectives of the ES and repository shaft performance monitoring programs are to:

1. Provide data from the two ESs for use in the design and construction of the repository shafts.
2. Provide data to verify the adequacy of design and construction procedures for all SRP shafts.
3. Provide data to modify design, if necessary, during construction of all SRP shafts.
4. Monitor the stability and performance of the repository shafts.
5. Collect data at potential locations for shaft decommissioning seals.
6. Collect and document data for use beyond immediate design requirements.

A successful performance monitoring program for the SRP shafts will meet certain basic requirements. For example, instrumentation will be compatible with expected geological, geohydrological, geochemical, and geotechnical conditions, and with proposed design and construction techniques. In addition, the instrumentation will provide data that represents the actual behavior of the shaft lining and surrounding strata. The monitoring program will not interfere unduly with construction and operation. Finally, monitoring instruments will be simple, rugged, and, where practicable, repairable and replaceable.

7.2 PHENOMENA TO BE MONITORED AND MEASURED

The phenomena to be monitored, measured, and recorded in the shafts include:

1. Freeze wall formation.
2. Groundwater pressures.
3. Rock and lining strains and displacements.
4. Lining loads and stresses.
5. Rock and lining temperatures.
6. Groundwater migration.

Brief descriptions of the activities required to monitor each of these phenomena and suitable measuring devices for them follow.

7.2.1 Freeze Wall Formation

To assess the formation of a freeze wall the following data are required:

1. Freeze wall temperatures during freezing, thawing, and construction.
2. Freeze wall thickness.
3. Surface uplift.
4. Groundwater levels inside and outside the freeze wall cylinder.

Certain guidelines should be followed while monitoring freeze wall formation and maintenance. Test holes should be drilled within the area to be frozen before freezing starts. During freezing and after the freeze wall has formed, cross hole ultrasonic measurements should be made to monitor the wall's development and thickness. Also, after the freeze wall has formed, temperature profiles over its entire depth should be made periodically. Finally, shallow groundwater wells should be used to monitor flow patterns both inside and outside the wall.

7.2.2 Groundwater Pressures

Sections of watertight lining that seal aquifers will be loaded not only by rock pressure, but also by groundwater pressure. Because this pressure will tend to become hydrostatic, the lining must be capable of

supporting at least a uniform radial load equal to the full weight of a water column at that depth. In addition, groundwater in strata surrounding nonwatertight shaft sections could be a major factor in creating stresses on the shaft lining.

Peak groundwater loads should occur soon after the linings are installed. Therefore, to assess the adequacy of the lining design, it is important to begin monitoring groundwater loads as early as possible.

Groundwater pressures can be measured using a variety of piezometers. For shaft instrumentation, the vibrating wire piezometer installed in conjunction with a pneumatic piezometer is suitable. However, measurement of groundwater pressure presents the designer with a serious challenge because penetrations through the steel and concrete lining in the major aquifers should be avoided (see Section 7.4.1.1, Preservation of Lining Integrity).

7.2.3 Displacements

Measurements of rock and shaft lining displacement indicate how stable the shaft structure is. A stable or decreasing rate of displacement indicates improving stability, while an increasing rate of displacement generally indicates declining stability. However, a more rigorous analysis is required to determine the stability of various components especially under creeping ground conditions. Displacements are usually measured at extensometer and convergence stations placed at various locations in a shaft. Information on lining displacements using extensometer/convergence stations will be augmented by strain measurements (see Section 7.2.5, Strain). Relative displacements of lining components are measured by joint meters installed within the lining.

7.2.4 Loads and Stresses

Load and stress measurements verify the geomechanical values used in lining design. A number of stress and load measuring devices, such as pressure cells, load cells, flat jacks, borehole deformation gauges, and vibrating-wire stress meters are available. Pressure cells, which are flat, circular, mercury-filled cavities coupled to sensing elements and embedded in the concrete, are generally used in shaft instrumentation. However, maintenance and replacement of such cells may be difficult.

7.2.5 Strain

Measurements of the magnitude and distribution of strain in the shaft lining are used not only to verify lining design criteria but more importantly, to warn of impending problems. Strain measurements are particularly useful where large but uncertain loads are expected. Strain data can be used to estimate stresses and loads, and the measurements are simpler to perform (and often more reliable) than stress measurements.

Strain measurements can be made in conjunction with displacement monitoring, since strain is a dimensionless parameter of displacement per unit length. Vibrating wire strain gauges used for shaft instrumentation can be either concrete embedment or nonembedment types. The disadvantages of many strain gauges is that they are sensitive to temperature changes, and they can be damaged by construction activities.

7.2.6 Temperature

The temperature in the concrete shaft lining will be measured to monitor the hydrating effect of the cement. These temperature measurements are particularly important in the upper shaft where ground freezing will be used to control groundwater during construction. Monitoring during emplacement of hot asphaltic sealant material (ASM) will also be required to ensure that the freeze wall is not affected. The relative effects of hydration/ASM temperatures on the frozen zone, and vice versa, are of critical importance during construction. Similarly, thawing should be monitored through the buildup of temperature and groundwater pressure. In addition, temperature data will provide corrections for stress and strain measurements.

Thermocouples, vibrating wire temperature gauges, or resistance temperature devices, such as semiconductor thermistors, can be used to measure lining temperatures.

7.2.7 Groundwater Migration

The vertical migration of water in the rock zone near the shaft will be monitored to determine the effectiveness of any grouting undertaken during or after construction. Hydraulic conductivity testing and piezometric monitoring will provide indications of potential groundwater migration past operational seals. Tracer testing should be implemented to provide long-term indications of groundwater flow.

7.2.8 Other Monitoring Requirements

Other parameters and phenomena that require monitoring include:

1. Deviation of the shaft lining relative to its centerline.
2. Leakage across a seal either through the rock adjacent to the seal, or through openings created in the seal by structural failure.
3. Loss of ASM.
4. Water inflow into the salt.
5. Corrosion of concrete and steel.
6. In situ stresses.
7. Subsidence/uplift.
8. Seismic events.

In situ stress measurement is a complex process and may not readily be possible in the repository shafts. However, measurement in the ESs should be considered. Water inflow and corrosion of concrete and steel can be monitored during periodic visual inspections of the shaft. Other methods to monitor the above items may be available and they should be evaluated during development of the monitoring plans.

7.3 MONITORING SEQUENCES AND TIME PERIODS

The sequence of shaft construction and the individual life span of each shaft can be divided into four phases:

1. Design and construction of the ESs followed by a period of in situ testing and observation.
2. Design and construction of repository shafts and possible integration with the ESs.
3. Operation of the repository and the collection of long-term shaft monitoring data.
4. Pre-closure assessment of shafts and shaft decommissioning seal designs followed by backfilling and construction of the seals.

Data acquired from the ESs will be available for full-scale shaft design. These data can also be used to design the instrumentation for each repository shaft and will be restricted mainly to the first few years of ES operation.

The life span of any particular shaft can be divided into the following phases:

1. Construction - very early monitoring.
2. Year 1 of Operation - early monitoring.
3. Years 2 to 5 - conventional monitoring.
4. Years 5 to End of Operating Life - long-term monitoring.

Very early monitoring should be directed at determining the initial loads upon linings, the initial stresses and strains within linings and foundation structures, and the initial effectiveness of seals. It should also produce data describing the effects of freezing and thawing upon the shaft structure.

Early monitoring should be directed at plotting the time dependent development of lining loads, stresses, and displacements; determining the loads upon, and stresses within, foundation structures; and indicating the effectiveness of seals.

Conventional monitoring should be aimed at collecting data, detecting anomalous behavior in shaft structures, and assessing the effects of use on the behavior of the shaft and shaft lining. With age, many of the instruments used during early monitoring will fail. Although failed instruments should be replaced if possible, it is expected that many instruments will not be replaceable.

Long-term monitoring should also be directed at detecting anomalous behavior including the effects on the shaft structure of long-term use, expansion of the underground facility, and waste storage. It is not possible to predict at this time what data acquisition schedules should be developed because they will depend on the behavior of the shaft at that time. Monitoring facilities and procedures will have to be designed as needed. However, because the long time spans involved will increase the likelihood of losing continuity of data acquisition, a special effort should be made to prevent data loss.

7.4 INSTRUMENTATION

Instruments and instrument installation should maximize:

1. Long-term reliability.
2. Ease of replacement and calibration if feasible.
3. Combined remote and local recording.
4. Redundancy.

Although the shafts could be operated for as long as 100 years, most instruments cannot be expected to produce continuous data records for that period of time. Some instruments will fail soon after installation in spite of careful design and manufacture. Therefore, sufficient numbers of instruments should be installed to provide adequate redundancy. Also, in order to extend the data acquisition period as far as possible into the period of full-scale repository operation, the design and locations of instruments should maximize reliability and facilitate replacement and recalibration wherever possible. However, because it will not be possible to replace all instruments, e.g., those that are embedded within the shaft lining or wall rock, data acquisition will taper off as irreplaceable instruments fail.

Continuous data gathering can be maximized by commencing acquisition as soon as possible, and by providing for backup acquisition during periods when instruments are being repaired or replaced.

7.4.1 Factors Affecting Instrumentation

The instrumentation program will evolve with shaft design and as data needs become clearer. For this reason, instrumentation planning must be based on precise objectives and a clear rationale, and instrumentation must be coordinated with subsurface design, shaft design, and construction. The following subsections provide guidance in this area.

7.4.1.1 Preservation of Lining Integrity

Penetration of the steel membranes in the watertight lining sections should be avoided. Emphasis should be placed on selecting and developing instrumentation and monitoring methods which do not require penetration of the lining structures. Geophysical methods such as ultrasonic and gamma radiation techniques are available and reliable. Other methods include the 'Petite Seismique' technique for determining rock fracture density, and elastic wave velocity instrumentation using the principle of pulsed-phase-locked-loop for measuring bolt tension. Many geophysical methods are in the development stage and should be carefully evaluated for their applicability. If penetrations are necessary, they must be designed, constructed, and maintained to remain watertight for the life of the shaft.

7.4.1.2 Geologic Conditions

Shaft design is governed largely by the geological, geotechnical, and geohydrological conditions that are likely to be encountered during shaft sinking. Geologic considerations take into account lithology and any

discontinuities such as bedding planes, joints, and faults. Geotechnical considerations require data on the magnitude and direction of in situ stresses and the geomechanical properties of soils and rock. Geohydrological considerations take into account aquifers, aquitards, and aquicludes. These considerations require data on hydrostatic pressure. In addition, aquifer intermixing is a key geohydrological concern. Geohydrologic pre-design studies will be necessary to determine if special construction methods in addition to freezing, such as grouting or dewatering, will be required to prevent intermixing.

During shaft design, underground parameters such as in situ stresses, hydrostatic pressures, and geomechanical properties are often estimated from limited field investigations. Wherever possible, these parameters should be measured during construction to check the accuracy of the estimated values and thus verify the adequacy of the design.

7.4.1.3 New Monitoring Techniques

The designer must consider that new techniques and equipment may be required for effective monitoring (as discussed in Section 7.4.1.1, Preservation of Lining Integrity). For example, the use of ASM as part of the shaft lining will entail the use of special instrumentation for monitoring its performance.

7.4.1.4 Other Design Considerations

Other design considerations include construction methods, regulatory requirements, shaft functions, and shaft operational life. These considerations also influence monitoring techniques and the selection of instrumentation. The instrumentation program must therefore be carefully designed to ensure compatibility with the lining design and the construction program.

Instruments will typically be installed in the rock behind the lining, at the interface between the rock and the lining, or within the shaft lining itself. Instrument locations and placement should not compromise the integrity of the shaft design and performance, or the strata where operating seals or decommissioning bulkheads will be installed.

Since space in the shaft is limited, access to instrument locations will be difficult, and remote data acquisition systems will be installed wherever possible. However, both instruments and remote data acquisition systems are extremely vulnerable to damage and corrosion. Furthermore, the installation,

reading, and maintenance of monitoring instruments and data acquisition systems will increase construction time. These factors must be considered when preparing the schedule.

7.5 IMPACTS OF SHAFT OPERATIONS

In designing shaft instrumentation systems, the designer must take into account the impacts of shaft operations and requirements for periodic maintenance and repair. Impacts to consider include:

1. Falling rock and debris in all shafts but especially in the mined-salt hoisting and service shafts.

2. Changes in shaft temperature and humidity due to normal seasonal fluctuations, and to excavation and waste storage operations.

3. Potentially corrosive salt dust in ventilation exhaust shafts.

4. Requirements for access to instrumentation stations, control boxes, power lines, and communications lines for data recording and maintenance.

5. Possible high air velocity in ventilation shafts.

6. Presence of gas in ventilation exhaust shafts.

7. Presence of pipes, power cables, and communication lines permanently affixed around the shaft perimeters.

Falling rock and debris can damage instruments, control boxes, power lines and communication lines. These facilities must be covered by strong protective covers or conduits as appropriate. If feasible, instrument reading facilities should be recessed into the inner lining wall.

Instrument locations within the shafts can be accessed either by small man hoists attached to the shaft walls, or by working platforms hung in the shafts and temporarily fastened to the walls at work areas. If hoists are used, scaffolding will have to be placed around the shafts at each measuring station. If working platforms are used, stabilization fixtures must be installed at each measurement station. A separate man hoist

may also be required. In ventilation shafts the platform must not interfere unduly with the passage of large quantities of air. In either case, all work areas must be protected from falling debris.

The design of all instruments and electrical devices must consider corrosion and related problems. All electrical devices in shafts must satisfy Federal mining regulations.

Instrumentation design must be closely coordinated with shaft design to ensure that design conflicts do not arise during construction and monitoring.

Access to instruments must not be hindered by pipes, cables, or structural members affixed to shaft walls.

8 REFERENCES

8.1 GENERAL REFERENCES

ACI, see American Concrete Institute.

AISC, see American Institute of Steel Construction.

American Concrete Institute, 1979. **Specification for the Design and Construction of Reinforced Concrete Chimneys**, ACI 307-79, Detroit, MI.

American Concrete Institute, 1983. **Building Code Requirements for Concrete Masonry Structures**, ACI 531-79, Table 10-1, Detroit, MI.

American Concrete Institute, 1985. **Building Code Requirements for Reinforced Concrete**, ACI 318-83, 3rd Printing, Detroit, MI.

American Concrete Institute, 1986. **Building Code Requirements for Structural Plain Concrete and Commentary**, ACI 318.1-83/318.1R-83, 4th Printing, Detroit, MI.

American Institute of Steel Construction, 1978. **Specification for the Design, Fabrication and Erection of Structural Steel for Buildings**, Chicago, IL.

American Society of Civil Engineers, 1983. **Seismic Response of Buried Pipes and Structural Components**, Committee on Seismic Analysis, New York, NY, pp. 15-16.

American Society for Testing and Materials, 1984. **Standard Specification for Ductile Iron Castings**, A536-84, Philadelphia, PA.

American Society for Testing and Materials, 1985. **Specification for Deformed and Plain Billet-Steel Bars for Concrete Reinforcement**, A615-85, Philadelphia, PA.

American Society for Testing and Materials, 1979. **Standard Specification for Pig Lead**, B29-79 (Reapproved 1984), Philadelphia, PA.

American Society for Testing and Materials, 1986. **Specifications for Chemical Admixtures for Concrete**, C494-86, Philadelphia, PA.

American Society for Testing and Materials, 1980. **Specification for Calcium Chloride**, D98-80, Philadelphia, PA.

American Society for Testing and Materials, 1980. **Methods of Sampling and Testing Calcium Chloride for Roads and Structural Applications**, D345-80, Philadelphia, PA.

American Society for Testing and Materials, 1985. **Standard Methods of Tension Testing of Metallic Materials**, E8-85a, Philadelphia, PA.

American Society for Testing and Materials, 1985. **Standard Practice for Ultrasonic Pulse-Echo Straight-Beam Examination by the Contact Method**, E114-85, Philadelphia, PA.

American Society for Testing and Materials, 1986. **Controlling Quality of Radiographic Testing**, E142-86, Philadelphia, PA.

American Society for Testing and Materials, 1979. **Standard Reference Radiographs for Ductile Iron Castings**, E689-79 (Reapproved 1984), Philadelphia, PA.

American Welding Society, 1986. **Structural Welding Code - Steel**, D1.1-86, Miami, FL.

Amstutz, E., 1970. "Buckling of Pressure-Shaft and Tunnel Linings," **Water Power**, Vol. 22, No. 11, pp. 1391-1399.

Andersland, O.B., F.H. Sayles, and B. Ladanyi, 1978. "Mechanical Properties of Frozen Ground", **Geotechnical Engineering for Cold Regions**, McGraw-Hill, New York, NY, pp. 216-275.

ASCE, see American Society of Civil Engineers.

ASTM, see American Society for Testing and Materials.

AWS, see American Welding Society.

Brown, E.T., J.W. Bray, B. Ladanyi, and E. Hoek, 1983. "Ground Response Curves for Rock Tunnels", **Geotechnical Journal**, American Society of Civil Engineer, V. 109, No. 1.

Burghardt, G.A., H. Link, V. Scharf, and K. Stoss, 1982. "Temperaturbedingte Rissbildungen beim Abteufen von Gefrierschächte im Salzgebirge" ("Thermal Cracking of Frozen Shafts During Sinking in Salt Formations"), **Kali und Steinsalz**, Vol. 9, 1982, Verlag Glückauf, Essen, pp. 294-315.

Chang, C. Y., M.S. Power, I.M. Idriss, P.G. Somerville, W.J. Silva, and P.C. Chen, 1986. **Observational Data on Spatial Variations of Earthquake Ground Motion**, Vol. 3, NUREG/CR-3805, Nuclear Regulatory Commission, Washington, DC.

Chang, C. Y., J.E. O'Rourke, W.J. Silva, and Z. Zheng, 1984. **A Wellbore Breakout Model**, prepared by Woodward-Clyde Consultants, Walnut Creek, CA for the U.S. Geological Survey, Menlo Park, CA.

Chen, J. C., J. Lysmer, and H.B. Seed, 1981. **Analysis of Local Variations in Free Field Seismic Ground Motion**, UCB/EERC-81/03, University of California, Berkeley, CA.

Coates, D.F., 1981, **Rock Mechanics Principles**. Canadian Department of Energy, Mines, and Resources, Ottawa.

Curtis, R.H., R.J. Wart, and E.L. Skiba, 1983. **A Summary of Repository Design Models**, NUREG/CR-3450, prepared by Acres American, Inc., for U.S. Nuclear Regulatory Commission, Washington, DC.

Daleboudt, C.H. and J.M. Weehuizen, 1958. "Eine Schachtauskleidung aus Stahlbeton" ("A Reinforced Concrete Shaft Lining"), **Glückauf**, Vol. 1/2, No. 1/2, January, pp. 17-28.

DIN 1693, 1973. **Cast Iron with Nodular Graphite**, Part 1, 1973 and Part 2, 1977, Beuth Verlag GmbH, Berlin.

DIN 21501, 1963. **Shaft Linings of Cast Iron Tubbing**, Beuth Verlag GmbH, Berlin.

DIN 21525, 1964. **Concrete Blocks for Mine Support**, Beuth Verlag GmbH, Berlin.

Dobry, R., I.M. Idriss, and E. Ng, 1978. "Duration Characteristics of Horizontal Components of Strong-Motion Earthquake Records", **Bulletin of the Seismological Society of America**, Vol. 68, No. 5, pp. 1487-1520.

DOE, see U.S. Department of Energy.

Dowell Division of The Dow Chemical Company, Undated. **Dowell Chemical Seal Ring and Dowell Chemical Seal Ring Gasket: Technical Report**, Tulsa, OK.

Goodman, R.E., 1980. **Introduction to Rock Mechanics**, John Wiley & Sons, New York, pp. 240-247.

Grant, P.M. 1983, "Practical Aspects of Shaft Lining Design," **Proceedings of First International Conference on Stability in Underground Mining** (August, 1982, Vancouver, B.C., Canada), Society of Mining Engineers, AIME, New York, NY.

Grutzeck, M.W. and D.M. Roy, 1985. **Experimental Characterization and Stability of Salt- and Nonsalt-Containing Grouts and Mortars**, BMI-ONWI-568. Prepared for the Office of Nuclear Waste Isolation by Materials Research Laboratory, Pennsylvania State University, PA.

Hendron, A.G., and G. Fernandez, 1983. "Dynamic and Static Design Considerations for Underground Chambers," **Proceedings of a Symposium on the Seismic Design of Embankments and Caverns** (May 16-20, Philadelphia, PA), American Society of Civil Engineers, New York, NY, pp. 157-197.

Hertrich, F., 1965. "Die Gefahr des Einbeulens bei Gusseisernen Tubbingringen" ("The Danger of Buckling with Cast Iron Tubbing Rings"), **Forschunschefte**, Glückauf, Essen.

Heuze, F.E. 1980. "Scale Effects in the Determination of Rock Mass Strength and Deformability," **Rock Mechanics**, Volume 12, Springer-Verlag, Berlin, pp. 167-192.

Hoek, E. and E.T. Brown, 1980. **Underground Excavations in Rock**, The Institution of Mining and Metallurgy, London, pp. 175-177, 218.

Hoek, E. and E.T. Brown, 1982. **Underground Excavations in Rock**, The Institution of Mining and Metallurgy, London, Rev. 2.

International Society for Rock Mechanics, 1979. **Rock Characterization Testing and Monitoring: ISRM Suggested Method**, prepared for The Commission on Testing Methods, ISRM, Pergamon Press, Inc., Elmsford, NY.

ISRM, see International Society for Rock Mechanics.

Jaeger, J.C., 1969, **Elasticity, Fracture and Flow: With Engineering and Geological Applications**, Methuen and Co. Ltd., London.

Jaeger, J.C., and N.G.W. Cook, 1969. **Fundamentals of Rock Mechanics**, Methuen and Co. Ltd., London.

Jessberger, H.L., 1980. "State-of-the-art Report: Ground Freezing Mechanical Properties, and Processes and Design," **Proceedings of 2nd International Symposium on Ground Freezing**, (June 24-26, Trondheim, Norway), Norwegian Institute of Technology, Trondheim, Norway, pp. 1-33.

Johnson, J.J., 1981. **Soil Structure Interaction: The Status of Current Analysis Methods and Research**, NUREG/CR-1780, Nuclear Regulatory Commission, Washington, DC.

Kampschulte, R.M., W. Lehmann, and H. Link, 1964. "Das Abteufen und Ausbauen der Gefrierschächte Wulfen 1 und 2", ("The Sinking and Lining of the Frozen Shafts Wulfen 1 and 2,") **Glückauf**, Vol. 100, No. 25, pp. 1473-1495.

Kelsall, P.C., J.B. Case, J. Meyer, and W.E. Coons, 1982. **Schematic Designs for Penetration Seals for Reference Repository in Bedded Salt**, ONWI-405, prepared by D'Appolonia Consulting Engineers, Inc., for the Office of Nuclear Waste Isolation, Battelle Memorial Institute, Columbus, OH.

Kelsall, P.C., J.B. Case, J. Meyer, and W.E. Coons, 1983. **Schematic Designs for Penetration Seals for a Repository in the Paradox Basin**, BMI/ONWI-563, prepared by IT Corporation for the Office of Nuclear Waste Isolation, Columbus, OH.

Kelsall, P.C., J. Meyer, J.B. Case, and W.E. Coons, 1985. **Schematic Designs for Penetration Seals for a Repository in the Permian Basin**, BMI/ONWI-564, prepared by IT Corporation for the Office of Nuclear Waste Isolation, Columbus, OH.

Klein, J., ed., 1985. **Handbuch des Gefrierschachtbaus (Handbook of Frozen Shaft Construction)**, Glückauf-Betriebsbucher, Band 31, Verlag Gluckauf GmbH, Essen.

Klein, J. and F. Reimann, 1985. "Schachtausbau aus Gusseisen mit Kugelgraphit" ("Shaft Lining Construction Using Nodular Graphite Cast Iron,") **Glückauf**, Vol 121, No. 22, pp. 486-487, 1693-1696.

Koplick, C.M., D.L. Pentz, and R. Talbot, 1979. **Borehole and Shaft Sealing**, NUREG/CR-0495, TR-1210-1, Vol. 1 of Information Base for Waste Repository Design, Nuclear Regulatory Commission, Washington, DC.

Kratzsch, H., 1983. **Mining Subsidence Engineering** (Translated by R.F. S. Fleming), Springer-Verlag, New York.

Lang, T.A., J.A. Bishoff, P.L. Wagner, 1980. **A Program Plan for Determining Optimum Roof Bolt Tension - Theory and Application of Rock Reinforcement Systems in Coal Mines**, Volume 1: PB-80-175-195, Volume 2: PB-80-179-187, U.S. Bureau of Mines.

Link, H., 1959. "Zur Spannungsermittlung in Schachtauskleidungen (Determining Stress in Shaft Linings)," **Research and Development**, Gutehoffnungshuette Sterkrade A.G., No. 29., p. 9.

Link, H., 1986. "Die Stabilitätsgrenze des Star Ummantelten Kreisrohres unter äusserer Wasserdruckbelastung" ("Stability Limits of a Solidly Encased Round Hollow Section Subjected to External Water Pressure"), **Stahlbau**, Vol. 7, pp. 201-204.

Link, H., H.O. Lutgendorf, and K. Stoss, 1985. **Richtlinien Zur Berechnung Von Schachtauskleidungen In Nicht Standfestem Gebirge (Guidelines for Calculating Shaft Linings in Incompetent Strata)**, Third Edition, **Glückauf**, Essen.

Lysmer, J., 1978. **Analytical Procedures in Soil Dynamics**, Report No. UCB/EERC-78/29, University of California, Berkeley, CA.

Lysmer, J., M. Tabatabaie-Raissi, F. Tajirian, S. Vahdani, and F. Ostadan, 1981. **SASSI: A System for Analysis of Soil-Structure Interaction**, UCB/GT/81-02, University of California, Berkeley, CA.

National Concrete Masonry Association, 1985. **Specification for the Design and Construction of Load-Bearing Concrete Masonry**, 13th Printing, Herndon, VA.

NAVFAC, 1971. **Design Manual - Soil Mechanics, Foundations and Earth Structures**, NAVFAC DM-7, Department of the Navy, Naval Facilities Engineering Command, Alexandria, VA, pp. 7-14-3.

NCMA, see National Concrete Masonry Association.

Newmark, N.M., and W.J. Hall, 1978. **Development of Criteria for Seismic Review of Selected Nuclear Power Plants**, NUREG/CR-0098, U.S. Nuclear Regulatory Commission, Washington, DC.

NRC, see U.S. Nuclear Regulatory Commission.

Obert, L. and W.I. Duvall, 1967. **Rock Mechanics and the Design of Structures in Rock**, published by John Wiley and Sons, Inc., New York, NY, p. 289.

Odquist, F.K.G., 1966, **Mathematical Theory of Creep and Creep Rupture**, Oxford at Clarendon Press, p. 168.

Oellers, T., 1983. "Bitumen as an Active Sealant for Shaft Linings," **Glückauf**, Vol. 119, No. 12, pp 567-570.

Oellers, T., and P. Sitz, 1985. "Entwurf und Berechnung Gas- und Flüssigkeitsdichter Schachtverschlüsse" ("Design and Analysis of Gas- and Fluidtight Seals in Shafts"), **Symposium on Shafts and Tunneling**, Verlag Glückauf, Essen, pp. 48-56.

O'Rourke, J.E., D. Allirot, and K. O'Connor, 1982. "Design Approaches for Access Plugs in a Basalt Repository," **The Technology of High-Level Nuclear Waste Disposal**, DOE/TIC-4621, Vol. 2, Tech-Information Center, Office of Science & Technology Information, U.S. Department of Energy, Washington, DC.

Ostrowski, W.J.S., 1972. "Design Considerations for Modern Shaft Linings," **CIM Transactions**, Vol. LXXV, pp. 184-198.

Owen, G.N., and R.E. Scholl, 1981. **Earthquake Engineering of Large Underground Structures**, FHWA/RD-80/195, prepared for the Federal Highway Administration by URS/John A. Blume & Associates, San Francisco, CA.

PCI, see Prestressed Concrete Institute.

Pfeifle, T.W., K.D. Mellegard, and P.E. Senseny, 1983. **Preliminary Constitutive Properties for Salt and Nonsalt Rocks from Four Potential Repository Sites**, ONWI-450, prepared by RE/SPEC, Inc., for Office of Nuclear Waste Isolation, Battelle Memorial Institute, Columbus, OH.

Popov, E.P., 1968. **Introduction to Mechanics of Solids**, Prentice-Hall, Inc., Englewood Cliffs, NJ.

Prestressed Concrete Institute, 1985. **PCI Design Handbook: Precast and Prestressed Concrete**, 3rd Edition, Prestressed Concrete Institute, Chicago, IL.

Roesner, E.K., S.A.G. Poppen, and J.C. Kanopka, 1983. "Stability During Shaft Sinking (A Design Guideline for Ground Support of Circular Shafts)," **First International Conference on Stability in Underground Mining** (August 16-18, 1982, Vancouver, BC), Society of Mining Engineers, AIME, New York, NY, pp. 749-769.

Roy, D.M., M.W. Grutzeck, and L.D. Wakeley, 1985. **Salt Repository Seal Materials: A Synopsis of Early Cementitious Materials Development**, BMI-ONWI-536, Prepared for the Office of Nuclear Waste Isolation by Materials Research Laboratory, Pennsylvania State University, PA.

Sage, J.D., and R.A. D'Andrea, 1982. "Measurement of Soil Thaw Weakening," **Proceedings of 3rd International Symposium on Ground Freezing**, U.S. Army Corps of Engineers, Hanover, NH.

Saunders, R., 1985. "Ductile Cast Iron as a Watertight Shaft Lining," **RETC Proceedings** (June 16-20, New York), Vol. 2, Society of Mining Engineers, AIME, New York, NY, pp. 1191-1210.

Schnabel, P.B., J. Lysmer, and H.B. Seed, 1972. **SHAKE: A Computer Program for Earthquake Response Analysis of Horizontally Layered Sites**, EERC72-12, University of California, Berkeley, CA.

Seed, H.B. and I.M. Idriss, 1970. **Soil Moduli and Damping Factors for Dynamic Response Analyses**, Report No. EERC 70-10, University of California, Berkeley, CA.

Seed, H.B. and J. Lysmer, 1978. "Soil-Structure Interaction Analysis by Finite Element Methods - State-of-the-Art," **Nuclear Engineering and Design**, Vol. 46, No. 1, pp. 349-365.

Senseny, P.E., T.W. Pfeifle, and K.D. Mellegard, 1985. **Constitutive Parameters for Salt and Nonsalt Rocks from the Detten, G. Friemel, and Zeeck Wells in the Palo Duro Basin, Texas**, BMI/ONWI-549, prepared by RE/SPEC, Inc., for Office of Nuclear Waste Isolation, Battelle Memorial Institute, Columbus, OH.

Silling, S.A., 1983. **Final Technical Position on Documentation of Computer Codes for High-Level Waste Management**, NUREG-0856, U.S. Nuclear Regulatory Commission, Washington, DC.

Silva, W.J., 1978. "Wave Propagation in An Elastic Medium with Applications to Seismology," Ph.D. Thesis, University of California, Berkeley, CA.

Springer, J.E., R.K. Thorpe and H.L. McKague, 1984. **Borehole Elongation and Its Relation to Tectonic Stress at the Nevada Test Site**, UCRL-53528, Lawrence Livermore National Laboratory, Livermore, CA, p. 13.

St. John, C.N., and T.F. Zahrah, 1985. **A Seismic Design of Underground Structures**, Report No. R-8411-5616, National Science Foundation, Washington, DC.

St. John, C.M., D.E. VanDillen, and E. Detournay, 1985. **An Investigation of the Failure of Rockbolted Tunnels for Deep Missile Basing**, R-8227-5534, prepared by Agbabian Associates, El Segundo, CA, for Defense Nuclear Agency, Washington, DC.

Storck, U., 1968. "First Use of a Double Steel and Concrete Composite Lining for Keeping High-Pressure Water Out of Potash Shaft," **Kali and Steinsalz**, Vol. 5, No. 3, pp. 87-94.

Stoss, K. 1957. "Temperature Stresses in Totally Welded Composite Shaft Linings of Steel and Concrete," **Krupp's Technical News**, Vol. 15, No. 8, pp. 263-271.

Stoss, K. and T. Oellers, 1985. "The Influence of Freezing on Strata Behavior", **Glückauf Translation**, Vol. 121, pp. 434-438.

Stoss, K. and T. Oellers, 1985. "Der Einfluss des Gefrierens auf das Gebirgsverhalten" ("The Influence of Freezing on Strata Behavior"), **Glückauf**, Vol. 121, No. 19, pp. 1438-1444.

Stoss, K., G.A. Burghardt, and H. Link, 1983. "Temperaturbedingte Rissbildung beim Abteufen von Tiefgefrierschächten im Salzgebirge" ("Thermal Cracking of Deep-Frozen Shafts During Sinking in Salt Formations"), **Glückauf**, Vol. 119, No. 20, pp. 979-984.

Szechy, K., 1973. **The Art of Tunnelling** (Second English Edition), Akadémiaikiadó, Budapest, Hungary.

Timoshenko, S., 1956. **Strength of Materials, Part II - Advanced Theory and Problems**, D. Van Nostrand Co., Inc., New York, NY.

Timoshenko, S., and D.H. Young, 1962. **Elements of Strength of Materials**, 4th Edition, D. Van Nostrand Co., Inc., Princeton, NJ.

Timoshenko, S.P., and J.N. Goodier, 1970. **Theory of Elasticity**, 3rd Edition, McGraw-Hill Book Co., New York, NY.

U.S. Corps of Engineers, 1980. "Rock Reinforcement - Engineering and Design," **Engineering Manual** EM1110-1-2907, Department of the Army, Corps of Engineers, Office of the Chief of Engineers, Washington, DC.

U.S. Department of Energy (DOE), 1985a. **Mission Plan for the Civilian Radioactive Waste Management Program.** DOE/RW-0005, Office of Civilian Radioactive Waste Management, Salt Repository Project Office, Columbus, OH.

U.S. Department of Energy (DOE), 1985b. **Generic Requirements for a Mined Geologic Disposal System.** SRP/B-2, Office of Civilian Radioactive Waste Management, Salt Repository Project Office, Columbus, OH.

U.S. Department of Energy (DOE), 1986. **Synthetic Geotechnical Design Reference Data for the Deaf Smith Site.** (Revision 1), SRP/B-11, Office of Civilian Radioactive Waste Management, Salt Repository Project Office, Columbus, OH.

U.S. Department of Energy (DOE), 1987. **SRP Input to Seismic Design**, Office of Civilian Radioactive Waste Management, Salt Repository Project Office, Columbus, OH.

U.S. Department of the Navy, 1981. **Soil Mechanics Design Manual**, DM-7.1, Naval Facilities Engineering Command, Alexandria, VA, p. 7.1-201.

U.S. Nuclear Regulatory Commission (NRC), 1983. **Disposal of High-Level Radioactive Wastes in Geologic Repositories Technical Criteria**, 10 CFR 60, Section 60.113 and 60.134, Washington, DC, June.

U.S. Nuclear Regulatory Commission (NRC), 1986a. **Reporting of Defects and Noncompliance**, 10CFR21, Washington, DC, January.

U.S. Nuclear Regulatory Commission (NRC), 1986b. **Quality Assurance Criteria for Nuclear Power Plants and Fuel Reprocessing Plants**, 10CFR50 Appendix B, Washington, DC, January.

Vyalov, S.S., ed., V.G. Omoshinkskii, S.E. Gorodetskii, V.G. Grigorieva, Iu. K. Zaretskii, N.K. Pekarskaia, and E.P. Shusherina, 1962. **The Strength and Creep of Frozen Soils and Calculations for Ice-Soil Retaining Structures**, U.S. Army CRREL Translation 76, 1965, prepared for U.S. Army Corps of Engineers by Cold Regions Research and Engineering Laboratory, Hanover, NH.

Wakeley, L.D. and D.M. Roy, 1986. **Nature of the Interfacial Region Between Cementitious Mixtures and Rocks from the Palo Duro Basin and Other Seal Components**, BMI/ONWI-580, prepared by Materials Research Laboratory, The Pennsylvania State University, for Office of Nuclear Waste Isolation, Battelle Memorial Institute, Columbus, OH.

Wallner, M., 1981, "Analysis of Thermomechanical Problems Related to the Storage of Heat Producing Radioactive Wastes in Rock Salt," **1st Conference on the Mechanical Behavior of Salt** (November 9, Pennsylvania State University), Trans Tech Publications, Clausthal-Zellerfeld, Federal Republic of Germany (1984), p. 739.

Wolf, J.P., 1985. **Dynamic Soil-Structure Interaction**, Prentice-Hall, Inc., Englewood Cliffs, NJ.

Yeh, G.C., 1974. "Seismic Analysis of Slender Buried Beams," **Bulletin of the Seismological Society of America**, Vol. 64, No.5, pp. 1551-1562.

9 BIBLIOGRAPHY

9.1 GENERAL BIBLIOGRAPHY

Abel, J.F., J.E. Dowis, and D.P. Richards, 1979. "Concrete Shaft Lining Design," **Proceedings of the 20th U.S. Symposium on Rock Mechanics** (June 4-6, University of Texas, Austin, TX), Society of Mining Engineers, AIME, New York, NY, pp. 627-640.

American Institute of Steel Construction (AISC), 1980. **Manual of Steel Construction**, Eighth Edition, AISC, Chicago, IL.

American Society for Testing and Materials (ASTM), 1984. **Specification for Structural Steel**, A36/A36M-84a, Philadelphia, PA.

American Society for Testing and Materials (ASTM), 1985. **Specification for High-Strength Low-Alloy Structural Steel with 50ksi (345 MPa) Minimum Yield Point to 4 in. Thick**, A588/A588M-85, Philadelphia, PA.

Amstutz, E., 1969. "Das Einbeulen von Schacht und Stollenpanzerungen," ("The Buckling of Shaft and Tunnel Linings"), **Swiss Construction News**, Vol. 87, No. 28, pp. 541-549.

Bechtel National, Inc., 1985. **Quarterly Geotechnical Field Data Report**, WIPP-DOE-218, prepared for the U.S. Department of Energy, Carlsbad, NM.

Bradshaw, R.I., and W.C. McClain, 1971. **Project Salt Vault: A Demonstration of Disposal of High-Activity Solidified Wastes in Underground Salt Mines**, ORNL-4555, Oak Ridge National Laboratory, Union Carbide Corporation, Nuclear Division, Oak Ridge, TN.

Brown, E.T., and J.W. Bray, 1982. "Rock Support Interaction Calculations for Pressure Shafts and Tunnels," **Proceedings of International Society of Rock Mechanics (ISRM) Symposium** (May 26-28, Aachen), A.A. Balkema, Rotterdam, Vol. II, pp. 555-565.

Chao-Chow, Mow, and Yih-Hsing Pao, 1973. **Diffraction of Elastic Waves and Dynamic Stress Concentrations**, Rand Corporation, New York, NY.

Coates, D.F., 1981. **Rock Mechanics Principles**, Canadian Department of Energy, Mines, and Resources, Ottawa, Canada.

Fluor (Fluor Technology, Inc.), 1987a. **Repository Design Sensitivity Study Report**, Prepared for U.S. Department of Energy, Salt Repository Project Office, Columbus, OH.

Hays, W.W., 1980. **Procedure for Estimating Earthquake Ground Motions**, U.S. Geological Survey Professional Paper 1114, U.S. Government Printing Office, Washington, DC.

Hoff, N.J., 1963. "Creep Effect," **The Effect of High Temperatures on Structures**, Part III, Stanford University, CA.

Kastner, H., 1962. **Statik des Tunnel - und Stollenbaus (Statics of Tunnels and Crosscut Structures)**, Springer-Verlag, Berlin/Goettingen/Heidelberg.

Lang, T.A. and J.A. Bischoff, 1982. **Research Study of Coal Mine Rock Reinforcement**, U.S. Bureau of Mines, PB-82-218-041, U.S. Bureau of Mines, Washington, DC.

Link, H., 1962. "Über den geraden Druckstab in Flüssigkeit" (A Bar Under Axial Compression Suspended in a Fluid), **Engineering Archives**, Springer, Vol. 31, No. 3, Berlin, pp. 149-167.

Link, H., 1965. **Die Beanspruchungen eines Schachtausbau aus verschweissten Stahlblechen mit Zwischenbeton und Asphalt - Gleitfuge (Stresses in a Shaft Lining Consisting of Welded Double Steel Sheets with Load Bearing Concrete and Surrounded by Bitumen)**, Glückauf Forschungshefte, Heft 6, Gluckauf-Verlag, Essen, Germany, pp. 1-15.

Link, H., 1985. "Schachtbau, Stollenbau, Tunnelbau" ("Construction of Shafts, Drifts and Tunnels"), **Stahlbau-Handbuch für Studium und Praxis**, Deutscher Stahlbau-Verband, Köln, Vol. 2, Ch. 35, pp. 1037-1069.

Mente, L.J., and F.W. French, 1964. "Response of Elastic Cylinders to Plane Shear Waves," **Journal of the Engineering Mechanics Division**, Vol. 64, No. EM5, ASCE, New York, NY, pp. 103-125, October.

Nelson, J.W. and P.C. Kelsall, 1984. "Prediction of Long-Term Creep Closure in Salt," **Proceedings, 25th Symposium on Rock Mechanics** (June 25-27, Northwestern University, Evanston, IL), Society of Mining Engineers, AIME, New York, NY, pp. 1115-1125.

U.S. Corps of Engineers, 1978. "Tunnels and Shafts in Rock," **Engineering Manual 1110-2-2901**, Department of the Army, Corps of Engineers, Office of the Chief of Engineers, Washington, DC.

U.S. Department of Energy (DOE), 1980. **Considerations for Developing Seismic Design Criteria for Nuclear Waste Storage Repositories**, JAB-00099-128, URS/John A. Blume & Associates, Engineers, San Francisco, CA.

U.S. Department of Energy (DOE), 1986. **Quality Assurance Plan for High-Level Radioactive Waste Repositories**, (OGR/B-3), Attachment A of Supplement No. 3, Office of Civilian Radioactive Waste Management, Washington, DC.

Van Dillen, D., R.W. Fellner, and B. Dendrou, 1979. "A Two-Dimensional Finite Element Technique for Modeling Rock/Structure Interaction of a Lined Underground Opening," **20th U.S. Symposium on Rock Mechanics** (Austin, TX, June 4-6), University of Texas, Austin, TX, pp. 251-258.

Vaughan, P.R., 1969. "A Note on Sealing Piezometers in Borehole," **Geotechnique**, Vol. 19, No.3, pp. 405-413.

Weston, R.F., 1984, **Generic Requirements for a Mined Geologic Disposal System**, DOE/NE 44301-1, DOE, Washington, DC.

Wright, F.D., 1973. "Roof Control Through Beam Action and Arching," **SME Mining Engineering Handbook**, Vol. 1, Society of Mining Engineers, AIME, New York, NY, pp. 13-80 through 13-96.

10 GLOSSARY, ACRONYMS, ABBREVIATIONS, AND SYMBOLS

10.1 GLOSSARY

anisotropy	The condition of having properties with different values when measured along axes in different directions.
anneal	The process by which a material heals itself in the presence of heat (e.g., creep deformation of salt to heal fractures).
aquiclude	1) rock formation which, although porous and capable of absorbing water slowly, does not transmit water fast enough to furnish an appreciable supply for a well or spring. 2) An impermeable rock formation that may contain water but which is incapable of transmitting significant water quantities. Usually functions as an upper or lower boundary of an aquifer.
aquifer	1) A water-bearing layer of permeable rock or soil. (Re. DOE/EIS-0046-D) 2) A formation, a group of formations, or a part of a formation that contains sufficient saturated permeable material to yield significant quantities of water to wells and springs. (Re.: 10CFR960; DOE/RW-0014, 12/84) 3) An underground geological formation, group of formations, or part of a formation that is capable of yielding a significant amount of water to a well or spring. (Re.: 40CFR191) 4) A layer of permeable rock or soil through which water flows. (Re.: DOE/NE-0007) 5) A water-bearing layer of permeable rock that yields water in usable quantities to wells. (Re.: Study of Isolation System for Geologic Disposal of Wastes, 83)
aquitard	A formation that retards but does not prevent water moving to or from an adjacent aquifer. It does not yield water readily to wells or springs, but may store groundwater. (Re.: DOE/RW-0014, 12/84)

artesian condition	Groundwater confined under hydrostatic pressure. The water level in an artesian well stands above the top of the artesian water body it taps. If the water level in an artesian well stands above the land surface, the well is a flowing artesian well.
asphalt	A dark brown to black cementitious material in which the predominating constituents are bitumens which occur in nature or are obtained in petroleum processing. Asphalt is a constituent in varying proportions of most crude petroleums.
average lithostatic gradient	An approximation of the increase in lithostatic stress with depth.
brine	1) Water containing dissolved salts at or near saturation. (Re.: DOE/RW-0014, 12/84) 2) Water containing dissolved salts in greater concentration than ordinary seawater. In salt deposits, brine may be present as fluid inclusions which are in equilibrium with the surrounding crystalline salt. (Re.: Draft Test Plan for In Situ Testing in an Exploratory Shaft in Salt, ONWI, 3/85)
caprock	A local designation in the Texas panhandle area for a hard caliche zone at a depth of 50 to 85 ft (15.2 to 25.9 m) at the Deaf Smith County site. Also, layers of insoluble mineral deposits that may be derived from the dissolution of a salt dome, ''capping'' the dome. Usually caprock is impervious.
clastic	A material consisting of fragments of rocks or organic structures that have been moved individually for some distance from their place of origin.
cohesion	A measure of the shear strength of a material along a surface with no perpendicular stress applied to that surface.

competent rock	Structurally strong rock, which under a specific set of conditions is able to support tectonic forces and localized stresses caused by excavating without undergoing significant deformation. (Re.: Study of Isolation System for Geologic Disposal of Wastes, 1983)
controlled blasting techniques	Use of patterned drilling and optimum amounts of explosives and detonating devices to control blasting damage.
creep closure	Closure of underground openings, especially openings in salt, by plastic flow of the surrounding rock under lithostatic pressure.
creep parameters	Variables that are incorporated into a constitutive relationship that describes the creep behavior of a material.
decommissioning	Activities associated with removing a repository from service, i.e., backfilling, shaft sealing, and the end of surface-facility use (including demolition, dismantling, etc.)
deviatoric stress	The difference between each principal stress value and the average of the three principal stresses.
discretization	Subdivision of a continuum into a finite number of blocks, elements, or membranes.
drill-and-blast	A method of mining in which small-diameter holes (less than 1 ft, 0.3 m) are drilled into the rock and then loaded with explosives. The blast from the explosives fragments and breaks the rock away from the face so that the rock can be removed. The underground opening is advanced by repeated drilling and blasting.
elastic	Describes a material or a state of a material where strain or deformation is recoverable, nominally instantaneously but actually within certain tolerances and within some arbitrary time. Capable of sustaining stress without permanent deformation.

elastic rock zone	The zone outside the relaxed rock zone where excavation has altered the in situ stress field. Rock in the elastic zone undergoes recoverable elastic deformation.
elastic polymeric	A chemical compound or a mixture of compounds formed by a chemical reaction in which two or more molecules form a larger molecule. This compound is capable of recovering size and shape after deformation.
engineered-barrier system	The man-made components of a nuclear waste disposal system which prevent the release of radionuclides from the subsurface facility or into the geohydrologic setting.
expansive material	A material such as earthfill, concrete, or grout that has clay additives which increase in volume in response to chemical absorption of water.
exponential-time creep law	A constitutive relationship used to describe the creep behavior of salt.
finite element method	The representation of a structure as a finite number of two-dimensional and/or three-dimensional components called finite elements.
ground control	Any technique used to stabilize a disturbed or unstable rock mass.
grout	A cementitious material of high water content, fluid enough to be poured or injected into spaces and thereby fill or seal them (such as the fissures in the foundation rock of a dam, or the interstices between fragments in a brecciated rock, or the space between the lining of a shaft and the surrounding earth).
hydrostatic pressure	The pressure exerted on an immersed body by a fluid at rest.
isoparametric	The finite element shape which is described by the same mathematical function as the general displacement field on that finite element.

isotropic horizontal stress	Stress that is uniform when measured along all horizontal axes.
keyway	A diametrical enlargement in an excavation such as an entryway, shaft, or borehole which is designed to stabilize the rock mass to a higher degree than the excavation itself.
lithology	The character of a rock described in terms of its structure, color, mineral composition, grain size, and arrangement of its component parts.
lithostatic pressure	The vertical pressure at a point in the earth's crust that is equal to the pressure that would be exerted by a column of the overlying rock or soil.
operational seal	The seal installed at the top and bottom of a watertight shaft lining section to prevent groundwater from flowing into the shaft.
phreatic surface	That surface of a body of unconfined ground water at which the pressure is equal to that of the atmosphere.
picotage	Vertical seal for watertight shaft lining constructed from wooden blocks, wedges, and needles tightly packed between a heavy steel or cast iron ring and the excavation wall.
plastic	Said of a body in which strain produces continuous, permanent deformation without rupture.
potentiometric surface	An imaginary surface representing the static head of groundwater and defined by the level to which water will rise in a well; piezometric surface. A water table is a particular potentiometric surface.
principal stress	A stress that is perpendicular to one of three mutually perpendicular planes that intersect at a point on which the shear stress is zero; a stress that is normal to a principal place of stress. The three principal stresses are identified as least or minimum, intermediate, and greatest or maximum.

probable maximum flood	The flood that may be expected from the most severe combination of critical meteorologic and hydrologic conditions that are reasonably possible in the region.
P waves	Compressional waves.
relaxed rock zone	The zone immediately around the shaft where excavation has altered the in situ stress field. Rock in this zone undergoes permanent plastic deformation. The outer edge of the relaxed rock zone is the boundary between plastic and elastic rock behavior.
repository horizon	The stratigraphic interval in which the roof, pillars, and floor of the underground repository will be located.
retrievability	The capability built into the repository by means of design approaches, construction methods, and operational procedures to allow emplaced nuclear waste to be retrieved.
rheology	The study of the deformation and flow of matter.
radionuclide	The radioactive form of a chemical element which exhibits spontaneous decay or disintegration, usually accompanied by the emission of ionizing radiation. (Re.: DOE/NE-0007)
seal	A device, mechanism, or material utilized to retard the flow of liquids or gases. (Re.: Draft Test Plan for In Situ Testing in an Exploratory Shaft in Salt; ONWI, 3/85)
semi-empirical	A combination of empirically and theoretically derived relationships.

shaft	A vertical or steeply inclined excavation from surface accessing specific horizons. The shaft may include the shaft lining, shaft seal material, all the equipment in the shaft, the collar, shaft stations, and the sump. This includes a zone of rock surrounding the shaft excavation which is affected by construction.
shaft lining	The concrete or concrete and steel structure fixed around the shaft to support the opening and, if required, to prevent water inflow.
SH waves	Horizontally polarized shear waves.
steady-state (secondary) creep	The second stage of deformation of a creep-prone material when subjected to a constant deviatoric stress. Creep rate is constant during this stage.
SV waves	Vertically polarized shear waves.
tilt	The slope of a plane. The slope of a geological stratum.
transient heat analysis	Time-dependent thermal analysis.
transient (primary) creep	The first stage of deformation of a creep-prone material when subjected to a constant deviatoric stress. Creep rate is initially high and then slowly decreases to a steady-state value.
viscoelastic	Said of a material in which instantaneous elastic strain, under stress below the elastic limit, is followed by continuously developed permanent strain under long sustained stress of constant magnitude. If the strain is kept constant at some point beyond the elastic limit, the stress is reduced exponentially.
viscoplastic	Said of a material which yields in the plastic domain where stresses are a function of the deformation rate.

10.2 LIST OF ACRONYMS

A/E	Architect/Engineer
ACI	American Concrete Institute
AIME	American Institute of Mining, Metallurgical, and Petroleum Engineers
AISC	American Institute of Steel Construction
ANSI	American National Standards Institute, Inc.
ASCE	American Society of Civil Engineers
ASM	Asphaltic Sealant Material
ASME	American Society of Mechanical Engineers
ASTM	American Society of Testing and Materials
AWS	American Welding Society
BLM	Bureau of Land Management
CFR	Code of Federal Regulations
CRWM	Civilian Radioactive Waste Management, Committee on Radioactive Waste Management
CSIR	Council for Scientific and Industrial Research (South Africa)
DBE	design basis earthquake
DOE	U.S. Department of Energy
DIN	Deutsche Industrie Normen (German Industry Standards)
EA	Environmental Assessment, Deaf Smith County Site, Texas: May 1986
EDBH	engineering design borehole
EPA	U.S. Environmental Protection Agency
ESF	exploratory shaft facility
ESs	exploratory shafts
GR	Geologic Repository
GTP	Generic Technical Position
HEPA	high-efficiency particulate air
HLW	high-level waste
ISD	SRP Input to Seismic Design
ISRM	International Society for Rock Mechanics
LSA	Lower San Andres formation

MGDS	Mined Geologic Disposal System
MSHA	Mine Safety and Health Administration
NAVFAC DM	Naval Facility Engineering Command Design Manual
NCMA	National Concrete Masonry Association
NFPA	National Fire Protection Agency
NGI	Norwegian Geotechnical Institute
NQA	Nuclear Quality Assurance
NRC	U.S. Nuclear Regulatory Commission
NUREG	Nuclear Regulatory Commission document
NWPA	Nuclear Waste Policy Act of 1982
NWTS	National Waste Terminal Storage (replaced by CRWM)
OGR	Office of Geologic Repositories
OSHA	Occupational Safety and Health Administration
PCI	Prestressed Concrete Institute
PMF	probable maximum flood
PGA	peak ground acceleration
PGD	peak ground displacement
PGV	peak ground velocity
QA	quality assurance
QC	Quality Control
R/A	radioactive
RETC	Rapid Excavation and Tunneling Conference
RMS	root mean square
RSDR	Repository Subsystem Design Requirements
SCP-CDR	Site Characterization Plan - Conceptual Design Report
SDG	SRP Shaft Design Guide
SSI	soil-structure interaction
SRP	Salt Repository Program
SRPO	Salt Repository Project Office
TDS	total dissolved solids
TDWR	Texas Department of Water Resources
TWDB	Texas Water Development Board
TWC	Texas Water Commission

UBC	Uniform Building Code
USA	Upper San Andres formation
USGS	U.S. Geological Survey
WIPP	Waste Isolation Pilot Plant

10.3 ABBREVIATIONS AND SYMBOLS (used in Section 5.4)

E_d = dynamic Young's modulus of the soil

E'_d = dynamic Young's modulus of the lining material

σ_a = longitudinal (axial) stress in the shaft lining

σ_x, σ_y, σ_z = normal stresses acting parallel to the x, y and z Cartesian coordinates, respectively (see Figure 5.6)

σ_t, σ_r = normal stresses acting parallel to the t and r cylindrical coordinates, respectively (see Figure 5.6)

ϵ_{xx}, ϵ_{zz} = normal strains acting parallel to the x and z Cartesian coordinates, respectively

ϵ_t, ϵ_r = normal strains acting parallel to the t and r cylindrical coordinates, respectively

τ_{xz}, τ_{xy}, τ_{yz} = shear stresses in the Cartesian coordinate system where, in general, τ_{ij} is the shear stress on a plane normal to the i axis, acting in the j direction. Also, $\tau_{ij} = \tau_{ji}$

τ_{rt}, τ_{rz}, τ_{tz} = shear stresses in the cylindrical coordinate system where, in general, τ_{ij} is the shear stress on a plane normal to the i axis, acting in the j direction. Also, $\tau_{ij} = \tau_{ji}$

γ_{xz}, γ_{xy}, γ_{yz} = shear stresses in the Cartesian coordinate system where, in general, γ_{ij} is the shear strain associated with the shear stress τ_{ij}

γ_{rt}, γ_{rz}, γ_{tz} = shear strains in the cylindrical coordinate system where, in general, γ_{ij} is the shear strain associated with the shear stress τ_{ij}

γ^*_{zy}, γ^*_{zx} = shear strains induced in the lining by the free-field shear strains γ_{zy} and γ_{zx}, respectively

I = moment of inertia of the shaft cross section

G_d = dynamic shear modulus of the soil

G'_d = dynamic shear modulus of the lining material

A = cross-sectional area of the shaft lining, and coefficient in three-dimensional analytical solution for lining stress

L = wavelength corresponding to the predominant frequency of the maximum shear strain

R = outer radius of liner

a = inner radius of liner

σ_b = longitudinal flexural stress in the shaft lining

κ = curvature along the shaft centerline

r = radial distance from shaft centerline to point under consideration (see Figure 5.9)

λ_d = dynamic Lamé's constant of the soil

ν_d = dynamic Poisson's ratio of the soil

σ_1, σ_3 = maximum and minimum principal stresses, respectively

θ = angle measured from σ_1 to point under consideration (see Figure 5.9)

ϵ_{t_A}, ϵ_{t_B} = components of normal strain parallel to the t coordinate axis

ν'_d = dynamic Poisson's ratio of the lining material

T = radius ratio = $\frac{r}{a}$

P = mean stress = $\frac{\sigma_1 + \sigma_3}{2}$

S = deviator stress = $\frac{\sigma_1 - \sigma_3}{2}$

E^*_d, E'^*_d = modified dynamic Young's moduli used to convert three-dimensional stress solution to plane stress solution

ν^*_d, ν'^*_d = modified dynamic Poisson's ratio used to convert three-dimensional stress solution to plane stress solution

B = coefficient in three-dimensional analytical solution for lining stress

C = coefficient (see B)

D = coefficient (see B)

Δ, Δ^* = coefficients (see B)

F_1, F_2, F_3, F_4 = coefficients (see B)

APPENDIX A
GROUND PRESSURE GUIDELINES

A.1 INTRODUCTION

The calculation of rock pressures and analysis of rock behavior is based on the characterization of the rock mass as an elastic, plastic, or viscoelastic homogeneous isotropic continuum.

A.1.1 Elastic Rock Condition

Hard, competent rock is generally assumed to be elastic if (1) the rock is reasonably homogeneous and isotropic, and it is without major discontinuities such as gouge-filled joints and (2) the in situ elastic strength of the rock is not exceeded by any excavation-induced or thermally induced stress increases. Young's modulus and Poisson's ratio describe the stress/strain relationship of the rock under all load changes for this condition.

A.1.2 Plastic Rock Condition

In the analysis of discontinuous rock masses, including those with tight or filled-in joints, a plastic rock condition is assumed in the analysis of load variations and changes in the stress/strain relationship of the rock mass. These analyses assume a Mohr-Coulomb strength criterion which is defined by the angle of internal friction and cohesive strength.

An assumed initial elastic condition can be changed to a plastic condition wherever the in situ elastic rock strength has been exceeded by an excavation-induced or thermally-induced stress increase.

A.1.3 Viscoelastic Rock Condition

A viscoelastic rock condition should be assumed in the analysis of the stress/strain response of salt (and any other creep sensitive geologic units) to the initial stress concentrations caused by excavation. The viscoelastic determination should be composed of an elastic strain component, defined by the Young's modulus and Poisson's ratio, a transient state creep (viscous) component, and for practical purposes, a steady state creep component defined by a temperature-dependent and stress-dependent creep law.

A.1.4 Viscoplastic Rock Condition

A viscoplastic rock condition should be assumed in the analysis of the long-term, steady state creep of salt into an unsupported, excavated opening. The steady state creep phase is completely defined by the same temperature- and stress-dependent creep law used in the viscoelastic analysis. The steady state condition develops asymptotically, but it should be assumed after some initial time period when creep rates are nearly constant.

Linings that will be subjected to ground pressures resulting from salt creep must be designed for full lithostatic pressures (see Chapter 4). Alternately, creep pressures may be isolated from the lining over the operational life of the shaft by installing compressible backfill materials between the shaft lining and the excavated shaft wall. Methods for designing such a lining can be found in the literature (e.g., Goodman, 1980). Refer to Jessberger (1980), Vyalov, et. al., (1962), and Klein (1985) for design methods in creeping frozen ground conditions.

A.2 ELASTIC CONDITIONS

The stress surrounding a circular hole in an ideally elastic medium with an internal pressure acting within the hole can be expressed as (Coates, 1981):

$$\sigma_r = \sigma_h + (P_g - \sigma_h)\left(\frac{a}{r}\right)^2 \qquad \text{(A-1)}$$

$$\sigma_t = \sigma_h - (P_g - \sigma_h)\left(\frac{a}{r}\right)^2 \qquad \text{(A-2)}$$

where:
- σ_r = radial stress
- σ_t = tangential stress
- σ_h = in situ horizontal stress acting in all directions in the ground prior to shaft excavation
- a = radius of shaft excavation
- r = radial distance to the point of interest
- P_g = radial support pressure acting at radius a

The various stresses are shown on Figure A-1. For the case where P_g equals zero, i.e., in an unlined shaft, the stresses that develop in the elastic ground around the shaft are shown as dashed curves. For this case, the radial stress at ($\frac{R}{a}$ = 1) is zero, and the tangential stress at ($\frac{R}{a}$ = 1) is 2 σ_h. If a lining is provided, the radial pressure acting at ($\frac{R}{a}$ = 1) becomes P_g and the tangential stress at ($\frac{R}{a}$ = 1) is decreased by the amount of the lining pressure P_g as shown by the solid curves on Figure A-1.

A.3 ELASTIC/PLASTIC CONDITIONS

If the rock surrounding the shaft cannot sustain the radial and tangential stresses, failure will occur. The resulting stresses may be as shown on Figure A-2, where R is the radius to the unfailed elastic zone. The space between (r = a) and (r = R) represents a zone of relaxed ground. This zone is in a plastic state of equilibrium in which the stress relationship is governed by the Mohr-Coulomb strength theory. The zone remains in tact and has sufficient strength to sustain a tangential stress consistent with the elastic distribution of stresses at radius R.

The extent of the relaxed zone is influenced by support pressure as well as by the strength and properties of the rock mass as defined by the Mohr-Coulomb strength theory. Shaft excavation may diminish the in situ strength and other properties of the rock mass, thus increasing the area of the relaxed zone. It is therefore important that the lining design and construction methods control the relaxed zone.

Jaeger (1969) gives the equation for calculating the radius R of the disturbed rock zone on a shaft lining:

$$\frac{R}{a} = \left\{ \left(\frac{2}{t^2 + 1} \right) \frac{\sigma_h (t^2 - 1) + 2c \cdot t}{P_g (t^2 - 1) + 2c \cdot t} \right\}^{\frac{1}{t^2 - 1}} \qquad \text{(A-3)}$$

where: $t^2 = \tan^2 (45° + \frac{\phi}{2}) = \frac{1 + \sin \phi}{1 - \sin \phi}$

ϕ = internal friction angle of elastic rock mass

c = cohesion of the rock mass

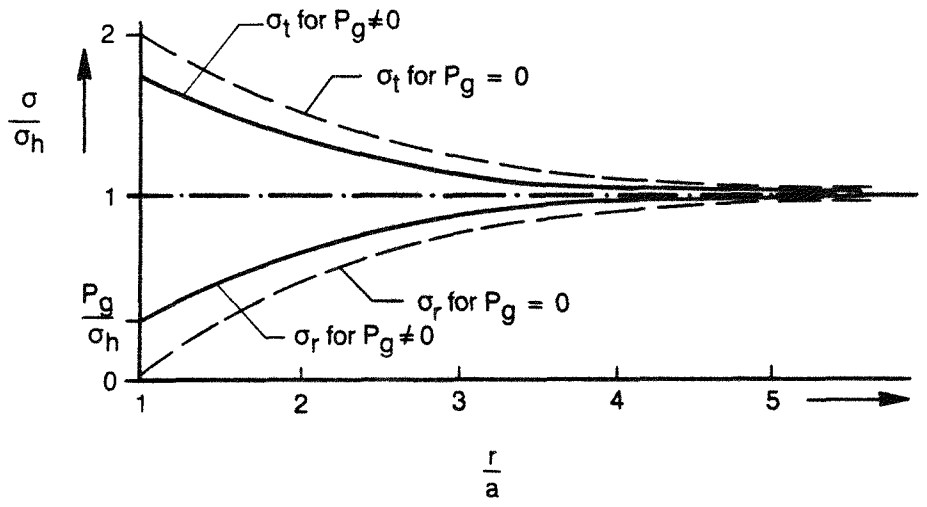

EFFECTS ON STRESSES AROUND SHAFT FROM LINING BACK PRESSURE P_g

FIGURE A 1

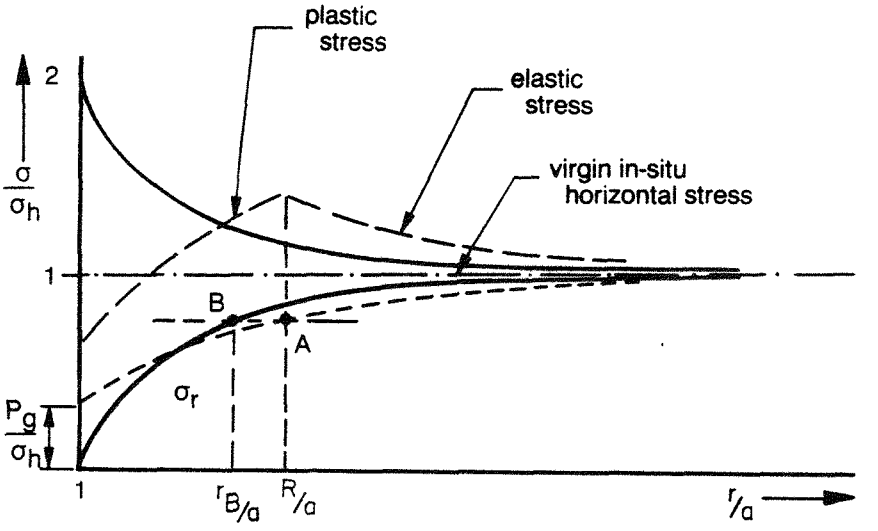

A = Plastic/Elastic Boundary

B = Approximation of Location of Pt. A on the Elastic Curve

RADIAL AND TANGENTIAL STRESS DISTRIBUTIONS FOR ELASTIC AND PLASTIC CONDITIONS

FIGURE A.2

The shaft lining pressure P_g is a function of the relaxed zone thickness (R − a) and, conversely, the relaxed zone thickness is a function of the shaft lining pressure. A conservative first estimate of R can be made by referring to Figure A-2. At the transition point between the elastic and plastic zones (r = R) there exists a radial stress σ_{rR} and a tangential stress σ_{tR}. Both elastic and plastic criteria hold at this point (Jaeger, 1969).

$$\sigma_{tR} = 2\,\sigma_h - \sigma_{rR} \tag{A-4}$$

$$\sigma_{tR} = \sigma_{rR} \cdot t^2 + 2\,c \cdot t \tag{A-5}$$

Equating σ_{tR} from Equations A-4 and A-5 yields:

$$\sigma_{rR} = \frac{2\,(\sigma_h - c \cdot t)}{t^2 + 1} = (\sigma_h - c \cdot t)\,(1 - \sin\phi) \tag{A-6}$$

Equation A-6 defines the radial rock stress at Point A in Figure A-2. The radial rock stress at Point A could be defined in terms of radial distance R if support pressure P_g were known. The distance to Point A across the plastic rock zone in fractured rock will vary according to the amount of support pressure P_g provided to the excavated shaft wall. The greater the support pressure P_g the smaller the radial distance R. In other words, the radius R is a function of P_g and vice versa. For practical ranges of support pressure in fractured rock, the distance R to Point A across a plastic zone will always be greater than the distance r_B to the same radial stress at Point B on a theoretical curve for the case of no support pressure P_g and where all the rock would remain elastic.

The expression for determining r_B in terms of shaft exavation radius a and in situ stress σ_h, according to elastic stress distribution, is (Jaeger, 1969, p. 126):

$$\sigma_{r_B} = \sigma_h\left[1 - \left(\frac{a}{r_B}\right)^2\right] \tag{A-7}$$

Equating Equation A-6 and Equation A-7, and setting $t^2 = \frac{1 + \sin\phi}{1 - \sin\phi}$, an expression is obtained for $\frac{a}{r_B}$, which will serve as a conservative approximation of $\frac{a}{R}$:

$$\left(\frac{a}{R}\right)^2 = \sin\phi + \left(\frac{c}{\sigma_h}\right)\cos\phi \tag{A-8}$$

The approximation method gives an explicit solution for determining radius r_B on a theoretical elastic curve. Thus, the radius r_B can serve as an approximation to the true radius R, and it will be a conservative approximation since, being smaller, it will lead to a larger required support pressure.

Jaeger (1969) presents the solution of σ_r in the relaxed zone:

$$\sigma_r = \left(P_g + \frac{2c \cdot t}{t^2 - 1}\right)\left(\frac{r}{a}\right)^{t^2 - 1} - \frac{2c \cdot t}{t^2 - 1} \qquad \text{(A-9)}$$

Applying the boundary condition $\sigma_r = \sigma_{rR}$ for $r = R$:

$$\sigma_{rR} = \left(P_g + \frac{2c \cdot t}{t^2 - 1}\right)\left(\frac{R}{a}\right)^{t^2 - 1} - \frac{2c \cdot t}{t^2 - 1} \qquad \text{(A-10)}$$

Combining A-6 and A-10 and setting $\frac{2t}{t^2 - 1} = \cot\phi$,

$$P_g = (\sigma_h + c \cdot \cot\phi)(1 - \sin\phi)\left(\frac{a}{R}\right)^{t^2 - 1} - c \cdot \cot\phi \qquad \text{(A-11)}$$

It is the intent of the guidelines to set an upper limit to $\frac{R}{a}$, e.g., to limit the extent of the plastic zone. If the compressive strength of the rock is strong relative to the in situ stress, it can be shown that $\frac{R}{a}$ approaches $\sqrt{e}$ as a limit for the case of no support pressure, even for rock with a very low friction angle. If the compressive strength of the rock is low relative to the in situ stress, it will be necessary to supply a certain minimum support pressure to limit the $\frac{R}{a}$ to less than $\sqrt{e}$. The demonstration of the limit $\frac{R}{a}$ for the two uses, together with the governing ratios of $\frac{q_u}{\sigma_h}$, is given following:

Condition 1 - Compressive strength of rock is high relative to the in situ stress

Let: $\frac{q_u}{2} < \sigma_h \leq q_u = 2c \cdot t$

and: $\sigma_{r(min)} = 0$ (i.e. $P_g = 0$)

since: $$\frac{R}{a} = \left[\frac{2}{t^2+1} \bullet \frac{\sigma_h (t^2-1) + 2c \bullet t}{P_g (t^2-1) + 2c \bullet t}\right]^{\frac{1}{t^2-1}}$$

then: $$\max \frac{R}{a} = \left[\frac{2}{t^2+1} \bullet \frac{\sigma_h (t^2-1) + 2c \bullet t}{2c \bullet t}\right]^{\frac{1}{t^2-1}}$$

and: $$\max \frac{R}{a} = \left[\frac{2}{t^2+1} \bullet (t^2-1+1)\right]^{\frac{1}{t^2-1}}$$

$$= \left(\frac{2t^2}{t^2+1}\right)^{\frac{1}{t^2-1}} = (1+\sin\phi)\ \frac{1-\sin\phi}{2\sin\phi}$$

then: taking the limits of the above equation as ϕ approaches 0, we have

$$\lim_{\phi \to 0}\left[(1+\sin\phi)^{\frac{1-\sin\phi}{2\sin\phi}}\right] = \lim_{\phi \to 0}\left[e^{\frac{1-\sin\phi}{2\sin\phi} \bullet \ln(1+\sin\phi)}\right]$$

since: $$\lim_{\phi \to 0}\left(\frac{\ln(1+\sin\phi)}{\sin\phi}\right) = \lim_{\phi \to 0}\left(\frac{\frac{\cos\phi}{1+\sin\phi}}{\cos\phi}\right) = 1$$

where: $$\left[\lim \frac{f(x)}{g(x)} = \lim \frac{f'(x)}{g'(x)}, \text{ if } \lim f(x), \lim g(x) \to 0\right]$$

then: $$\max \frac{R}{a} = \sqrt{e}$$

Condition 2 – Compressive strength of the rock is low relative to the in situ stress.

Let: $$\sigma_h > q_u = 2c \bullet t$$

with: $(\sigma_r)_{min} = P_g$

and: $\sigma_h = 2c \bullet t + (\sigma_r)_{min} \bullet t^2$

(Mohr-Coulomb criteria)

then: $$\frac{R}{a} = \left[\frac{2}{t^2+1} \bullet \frac{(t^2 \bullet P_g + 2c \bullet t)(t^2 - 1) + 2c \bullet t}{P_g (t^2 - 1) + 2c \bullet t}\right]^{\frac{1}{t^2-1}}$$

$$= \left(\frac{2t^2}{t^2+1}\right)^{\frac{1}{t^2-1}}$$ therefore, it is the same as Condition 1.

and: $\max \frac{R}{a} = \sqrt{e}$ (for c, $\phi \rightarrow 0$)

Thus, to limit $\frac{R}{a} \leq \sqrt{e}$, a support pressure is needed:

Summarizing Conditions 1 and 2:

1. Calculate $(\sigma_r)_{min}$ to limit the $\frac{R}{a} < \sqrt{e}$

If: $\sigma_h > q_u = 2c \bullet t$

then: $$\sigma_{r(min)} = \frac{\sigma_h - 2c \bullet t}{t^2} = \sigma_h \bullet \left(\frac{1 - \sin\phi}{1 + \sin\phi}\right) - 2c\sqrt{\frac{1 - \sin\phi}{1 + \sin\phi}}$$

where: $\sigma_{r(min)} = P_g$

if: $\frac{q_u}{2} < \sigma_h \leq q_u = 2c \bullet t$

then: $(\sigma_r)_{min} = 0$, then no support pressure is required to limit the plastic zone.

Selection of the Design Support Pressure, P_g

a. Calculate the $\frac{R}{a}$ from the approximation method as obtained from Equation A-8. If less than 1.65, compute P_g from Equation A-11.

b. If $\frac{R}{a}$ from the approximation method is greater than 1.65, assess the $\frac{q_u}{\sigma_h}$ ratio and compute P_g from Condition 1 or 2 as given above. This will limit the $\frac{R}{a}$ to 1.65.

APPENDIX B
SALT CREEP

B.1 INTRODUCTION

This appendix describes an analytic solution of stress distribution around a circular opening with a given hydrostatic stress at infinity. Its objective is to provide a method for predicting the closure rate of the opening. The opening is assumed to exist in plane strain conditions beyond the influence, for example, of the shaft station floor, and shaft bottom. The material analyzed is rock salt considered as a non-Newtonian fluid which has been under loading for a long period of time.

B.2 DEFORMATION OF ROCK SALT

The deformation of rock salt for a given loading can be illustrated with the strain/time relationship shown in Wallner (1981). The strain rate can be divided into:

$$\dot{\epsilon}_{ij} = \dot{\epsilon}^{E}_{ij} + \dot{\epsilon}^{P}_{ij} + \dot{\epsilon}^{C}_{ij} \qquad \text{(B-1)}$$

where: $\dot{\epsilon}^{E}_{ij}$ = the elastic component

$\dot{\epsilon}^{P}_{ij}$ = the primary creep component

$\dot{\epsilon}^{C}_{ij}$ = is the secondary creep component.

Since the primary creep dissipates rapidly, it can be treated as a nonlinear elastic response.

Long after excavation, the stress around the opening reaches steady state, and all incremental deformation is the result of secondary creep. Therefore:

$$\dot{\epsilon}_{ij} = \dot{\epsilon}^{C}_{ij} \qquad \text{(B-2)}$$

The constitutive equation for secondary creep can be expressed as:

$$\dot{\epsilon}_e = \bar{A}\sigma_e^{\,n} \tag{B-3}$$

where:
- $\dot{\epsilon}_e$ = effective strain rate
- $\bar{A}$ = fitting parameter of material properties ($\bar{A} = A \cdot e^{-\frac{Q}{RT}}$)
- σ_e = effective stress
- n = fitting parameter of material properties
- Q = activation energy (cal $mole^{-1}$)
- R = Universal Gas Constant (1.987 cal $mole^{-1}$ $°K^{-1}$)
- T = absolute temperature (°K)

If no volumetric change is associated with secondary creep, the material described by Equations B-2 and B-3 is an incompressible non-Newtonian fluid. The constitutive equation becomes (see Attachment A):

$$\dot{\epsilon}_{ij} = \bar{A} \cdot \frac{3}{2} (\sigma_e)^n \cdot \frac{S_{ij}}{\sigma_e} \tag{B-4}$$

where: S_{ij} = the component of the deviatoric stress sensor

B.3 CYLINDRICAL OPENING IN STATE OF PLANE STRAIN

Considering a cylindrical opening in the state of plane strain (Odquist, 1966):

$$\dot{\epsilon}_\gamma = \frac{dv}{dr} \tag{B-5}$$

$$\dot{\epsilon}_\theta = \frac{v}{r} \tag{B-6}$$

$$\dot{\epsilon}_z = 0 \tag{B-7}$$

where: υ = the radial velocity.

At steady state, the incompressibility of material results in:

$$\frac{d\upsilon}{d_r} + \frac{\upsilon}{r} = 0 \tag{B-8}$$

Solving this differential equation,

$$\upsilon = \frac{C}{r} \tag{B-9}$$

where: C = an integration constant.

Substituting Equation B-9 into Equations B-5 and B-6:

$$\dot{\epsilon}_r = -\frac{C}{r^2} \tag{B-10}$$

$$\dot{\epsilon}\theta = \frac{C}{r^2} \tag{B-11}$$

The relationship between stress and strain, which is derived from the constitutive equation in Equation B-4, is shown in Equation BT-11 Attachment B. Combining Equations B-10 and BT-11:

$$\sigma_\theta - \sigma_r = \left(\frac{C}{A}\right)^{\frac{1}{n}} \cdot \left(\sqrt{\frac{2}{3}}\right)^{\frac{n+1}{n}} \cdot r^{-\frac{2}{n}} \tag{B-12}$$

$$= D_r^{-\frac{2}{n}}$$

The equilibrium condition for the cylindrical opening requires that (Odquist, 1966):

$$\frac{d\sigma_r}{d_r} = \frac{\sigma_\theta - \sigma_r}{r} \tag{B-13}$$

Therefore:

$$\frac{d\sigma_r}{d_r} = D_r^{-\frac{2}{n}-1} \tag{B-14}$$

The solution of this differential equation is:

$$\sigma_r = -D \bullet \frac{n}{2} \bullet r^{\frac{2}{n}} + E \tag{B-15}$$

$$\sigma_\theta = D \bullet (1 - \frac{n}{2}) \bullet r^{\frac{2}{n}} + E \tag{B-16}$$

The boundary conditions for a cylindrical opening in an infinite medium are:

$$\sigma_r = 0 \quad \text{at} \quad r = a \tag{B-17}$$

$$\sigma_r = -\sigma_0 \quad \text{at} \quad r = \infty \tag{B-18}$$

where: σ_0 = the far field horizontal stress.

D and E can be determined from these boundary conditions:

$$D = -\frac{2}{n} \bullet a^{\frac{2}{n}} \bullet \sigma_0 \tag{B-19}$$

$$E = -\sigma_0 \tag{B-20}$$

and:

$$\sigma_r = [\left(\frac{r}{a}\right)^{-\frac{2}{n}} - 1]\,\sigma_0 \tag{B-21}$$

$$\sigma_\theta = -[\left(\frac{2}{n} - 1\right) \bullet \left(\frac{r}{a}\right)^{-\frac{2}{n}} + 1]\,\sigma_0 \tag{B-22}$$

$$\sigma_\theta - \sigma_r = -\frac{2}{n} \cdot \left(\frac{r}{a}\right)^{-\frac{2}{n}} \cdot \sigma_0 \qquad (-23)$$

From Equation BT-12:

$$\dot{\epsilon}_\theta = \bar{A} \cdot \left(\frac{\sqrt{3}}{2}\right)^{n+1} \cdot \left(\frac{2}{n}\right)^n \cdot \left(\frac{r}{a}\right)^{-2} \cdot \sigma_0^n$$

$$= \bar{A} \cdot \left(\frac{\sqrt{3}}{2}\right)^{n+1} \cdot \left(\frac{r}{a}\right)^{-2} \cdot \left(\frac{\sigma_0}{n}\right)^n \qquad (B\text{-}24)$$

at r = a

$$\dot{\epsilon}_\theta = \bar{A} \cdot \left(\frac{\sqrt{3}}{2}\right)^{n+1} \cdot \left(\frac{\sigma_0}{n}\right)^n \qquad (B\text{-}25)$$

The rate at which the opening converges can be obtained by inserting $\dot{\epsilon}_\theta$ into Equation B-6.

$$v = \dot{\epsilon}_\theta \cdot a = \bar{A} \left(\frac{\sqrt{3}}{2}\right)^{n+1} \cdot a \cdot \left(\frac{\sigma_0}{n}\right)^n \qquad (B\text{-}26)$$

The stress rates, strain rates, and convergence rates calculated using the above equations apply to a steady state condition. They represent the long-term mechanical behavior of a shaft in a rock salt formation. Theoretically, the stresses reach steady state immediately after the excavation of a cylindrical opening in an incompressible material. However, if the material is elastically compressible, an infinite amount of time is required to redistribute the stresses around the opening from an elastic state to the steady state.

Wallner (1981), presents the time history for a similar creep analysis using a finite-element method. The same creep law is used to show the stress distribution over 200 days and 1,122 days respectively for a case of $\bar{A} = 2.25 \times 10^{-10} \left(\frac{1}{(MPa)^n \cdot DAY}\right)$, n = 5, a = 157mm and σ_0 = 22.5MPa. The elastic constants for this analysis are set for E = 25,000 MPa and ν = 0.25. These creep parameters approximate estimated values for the Permian Basin in Texas.

The analytic solution for the convergence rate at t = ∞ is 0.88×10^{-3} mm/day. The numerical solution of $\sigma_\theta - \sigma_r$ at r = a at t = 200 days is about 1.6 times the analytic solution at t = ∞. As shown in Equation BT-12, $\dot{\epsilon}_\theta$ at t = 200 days should be $(1.6)^5 = 10.5$ times $\dot{\epsilon}_\theta$ at t = ∞. Similarly, $\sigma_\theta - \sigma_r$ at r = a at t = 1,122 days is about 1.47 times the analytic solution at t = ∞. The $\dot{\epsilon}_\theta$ at t = 1,122 days should be $(1.47)^5 = 6.8$ times $\dot{\epsilon}_\theta$ at t = ∞. Wallner shows the convergence rate at 200 days at about 0.016 mm/day which will give a convergence rate at t = ∞ of about 0.0015 mm/day. It is 1.7 times the analytic solution derived from Equation B-26.

The comparison between the numerical finite element method solution for creep rate of convergence with respect to time after excavation and the analytical solution of creep rate given by Equation B-26 is shown in Figure B-1. The higher rates of creep during the early time history of the excavation in the finite element method solution are largely due to the initial stress concentrations around the opening caused by the excavation, which are not considered in the steady-state analytical solution.

ATTACHMENT A: STRESS/STRAIN DECOMPOSITION, INVARIENTS, AND FLOW RATE

$$\sigma_m = \frac{1}{3}(\sigma_{11} + \sigma_{22} + \sigma_{33}) \tag{AT-1}$$

$$\sigma_{ij} = S_{ij} + \delta_{ij}\sigma_m \tag{AT-2}$$

$$\sigma_e = \sqrt{\frac{3}{2}}\,(S_{ij}S_{ij})^{\frac{1}{2}} \tag{AT-3}$$

$$|S| = (S_{ij}S_{ij})^{\frac{1}{2}} \tag{AT-4}$$

$$\epsilon_m = \frac{1}{3}(\epsilon_{11} + \epsilon_{22} + \epsilon_{33}) \tag{AT-5}$$

$$\epsilon_{ij} = e_{ij} + \delta_{ij}\epsilon_m \tag{AT-6}$$

$$\epsilon_e = \sqrt{\frac{2}{3}}\,(e_{ij}e_{ij})^{\frac{1}{2}} \tag{AT-7}$$

NOTE: THAT AT THE END OF A 3 YEAR PERIOD, THE NUMERICAL FINITE ELEMENT SOLUTION OF SALT CREEP (SIMILAR TO PERMIAN BASIN SALT CREEP PARAMETERS) IS APPROXIMATELY 8 TIMES THE CLOSED-FORM ANALYTICAL SOLUTION. USE A FACTOR OF 10 FOR A TIME-AVERAGED SOLUTION OF CREEP WITH THE CLOSED-FORM METHOD DURING EARLY LIFE OF EXCAVATED OPENINGS.

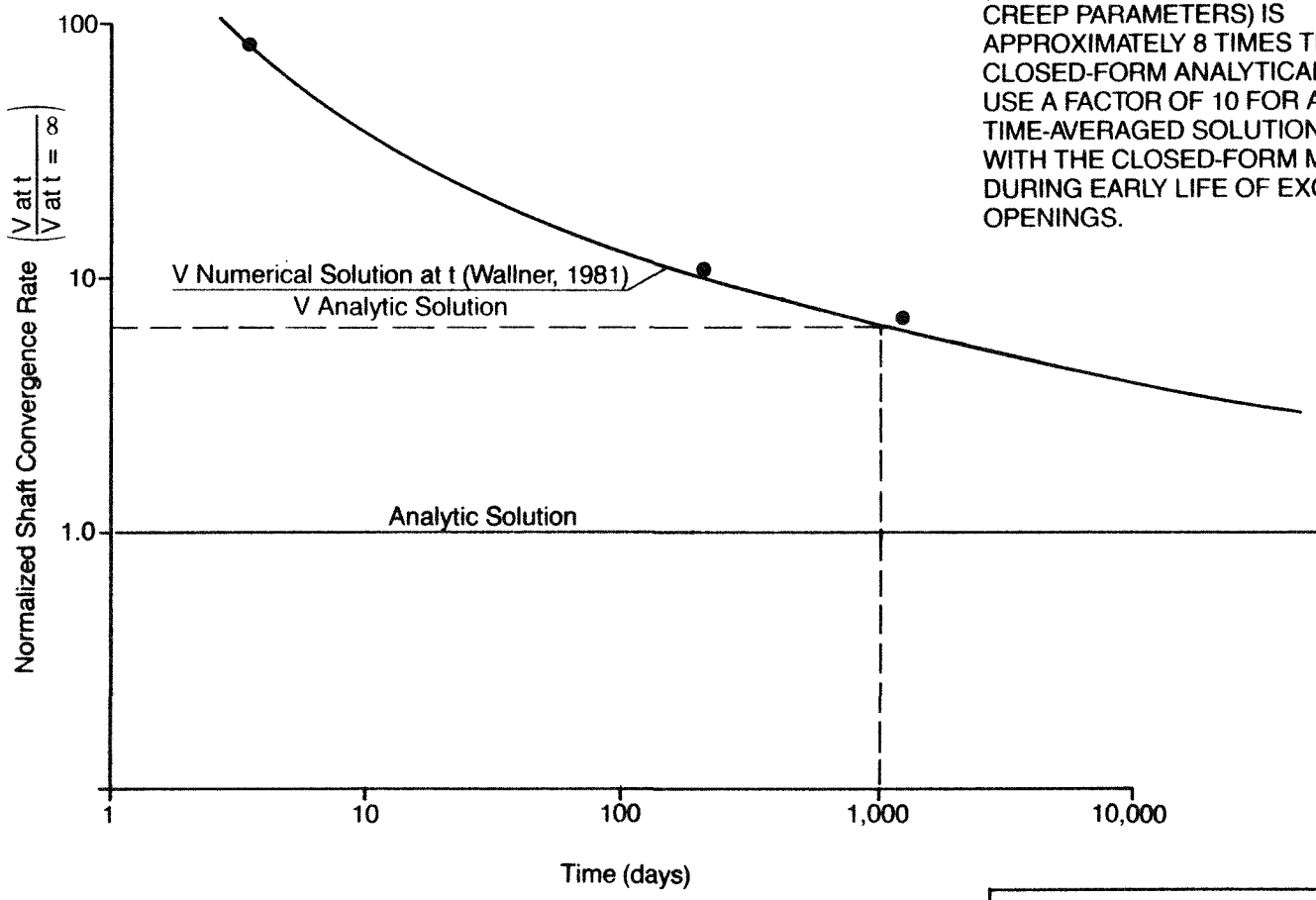

COMPARISON OF CONVERGENCE RATES DUE TO CREEP: NUMERICAL SOLUTION VS. ANALYTICAL SOLUTION

FIGURE B.1

Changing strain term (ϵ) to strain rate term ($\dot{\epsilon}$), the equality in Equations AT-5 through AT-7 holds.

The creep law for the material is:

$$\epsilon_e = \bar{A}\ \sigma_e^n \tag{AT-8}$$

It is assumed that for an isotropic medium, the principal directions of the stress and strain-rate tensors coincide, i.e.,

$$\dot{e}_{ij} = \dot{\lambda}\ \frac{S_{ij}}{|S|} = \dot{\lambda}\sqrt{\frac{3}{2}}\ \frac{S_{ij}}{\sigma_e} \tag{AT-9}$$

In a cylindrical opening in an infinite medium or in a thick-walled cylinder, this assumption becomes a true situation. For incompressible material, Equation AT-9 becomes:

$$\dot{e}_{ij} = \dot{\lambda}\sqrt{\frac{3}{2}}\ \frac{S_{ij}}{\sigma_e} \tag{AT-10}$$

where $\dot{\lambda}$ is a positive scalar. Furthermore:

$$\dot{\epsilon}_e = \sqrt{\frac{2}{3}}\left(\dot{\lambda}\sqrt{\frac{3}{2}}\ \frac{S_{ij}}{\sigma_e} \cdot \dot{\lambda}\sqrt{\frac{3}{2}}\ \frac{S_{ij}}{\sigma_e}\right)^{\frac{1}{2}} = \dot{\lambda} \cdot \frac{1}{\sigma_e} \cdot \sqrt{\frac{2}{3}} \cdot \sigma_e = \sqrt{\frac{2}{3}}\ \dot{\lambda} \tag{AT-11}$$

Substituting Equation AT-8 into Equation AT-11:

$$\dot{\lambda} = \bar{A}\sqrt{\frac{3}{2}}\ (\sigma_e)^n \tag{AT-12}$$

Substituting Equation AT-12 into Equation AT-10:

$$\dot{\epsilon}_{ij} = \bar{A} \cdot \frac{3}{2} \cdot (\sigma_e)^n \cdot \frac{S_{ij}}{\sigma_e} \tag{AT-13}$$

The flow rate of the material is determined using Equation AT-13.

ATTACHMENT B: STRESS/STRAIN FOR PLANE STRAIN CYLINDRICAL OPENING IN INCOMPRESSIBLE MEDIUM

$$\dot{\epsilon}_z = \dot{e}_z = 0 \tag{BT-1}$$

$$\dot{\epsilon}_z = \dot{\epsilon}_z - \frac{1}{3}(\dot{\epsilon}_z + \dot{\epsilon}_r + \dot{\epsilon}_\theta) = -\frac{1}{3}(\dot{\epsilon}_r + \dot{\epsilon}_\theta) = 0 \tag{BT-2}$$

$$\dot{\epsilon}_\theta = -\dot{\epsilon}_r \tag{BT-3}$$

$$\dot{\epsilon}_e = \sqrt{\frac{2}{3}}\left(\dot{\epsilon}_r^2 + \dot{\epsilon}_\theta^2\right)^{\frac{1}{2}} = \frac{2}{\sqrt{3}} \cdot \dot{\epsilon}_\theta \tag{BT-4}$$

Combining Equations AT-13, BT-1, and BT-3:

$$S_\theta = -S_r \text{ and } S_z = 0 \tag{BT-5}$$

$$S_z = \sigma_z - \frac{1}{3}(\sigma_\theta + \sigma_r + \sigma_z) = 0 \tag{BT-6}$$

Equations BT-5 and BT-6 give:

$$\sigma_z = \frac{1}{2}(\sigma_r + \sigma_\theta) \tag{BT-7}$$

$$S_\theta = -\frac{1}{2}(\sigma_r - \sigma_\theta) \tag{BT-8}$$

$$S_r = \frac{1}{2}(\sigma_r - \sigma_\theta) \tag{BT-9}$$

$$\sigma_e = \frac{\sqrt{3}}{2}(\sigma_r - \sigma_\theta) \tag{BT-10}$$

Inserting Equations BT-7 through BT-10 into Equation AT-13:

$$\dot{\epsilon}_r = \bar{A} \cdot \frac{3}{2} \cdot \left(\frac{\sqrt{3}}{2}\right)^n \cdot (\sigma_r - \sigma_\theta) \cdot \frac{\frac{1}{2}(\sigma_r - \sigma_\theta)}{\frac{\sqrt{3}}{2}(\sigma_r - \sigma_\theta)} \qquad \text{(BT-11)}$$

$$= \bar{A} \cdot \left(\frac{\sqrt{3}}{2}\right)^{n+1} \cdot (\sigma_r - \sigma_\theta)^n$$

$$\dot{\epsilon}_\theta = \bar{A} \cdot \frac{3}{2} \cdot \left(\frac{\sqrt{3}}{2}\right)^n \cdot (\sigma_r - \sigma_\theta)^n \cdot \frac{-\frac{1}{2}(\sigma_r - \sigma_\theta)}{\frac{\sqrt{3}}{2}(\sigma_r - \sigma_\theta)} \qquad \text{(BT-12)}$$

$$= -\bar{A} \cdot \left(\frac{\sqrt{3}}{2}\right)^{n+1} \cdot (\sigma_r - \sigma_\theta)^n$$

APPENDIX C
DECOMMISSIONING BULKHEAD SIZING CRITERIA

C.1 BULKHEAD SIZING

The following criteria must either be measured or estimated in order to size a decommissioning bulkhead:

1. **Permeability**. In order to plan the sizes and locations of decommissioning bulkheads, some approximations are needed to estimate the maximum allowable host rock permeability at a seal location, and the total rock thickness needed to accommodate the necessary seal length. To achieve the requirements of 10 CFR 60.113 and 10 CFR 60.134, seal permeabilities may need to approach that of the host rock mass, or be as low as can be reasonably achieved and still not compromise the repository performance.

   When an opening is excavated in salt, a disturbed rock zone is created around it. This disturbed zone can be characterized as comprising two distinct zones outside the radius of excavation; a thin, fractured zone due to excess excavation energy imparted by blasting or machine boring, and a deeper plastic zone caused by redistribution and concentration of the in situ stresses. Koplick, et. al., (1979) estimates the maximum radius to the outer limit of the general fracture zone (plastic zone) in salt as 3.5 (R + 1) where R is the shaft radius in meters. It is assumed that outside this radius, the permeability of the in situ rock salt mass is unchanged.

   The maximum depth of the excavation-disturbed zone can be estimated and should be on the order of 2 ft to 5 ft (0.6 m-1.5 m). The permeability within this zone must also be estimated. Koplick, et, al., (1979) estimates it to be 0.3×10^{-1} ft/yr (10^{-5} cm/sec), which is at the upper limit of fracture flow in salt. The average permeability within the stress-disturbed zone, outside the blasting-disturbed zone, should be estimated to be on the order of 0.3×10^{-3} ft/yr (10^{-7} cm/sec). This is at the midpoint of the range for fracture flow in salt as estimated by Koplick, et. al., (1979). This should also be the maximum allowable permeability of the in situ host rock strata at the seal location. Finally, it is assumed that seal material can be backfilled into the opening upon decommissioning with an in situ permeability of about 0.3×10^{-4} ft/yr (10^{-8} cm/sec).

2. **Estimating Seal Length.** Without any future site-specific detail, one or more of the design approaches used by O'Rourke, et al., (1982) to estimate seal lengths might be adopted in order to model conservatively-based flow conditions through the seal. The worst-case condition for flow moving out of the repository toward the accessible environment was assumed to be a pressure head of brine at the saturation pressure of repository backfill pore fluid changed to steam at a temperature of approximately 392°F (200°C). It is assumed that this condition may exist for some time after the repository is decommissioned, until the groundwater system recharges above the temperature-induced pressure head. An allowable flow quantity must be selected for seal design and analysis. Preliminary estimates are on the order of 35 ft^3/yr (0.99 m^3/yr).

The required seal length must be available within the length of penetration access between the waste emplacement area and the accessible environment. The accessible environment is assumed to be the lowest economically useful aquifer within the overburden. It is assumed that the total required seal length may be made up of increments that may be separated from each other as long as the total required seal length can be accommodated.

Guidelines for evaluating geologic strata for shaft seal placement are to locate seal systems in strata that have stimulated hydraulic conductivities of less than about 0.1 md (10^{-7} cm/sec). Implicit in these criteria is the consideration that if the host rock permeability is not higher than the permeability for the stress-disturbed zone in the seal model, the allowable concentration of radionuclides at the end of the design seal length, for the worst-case failure scenario, will not be exceeded. If the stratum is estimated to be more permeable than this standard, a thicker seal is required. The appropriate thickness must be defined on the basis of the estimated hydraulic conductivity. The assessment of permeability should not only consider interstitial permeability, but also the permeability of rock mass discontinuities.

Deficiencies in site-specific permeability data require that judgments be made on the general range of permeabilities that might be expected from a given rock formation. These judgements should be based on the type and composition of the geologic strata, the degree of fracturing, and the characteristics of these fractures. In selecting candidate seal locations, consideration should be given to isolating known aquifers to prevent interaquifer contamination and to minimize the possibility of fresh water reaching salt horizons and causing salt dissolution.

3. **Stratum Thickness.** Kelsall, et. al., (1985) suggests that a minimum thickness of 20 ft to 40 ft (6.1 m to 12.2 m) is required for a permanent bulkhead seal. However, without more supportive field data 50 ft (15.2 m) should be used as a conservative minimum thickness. This minimum is felt to be necessary because of (1) the lack of site-specific data, and (2) the possible lateral variations in a given sedimentary, stratigraphic horizon. Because of the lack of site-specific data, formations or parts of formations, rather than specific locations, must be identified .. likely to be composed of low-permeability material with a minimum thickness of 50 ft (15.2 m).

   For design and construction purposes, seals should also be located within strata of uniform vertical and lateral lithology and uniform rock mass properties (i.e., rock type, strength, porosity, density, and elastic modulus). The strata should contain as few rock mass discontinuities (such as joints or shears) as possible, since they may alter the permeability, the engineering properties, and the performance characteristics of the strata.

4. **Rock Strength.** Seals should be placed within strata that have sufficient strength (i.e., unconfined compressive and tensile) to minimize structural engineering problems associated with shaft development and bulkhead emplacement. In particular, the compressive strength of the rock wall (Chang, et. al., 1984) should be considered in selecting candidate seal locations because stress concentrations at shaft walls in excess of rock strength may damage the rock, and greatly increase the permeability of the rock along the shaft.

   For elastic response, this damage potential can be expressed in terms of a stress concentration ratio S_R:

$$S_R = \frac{\sigma}{C_o} = \frac{3\sigma_1 - \sigma_3}{C_o} < 1, \qquad \text{(C-1)}$$

where: S_R = ratio of the stress to the strength
σ_1 = maximum stress normal to borehole axis (psi, kPa)
σ_3 = minimum stress normal to borehole axis (psi, kPa)
C_o = uniaxial compressive strength of rock (psi, kPa)
and: $\sigma = 3\sigma_1 - \sigma_3$ = stress field around circular openings (Timoshenko, 1956)

A value of S_R that is less than 1 is safe, based on the elastic model.

Until site specific data are available, subsurface stress conditions at the repository site are assumed to be lithostatic, with a hydrostatic pressure that varies with depth. So:

$$\sigma_V = \sigma_H = \sigma_1 = \sigma_3 = \gamma Z \qquad \text{(C-2)}$$

where: γ = average unit weight (psi/ft, kPa/m)

σ_V = vertical stress (psi, kPa)

$\sigma_H = \sigma_1 = \sigma_3$ = horizontal stress (psi, kPa)

and: Z = depth (ft, m)

Seals should be located in rock strata where the ratio of $\frac{\sigma_V}{C_o}$ is less than the minimum value for wall rock damage. From Equations C-1 and C-2:

$$\frac{\sigma_V}{C_o} < 0.5 \qquad \text{(C-3)}$$

Field experience suggests that the stress ratio should be less than 0.5 (Hoek and Brown, 1980) to control wall rock problems, and perhaps less than 0.2 to avoid slight spalling damage from variable in situ stress conditions and anisotropies. Ideally, the site-specific characteristics of candidate seal locations should be reviewed to ensure that the $\frac{\sigma_V}{C_o}$ ratio is less than the suggested values.

The following table summarizes the minimum rock compressive strengths needed to meet the theoretical empirical ratio of $\frac{\sigma_V}{C_o}$:

Depth (feet)[a]	Compressive Strength (psi)[b] for $\frac{\sigma_V}{C_o} = 0.2$[c]	Compressive Strength (psi)[b] for $\frac{\sigma_V}{C_o} = 0.5$[c]
1,000	5,500	2,200
2,000	11,000	4,400
3,000	16,500	6,600

[a] Multiply by 0.305 to obtain m

[b] Multiply by 6.89 to obtain kPa

[c] γ assumed to be 1.1

It is apparent that a seal will require fairly competent, medium-strength rock in order to limit the $\frac{\sigma_v}{C_o}$ ratio to 0.2. Salt strata do not exhibit breakout or spalling phenomena due to creep, so these criteria do not apply in salt. If the criteria must be exceeded for a seal in a strategic location, then more control excavation techniques should be implemented.

5. **In Situ Mechanical Conditions.** To minimize any mechanical incompatibility of seal and strata, the in situ temperatures, pressures, and the mechanical properties of the strata (i.e., bulk modulus, Young's modulus, Poisson's ratio, index properties) should be considered when selecting candidate seal locations.

6. **Geochemistry**. Candidate seal locations should have water chemistry parameters (e.g., E_H, pH, temperature, total dissolved solids (TDS), specific conductance, alkalinity, dissolved oxygen) that are compatible with the longevity of backfill and bulkhead materials.

7. **Hydrochemistry**. The hydrochemical stability of minerals and rocks such as gypsum, anhydrite, and salt, including the rates of geochemical processes, of salt dissolution (if any), of mineral transformations (specification), and of diagenesis, should be considered when selecting candidate seal locations and their frequency.

C.2 EXCAVATION EFFECTS

In determining the properties and response of the excavation disturbed zone, the shaft sinking method used must be considered. Different excavation techniques induce a different degree of disturbance on the adjacent host rock. These effects influence the size of the bulkhead necessary to perform the proper sealing function.

The drill-and-blast excavation technique is typically utilized for conventional shaft sinking and is acceptable in many mining operations. However, the shaft wall damage from a blast detonation wave contravenes the repository shaft decommissioning criteria for minimizing the disturbed rock zone. Blasting in association with stress redistribution from the excavation geometry can contribute to a zone of rock disturbance around the excavation. This disturbance can cause an increase in the fracture network with a consequent increase in permeability.

Mechanical and hand excavation techniques are available as alternatives to blasting. These techniques include using vertically mounted roadheader units, high-energy impact breakers, pneumatic hammers, and pneumatic splitters. Flexibility is inherent in the techniques, and they may utilize a free face blasted in the center of the shaft. With blasting damage eliminated at the shaft wall, the excavation at a decommissioning seal location can be kept to a minimum. Although surface preparation may be required, additional excavation should not be necessary prior to bulkhead shell or bulkhead construction.

APPENDIX D

DERIVATION OF EQUATIONS 5-45, 5-46, 5-49, 5-62, AND 5-63.

D.1 Equation 5-45

For a sinusoidal wave of amplitude a and wave length L the shear-induced displacement u of the shaft centerline is given by:

$$u = a \sin \frac{2\pi z}{L} \qquad \text{(D-1)}$$

where: u = horizontal (transverse) displacement of shaft centerline (in, mm)
a = maximum amplitude of shaft centerline displacement (in, mm)
z = vertical coordinate (in, mm) (see Figure 5.6)
L = wave length of displacement pattern (in, mm)

Consider the shaft lining as a vertical beam of hollow, circular section. The transverse shear V in such a beam can be expressed by:

$$V = -E'_d I \frac{d^3u}{dz^3} \qquad \text{(Timoshenko, 1956) (D-2)}$$

where: V = beam shear (lb, N)
E'_d = dynamic Young's modulus of the lining material (psi, N/mm^2) (The usual psi to kPa conversion used elsewhere in the SDG does not apply due to the use of lb to N conversion)
I = moment of inertia of the shaft cross section (in^4, mm^4)

The corresponding maximum shear stress for a thin-walled circular tube acting as a beam is given by:

$$\tau_{zy} = 2\frac{V}{A} \qquad \text{(Popov, 1968) (D-3)}$$

where: τ_{zy} = maximum shear stress on the cross section (psi, N/mm^2)
A = cross-sectional area of the shaft lining (in^2, mm^2)

The maximum shear strain corresponding to the shear stress given in Equation D-3 is:

$$\gamma^*_{zy} = \frac{2V}{G'_d A} \tag{D-4}$$

where: γ^*_{zy} = maximum shear strain on the shaft cross section (in/in, mm/mm). (The * has been added to denote an induced strain arising from the imposed shear force, V)
G'_d = dynamic shear modulus of the lining material (psi, N/mm^2)

Differentiating Equation D-1 and combining it with Equations D-2 and D-4 yields:

$$\gamma^*_{zy} = \frac{2E'_d I}{G'_d A}\left(\frac{2\pi}{L}\right)^3 a \bullet \cos\frac{2\pi z}{L} \tag{D-5}$$

Now the free-field shear strain produced by the sinusoidal wave is given by:

$$\gamma_{zy} = \frac{\partial u}{\partial z} \qquad \text{(Timoshenko and Goodier, 1970)} \tag{D-6}$$

where: γ_{zy} = free field shear strain (in/in, mm/mm)

Differentiating Equation D-1 and substituting into Equation D-6 gives:

$$\gamma_{zy} = a\left(\frac{2\pi}{L}\right)\cos\frac{2\pi z}{L} \tag{D-7}$$

The calculated maximum free-field shear strain is available from the site analysis in the SRP Input to Seismic Design (DOE, 1987). Substituting this value into Equation D-7, setting the cosine term equal to its maximum value of unity, and solving for the value, a, gives:

$$a = \gamma_{zy}\left(\frac{L}{2\pi}\right) \tag{D-8}$$

Equations D-5 and D-8 are combined and simplified to give:

$$\gamma^*_{zy} = \frac{2E'_d I}{G'_d A}\left(\frac{2\pi}{L}\right)^2 \cdot \gamma_{zy} \cdot \cos\frac{2\pi z}{L} \qquad \text{(D-9)}$$

The maximum induced shear strain from Equation D-9 is then:

$$\gamma^*_{zy} = \frac{8\pi^2 E'_d I}{G'_d A L^2}\gamma_{zy} \qquad \text{(D-10)}$$

which is Equation 5-45.

D.2 Equation 5-46

For a long circular vertical shaft with prescribed stresses at infinity (free field) it may be assumed that the horizontal displacements u and v are independent of the vertical coordinate z and the strain $\epsilon_{zz} = \frac{\partial w}{\partial z}$ is a constant ϵ. With zero body forces the equation of equilibrium, in terms of displacements, can be written in cylindrical coordinates as:

$$\frac{\partial^2 w}{\partial r^2} + \frac{1}{r} \cdot \frac{\partial w}{\partial r} + \frac{1}{r^2} \cdot \frac{\partial^2 w}{\partial \theta^2} = 0 \qquad \text{(Jaeger and Cook, 1969) (D-11)}$$

where: w = vertical displacement along the z axis (in, mm)
r = radial coordinate (in, mm) (see Figure 5.9)
θ = angular coordinate measured from the x axis (see Figure 5.9)

The shear stress of concern is:

$$\tau_{zr} = \tau_{rz} = G\gamma_{rz} = G\frac{\partial w}{\partial r} \qquad \text{(Jaeger and Cook, 1969) (D-12)}$$

where: τ_{rz} = shear stress expressed in cylindrical coordinates (psi, kPa) (see Figure 5.6)
G = shear modulus of the soil (psi, kPa)

The general solution of Equation D-11 is:

$$w = (Ar + Br^{-1}) \cos\theta + (Dr + Er^{-1}) \sin\theta + \epsilon z \qquad \text{(D-13)}$$

where: A, B, D and E are constants.

Using the definition of Equation D-13 in Equation D-12 yields the general solution:

$$\tau_{rz} = G\,(A - Br^{-2}) \cos\theta + G\,(D - Er^{-2}) \sin\theta \qquad \text{(D-14)}$$

Equations D-13 and D-14 apply for a region outside a circular hole and also for a cylindrical annulus within that hole, viz., the shaft lining with inside radius a and outside radius R. To distinguish between the region outside the annulus and the annulus, a prime (′) is added to the equations for the annulus, i.e.:

$$w' = (A'r + B'r^{-1}) \cos\theta + (D'r + E'r^{-1}) \sin\theta + \epsilon z \qquad \text{(D-15)}$$

$$\tau'_{rz} = G'(A' - B'r^{-2}) \cos\theta + G'(D' - E'r^{-2}) \sin\theta \qquad \text{(D-16)}$$

where: G' = the shear modulus of the annulus (lining) (psi, kPa).

For the annulus (lining) the shear stress vanishes at the interior surface, i.e., at $r = a$, $\tau'_{rz} = 0$ for all values of θ. Hence, from Equation D-16, it follows that:

$$A' = B'a^{-2}$$

$$D' = E'a^{-2}$$

and:
$$\tau'_{rz} = G'(A' \cos\theta + D' \sin\theta)(1 - \frac{a^2}{r^2}) \qquad \text{(D-17)}$$

Further, stresses and displacements must be continuous at the lining-soil interface, $r = R$

where:
$$w' = R\{(A' \cos\theta + D' \sin\theta)(1 + \frac{a^2}{R^2})\} + \epsilon z \qquad \text{(D-18)}$$

$$\tau'_{rz} = G'(A' \cos\theta + D' \sin\theta)(1 - \frac{a^2}{R^2}) \qquad \text{(D-19)}$$

For the region well removed from the hole, the stresses at infinity are known, i.e., at $r = \infty$ and $\theta = 0$, Equation D-14 gives:

$$\tau_{rz} = \tau^{\circ}_{xz} = GA \tag{D-20}$$

and at $r = \infty$, $\theta = 90°$, Equation D-14 gives:

$$\tau_{rz} = \tau^{\circ}_{yz} = GD \tag{D-21}$$

where: τ°_{xz} and τ°_{yz} = the free-field shear stresses in the soil.

Equations D-20 and D-21 may now be solved for A and D as follows:

$$A = \frac{\tau^{\circ}_{xz}}{G} \tag{D-22}$$

$$D = \frac{\tau^{\circ}_{yz}}{G} \tag{D-23}$$

At the lining-soil interface, the shear stress and displacement corresponding to the soil surface of the hole ($r = R$) can be expressed by combining Equations D-22 and D-23 with Equations D-13 and D-14 as follows:

$$w = R\{(\frac{\tau^{\circ}_{xz}}{G} + BR^{-2}) \cos\theta + (\frac{\tau^{\circ}_{yz}}{G} + ER^{-2}) \sin\theta\} + \epsilon z \tag{D-24}$$

$$\tau_{rz} = G(\frac{\tau^{\circ}_{xz}}{G} - BR^{-2}) \cos\theta + G(\frac{\tau^{\circ}_{yz}}{G} - ER^{-2}) \sin\theta \tag{D-25}$$

Because the stresses and displacements must be continuous at the lining-soil interface, Equations D-19 and D-25 can be equated to give:

$$G'A'(1 - \frac{a^2}{R^2}) = -GBR^{-2} + \tau^{\circ}_{xz} \tag{D-26}$$

$$G'D'(1 - \frac{a^2}{R^2}) = -GER^{-2} + \tau^{\circ}_{yz} \tag{D-27}$$

Likewise, Equations D-18 and D-24 can be equated to yield:

$$A'\left(1+\frac{a^2}{R^2}\right)=\frac{\tau^{\circ}_{xz}}{G}+BR^{-2} \tag{D-28}$$

$$D'\left(1+\frac{a^2}{R^2}\right)=\frac{\tau^{\circ}_{yz}}{G}+ER^{-2} \tag{D-29}$$

Equations D-26 and D-28 may now be solved for A′ and B as follows:

$$A'=\frac{2\tau^{\circ}_{xz}}{G'\left(1-\frac{a^2}{R^2}\right)+G\left(1+\frac{a^2}{R^2}\right)} \tag{D-30}$$

$$BR^{-2}=\frac{\tau^{\circ}_{xz}}{G}\cdot\frac{\left\{G\left(1+\frac{a^2}{R^2}\right)-G'\left(1-\frac{a^2}{R^2}\right)\right\}}{\left\{G\left(1+\frac{a^2}{R^2}\right)+G'\left(1-\frac{a^2}{R^2}\right)\right\}} \tag{D-31}$$

Solving Equations D-27 and D-29 for D′ and E yields similar relationships, but involving τ°_{yz}, i.e.,

$$D'=\frac{2\tau^{\circ}_{yz}}{G'\left(1-\frac{a^2}{R^2}\right)+G\left(1+\frac{a^2}{R^2}\right)} \tag{D-32}$$

$$ER^{-2}=\frac{\tau^{\circ}_{yz}}{G}\cdot\frac{\left\{G\left(1+\frac{a^2}{R^2}\right)-G'\left(1-\frac{a^2}{R^2}\right)\right\}}{\left\{G\left(1+\frac{a^2}{R^2}\right)+G'\left(1-\frac{a^2}{R^2}\right)\right\}} \tag{D-33}$$

The lining stress is obtained by substituting Equations D-30 and D-32 into Equation D-19 which gives:

$$\tau'_{rz}=\frac{2\left(1-\frac{a^2}{r^2}\right)}{\frac{G}{G'}\left(1+\frac{a^2}{R^2}\right)+\left(1-\frac{a^2}{R^2}\right)}\left(\tau^{\circ}_{xz}\cos\theta+\tau^{\circ}_{yz}\sin\theta\right) \tag{D-34}$$

Equation D-34 can be simplified by considering the case of free-field shear in the y–z plane only, i.e., let $\tau^{\circ}_{xz} = 0$, and evaluating the maximum shear stress which occurs at $r = R$ and $\theta = 90°$. For this case, Equation D-34 reduces to:

$$\tau'_{rz} = \frac{2(1 - \frac{a^2}{R^2})\,\tau^{\circ}_{yz}}{\frac{G}{G'}(1 + \frac{a^2}{R^2}) + (1 - \frac{a^2}{R^2})} \qquad \text{(D-35)}$$

The stresses in Equation D-35 can be expressed in terms of strains by noting that:

$$\tau'_{rz} = G'\gamma'_{rz} \qquad \text{(D-36)}$$

$$\tau^{\circ}_{yz} = G\gamma_{yz} \qquad \text{(D-37)}$$

where: γ'_{rz} = shear strain in the lining
γ_{yz} = free-field shear strain in the soil

Substituting Equations D-36 and D-37 into Equation D-35 gives:

$$\gamma'_{rz} = \frac{2(1 - \frac{a^2}{R^2})\,\gamma_{yz}}{(1 + \frac{a^2}{R^2}) + \frac{G'}{G}(1 - \frac{a^2}{R^2})} \qquad \text{(D-38)}$$

Noting that $\gamma_{yz} = \gamma_{zy}$, letting $\gamma'_{rz} = \gamma^*_{zy}$, and letting $G' = G'_d$ and $G = G_d$ (to denote dynamic moduli), Equation D-38 becomes Equation 5-46.

D.3 Equation 5-49

Curvature of a deflected beam is given by:

$$\kappa = \frac{d^2u}{dz^2} \qquad \text{(Timoshenko and Young, 1962)} \quad \text{(D-39)}$$

where: κ = beam curvature (1/in, 1/mm)

u = lateral displacement (in,mm)

z = vertical coordinate (in,mm) (see Figure 5.6)

Differentiating Equation D-1 and combining with Equations D-8 and D-39 yields:

$$\kappa = -\frac{2\pi}{L}\gamma_{zy}\sin\frac{2\pi z}{L} \tag{D-40}$$

Disregarding sign as not significant, the maximum curvature from Equation D-40 is:

$$\kappa = \frac{2\pi}{L}\gamma_{zy} \tag{D-41}$$

which is Equation 5-49.

D.4 Equations 5-62 and 5-63

The stress-strain equations for biaxial stress are given by:

$$E'_d\epsilon_t = \sigma_t - \nu'_d\sigma_z \qquad \text{(Timoshenko and Goodier, 1970)} \tag{D-42}$$

$$E'_d{}'\epsilon_{zz} = \sigma_z - \nu'_d\sigma_t \tag{D-43}$$

Equations D-42 and D-43 are solved simultaneously to obtain:

$$\sigma_t = \left(\frac{E'_d}{1-\nu'^2_d}\right)(\epsilon_t + \nu'_d\epsilon_{zz}) \tag{D-44}$$

and:

$$\sigma_z = \left(\frac{E'_d}{1-\nu'^2_d}\right)(\epsilon_{zz} + \nu'_d\epsilon_t) \tag{D-45}$$

which are Equations 5-62 and 5-63, respectively.

APPENDIX E

DERIVATION OF TABLE 5.6

Table 5.6 shows correction factors that should be used for determining the tangential stresses at the outside surface of the shaft lining where the ratio of lining thickness to shaft radius $\left(\frac{t}{r_i}\right)$ is greater than 0.3.

The following equation is a linear approximation of the tangential stresses in the wall of a hollow cylinder subjected to an external pressure P_o.

$$\sigma_t = -\frac{P_o \cdot r_a}{t}\left(1 + \frac{y}{r_s}\right) \qquad \text{(Link, et. al., 1985) (E-1)}$$

where: σ_t = tangential stress (psi, kPa)

r_a = radius to outer surface of the cylinder (in, mm)

t = thickness of the cylinder wall (in, mm)

r_s = radius to the neutral axis of the cylinder wall (in, mm)

y = distance from the neutral axis to any point in the wall (in, mm). In addition, y is positive when measured toward the inside of the cylinder.

This linear equation is based on the simple formula for thin-walled cylinders:

$$\sigma_t = \frac{P_o\, r_a}{t} \qquad \text{(Link, et. al., 1985) (E-2)}$$

It can be readily seen that for a thin-walled cylinder the value of $\frac{y}{r_s}$ is small, and the error introduced by using Equation E-1 is also small.

For thicker-walled cylinders, however, a more precise stress determination is obtained by using the following equation derived from the classic Lamé formula for thick-walled cylinders:

$$\sigma_t = \frac{P_o \cdot r_a^2}{r_a^2 - r_i^2}\left(1 + \frac{r_i^2}{r^2}\right) \qquad \text{(Link, et. al., 1985) (E-3)}$$

where: r_i = internal radius of the cylinder

r = radius to any point in the cylinder wall ($r_i < r \leq r_a$)

Figure E-1 illustrates the stress distribution for a 15 ft (4.6 m) inside diameter (r_i = 90 in, 2,286 mm) cylinder with a 48 in (1,219 mm) thick wall ($\frac{t}{r_i}$ = 0.53) subjected to an external pressure of P_o.

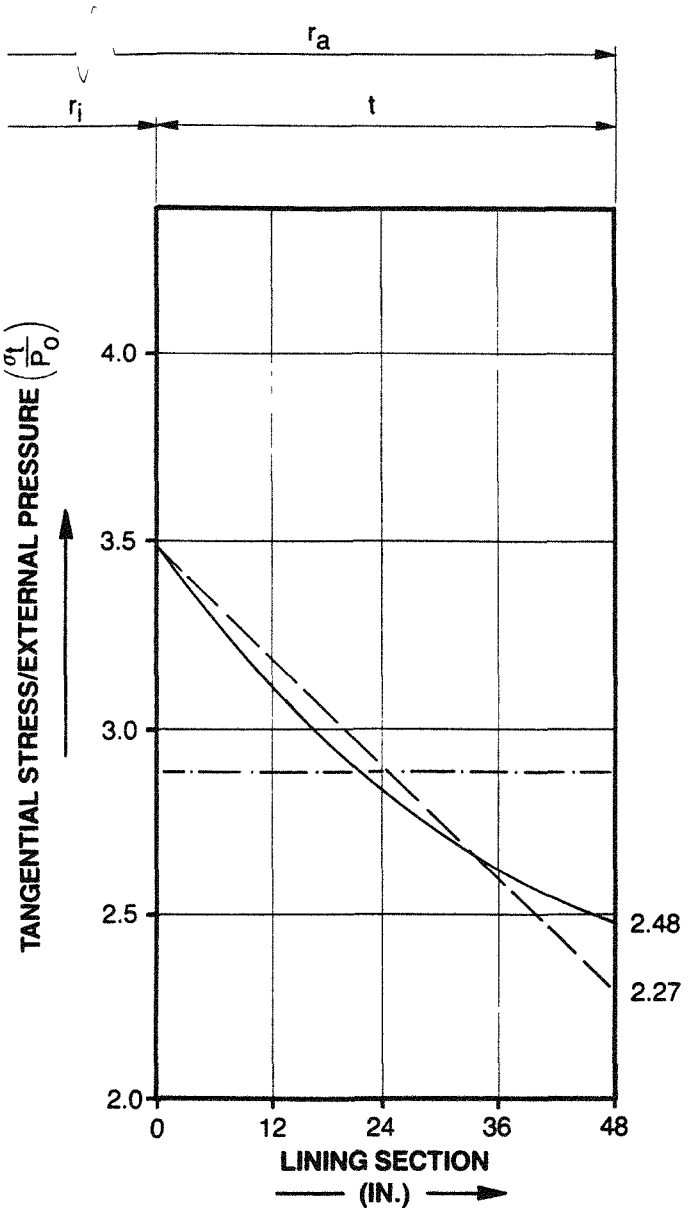

LEGEND

Thin Wall Equation E-2

Linear Equation E-1

Quadratic Equation E-2

STRESS DISTRIBUTION FOR A 15 FOOT DIAMETER CYLINDER

FIGURE E.1

APPENDIX F

VERIFICATION OF EQUATION 4-20

From Figure F-1:

ab = L = length of the shaft
ao = R = radius of curvature of liner
bc = f = maximum relative horizontal displacement of the shaft axis over length L

Since f is very small with respect to L, the distance ab is approximately equal to ac.

$ac \cong ab = L$
$bc = ao\,(1 - \cos\theta)$
$f = R\,(1 - \cos\theta)$

or: $$\cos\theta = 1 - \frac{f}{R} \qquad \text{(F-1)}$$

$ac = R \sin\theta$
$L = R \sin\theta$

or: $$\sin\theta = \frac{L}{R} \qquad \text{(F-2)}$$

from Equations F-1 and F-2

$$\sin^2\theta + \cos^2\theta = 1 = \frac{L^2}{R^2} + 1 + \frac{f^2}{R^2} - \frac{2f}{R} \qquad \text{(F-3)}$$

then: $$\frac{L^2 + f^2 - 2fR}{R^2} = o$$

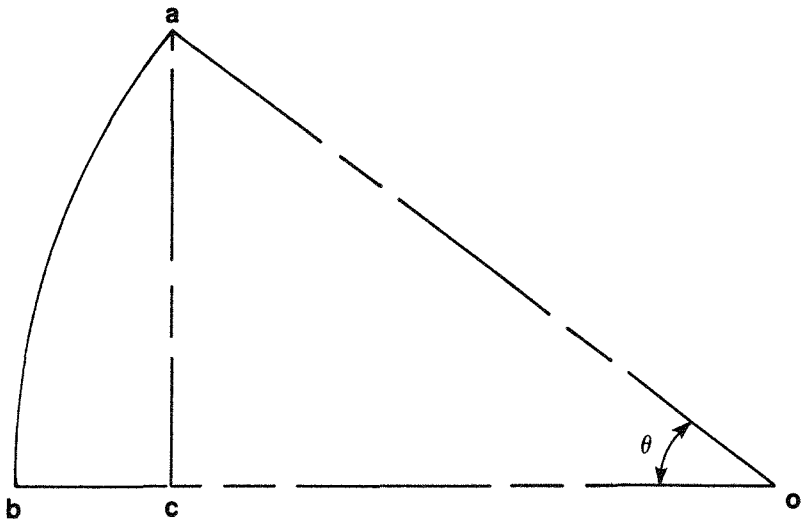

IDEALIZED BENDING DIAGRAM

FIGURE F.1

and: $L^2 + f^2 - 2fR = o$

and: $R = \frac{L^2 + f^2}{2f}$

Neglecting the value of f^2 since L^2 is much greater than f^2:

then: $R = \frac{L^2}{2f}$ (F-4)

Equation F-4 becomes Equation 4-20.